UNIVERSITY OF THE WITWATERSRAND, JOHANNESBURG

Palynology and organic geochemistry analysis of borehole cores from the Maniamba Basin, northern of Mozambique: Potential for hydrocarbon

Nelson Ernesto Nhamutole

Student number: 2275773 **Orcid number:** 0000-0002-6578-4622

Thesis submitted to the Faculty of Science at the University of the Witwatersrand, Johannesburg, in fulfilment of the requirements for the degree of Doctor of Philosophy.

Johannesburg, May of 2025

Main supervisor

Prof. Marion Bamford (ESI, Wits)

Co-supervisors

Prof. Paulo Alves de Souza (UFRGS)

Prof. Dermeval Aparecido do Carmo (UnB)

Declaration

I hereby certify that this doctoral thesis is completely my own unaided work, and has not been submitted before for any degree or examination at any other University.

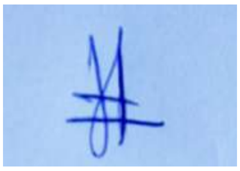

(Signature of candidate)

28th day of May 2025

Abstract

The Maniamba Basin in northern Mozambique, southern Africa, is one of the well-known coal bearing basins within the country. Their geological formations are contemporaneous with the Karoo Supergroup with an almost complete record of sediment deposition occurring during the Late Carboniferous to Early Jurassic. The basins are linked to regions of old crustal sutures where high-strain structures formed during the Pan-African Orogeny. Since studies of the organic facies are scarce, the main objective of this thesis is to determine the potential for hydrocarbon generation together with a good understanding of the biostratigraphy of organic-rich rock sequences intercepted by four boreholes. JOG16N-5, JOG16N-6, JOG16-7, and JOG16N-8 together with four outcrops at Luiga, Luchai, Michunwa and Nhamago, in the Maniamba Basin. The multiproxy analysis includes palynology, palynofacies, elemental analysis, XRD, vitrinite reflectance, TOC, Rock Eval pyrolysis and biomarkers. Two hundred thirty-seven rocks were subsampled from borehole cores, together with twenty samples from outcrop were analyzed for the type, content, quality, thermal maturity, age of deposition, palaeoenvironments for hydrocarbon potential of the Basin. The lithostratigraphic units are organically rich in regard to TOC, thermally matured into gas and oil windows, however more gas with minor oil is generated given the preservation of the organic matter in a proximal - distal environment under oxic conditions (type III kerogen, mixed type II/III and type IV kerogen). Over-maturation occurrence is linked to kimberlite emplacement that is associated with the first or second graben faulting stages in the Basin.

The Maniamba Basin organic-rich rocks differ geochemically from oil fluids in the Rovuma and Mozambique basins that has been assumed to be the same since the latter fluids are suggested to be sourced from marine shales.

Biostratigraphically, a Guadalupian age was inferred for outcrop strata of the Luchai and Nhamago sites being coeval with the K4 Formation and Changhsingian-Induan for Luiga site suggesting correlation with the K5 Formation. No age was assigned to the Michunwa outcrop strata due to their poor preservation. Additionally, a Wuchiapingian age was suggested for the K4 Formation, whereas a Changhsingian-Induan age is inferred for the K5 formations in the Maniamba Basin contradicting previous findings.

In the K5 Formation for the first time the Permo-Triassic transition is recorded reinforcing correlations in Central Gondwana. In its turn, in the K4 Formation, intra Gondwanan provincialism is observed with the northern Karoo palynoevents differing from their southern Karoo counterpart. The revised coal biostratigraphy could potentially spark interest for coal bed methane in the world seeking for cleaner energy.

The Basin palaeoenvironment is characterised by oscillating paleoredox conditions that could have been influenced by sediment infilling during the Permian-Triassic boundary to possibly the end of the thermal uplift caused by the jurassic Karoo magmatism. Yet, during the middle-late Permian to Early Triassic this Basin was made up of meandering and braided rivers together with coal-bearing beds that comprise floodplains, crevasse splay and fluvial channel lithofacies associations. This is a representative of a typical fluvial/lacustrine settings marked by the co-existence of sub environments and hypautocthonous sedimentation.

In conclusion, this multiproxy study has demonstrated that the integration of approaches has given a deeper understanding of the evolutionary history of the Maniamba Basin.

Keywords: Karoo deposits, Hydrocarbon, Stratigraphy, Gondwana coals, Palaeoenvironment.

Acknowledgements

The PhD journey was not the easiest whatsoever but there was a certain individual that made it a bit smoother. To my main PhD supervisor Prof. Marion Bamford for your endless and unwavering support, encouragement, guidance, friendship, and much more. Words are not enough to describe everything you have done to me during all this process. Prof. Paulo Alves de Souza (Federal University of the Rio Grande do Sul, Brazil) your constructive criticism, corrections and readiness were very essential. Thanks for your hospitality and kindness during my stay in Brazil. Prof. Dermeval Aparecido do Carmo thanks for your positive criticism and for host me in Brasilia University. I would like to extend my deepest gratitude to Direcção Nacional de Geologia e Minas for the invaluable support, and assistance in providing and giving permission to use borehole cores. The Instituto Nacional de Petróleos (INP, MIREME) is acknowledged due to its financial support towards this research. Thanks go out to Prosper Bande from Evolutionary Studies Institute, University of the Witwatersrand who assisted during palynological preparation, Deran Reddy from the Microscopy and Microanalysis Unit (MMU), University of the Witwatersrand who helped during fluorescence analysis. Juliana Marinho, Humberto, Bruno, Kawane from Federal University of the Rio Grande do Sul (UFRGS) are acknowledged for their assistance during Rock Eval pyrolysis and vitrinite reflectance analysis. To the ESI staff, thank you for giving me assistance since my master studies and later on in my PhD journey. The support received from my family played a pivotal role in ensuring my resilience skill during this demanding time. I would like sincerely to thank Dr. Costa Junior (may his soul rest in peace) for have discovered my potential while I was an undergraduate student and for his advises that is always possible to defeat the odds. The National Museum of Geology, Mozambique, PAST (The Palaeontological Scientific Trust, Johannesburg), National Research Fund (NRF), Jim and Gladys Taylor Trust, Genus (DSI-NRF Centre of Excellence in Palaeosciences, UID 86073) towards this research is hereby acknowledged. Opinions expressed and conclusions arrived at, are those of the author and are not necessarily to be attributed to the Genus.

Lastly, I would like say that the list is endless and thank you to all who helped in their way to make this project possible.

Co-author's contributions

Prof. Marion Bamford (Evolutionary Studies Institute), main supervisor, Prof. Paulo Alves de Souza (Federal University of Rio Grande do Sul), Dermeval Aparecido do Carmo (University of Brasilia) as my supervisors who have guided through the research process.

- Prof. Tais Freitas da Silva from Federal University of Rio Grande do Sul, Brazil (UFGRS), supported the Rock Eval analysis.
- Prof. Egberto Pereira, Dr. Lucas Bastos (Rio de Janeiro State University), Prof. Sidney Gonçalo de Lima, Dr. Artur Barros, Lorena Tuane (Piauí Federal University) provided their expertise in biomarker analysis and data interpretation.
- Cristina Moreira Felix (Federal University of Rio Grande do Sul) contributed as an expert in Palaeozoic palynomorph identification.
- Jardel Peu, Aldevina Zimba and Olimpio de Deus (Eduardo Mondlane University) assisted with core subsampling, statistic software and 3D Basin model.
- Prosper Bande (Evolutionary Studies Institute, University of the Witwatersrand) provided assistance during palynological preparation.
- Manuel Nopeia (Akita University) and Laura Mendes (Eduardo Mondlane University) assisted with XRD and Raman analysis. Unfortunately, Raman analysis was not included in the present research.
- The elemental analysis was performed by JOGMEC.

Contents

List of Figures

List of Tables

Part I - Introduction

1. General Introduction

Mozambique over the last decades has proven to be a wealth country in terms of hydrocarbon reserves. The exploration in the country has been focused in the Mozambique Basin and the Rovuma basins (Fig. 1). The first Basin covers the onshore and offshore sections of south and Centre of the country (Fig. 1). Similarly, the Rovuma Basin occurs onshore and offshore but it is located in the north part of Mozambique. Albeit the fact of being economically the most exploited basins in the country, published data highlighting hydrocarbon potential based on palynology and petroleum geochemistry do not exist for these two basins (Fig.1).

Most of the published studies in the Mozambique Basin and the Rovuma Basin are related to seismic methods (Salman and Abdula, 1995; Mahanjane, 2012; 2014 and others). Data in which palynology and petroleum geochemistry were applied are owned by the oil companies (ECL, 2000; Lineback et al., 1986; Salman et al., 1990). Apart from internal reports of oil companies there are very few publications on petroleum geochemistry for these two basins with Lineback et al. (1986) and Mussa (2017) being two examples.

On the opposite side, a quite considerable number of biostratigraphy studies in the Main Karoo Basin have been undertaken (Falcon et al., 1984, 1986; MacRae, 1988, Aitken, 1998, Barbolini et al., 2014). The Main Karoo Basin (MKB) represents the most extensive and continuous geological record spanning from Late Carboniferous to mid-Jurassic in southern Africa (Smith, 1990; Catuneanu et al., 1998). The MKB, was mainly controlled by tectonism as a consequence of the development of the Karoo foreland basin with the subduction of the palaeo-Pacific plate beneath the Gondwana (Catuneanu et al., 1998, 2005). During the Late Carboniferous/Early Permian, Gondwana was dominated by glaciation due to the‘‘decreasing of the global latitudinal distribution of the equilibrium line of altitude’’ (Isbell et al., 2008), which changed to progressive aridification in the Middle Permian-Triassic and eolian environment into the Early Jurassic (Smith, 1990; Johnson et al., 1996; Catuneanu et al., 2005). This climate oscillation affected vegetation, having a direct link with biomass production, coal, gas, etc. In the Karoo Basin, the Ecca Group represents the most economically important deposits as it comprises the main coal bearing strata of the Karoo Supergroup (MKB) characterised by a complex system that comprises fluvial and delta plains. In the MKB, the organic rich rocks were deposited in typical lacustrine and swampy environment. (Smith, 1984; Bordy, 2019). Although there are a number of studies in the MKB including the Tete Province in Mozambique (Fernandes et al., 2015, Hancox, 2016; Perreira et al., 2016; Gotz, 2017; Galasso et al., 2019), some subsidiary basins remain completely overlooked.

An example of these subsidiary basins is the Maniamba Basin (MB) located in the Niassa Province (northern Mozambique). The formation of the MB is linked to the Permian-Triassic rifting system which is referring to the development of Karoo grabens that the occurred before the break-up of Gondwana. According to Delvaux (1991), the largest Karoo basins in South Africa, Zimbabwe, Mozambique were formed during that time. Most of the basins originated from rifts that were initially formed as tectonic sedimentary basins, however during the Permian-Triassic they evolved into grabens and half grabens as a consequence of descendant faulting and deformation during Early Jurassic (Catuneanu et al., 2005). In the Maniamba Basin, the most detailed palynology studies were done by Verniers et al. (1989). In that study three palaeozones were established. However, these biozones were only identified for some sections of the upper Karoo. Due to the poorly preserved assemblages of spores and scarce available data of material, the work of Verniers and colleagues only identified the palynomorphs to the generic level. Other recent studies regarding the sedimentary facies of the Maniamba Basin are referred to by Norconsult (2007), Vale Moçambique (2014), JOGMEC (2015) and Paz (2018), however none of them dealt with palynology, palynofacies, thermal maturation (vitrinite reflectance, spore colour index), Total Organic Carbon (TOC) or organic geochemistry (Rock Eval Pyrolysis, biomarkers). Thus, this project represents the first to combine all the proxies that have been proved to be successful worldwide (e.g., Mendonça Filho et al., 2010; Aggarwal et al., 2019; Bastos et al., 2021).

This study uses data from the Maniamba site in order to understand a likely potential for hydrocarbon reserves in the Karoo sediments aligned to the fact that there is a worldwide growing interest for exploration of unconventional hydrocarbons in the Palaeozoic rocks despite current clean energy policies. Concomitantly, the results from the Maniamba Basin could be extrapolated to the Mozambique and Rovuma Basins where Karoo sediments buried by younger sedimentary sequences are poorly studied by the oil companies. All in all, the assignment of the relative ages of the strata, reconstruction of depositional environments, determination of source rock potential, and paleoclimate will deepen the understanding regarding the evolutionary history of this basins over time.

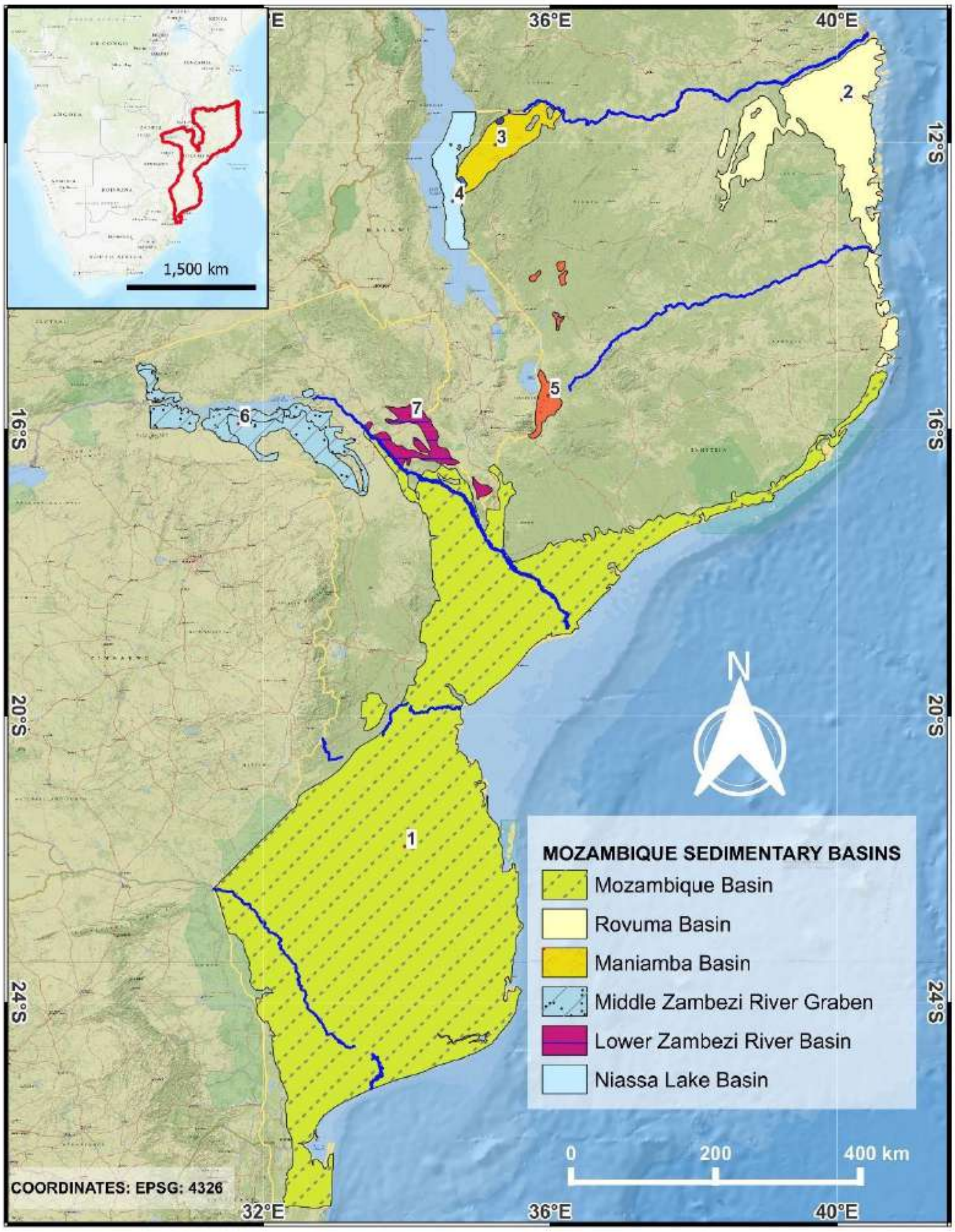

Figure 1. Map of Mozambican sedimentary basins adapted from ECL, 2000.

2. Objectives

The general objective of the thesis is to integrate palynology and organic geochemistry in order to evaluate the potential for hydrocarbon in the Maniamba Basin. In this regard, several objectives were established:

- Identification and classification of palynomorphs encountered in the studied areas.
- Determination of the age of the sequences.
- Determination of the type of organic matter.
- Evaluation of the organic thermal evolution.
- Characterization of the palaeoenvironments.
- Determination of provenance, sediment maturity, and tectonic settings.
- Assessment of the petroleum generation potential of the source rocks.
- Correlation of the Maniamba Karoo Basin with other coeval Karoo basins in regard to hydrocarbon potential.
- Determination of the contribution of Karoo aged rocks to the petroleum fluids from the Mozambique Basin and Rovuma Basin.

Therefore, in order to respond to the established variables, four boreholes (JOG16N-5, JOG16N-6, JOG16N-7, JOG16N-8) and four outcrops were selected and submitted to different multiproxy techniques such as palynology, palynofacies, vitrinite reflectance, Total Organic Carbon (TOC), elemental analysis, pyrolysis Rock Eval and biomarkers (hydrocarbon fingerprint).

3. Structure of the Thesis

The thesis is presented by published papers for the results chapters with a general introduction and discussion to link the sections and produce a cohesive body of work. It is presented as follows.

Part I consists of the general introduction together with objectives, and structure of the present thesis.

Part II consists of a literature review that highlights the main concepts used in the present study.

Part III consists of data regarding geography and geology of the Maniamba Basin.

Part IV consists of the laboratory techniques and methods used for the analysis of both sections of the organic matter (kerogen and bitumen).

Part V Includes the results and discussion of the present work. Here, seven papers are presented. These papers were submitted to international accredited journals where the papers are full length and peer-reviewed. Some papers are published (3), others are either submitted (3) or under review (2). This section is subdivided into four separate chapters that were based on the subject of the undertaken work.

Chapter One Includes one paper which deals with palynofacies in the sediments intercepted by the JOG16N-8, one of the four cores, and includes the upper Karoo sediments (age). Here, palynofacies are used to assess hydrocarbon potential.

- Nhamutole, N.; Bamford, M., Souza, P.A, Do Carmo, D. (2023). Palynofacies analysis of the JOG16N-8 borehole, K5 formation from the Maniamba Basin (middle Permian), Mozambique: *A contribution for hydrocarbon exploration.* Journal of African Earth Sciences, 205, 104997. (**Published**),

Chapter Two consists of one paper using the Rock eval pyrolysis data interpretation from outcrop units in the Maniamba Basin. This complements the borehole data for the same area however, outcrops data are used to assess hydrocarbon potential based on Rock Eval herein.

- Nhamutole, N., Bamford, M., Silva, T., Souza, P., Carmo, D., Moreira, C. 2024. Petroleum potential from Permian-Triassic strata of the Maniamba Basin, Mozambique: A preliminary characterisation. South African Journal of Geology, 127,117–130. (**Published**).

Chapter Three comprises three papers which are related to multiproxy analysis of the Maniamba Basin, including palynology, palynofacies, vitrinite reflectance, spore colour index, elemental analysis, XRD, pyrolysis rock eval and biomarkers. The first paper in this chapter includes almost all the proxies and is only lacking the biomarkers. It deals with sedimentary rocks from the JOG16N-5 borehole core. This paper complements the information obtained in the papers described in chapter one and two regarding hydrocarbon potential in the Basin.

The second paper in this chapter deals with the analysis of organic matter of the sedimentary rocks from JOG16N-6 and JOG16N-8 borehole core whereas the third paper focuses on the sedimentary units from outcrops. The latter two papers are more environmentally oriented albeit the fact that the second paper contributes to the understanding of the contribution of studied rocks into the oil fields from Rovuma Basin.

- Nhamutole, N., Bamford, M., Silva, T., Souza, P.A., Do Carmo, D., Felix, C. (2024). Shale-gas potential from K4 Formation (Permian), Maniamba Basin, Mozambique: Insights from integrated geochemical evaluation, elemental analysis and palynology. South African Journal of Geology. (**Under review**).
- Nhamutole, N., Bamford, M., Souza, P.A., Félix, C.M., Pereira, E., Bastos, L., Nopeia, M., Mendes, L., Deus, O. Reconstructing the Late Permian-Early Triassic environment of a coal-bearing succession in the Maniamba Basin, Mozambique (Central Gondwana): *A multiproxy palynological and geochemical approach*. International Journal of Coal Geology. (**Accepted for publication-*in press***).
- Nhamutole, N., Bamford, M., Lima, S., Barros, A., Almeida, L., Peu, J. Saturated hydrocarbons in source rocks from Maniamba Basin, Mozambique*:* A contribution for a better understanding of past environments. South African Journal of Chemistry. (**Under review**).

Chapter Four focuses on the palynostratigraphy of the Maniamba Basin using all four borehole cores. Two cores are described in the first paper: JOG16N-6 and JOG16N-8, while the remaining two are used for the second paper, (JOG16N-5 and JOG16N-7). The first paper investigated late Permian-Early Triassic transition whereas the last paper is focused solely in the late Permian. The papers are:

- Nhamutole, N, Bamford, M.K, Souza, P. A, Félix, C.M, Carmo, D.A, Peu, J. Palynology of two drilling cores from the Maniamba Basin, Mozambique (Central Gondwana):

Insights on age and palaeoenvironments. Review of Palaeobotany and Palynology, 334, 105271. (**Published**)

- Nhamutole, N, Bamford, M.K, Souza, P. A, Félix, C.M, Carmo, D.A, Bande, P. New palynological data from the Maniamba Basin, Mozambique: *Implication on Guadalupian and Lopingian Palaeoflora.* Review of Palaeobotany and Palynology. (**Published**).

The last part, **Part VI** of the thesis refers to the general conclusions, contribution to existing knowledge and recommendations for future research.

References

Aggarwal, N., Agrawal, S., Thaku, B., 2019. Palynofloral, palynofacies and carbon isotope of Permian coal deposits from the Godavari Valley Coalfield, South India: Insights into the age, palaeovegetation and palaeoclimate. Inter. J. Coal Geol. https://doi.org/10.1016/j.coal.2019.103285.

Aitken, G.A., 1998. A palynological and palaeoenvironmental analysis of Permian and early Triassic sediments of the Ecca and the Beaufort groups, Northern Karoo Basin, South Africa. Unpublished Ph.D. Thesis, University of the Witwatersrand.

Barbolini, N., 2014. Palynostratigraphy of the South African Karoo Supergroup and correlations with coeval Gondwanan successions. Unpublished PhD Thesis, University of the Witwatersrand, 386 pp.

Bastos, L. P. H., Rodrigues, R., Pereira, E., Bergamaschi, S., Alferes, C. L. F., Augland, L. E., Svensen, H. H., 2021. The birth and demise of the vast epicontinental Permian Irati-Whitehill sea: evidence from organic geochemistry, geochronology, and paleogeography. Palaeog. Palaeclimat. Palaeoecol. 562, 110103.

Bordy, E. 2019. Depositional style changes during the Permo-Carboniferous Early Jurassic evolution of the Central Kalahari Karoo Sub basin, Botswana. Geological Journal 55,5514–5539.

Catuneanu, O., Hancox, P.J., Rubidge, B.S., 1998. Reciprocal flexural behaviour and contrasting stratigraphies: a new basin development model for the Karoo retroarc foreland system, South Africa. Basin Research 10, 417-439.

Catuneanu, O., Wopfner, H., Eriksson, P.G., Cairncross, B., Rubidge, B.S., Smith, R.M.H., Hancox, P.J., 2005. The Karoo basins of south-central Africa. Journal of African Earth Sciences 43, 211-253.

Delvaux, D., 1991. Karoo rifting in western Tanzania: precursor of Gondwana break-up? in Contributions to Geology and Palaentology of Gondwana in Honor of Helmut Wopfner, 111-125.

ECL, 2000. The Petroleum Geology and Hydrocarbon Prospectivity of Mozambique. Empresa Nacional de Hidrocarbonetos (ENH), Unpublished report. 144pp.

Falcon, R., 1975. Palynostratigraphy of the Lower Karroo sequence in the central Sebungwe District, Mid-Zambezi Basin, Rhodesia. Palaeontol. afr. 18, 1–29.

Falcon, R.M.S., Pinheiro, H.J., Sheperd, P., 1984. The palynostratigraphy of the major coal seams in the Witbank Basin with lithostratigraphic, chronostratigraphic and palaeoclimatic implications. Comunicações dos Serviços Geológicos de Portugal 70, 215-243.

Fernandes, P., Cogné, N., Chew, D., Rodrigues, B., Jorge, R.C.G.S., Marques, J., Jamal, D., Vasconcelos, L., 2015. The thermal history of the Karoo Moatize-Minjova Basin, Tete Province, Mozambique: An integrated vitrinite reflectance and apatite fission track thermochronology study. J.Afr. Earth Sci. 112, 55-72.

Fernandes, P., Hancox, P., Mendes, M., Pereira, Z., Lopes, G., Marques, J., Jorge, R., Albardeiro, L. 2023. The age and depositional environments of the lower Karoo Moatize Coalfield of Mozambique: insights into the postglacial history of central Gondwana. Palaeoworld, 33, 979–996.

Galasso, F., Pereira, Z., Fernandes, P., Spina, A., Marques, J., 2019. First record of Permo-Triassic palynomorphs of the N'Condédzi sub-basin, Moatize-Minjova Coal Basin, Karoo Supergroup, Mozambique. Revue de Micropaléontologie, 64, 100357.

Gotz, A.E., Hancox, P.J., Lloyd, A., 2017. Permian climate change recorded in palynomorph assemblages of Mozambique (Moatize Basin, eastern Tete Province). Acta Palaeobotanica 57, 3–11.

Hancox, P.J. 2016. The coalfields of South-Central Africa: A current perspective. Episodes, 39, 407–428.

Isbell, J.L., Cole, D.I., Catuneanu, O., 2008. Carboniferous-Permian glaciation in the main Karoo Basin, South Africa: Stratigraphy, depositional controls, and glacial dynamics. In: Fielding, C.R., Frank, T.D., & Isbell, J.D. (Eds.), Resolving the Late Paleozoic Ice Age in Time and Space. Special Paper of the Geological Society of America, 441,71–82.

JOGMEC, 2015. The Results of Drilling Survey III in Mozambique. National Institute of Mines report.

Kent, P. E and Perry, J.T., 1973. The development of the Indian Ocean margin in Tanzania in Sedimentary basins of the African coasts. Drilling Project, 25, 679-654.

Lineback, J.A., Keal, J., Burroughs, K., 1986. Source rock potential of East Africa progress report and preliminary geochemical data and interpretation for Mozambique and additional wells in Somalia, Ethiopia and Madagascar. Robertson Research. 400pp.

Mahanjane, E., 2012. A geotectonic history of the northern Mozambique Basin including the Beira High – A contribution for the understanding of its development. Marine and Petroleum Geology, 36, 1-12.

Mahanjane, E., 2014. Maturity and Petroleum systems modelling in the offshore Zambezi delta depression and Angoche Basin, northern Mozambique. Journal of Petroleum Geology, 37, 329-348.

MacRae, C.S., 1988. Palynostratigraphic correlation between the Lower Karoo sequence of the Waterberg and Pafuri coal-bearing basins and the Hammanskraal plant macrofossil locality, Republic of South Africa. Memoirs of the Geological Survey of South Africa 75,1–217.

Mendonça Filho, J.G., Chagas, R.B.A., Menezes, T.R., Mendonça, J.O., Silva, F.S., Sabadini-Santos, E., 2010. Organic facies of the Oligocene lacustrine system in the Cenozoic Taubaté Basin, Southern Brazil. International Journal of Coal Geology 84, 166 - 178.

Mussa, A., 2017. O potencial de geração de hidrocarbonetos da Formação Pimenteiras, Bacia do Parnaíba. Unpublished PhD thesis. Universidade Federal do Rio Grande do Sul.

Norconsult, C., 2007. Notícia explicativa das áreas de Niassa, Cabo Delgado e partes de Zambézia e Nampula. Maputo, Moçambique: Direcção Nacional de Geologia. Unpublished report.

Paz, V., 2018. Sistemas Deposicionais e Fácies Sedimentares da Bacia Carbonífera de Maniamba. Bachelor Thesis. Universidade Eduardo Mondlane, p. 121 (in Portuguese).

Pereira, Z., Fernandes, P., Lopes, G., Marques, J., Vasconcelos, L., 2016. The Permian–Triassic transition in the Moatize–Minjova Basin, Karoo Supergroup, Mozambique: A palynological perspective. Rev. Palaeob. and Palynol. 226, 1–19.

Salman, G., Sheremetiev, Y., Koblents, A., 1990. The northern part of Mozambique Basin, a report on the geology and the oil and gas potential of Zambezi Licence Block, Mozambique. Empresa Nacional de Hidrocarbonetos, Mozambique, 127pp.

Salman, G., Abdula, I., 1995. Development of the Mozambique and Rovuma sedimentary basins, offshore Mozambique. Sedimentary Geology 96, pp. 7-41.

Smith, R.A., 1984. The lithostratigraphy of the Karoo Supergroup in Botswana. Bulletin of the Geological Survey of Botswana 26, 1-239.

Smith, R.M.H., 1990. A review of the stratigraphy and sedimentary environments of the Karoo basin of South Africa. Journal of African Earth Sciences 10,117-137.

Vale Moçambique, M., 2014. Projecto, desenvolvimentos e avaliação da ocorrência de carvão existente na Bacia Carbonífera de Maniamba. Provincia de Niassa em Moçambique, p. 100 (in Portuguese).

Verniers, J., Jourdan, P.P., Paulis, R.V., Frasca-Spada, L., De Bock, F.R., 1989. The Karroo graben of Metangula northern Mozambique. J. Afr. Earth Sci. 9, 137–158.

Part II – Organic matter concepts

4. Organic matter: Concepts and Classification

According to Durand (1980), sedimentary organic matter (SOM) depicts all kinds of organic matter with direct links to living or extinct organisms. Organic matter (OM) is mainly composed of organic molecules (e.g., hydrogen, oxygen, nitrogen, and sulphur). The OM can be either autochthonous or allochthonous depending on the deposition environment. It has been observed that a considerable supply of OM in continental margins due to high primary productivity in these regions as well as from continental allochthonous settings. In marine environments the OM is sourced from either marine phytoplankton or marine phytobenthic if photosynthesis occurs (Tissot and Welte, 1984).

The enrichment and accumulation of OM, relies on productivity of the biomass, degradation driven by biological and chemical processes, basin geological framework, and on the OM depositional processes (Tissot and Welte, 1984). In regard to preservation, the organic matter depends on the concentration of oxygen. For instance, in oxic waters the OM tends to be degraded whereas in anoxic waters a higher chance of much better preservation conditions is observed. In general, a water column is oxygenated, since there is an exchange between the atmosphere and the hydrosphere system. However, under conditions where the water column is strongly stratified or periods of high productivity occur, more anoxic conditions emerge and help in the preservation of OM (Meyers, 1997). Lastly, it should be highlighted that the OM consists of two fractions, kerogen and bitumen. The difference between the two fractions is their solubility in organic solvents. Kerogen depict 95% of the total OM is insoluble whilst bitumen is soluble (Tissot and Welte, 1984) (figure 2).

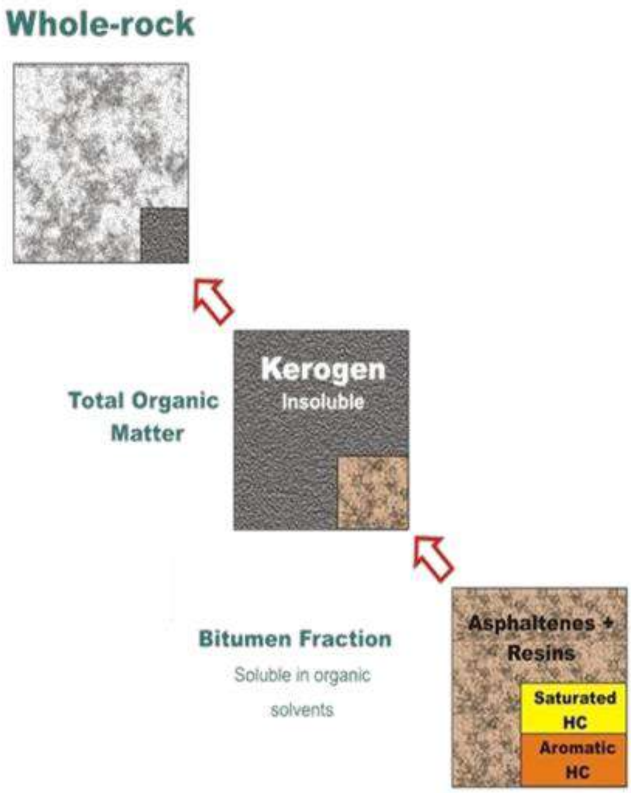

Figure 2. Compositional fractions of the OM adapted from Tissot and Welte (1984).

4.1. Kerogen: Type and Classification

The quality of hydrocarbons that have a potential to be preserved and later yielded depends in the amount of hydrogen and oxygen. These two elements are the essential part of the insoluble OM (Tissot and Welte, 1984). The different types of kerogens and their hydrocarbon potential are well-illustrated in the van Krevelen diagram. According to van Krevelen (1993) three types of kerogen exist and are classified according to the Hydrogen /Carbon versus Oxygen/Carbon ratios. Type I, type II, type III and type IV kerogens are identified based on the aforementioned ratios. The aforementioned diagram was initially restricted to coals; however, it was modified for its broader use by Tissot et al. (1974). The adapted diagram uses Hydrogen Index (HI) versus Oxygen Index (OI) based on Pyrolysis Rock Eval to assess depositional environments and potential for hydrocarbon for each group of kerogen.

According to the modified diagram, type I kerogen is enriched in lipids, and low heteroatomic bonds. Here, the H/C ratio is greater than the O/C ratio. Generally, lacustrine environments are linked to kerogen type I. Common occurrences includes fresh water algae, *Botryococcus*) and

OM characterised of enrichment in lipids linked to amorphous organic matter. Kerogen type I is oil prone (Tissot and Welte, 1984).

Type II is characterised by considerably lower H/C ratios if compared to kerogen type I. Chemically, it includes a dominance of chains made up by considerable aliphatic compounds together with naphthenic rings. Open marine sediments are linked to kerogen type II influenced by deposition in reducing environments bearing medium to high sulfur content. High content of sporomorphs together with cuticles is also linked to this kerogen. Similarly, Kerogen type II presents a potential for oil generation as kerogen type I. However, kerogen type II is lesser oil prone than kerogen type I. Most of the source rocks and shales widespread in the world are kerogen type II (Tissot and Welte, 1984).

The third type of kerogen is linked to terrestrial higher plants, and is linked to proximal environments. In this scenario, the source rocks are lesser oil prone comparatively to the previous two types of kerogens. However, abundant gas can be expected when maturity is reached (Tissot and Welte, 1984).

Lastly, the fourth kerogen type is characterised by a dominance of aromatic compounds. This kerogen is derived from oxidation, (pre- or post-depositional), combustion. Typically, the type IV is mainly composed of a high content of carbon and depletion in regard to hydrogen and oxygen. Type IV kerogen can generate small amounts of gas however the potential is considered to be low (Mendonça et al., 2011).

4.2. Thermal maturity

Biological (microbial) activities combined with temperature and pressure are considered the triggers of physicochemical changes of OM at the time of deposition and its burial (Tissot and Welte, 1984).

The set of processes linked to thermal maturity (temperature) are categorised into three consecutive phases. The stages are designated as diagenesis, catagenesis and metagenesis (Fig. 3) (Tissot and Welte, 1984).

4.2.1. Diagenesis

During the diagenesis (Fig. 3) physicochemical processes together with microbiological induced events occur at few hundred meters of depth. Reactions triggered by low temperature (to 65ºC) consisting of decarboxylation, reduction and polymerization characterise this stage. Vitrinite reflectance of approximately 0.4% indicates that during this stage the source rocks are considered immature however the same sequence of rocks if mature enough may generate oil or gas (Tissot and Welte, 1984).

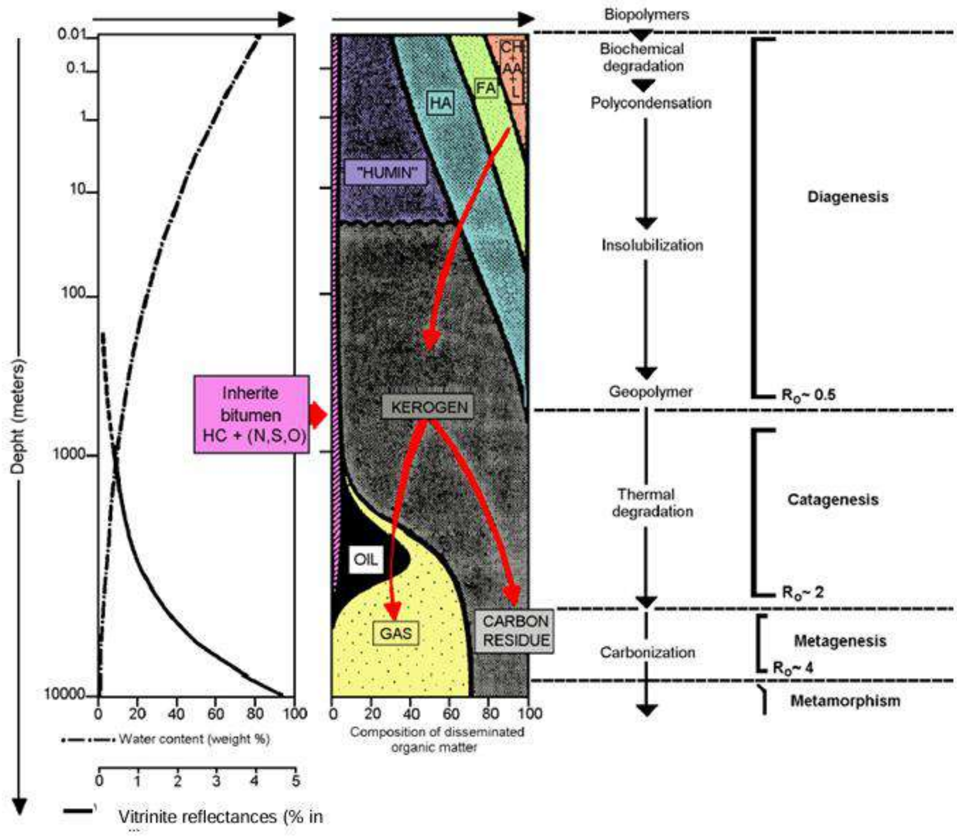

Figure 3. Thermal evolution of the OM adapted from Tissot and Welte (1984). CH: carbohydrates; AA: Amino acids; L: lipids; FA: fulvic acids; HA: Humic acids; HC: hydrocarbons; N, S, O: NSO compounds.

4.2.2. Catagenesis

During catagenesis, the OM is degraded as a result of increasing temperature and pressure during burial (50 - 200ºC) and pressure (300 to 1500 bars) (Hunt, 1995; Tissot and Welte, 1984). The catagenesis is the stage following the diagenesis. The temperature could reach 200ºC and pressure 1500 bars) (Hunt, 1995; Tissot and Welte, 1984). The OM degradation based on increasing of temperature is the main factor linked to the generation of hydrocarbon (Fig. 3). At this stage liquid oil is yielded first (oil window). Wet gas and condensate are produced at later stage together with methane. The catagenesis is defined by vitrinite values in the ranges of 0.5 to 1.35 % Rrandom (Tissot et al., 1974). At vitrinite reflectance values around 2.0% the heated organic matter is depleted from aliphatic chains and the catagenesis thermal stage is reached (Tissot and Welte, 1984).

4.2.3. Metagenesis

At this phase, the OM reaches great depth and highest temperature (Hunt, 1995). During catagenesis an arrangement of aromatic molecules is observed. Here, the source rocks are regarded supermature and only dry gas can be generated (Tissot and Welte, 1984).

4.2.4. Metamorphism

The metamorphism depicts the last stage of thermal evolution. During this stage both parameters, temperature and pressure reach high values. CH_4 (methane), CO_2 and graphite are yielded as consequence of OM transformation influenced by high temperature and pressure. According to Hunt at this stage, the appearance of greenschist facies is observed and vitrinite reflectance values are more than 4%.

In summary, it should be stressed that in addition to the aforementioned stages of thermal maturity, other components of a petroleum system do exist. Those components are related to the migration pathways when oil is generated to the reservoir (accumulation of oil before its exploitation); sealing rock, responsible for creating a barrier in order to prevent the possible final migration of the oil to the subsurface and others (Tissot and Welte, 1984).

Palynofacies

The introduction of the concept regarding palynofacies is attributed to Combaz (1964) as a definition for the bulk association of particulate OM embedded in sediments that remain after the removal of mineral matrix through acidification with hydrochloric and hydrofluoric acids. Later on, in 1995 the concept was expanded by Tyson, who defined palynofacies as a set of particulate OM found in a sedimentary rock that could be associated with any specific environmental condition of deposition and ultimately the hydrocarbon generating potential.

Traverse (1994) and Tyson (1995) adopted the terms, organic faciology and morphology of particulate OM in order to distinguish it into three categories: phytoclast, palynomorphs and amorphous groups (Table 1, Table 2 and Table 3) which were later applied and published by Mendonça Filho (1999) and others.

The palynofacies analysis is an effective parameter in the characterization of organic facies, since it allows a straightforward interpretation of the organic components. However, this classification could be subjective since the influence of factors such as thermal change, environmental, depositional, botanical classification, relationship between marine or terrestrial contribution, distance from the source, degree of degradation and allochthonous or autochthonous fractions that all should be taken into consideration, as suggested by Mendonça Filho et al. (1999). The characterization of these components is carried out based on their morphology, state of preservation aiming at identifying the provenance of OM, their relative proportions, state of preservation, level of thermal maturity, paleoenvironments, paleoredox conditions and hydrocarbon generation potential (Tyson, 1995).

Kerogen groups based on organic matter

The classification of kerogen has been a matter of debate due to the lack of standardization. However, some existing schemes are those proposed by Tyson (1995), Mendonça Filho (1999), Mendonça Filho et al. (2010). Key parameters including state of preservation, provenance, shape, optical variables, geochemical content are the most used in aforementioned classifications. However, a highly refined system is needed in order to yield a more robust interpretation. Based in the kerogen classification, three different groups can be identified and includes phytoclast, palynomorphs, and amorphous organic matter (AOM).

Phytoclast Group

Phytoclast represents plant tissues that can be linked to either gymnosperm and angiosperms (Tyson, 1995). Non-opaque (translucent) and opaque sub-categories are considered herein. The first sub-category includes mostly cuticles, membranes, and fungal hyphae. Paleoenvironment conditions determine the contribution of the phytoclast content in a given kerogen assemblage (Tyson, 1995).

Table 1 Main categories of phytoclast group and their refined description based on Tyson (1995) and Mendonça Filho et al. (2011).

<table>
<tr><th></th><th></th><th>Categories</th><th>Description</th></tr>
<tr><td rowspan="7">Dispersed Organic Matter (DOM)</td><td rowspan="3">Opaque</td><td>Black/ opaque</td><td>Absence of internal structure</td></tr>
<tr><td>Lath</td><td>Opaque with pitting</td></tr>
<tr><td>Corroded</td><td>Opaque and irregular</td></tr>
<tr><td rowspan="4">Non-opaque (Translucent)</td><td>Biostructured</td><td>Brown, lath to equant with pitting</td></tr>
<tr><td>Cuticle</td><td>Epidermal tissues from higher plants</td></tr>
<tr><td>Membrane</td><td>Pale yellow, sheet-like irregular display fluorescence</td></tr>
<tr><td>Fungal hyphae</td><td>Hyphae fragments, brown, represent the vegetation stages of fungi</td></tr>
</table>

Amorphous Group

The Amorphous Group comprises structureless organic matter under transmitted light microscopy. The AOM mostly comprises phytoplankton, AOM derived from bacteria, resins (Tyson, 1995). Paleoredox conditions and distal deposition are possible explanation that determine the content of AOM in a given kerogen association. Additionally, depending in the redox conditions the intensity of the fluorescence can be recorded (Tyson, 1995, Mendonça Filho et al. 2011).

Table 2 Highlight of AOM classification based on Tyson (1995) and Mendonça Filho et al. (2011).

Sub-categories	**Description**
Bacterially derived AOM	Structureless OM, no form, orange brown. It can contain inclusions of palynomoprhs, phytoclast, and pyrite. It can display fluorescence.
Resin (Yielded by terrestrial higher plants)	Structureless material, round, homogenous, fluorescence.

AOM=Amorphous organic matter

Palynomorph Group

Palynomorphs as part of the kerogen is referred to all organic walled microfossils that remain after the acidification process through hydrochloric and hydrofluoric acids (HCl and HF) in palynological preparations. Palynomorphs is one the well represented groups of particulate OM in the kerogen assemblage. However, its analysis relies on the nature of the assemblage which could be influenced by environment of deposition as well as by primary productivity (Tyson, 1995; Mendonça et al., 2011). In the present study, only sporomorphs were observed. In the present project, only sporomorphs (terrestrially derived palynomorphs) were observed. Based on their origin and complex morphology, spores and pollen can be divided into different subcategories (Table 3).

Table 3 Highlighted classification of palynomorph group based on Tyson (1995) and Mendonça Filho et al. (2011).

		Description	Subcategories
Palynomorphs	**Pollen**	Derived from gymnosperms and gymnosperms	Monosaccate Bisaccate striate Bisaccate non-striate Plicates
	Spores	Derived from Pteridophyte and bryophyte	Monolete Alete
	Other palynomorphs	---------------------	Acritarch Prasinophytes Chitinozoans Undetermined
Freshwater microplankton	***Botryococcus***	*Chlorococalles algae*	Globular colonies with irregular shape (30-2000 μm), sometimes display diversified lobes

----- Palynomorphs not observed in the present study.

4.3. Rock Eval Pyrolysis

The Rock-Eval pyrolysis technique is considered an important geochemical technique that allows the identification of kerogen types and conversion of OM into oil and gas (Espitalié et al., 1977). This tool is a laboratory simulation of the process of petroleum generation. The pyrolysis results are expressed in parameters such as S1 (free hydrocarbons present in the sample that become volatile due to considerable heating with temperature ranging from 200 to 250°C), S2 (Hydrocarbons generated at high temperatures by kerogen pyrolysis) and S3 (carbon dioxide released in organic matter and water). Another parameter used in pyrolysis includes T_{max} (ºC). The T_{max} depicts the maximum release of hydrocarbons occurs during the second peak (Tissot and Welte, 1984). For more robust interpretation of thermal evolution of sedimentary Basin and due to the fact that T_{max} values are influenced by other variables (e.g., clay mineral content, kerogen types, laboratory handling of the samples), thus their correlation with vitrinite reflectance, spore color index (SCI) and biomarkers data is inevitably important. Other pyrolysis data includes the hydrogen index (HI), index of oxygen (OI), production index (IP). These indexes are described in the methodology section and their importance for source rock assessment can found in detail in the table 4.

Table 4 Geochemical variables highlighting the different kerogen's type and expelled petroleum fluids adapted from Peters and Cassa (1994).

Kerogen	HI (mg HC/g TOC)	S_2/S_3	H/C atomic ratio	Expelled hydrocarbon at the peak of maturity
I	>600	>15	>1.5	Oil
II	300-600	10.0-15.0	1.2-1.5	Oil
II/III	200-300	5.0-10.0	1.0-1.2	Mixed oil and gas
III	50-200	1.0-5.0	0.7-1.0	Gas
IV	<50.0	<1.0	<0.7	None

*HI: Hydrogen Index; TOC: Total organic carbon; H/C: Hydrogen and Carbon ratios.

4.4. Biomarkers

The term biomarker was introduced for the first time by Seifert and Moldowan (1981). Biomarkers are traditionally called chemical fossils or biological markers and are organic compounds of a complex nature whose main structure did suffer significant changes during burial process (Peters et al., 2005). Biomarkers are always associated with their precursor of biological origin. These organic and petroleum fingerprints can be found in oils, extracts of sediment as well in other environments. The biomarker study is an important factor that helps to determine of the origin of OM, thermal evolution, palaeoenvironments, and source-source, source-oil, oil-oil correlations (Mendonça Filho, 2010). Overall, the quantity of biomarkers recovered has increased due to the development of better analytical techniques for detection and identification of organic compounds. The majority of biomarkers used in the study of source rocks are saturated and are summarized below (Table 5).

Table 5 Hydrocarbon biomarker according to Peters et al. (2005).

Biomarker	Structure	Precursor	Information
n-alkane (C15, C17, C19)		Marine algae	Origin of OM
n-alkane (C25, C27, C29, C31)		Terrestrial plants	Origin of OM
Pristane Phytane	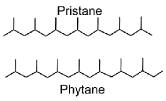	Phototrophic organisms	Depositional environment
Tricyclic terpanes	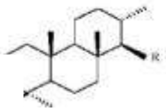	Prokaryotic organisms	Thermal maturation
Hopanes	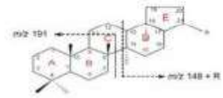	Prokaryotic organisms	Thermal maturation
Gammacerane	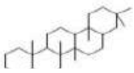	Protozoa	Hypersalinity conditions
Steranes	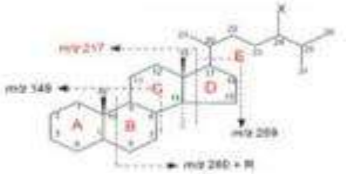	Eukaryotic organisms	Thermal maturation and OM origin
Diasteranes	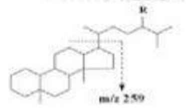	Eukaryotic organisms	Thermal maturity

*OM=organic matter

4.5. X-Ray Diffraction (XRD)

X-ray diffraction (XRD) represents a chemical analysis that allows the identification of mineral phases presented in a given sample. It consists of focusing electrons onto the sample and then measuring the angle at which the x-ray beam is diffracted and read by the detector. The angles read are recorded in the form of “peaks” in a diffractogram. By acknowledging that each mineral has a distinct and known diffraction, it is possible to discriminate the phases individually in the sample. The XRD technique analysis was crucial to help in the interpretation of tectonic settings, sediment maturity and provenance.

Elemental analysis

In the present study, elemental analysis was used to infer the maturation and paleoredox prevailing conditions during the process of sedimentation. For the interpretation of elemental analysis, the target elements in the kerogen assemblages were carbon, hydrogen, oxygen, nitrogen and sulphur.

References

Combaz, A., 1964. Les palynofacies. Reveu de Micropaléontologie, 7, 204-218.

Durand, B., 1980. Sedimentary organic matter and kerogen. Definition and quantitative importance of kerogen. Chapter 1, in: Durand, B. (Ed.), Kerogen - Insoluble organic matter from sedimentary rocks. Editions Technip, Paris, pp. 13-34.

Espitalié, J., Laporte, J.L., Madec, M., Marquis, F., Leplat, P., Paulet, J., Boutefeu, A., 1977. Méthode rapide de caractérisation des roches mètres, de leur potentiel pétrolier et de leur degré d'évolution. Revue de l'Institut Français du Pétrole, 32, 23-42.

Hunt, J.M., 1995. Petroleum Geochemistry and Geology. Freeman, San Francisco.

Mendonça Filho, J.G.M., 1999. Aplicação de estudos de palinofácies e fácies orgânica em rochas do Paleozóico da Bacia do Paraná, Sul do Brasil. PhD thesis. Universidade Federal do Rio Grande do Sul, pp. 254 (in Portuguese).

Mendonça Filho, J.G., Menezes, T.R., Mendonça, J.O., Oliveira, A.D., Carvalho, M.A., Sant'Anna, A.J., Souza, J.T., 2010. Palinofácies, in: Sousa, C.I. (Ed.), Paleontologia. Rio de Janeiro, Interciência, pp.379 – 413.

Mendonça Filho, J.G., Menezes, T.R., Mendonça, J.O., 2011. Organic Composition (Palynofacies Analysis). Chapter 5 in: ICCP Training Course on Dispersed Organic Matter, ISBN 978-9-89-826567-8, pp. 33-81.

Peters, K.E., Cassa, M.R., 1994. Applied source rock geochemistry. L.B. Magoon, W.G. Dow (Eds.), The Petroleum System—From Source to Trap: Tulsa, Okla, vol. 60, American Association of Petroleum Geologists, Memoir, pp. 93-117.

Peters, K.E., Walters, C.C., Moldowan, J.M., 2005. The Biomarker Guide, vol. 2, Biomarkers and Isotopes in Petroleum Exploration and Earth History, second ed. Cambridge University Press, London.

Seifert, W.K., Moldowan, J.M., 1981. Paleorecon-struction by biological markers. Geochimica et Cosmochimica Acta 45,783–794.

Tissot, B., Welte, D.H., 1984. Petroleum formation and occurrence, second ed. Springer Verlag, Hidelberg.

Traverse, A., 1994. Sedimentation of organic particles. Cambridge University Press, Cambridge, pp. 1–544.

Traverse, A., 2007. Paleopalynology, Second Edition (Topics in Geobiology 28). Springer, Netherlands, Dordrecht.

Tyson, R.V., 1995. Sedimentary Organic Matter, Organic Facies and Palynofacies. Chapman and Hall, London, 615pp.

van Krevelen, D.W., 1993. Coal: Typology - Chemistry - Physics - Constitution, 3rd ed. Elsevier, The Netherlands.

Part III – Geography and Geology

5. **Geography and Geology**

This study was developed in Niassa province, northern Mozambique (Fig. 4). The African continent is made up of a set of cratons and mobile belts of archaic age. These cratons and belts were united by elongated and folded belts during Proterozoic-Cambric. A later event consisted of the coverage of these geological features by associated undeformed and extrusive rocks assigned to late Carboniferous-Early Jurassic, and Cretaceous to Quaternary (GTK Consortium, 2006). The Mozambican geology is characterised by the occurrence of crystalline basement assigned to Archaic-Cambric and rocks assigned to Phanerozoic. The study area comprises rocks from the Phanerozoic. The Phanerozoic setting in Mozambique includes all lithologies deposited following the Pan-African cycle orogeny. These are generally, continental to marine sediments and volcanic rocks. The Phanerozoic coverage is subdivided (from oldest to youngest) in Karoo Supergroup (KSG) and sequences deposited during the development of East African Rift System (GTK Consortium). According to the stratigraphic record, the Karroo Supergroup includes from the base to the top the following formations: Dwyka, Ecca, Beaufort, Stormberg, and Drakensberg (Catuneanu et al., 2005). The Stormberg is either magmatic or sedimentary whilst the Drakenskerg is magmatic (Catuneanu et al., 2005).

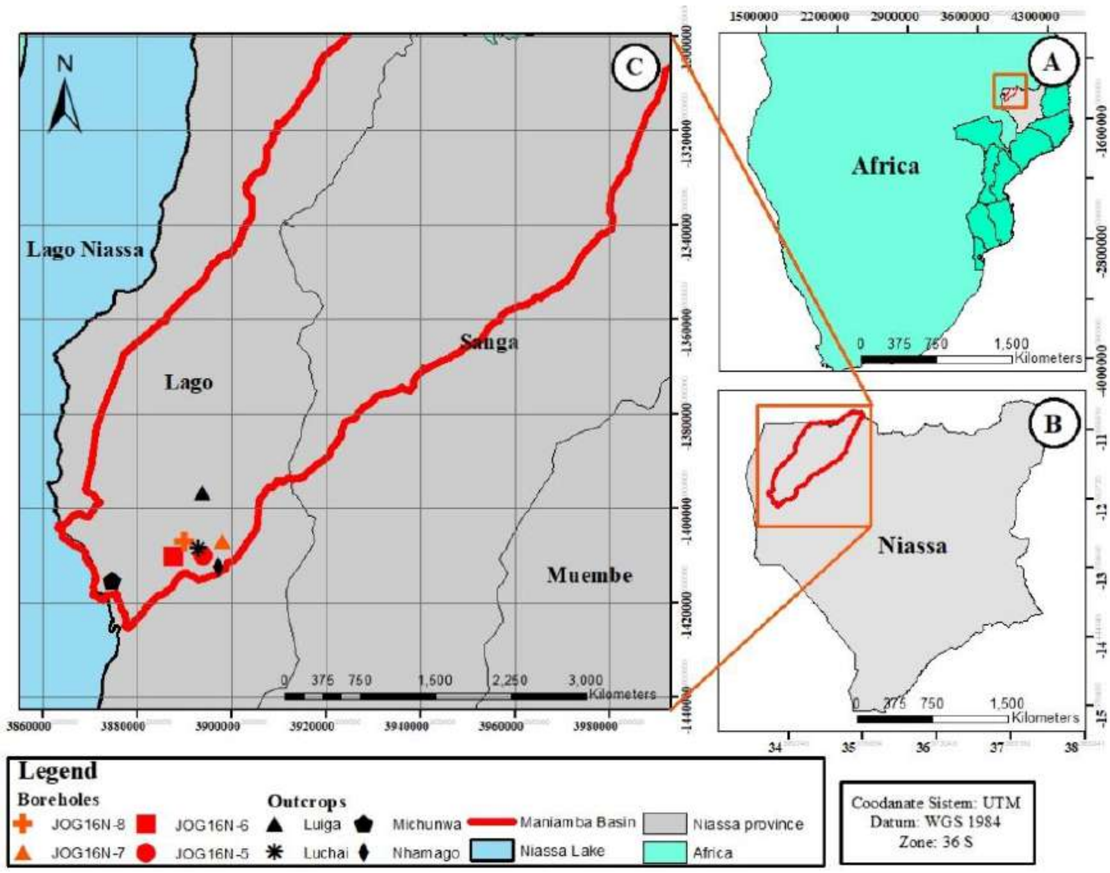

Figure 4. Geographical location of the Maniamba Basin.

It has been undoubtedly observed that almost all of the countries located in southern Africa have their geological framework contemporaneous with the Karoo Supergroup (KSG). The KSG in Mozambique, comprises igneous and sedimentary rocks overlying the Precambrian basement. Yet, the KSG is unconformably overlain by Middle Jurassic and younger rocks (Verniers et al., 1989; Norconsult Consortium, 2007). The KSG records the changes in facies from glaciogenic to temperate deltaic deposits that are found at the base. The aforementioned facies changed to fluvial/lacustrine, and at the top of the sequence more arid and continental facies are present (Verniers et al., 1989). The record of KSG sequences in Mozambique is restricted to basins that are regarded as being intracontinental and extensional (Fig. 5). Their formation has been suggested to have been influenced by existence of regions characterised by old crustal sutures in which structures derived from high-strain are linked to Pan-African Orogeny (620–530 Ma) (GTK Consortium, 2006). The sutures became reactivated during Early Permian to Early Jurassic due to lithospheric extension. This reactivation was responsible for driving subsidence which resulted in the formation of linear extensional basins morphology resembling half-graben to graben (GTK Consortium, 2006;

Norconsult Consortium 2007). Karoo coal-bearing rocks in Mozambique are illustrated in the figure 5, however, regarding palynology the Zambezi Valley Basin is the most studied (Pereira et al., 2016; 2019; Galasso et al., 2019; Fernandes et al., 2023 and others). The sub-basins pertaining to the Zambezi Valley are characterised by sedimentary and volcanic rocks assigned to Permian-Early Jurassic (GTK Consortium, 2006). Overall, the lithostratigraphic sequences of the KS in these basins are quite similar. Mainly, these basins consist of sandstone, mudstone together with significant layers of coal found at the base of the sequence. The aforementioned lithological sequence overlaps the glacial deposits (Afonso, 1975; Carvalho, 1977, Vasconcelos, 1995). Lastly, the Upper horizons of the KSG comprises volcanic rocks of bimodal pattern linked to the Karoo Igneous Province (Cox, 1992).

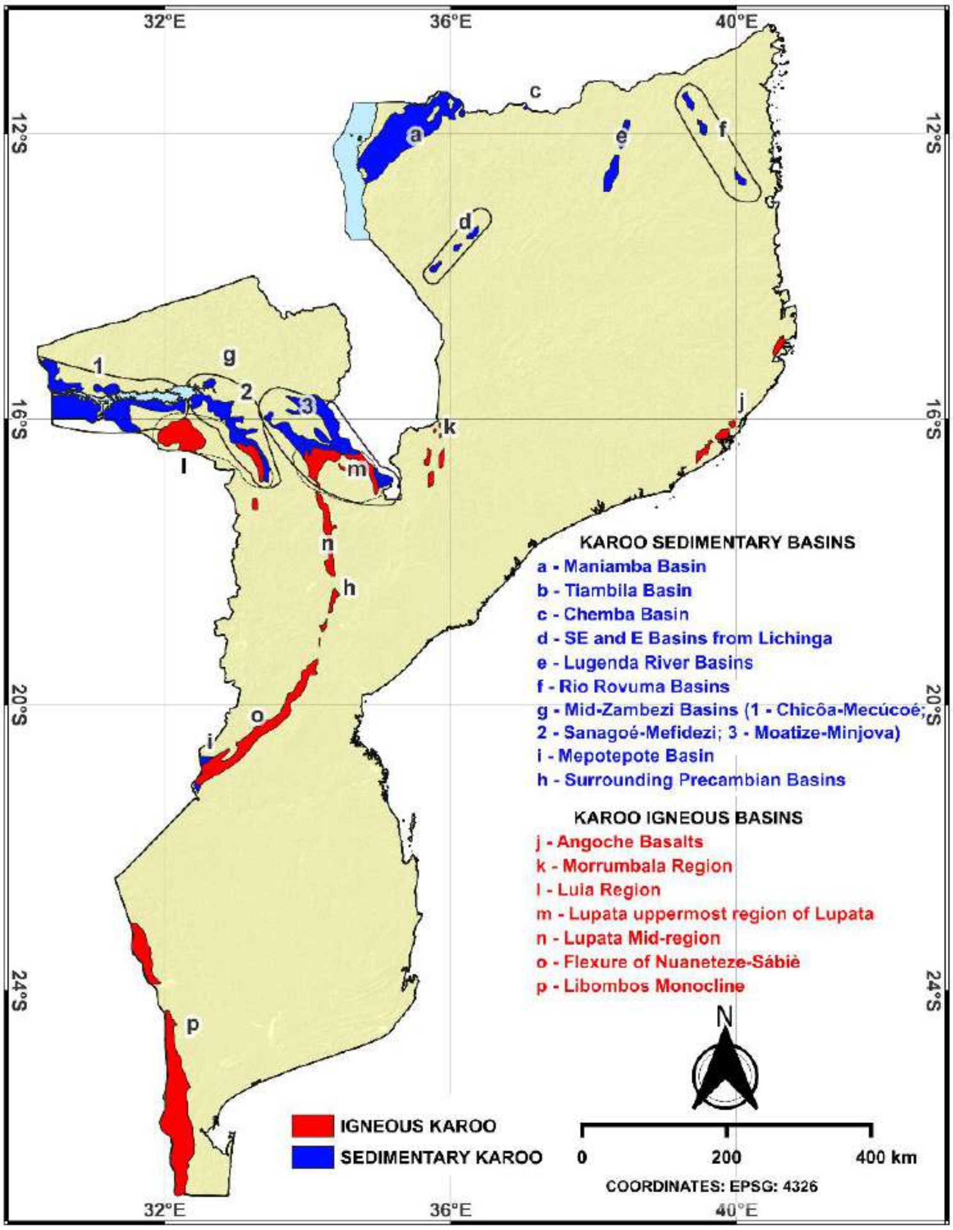

Figure 5. Map of sedimentary and igneous Karoo occurrences in Mozambique adapted from. Vasconcelos (2010).

5.1. Maniamba Basin

The Maniamba Basin lies within the Metangula Graben. The Karoo graben extends from South Africa to the coastal area of Kenya (Verniers et al., 1989). The Metangula Graben (Fig. 6) is subdivided into the following groups: Lower, Middle and Upper Karoo. The most comprehensive survey undertaken in the Basin was done by Jacques Verniers and colleagues from the “Brigadas de Cartografia Geológica da Bacia

Carbonífera de Metangula" from 1977 to 1980. According to them, the stratigraphy of the Maniamba Basin consists of Lower Karoo, which includes the K2, K3 and K4 formations. The Middle Karoo comprises two units, the K5 and K6 formations and the Upper Karoo consists of five units, KSa, KSb, KSc, KSd and KSe (Figs. 6 and 8). The description of each Karoo units is as follows:

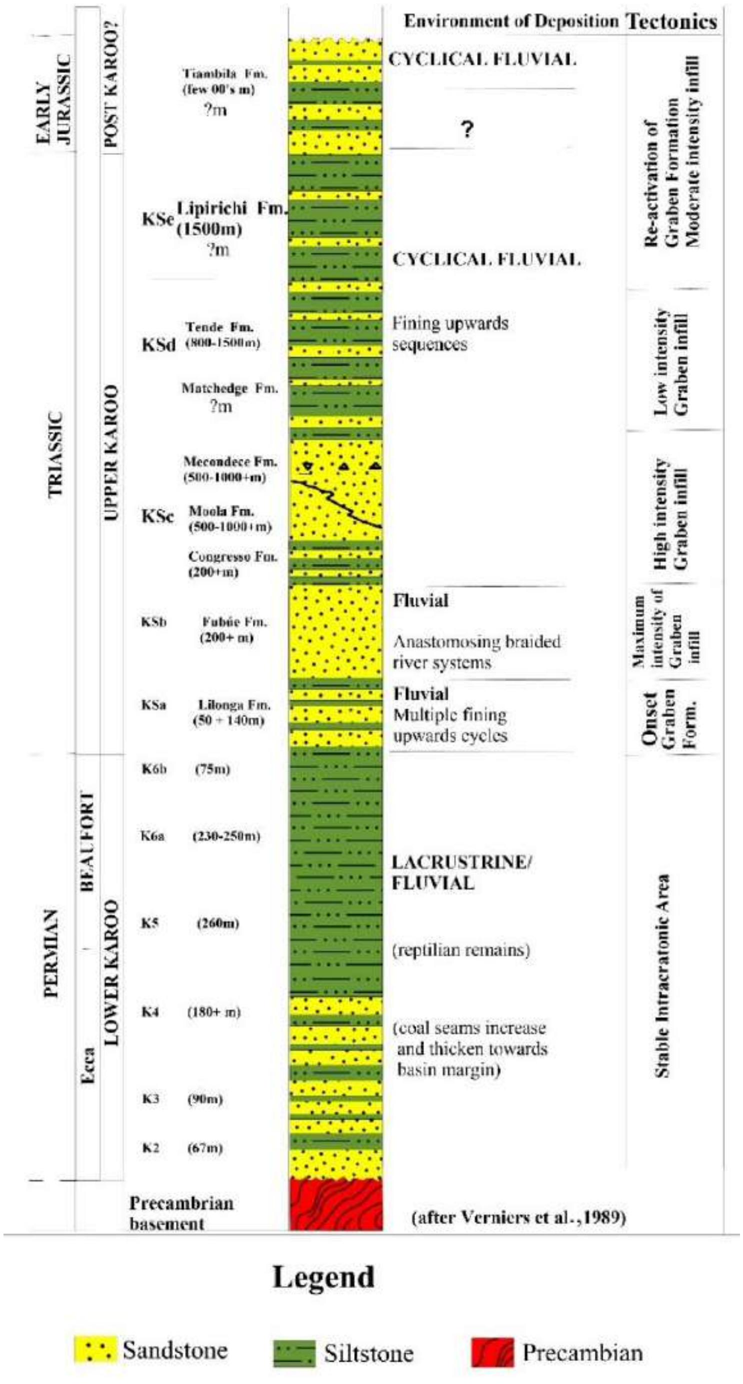

Figure 6. Stratigraphic sequence of the studied Basin adapted from Verniers et al. (1989).

5.1.1. Lower Karoo

Within the Lower Karoo, the K4 Formation was the main target. The K4 Formation (Lower Permian) comprises coal seams, carbonaceous intercalations and green, grey sandy siltstone. The palaeobotanical record is represented by *Glossopteris* leaves assigned to three different species: *Glossopteris ampla*, *G. browniana* and *G. indica* (Verniers et al., 1989). Furthermore, petrified material attributed to *Agathoxylon africanum* and *Prototaxoxylon uniseriale* occur and exhibit well-defined growth rings (Nhamutole et al., 2021). This Formation contains a thickness varying from 171 to 186 m.

5.1.2. Middle Karoo

The Middle karoo consists of two formations, K5 and K6 formations respectively. The K5 Formation is 250 to 260 meters thick and is subdivided into 3 members known as: K5a at the base, K5b in the middle, and then K5c on the top (Verniers et al., 1989; Araújo et al., 2020). The K5a member consists of dark grey, massive siltstones, minor tabular fine-grained sandstone. Araújo et al. (2020) suggest that the sedimentation occurred in well-drained and fully-vegetated river floodplains which is related to high-water tables (Araújo et al., 2020). In turn, the K5b member, generally consist of siltstones with fine to medium grain sizes, altering from dark to greenish grey. Several carbonaceous sediments are, however, observed in this member. Lastly, the K5c member contains rocks such as reddish grey, compact siltstone and claystone.

In its turn, the K6 Formation is divided into four members. The base is made up of the K6a1, K6a2, K6a3 members whereas the top only present one member, the K6b. A Permian age for the K6 Formation has been assigned based on the occurrence of *Glossopteris* leaves and vertebrate fossils (e.g., *Inostrancevia africana*). These fossil bones consist of fragmented skeletal and cranial elements of therapsids displaying a black colour (Araújo et al., 2020).

5.1.3. Upper Karoo

According to Verniers et al. (1989), the Upper Karoo units in the Maniamba basin are found in the central and northern part of the graben. This part of the Basin comprises the Lipirichi Formation (KSe), Tende Formation (KSd), Mecondece Formation (KSc), Fúbué Formation (KSb), Mount Lilonga Formation (KSb). In the present work, only outcrop samples from the KSb Formation were studied. The KSb Formation (Middle Triassic) conformably overlies the Mount Lilonga Formation (KSa, Early Triassic) (Araújo et al., 2020). The lithology of the Fubué Formation (KSb, Middle Triassic) consists of coarse-grained conglomeratic sandstones and the deposition of this unit seems to have occurred under a braided river system (Verniers et al., 1989). Typically, the thickness of the formation is up to 200 m.

In summary, the lower and middle Karoo in the Maniamba Basin were deposited in a cyclical fluvio-lacustrine environment differing from the upper Karoo graben. The formation and infilling of this graben occurred during the upper Karoo triggered by braided rivers and mostly by meandering rivers. These depositional environments broadly correspond with those of the MKB in South Africa where the Lower Karoo or Ecca Group environment was fluvio-deltaic and the Middle Karoo or Beaufort Group developed in more braided-stream environments (Catuneanu et al., 1998).

5.1.4. Kimberlite intrusions

Kimberlites occur in the MCB as dykes up to 3m thick. The kimberlite occurrences are reported along five zones (Fig. 7). One zone trends ENE-WSW and the remaining four zones trend NW-SE (Key et al., 2007) (Fig. 7). The presented trends of the kimberlites associated with their age indicate that their emplacement was mainly controlled by stress linked to Lower Cretaceous during the break up of Gondwana. This factor led to the dextral displacement of Madagascar with regard to mainland Africa. As a consequence, this stress reactivates the NW-SE and ENE-WSW trending bounding faults from the Karoo that host the kimberlites. Moreover, the shearing of dextral type along the bounding faults yielded fractures that were followed by infilling from kimberlite dykes (Key et al., 2007) (Fig. 7).

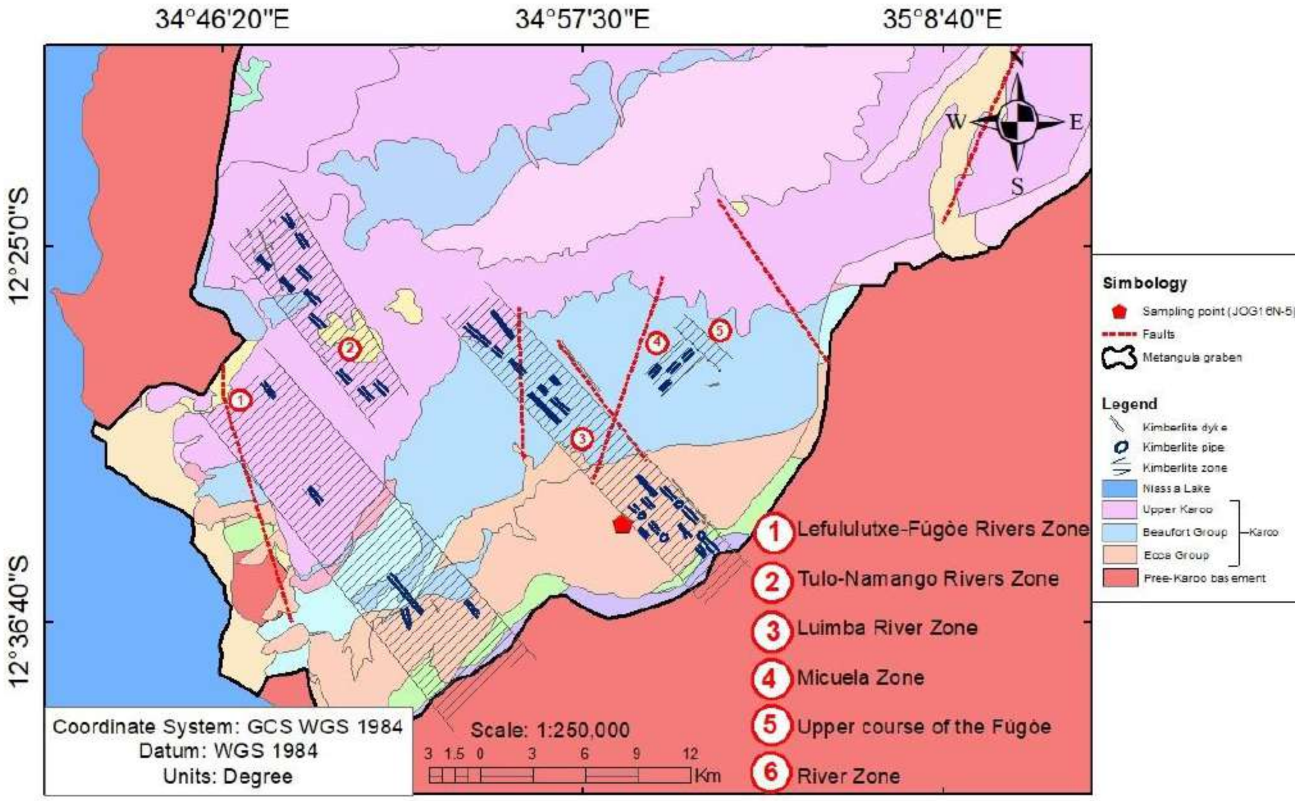

Figure 7. Geological map of the Maniamba Basin indicating the areas of occurrence of kimberlite intrusions adapted from (Key et al., 2007).

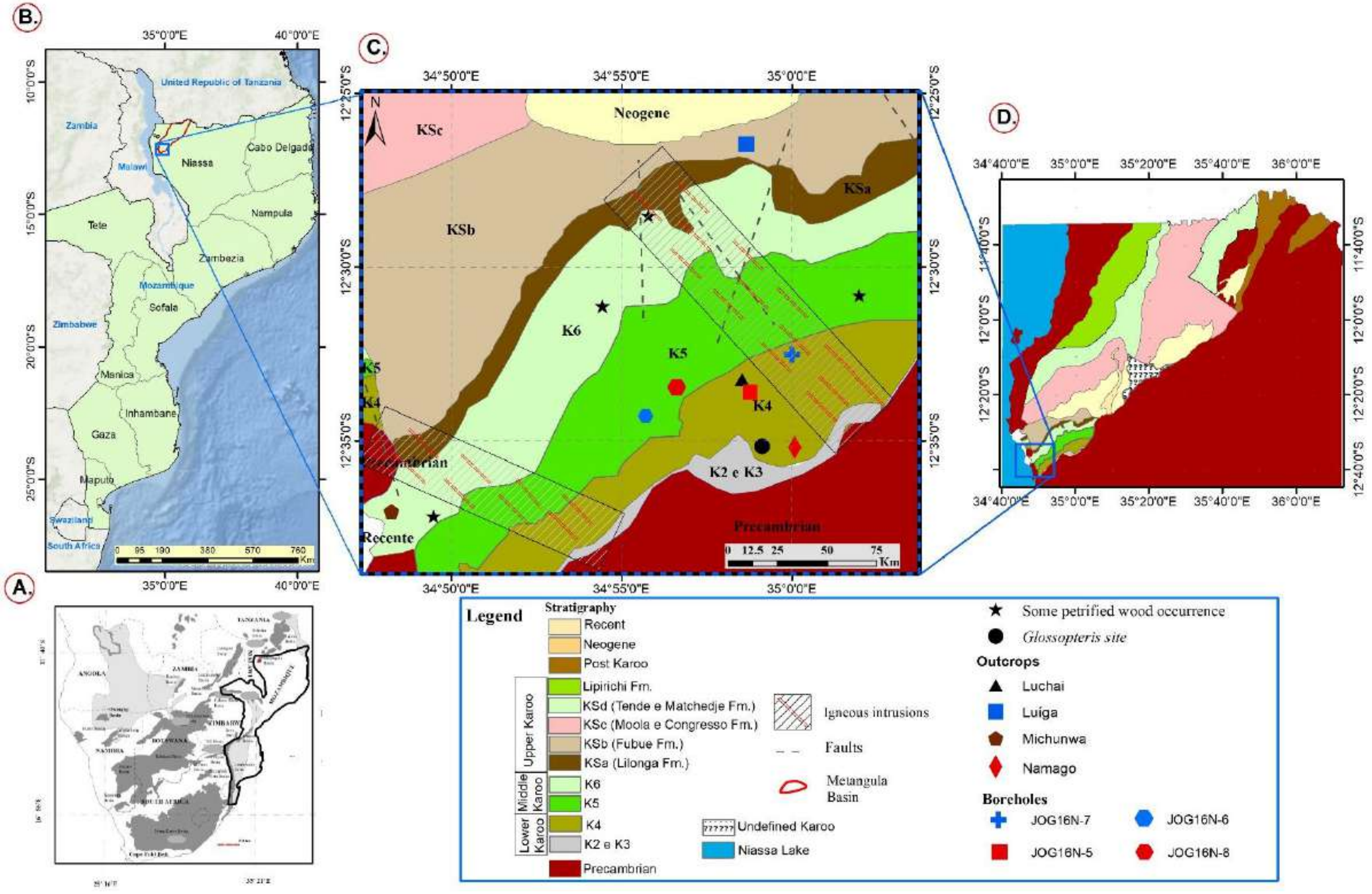

Figure 8. A. Southern Africa map illustrating the location of Mozambique, B. Map of Mozambique showing the location of the Maniamba Basin (Niassa), C and D. Geology and stratigraphy of the Maniamba Basin (modified from Verniers et al., 1989).

References

Afonso, R.S., 1975. Contribuição para o conhecimento da área de Tambara-Dôa (Folha Sul E-36, grau quadrado 1634). Boletim Serviços de Geologia e Minas, Lourenço Marques 38, 51–53.

Araújo, R., Macungo, Z., Smith, R., Tolan, S., Angielczyk, K., Crowley, J., Milisse, D., Mugabe, J., 2020. The first Lower Triassic tetrapod fossils from Metangula Graben (Niassa Province, Mozambique) and their biostratigraphic significance. Palaeontol. Afr. 54, 56–58.

Catuneanu, O., Wills, A.J., Mial, A.D., 1998. Temporal significance of sequence boundaries. Sediment. Geol. 121, 157-178.

Catuneanu, O., Wopfner, H., Eriksson, P.G., Cairncross, B., Rubidge, B.S., Smith, R.M.H., Hancox, P.J., 2005. The Karoo basins of south-central Africa. J. Afr. Earth Sci. 43, 211–253.

Carvalho, L.H.B., 1977. Formações vulcânicas de Carinde, Tete-Moçambique. Instituto Superior Técnico, Lisboa. Unpublished PhD Thesis. pp. 213.

Cox, K. G., 1992. Karoo igneous activity, and the early stages of the break-up of Gondwanaland. In: Storey, B. C., Alabaster, T. and Pankhurst, R. J. (eds.). Magmatism and the Causes of Continental Break-up. Geological Society Special Publication 68, 137-148.

Fernandes, P., Hancox, P., Mendes, M., Pereira, Z., Lopes, G., Marques, J., Jorge, R., Albardeiro, L., 2023. The age and depositional environments of the lower Karoo Moatize Coalfield of Mozambique: insights into the postglacial history of central Gondwana. Palaeoworld 33, 979–996.

Galasso, F., Pereira, Z., Fernandes, P., Spina, A., Marques, J., 2019. First record of Permo- Triassic palynomorphs of the N'Cond´ edzi sub-basin, Moatize-Minjova Coal Basin, Karoo Supergroup, Mozambique. Revue de Micropaleontol. 64, 100357.

GTK Consortium, 2006. Map explanation. Sheets 1631- 1934. Geology of Degree Sheets, Mecumbura, Chioco, Tete, Tambara, Guro, Chemba, Manica, Catandica, Gorongosa, Rotanda, Chimoio and Beira, Mozambique. Vol 2. Ministério dos Recursos Minerais, Direcção Nacional de Geologia, Maputo.

Lopes, G., Pereira, Z., Fernandes, P., Mendes, M., Marques, J., Jorge, R., 2021. Late Permian palaeoenvironmental evolution of the Matinde Formation in the Muar´adzi Sub-basin, Moatize-Minjova Basin, Mozambique. J. Afr. Earth Sci. https://doi.org/ 10.1016/j.jafrearsci.2021.104138.

Nhamutole, N.E., Bamford, M.K., Araújo, R., 2021. New species of *Protaxodioxylon* (conifer wood) from the middle permian of the Metangula graben (Niassa province, Mozambique) and their implications. J. Afr. Earth Sci. 183, 104323.

Norconsult Consortium., 2007. Notícia explicativa das áreas de Niassa, Cabo Delgado e partes de Zambézia e Nampula. Maputo, Moçambique: Direcção Nacional de Geologia. Unpublished report.

Pereira, Z., Fernandes, P., Lopes, G., Marques, J., Vasconcelos, L., 2016. The Permian– 685 Triassic transition in the Moatize–Minjova Basin, Karoo Supergroup, Mozambique: A 686 palynological perspective. Rev. Palaeobot. Palynol. 226, 1–19.

Pereira, Z., Fernandes, P., Lopes, G., Marques, J., Vaz, M., Costa, M., Correia, J., Castro, L., Galasso, F., 2019. Palynology of the Muara'dzi sub-basin, Moatize- Minjova Coal Basin, Karoo Supergroup, Mozambique. Rev. Palaeobot. Palynol. 269, 78–93.

Key, R.M., Bingen, B., Barton, E., Daudi, E.X.F., Manuel, S. and Moniz, A., 2007. Kimberlites in a Karoo graben of northern Mozambique: Tectonic setting, mineralogy and Rb-Sr geochronology. South African Journal of Geology, 110, 111-124.

Vasconcelos, L., 1995. Contribuição para o conhecimento dos carvões da Bacia Carbonífera de Moatize, Província de Tete, República de Moçambique. Ph.D. thesis. Faculdade de Ciências, Universidade do Porto, Porto, 231pp.

Vasconcelos, L., 2010. O carvão em Moçambique. In: Cotelo Neiva, J.M., Ribeiro, A., Mendes Victor, L., Noronha, F., Ramalho, M.M. (Eds.), Ciências Geológicas– Ensino e Investigação da sua História. Geologia das Ex-Colónias de África, Lisboa, Portugal, pp. 191–206.

Verniers, J., Jourdan, P.P., Paulis, R.V., Frasca-Spada, L., De Bock, F.R., 1989. The Karroo graben of Metangula northern Mozambique. J. Afr. Earth Sci. 9, 137–158.

Part IV - Methodologies and Samples

6. Materials and Methods

This part consists of a detailed description of the methodology used in the present project (Fig. 9). Bitumen and kerogen were analysed for a better characterization of the OM. In this research, palynology (stratigraphy), palynofacies, fluorescence analysis were performed at Evolutionary Studies Institute, University of the Witwatersrand, South Africa. Elemental analysis and XRD were performed in the Geology department, Eduardo Mondlane University, Mozambique. Rock Eval pyrolysis, vitrinite reflectance, palynology were performed at Federal University of Rio Grande do Sul, Porto Alegre (Brazil) between Laboratório de Palinologia Marleni Toigo and Núcleo dos Estudos de carvão e rochas geradoras de petróleo. Lastly, biomarkers (oil fingerprint) were undertaken in the Teresina Federal University (Organic Geochemistry laboratory) and Rio de Janeiro State University (Chemostratigraphy and Organic Geochemistry Laboratory).

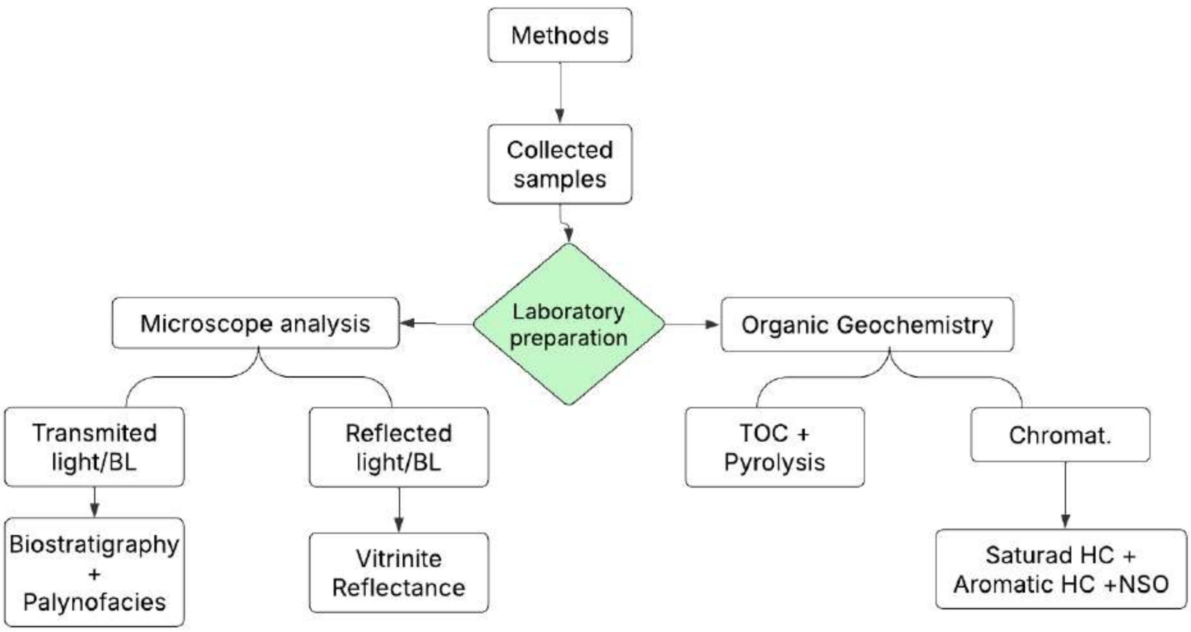

Figure 9. The main methods used to characterize the bitumen and kerogen in the present project. BL=Blue Light); TOC=Total Organic Carbon; HC=Hydrocarbon; NSO=Nitrogen, Sulfur and Oxygen (Polar); Chromat=Chromatography.

6.1. Organic Geochemical analysis

6.1.1. Pyrolysis rock eval analysis

The detailed geochemical analyses of the outcrop and borehole samples were carried out at the Núcleo de Estudos de Carvão e Rocha Geradora de Petróleo, Institute of Geosciences, Federal University of Rio Grande do Sul. Samples were sieved to pass mesh of 9 and 16µm and taken for Wildcat Technologies' HAWK Pyrolysis and Total Organic Carbon (TOC) analyses. TOC determines the petroleum potential or quantity of source rock. Rock Eval pyrolysis (Fig. 10), consists of heating the samples at elevated and programmed temperatures in an inert atmosphere (helium) in order to determine the type of kerogen, thermal maturity, and the transformation of the OM into petroleum and natural gas (Espitalié et al., 1977; Tissot and Welte, 1984). For analysis on the HAWK instrument, the samples were ground using a mortar and pestle to pass 60 mesh size and weighed to about 100 mg, after which they were pyrolysed in the HAWK for the following parameters: S1 (which represents the amount of free hydrocarbon liberated at 300º C without cracking the kerogen), S2 (the amount of hydrocarbon released from cracking of kerogen (mg HC/g rock) during temperature programmed pyrolysis (300 to 600º C), S3 (the amount of CO_2 from breaking oxygen-containing compounds in kerogen at 300 to 390º C)], and from the S2 peak, the Tmax values are obtained. The Tmax values represent the temperature at which the maximum generation of hydrocarbons from pyrolysis cracking of the kerogen occurs (°C). The interpreted parameters obtained from pyrolysis analysis are: Hydrogen Index (HI) (mg HC/ gTOC) and Oxygen Index (OI) (mg CO_2 /gTOC), which are related to the amount of oxygen and hydrogen respectively. The Production Index (PI) which characterises the level of maturation of the OM.

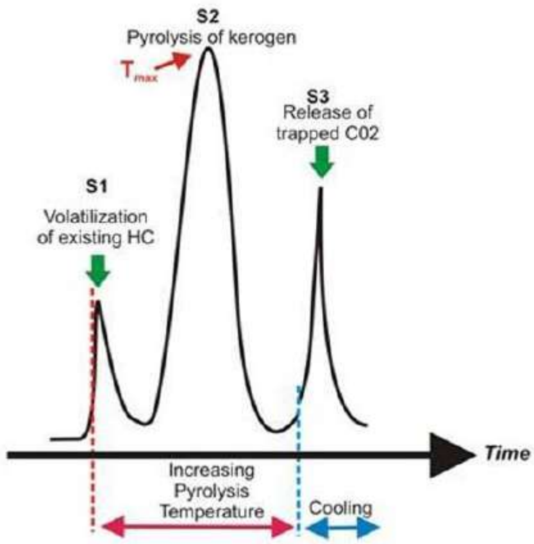

Figure 10. Diagram-Showing data from programmed Rock Eval pyrolysis modified from Tissot and Welte (1984).

6.1.2. Biomarkers

Gas chromatography (GC) together with mass spectrometry (MS) were used in order to obtain important insights regarding the biomarkers as it follows.

Extraction and fractionation of OM

The samples that underwent pulverization were kept in a desiccator with calcium chloride (CaCl2) to remove excess moisture for 24 hours before extraction. Approximately 20 g of pulverized rock were extracted with an aid of a Soxhlet based system to obtain the organic extract. For the removal of Sulphur around 500 mg of powdered metallic copper was added. Later on, occurred the filtration and evaporation of the extract and its placement into a glass bottle. The organic extracts obtained were then fractionated using column chromatography based on silica. The eluent-based system consisted on hexane (saturated), aromatics) and polar compounds.

Liquid Chromatography (LC) conditions

The extraction of soluble OM was done in a Soxhlet type extractor (250 ml). A chemical solvent, dichloromethane was used herein. The extracted bitumen undergone fractionation into saturated compounds, aromatics, resins, and asphaltenes compounds. The fractionation process occurred in a glass column (10 mm diameter/25 cm extension) together with a solid phase composed of silica gel (1/3) and alumina (2/3). A hexane mobile phase for extraction of the saturated compounds, a mixture of dichloromethane and hexane for the extraction of aromatic was part of the process.

Gas Chromatography-Mass Spectrometry (GC-MS) analysis conditions

The analysis of the saturated fractions was undertaken at a concentration of 2 mg mL 1. A gas chromatograph integrated to a Shimadzu spectrometer, model GCMS QP2010SE, equipped with an automatic sampler, model AOC-500. The separation based on chromatograph was carried out on a DB-5MS UI capillary column, 30 m × 0.25 mm, internal film thickness of 0.25 µm. The considered phase consisted of 5% diphenyl and 95% diphenyl dimethylpolysiloxane, following the standard procedures. The injector temperature was 290 °C in spitless mode and a volume of 1.0 µL of sample was injected. Helium gas (99.9%) with constant flow of 1.0 mL.min-1was used. The temperature of the interface was maintained at 320 °C. A full scan mode consisting of mass ranging from 57-600D was used in order to operate the quadrupole. However, a solvent cutoff of 4 minutes has also been considered herein. The source of the ion was operated at a temperature of 230 ºC. The energy of ionization used was around 70 eV.

6.2. Palynology

For palynological preparation standard methods adapted from Phipps and Playford (1984) and Traverse, (2007) were performed. Briefly, the techniques consisted at multiple treatments of the samples with hydrochloric (HCl) and hydrofluoric (HF) acids in order to eliminate the fraction of carbonates and silicates. The concentrated fraction without carbonates and silicates was thereafter sieved through a 10µm mesh. The aforementioned step preceded the mounting of permanent slides. The prepared slides are housed in the Evolutionary Studies Institute, Faculty of Sciences, University of the Witwatersrand, South Africa. The study of the slides was based on the qualitative (identification of organic components) and quantitative (abundance based on counting) under transmitted white light with a petrographic microscope. For precise qualitative interpretation, the preservation state of particulate components was taken into consideration.

6.2.1. Palynofacies and Spore Colour Index (SCI)

During laboratory analysis, each sample was crushed and treated with hydrochloric acid and hydrofluoric acid. The treatment with acids aimed at removing carbonates and silicates respectively (Tyson, 1995). Neutralisation occurred between the addition of each acid, and consisted with the addition of distilled water and centrifugation at 300 rpm for 5 min. The concentrated residues were then sieved through a 10 µm nylon mesh and subsequently mounted on glass slides with glycerine jelly. The palynofacies study was based on the counting of 300 kerogen components per slide and their identification under a transmitted light microscope (Zeiss® Axioskop microscope), at 200x magnification. Here, should be stressed that fluorescence mode was used when needed for particle identification. The OM groups were identified, and classified following Tyson (1995) and Filho et al. (2002). The data generated by counting of the organic components as previously described were used for statistical treatment. The absolute data for each variable were recalculated for percentage values for interpretation of relative abundance through the studied section. In order to identify similarities amongst the variables and determine the palynofacies assemblages in the studied successions, a cluster analysis was performed using Q-mode. Additionally, paleotemperatures reached by the sediments were assessed with an aid of well-established Spore Colour Index (SCI). Some of the useful palynotaxa included non-striate bisaccate pollen, *Scheuringipollenites maximus* and monolete spores, *Laevigatosporites plicatus*.

6.2.2. Biostratigraphy

The microphotographs were taken in transmitted light mode Zeiss Axioskop coupled with Olympus DP72 camera and Stream Essentials® software. Counting of three hundred (300) grains was undertaken per slide under 400x magnification in order to yield qualitative and quantitative data. Each palynomorph was analysed qualitatively by using the selected references for identification and classification of species. The identified palynomorph association was then compared with existing and published biozones, allowing thus the age constraints for the investigated units (e.g., Balme, 1980; Barbolini et al., 2018; Aggarwal et al., 2019; Pereira et al., 2019; Galasso et al., 2019 and other references included therein). For floral and palaeoenvironment inferences, palynological categories as described by Lindström and McLoughlin (2007) were used.

6.3. Organic Petrography

6.3.1. Vitrinite Reflectance

The collected samples from cores and outcrops were pulverized and followed by isolation of kerogen from bitumen. The latter process has consisted on the use of SOXTEC™ 2050 equipment, dichloromethane and methanol during 2-4 hrs. Later on, acidification process was performed aimed at removing silicates and carbonates. The measurements of Vitrinite reflectance were conducted on polished concentrated kerogen samples in order to make a precise determination of the thermal variability. The vitrinite was measured using a reflected light microscope (LEICA DM6000 M), a Discus-Fossil software with a magnification of 200x for coals and 500x for shales. During different stages, the calibration of the microscope occurred with aid of an aluminium-garnet with known reflectance of 0.895. It should be highlighted that the sample preparation followed the Standard procedures outlined by Vandenbroucke and Largeau (2007) as well as by the American Society for Testing and Materials (ASTM) D2797 (ASTM D7708-11, 2011).

The laboratory procedures were undertaken at the Núcleo dos Estudos de Carvão e Rochas Geradoras de Petróleo, Federal University of Rio Grande do Sul (UFRGS) Porto Alegre, Brazil.

6.4. Elemental analysis

This proxy is frequently used as aid for a detailed typification of kerogen. The kerogen typification is obtained through a van Kravelen diagram which combines H/C in the y axis and O/C ratios in x axis (Espitalie et al., 1977; Lafargue et al., 1998). Here, elements comprising, carbon, nitrogen, hydrogen, oxygen, and sulphur are analysed.

For these analyses only eight samples were chosen. The samples underwent a spraying process on a porcelain in order to proceed with acidification. The acidification process was aimed at removing the carbonates through washing the samples using hydrochloric acid. The obtained solution was then submitted for neutralization with distilled water followed by drying process and proper analysis. The mixture of 40 mg per sample with 89 mg of tungsten has been performed. The data are displayed as percentages of the analysed elements including the ash and oxides contents.

6.5. X-Ray diffraction (XRD)

X-ray diffractometry (XRD) is applied in several fields such as material sciences, mineral processing, petroleum research and others. For XRD analysis, 1 g of powder sample was used and prepared as pressed pellets, analysed as bulk, unoriented samples. The diffraction X-rays are produced when a monochromatic X-ray source hits the flat surface of samples. The diffractogram follows Bragg's law for calculating the resulting diffraction angle, which is phase-dependant. The quantification of phases is carried out by the Rietveld method. The specific directions appear as peaks on the diffraction pattern called reflections. The measured data are compared with the theoretical single-phase diffractogram for phase identification.

6.6. Samples

For the present research four boreholes drilled by JOMEC in the Maniamba Basin were subsampled. All the boreholes are located in the southwestern section of the Basin (Fig. 11). The studied material represents a frontier area where no hydrocarbon research has ever been carried out.

The studied cores were provided by MIREME including permission for publication of data. The geological description of each borehole is including in the different publications in section in the discussion section. Other samples used in this study were obtained from four outcrops. The collection of the samples in these outcrops resulted from previous field expeditions in which the process of sampling was entirely based on the degree of preservation. For sampling, the outermost parts of the outcrop were discarded as they are more likely to be either oxidized or contaminated with organic debris. A few hundreds of grams were sampled from outcrops in most cases. Samples were then, labelled and bagged to avoid cross contamination. Geological structures such as fractures and other penetrating surfaces were avoided as these represents preferential weathering “spots”. In addition, during the process of sampling, GPS coordinates and other relevant information such as lithology, colour, sedimentary structures, locality, were also recorded.

Both outcrops and cores we integrated in order to cover the maximum of stratigraphical units. The table below provides information regarding the selected boreholes and outcrops.

Table 6 Main information regarding the studied samples.

Borehole/Outcrops	**Drilling company**	**Number of samples**	**Depth (m)**	**Formation/Age (This study)**
JOG16N-5	JOGMEC	65.0	213.0	Late Permian
JOG16N-6	JOGMEC	39.0	318.0	Late Permian-Early Triassic
JOG16N-7	JOGMEC	64.0	279.0	Late Permian
JOG16N-8	JOGMEC	69.0	356.0	Late Permian-Early Triassic
Luiga	Field work	5.0	25.0	Late Permian-Early Triassic
Luchai	Field work	5.0	9.0	Middle Permian
Nhamago	Field work	5.0	8.0	Middle Permian
Michunwa	Field work	5.0	7.5	Undetermined

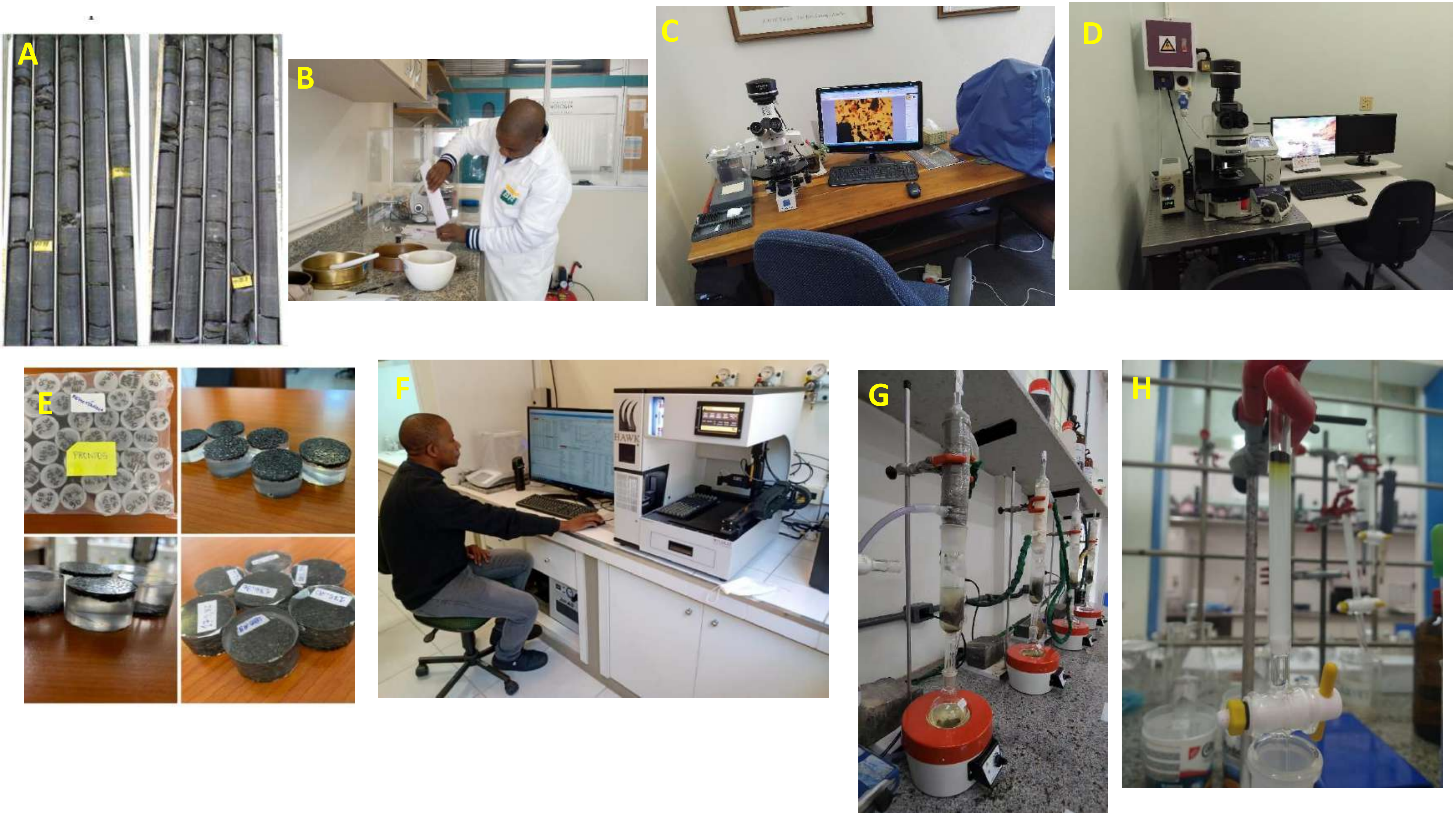
A
B
C
D
E
F
HAWK
G
H

Figure 11. Laboratory analysis performed during the present study. A. some subsampled cores from the Maniamba Basin. B. Preparation of samples for palynological processing, vitrinite analysis, and Rock Eval simulations. Microscope used during counting of slides for palynofacies analysis, and biostratigraphy D. Fluoresce microscope used for assessing hydrocarbon potential. E. Plugs prepared for vitrinite reflectance measurements. F. Rock analysis simulation using Rock Eval-6. G and H. Biomarker analysis (Chromatography).

References

Aggarwal, N., Agrawal, S., Thaku, B., 2019. Palynofloral, palynofacies and carbon isotope of Permian coal deposits from the Godavari Valley Coalfield, South India: Insights into the age, palaeovegetation and palaeoclimate. Inter. J. Coal Geol. https://doi.org/10.1016/j.coal.2019.103285.

ASTM D7708-11., 2011. Standard Test Method for Microscopical Determination of the Reflectance of Vitrinite Dispersed in Sedimentary Rocks: Annual Book of ASTM Standards: Petroleum Products, Lubricants, and Fossil Fuels, Gaseous Fuels, Coal and Coke. Sec. 5. V. 5.06. ASTM International, West Conshohocken, PA, pp. 823–830.

Balme, J., 1980. Palynology, and the Carboniferous-Permian boundary in Australia and other Gondwana continent. Palynol. 4, 43–55.

Barbolini, N., Rubidge, B., Bamford, M.K., 2018. A new approach to biostratigraphy in the Karoo retroarc foreland system: Utilising restricted-range palynomorphs and their 558 first appearance datums for correlation. J. Afr. Earth Sci. 140, 114–133.

Espitálie, J., Madec, M., Leplat, P., 1977. Source rock characterization method for petroleum exploration: Proceedings of the Ninth Offshore Technology Conference, Houston, 439-442.

Filho, J.G.M., Carvalho, M., Menezes, T., 2002. Palinofácies. In: Dutra, T.L. (Ed.), Técnicas e Procedimentos para o Trabalho com Fósseis e Formas Modernas Comparativas, pp. 20–24. Unisinos, São Leopoldo.

Galasso, F., Pereira, Z., Fernandes, P., Spina, A., Marques, J., 2019. First record of Permo-Triassic palynomorphs of the N'Condédzi sub-basin, Moatize-Minjova Coal Basin, Karoo Supergroup, Mozambique. Revue de Micropaléontologie 64, 100357.

Lafargue, E., Marquis, F. Pillot, D., 1998. Rock-Eval 6 applications in hydrocarbon exploration, production and soil contamination studies. Oil and Gas Science Technology 53, 421-437.

Pereira, Z., Fernandes, P., Lopes, G., Marques, J., Vaz, M., Costa, M., Correia, J., Castro, L., Galasso, F., 2019. Palynology of the Muara´dzi sub-basin, Moatize-Minjova Coal Basin, Karoo Supergroup, Mozambique. Rev. Palaeob. Palynol. 269, 78–93.

Tissot, B., Welte, D.H., 1984. Petroleum Formation and Occurrence, second ed. Springer Verlag, Heldelberg, 699pp.

Traverse, A., 2007. Paleopalynology, Second Edition (Topics in Geobiology 28). Springer, Netherlands, Dordrecht.

Tyson, R.V., 1995. Sedimentary Organic Matter, Organic Facies and Palynofacies. Chapman and Hall, London, 615pp.

Vandenbroucke, M., Largeau, C., 2007. Kerogen origin, evolution and structure. Org. Geochem. 38, 719–833. https://doi.org/10.1016/j.orggeochem.2007.01.001.

Part V-Results and Discussion

Chapter One

Palynofacies analysis of the JOG16N-8 borehole, K5 Formation from the Maniamba Basin (middle Permian), Mozambique: A contribution for Hydrocarbon exploration.

Adapted from Nelson E. Nhamutole, Marion K. Bamford, Paulo. A. Souza, Dermeval A. Carmo

Published by Journal of African Earth Sciences

Journal of African Earth Sciences 205 (2023) 104997

Contents lists available at ScienceDirect

Journal of African Earth Sciences

journal homepage: www.elsevier.com/locate/jafrearsci

Palynofacies analysis of the JOG16N-8 borehole, K5 formation from the Maniamba Basin (middle Permian), Mozambique: A contribution for hydrocarbon exploration

Nelson E. Nhamutole [a,b,*], Marion K. Bamford [a], Paulo A. Souza [c], Dermeval A. Carmo A [d]

[a] Evolutionary Studies Institute and School of Geosciences, University of the Witwatersrand, P Bag 3, Wits, 2050, Johannesburg, South Africa
[b] Museu Nacional de Geologia, Av. 24 de Julho, 355, Maputo, Mozambique
[c] Laboratório de Palinologia Marleni Marques Toigo, Instituto de Geociências, UFRGS, Brazil
[d] Laboratório de Micropaleontologia da Universidade de Brasília, Brasília, DF, Brazil

Abstract

The Maniamba Basin in Mozambique is surveyed mainly in regard to coal exploration. However, this basin is also known for containing well preserved fossil plants and vertebrate fossils that shed light to the understanding of Gondwana ecosystems. Nevertheless, organic matter analysis (palynofacies) and its implication for depositional environment and hydrocarbon source rock have not yet been performed. Here, we report for the first time in the Maniamba Basin, results from palynofacies analysis combined with thermal maturation and kerogen typification. Palynofacies analysis was applied on 69 samples from the sediments of the JOGN16N-8 borehole, K5 Formation (middle Permian). The results indicate that sediments are dominated by phytoclasts with less abundant sporomorphs and sparse amorphous organic matter (AOM). Three palynofacies were identified suggesting depositional settings in a general proximal and oxic lacustrine-fluvial deltaic environment. The dominance of opaque phytoclasts may be due to wildfires, oxidation conditions before or post deposition in proximity to terrestrial settings and an environment under obliquity cycle-controlled monsoon climate. The organic matter composition combined with Spore

Colour Index (SCI), pointed out the existence of an abundant type IV kerogen followed by type III in immature phase suggesting very little or no potential for gas exploration. Very few horizons suggest the existence of kerogen type II. This study, gives significant information for better understanding of the variation of organic matter, palaeonvironment and source rock potential of the studied area.

1. Introduction

Coal, oil and gas reserves are an important source of energy although their consumption is detrimental to the environment. Until sufficiently cost-effective and environmentally friendly resources become obtainable, these fossil fuels will continue to be used. Mozambique is no exception and as a developing country it is reliant on fossil fuels for internal use as well as export.

Mozambique, on the eastern side of southern Africa, was part of Gondwanaland and comprises several large basins with Permian-aged coal deposits. Although the basins can be correlated generally with the Main Karoo Basin, the underlying topography, local palaeoenvironmental conditions, faulting and erosion, have affected the coal seam thicknesses, coal quality, maturity and oil and gas potential which varies between basins (Vale, 2014, JOGMEC, 2015; Paz, 2018). Until now, research has focussed on the Rovuma and Mozambique Basins, while the Maniamba Basin has received little attention. The Maniamba Basin has been regarded as vitally importance for the understanding of the flora and fauna of this portion of Gondwana (e.g., Castanhinha *et al*., 2013; Araújo *et al*., 2020; Macungo *et al*, 2020; Nhamutole *et al*., 2021).

Palynological research in the Maniamba Basin’s Karoo-aged deposits has been scarce. The existing studies were only focused on the classical palynostratigraphic aspect (De Bock and Verniers, 1984; Verniers *et al*., 1989) aimed at refining the stratigraphy of the Maniamba Basin based on correlations with other Gondwana basins. More importantly, several works have been undertaken on the coal quality and geology of the Maniamba Basin (Amaro, 1950; Borges *et al*., 1950; Vincente *et al*., 1950; De Bock, 1983). Surprisingly none of the studies carried out to date has aimed at understanding the organic matter composition of the Maniamba Basin although this proxy has been recently undertaken in some Karoo equivalent areas in the Tete province, centre of Mozambique (Costa *et al*., 2016; Gotz *et al*., 2017; Vaz, 2017). The organic matter composition forming the basis of palynofacies studies has been used widely with the integration of other proxies to yield a more robust interpretation of the environmental deposition, such as the proximal-distal relationship with regard to source, oxic open marine, dysoxic-anoxic, brackish freshwater, as well as the hydrocarbon-generating potential (e.g., Batten, 1996; Tyson, 1995; El Beialy *et al*., 2008; Zobaa *et al*., 2012; Raafat *et al*., 2021,). This approach relies on the organic matter isolation through laboratory standardized procedures in conjunction with microscope techniques for acquisition of data, statistical treatment and its interpretation. Here, a detailed palynofacies study based on organic matter composition of a middle Permian borehole from Mozambique consisting of clay-coal-sandstone-mudstone-siltstone is presented. This is the first palynofacies study to be carried out in this basin. The study was undertaken aimed at improving our understanding regarding the organic matter variation and its contribution to the depositional environment and source rock for the K5 Formation in the Maniamba Basin.

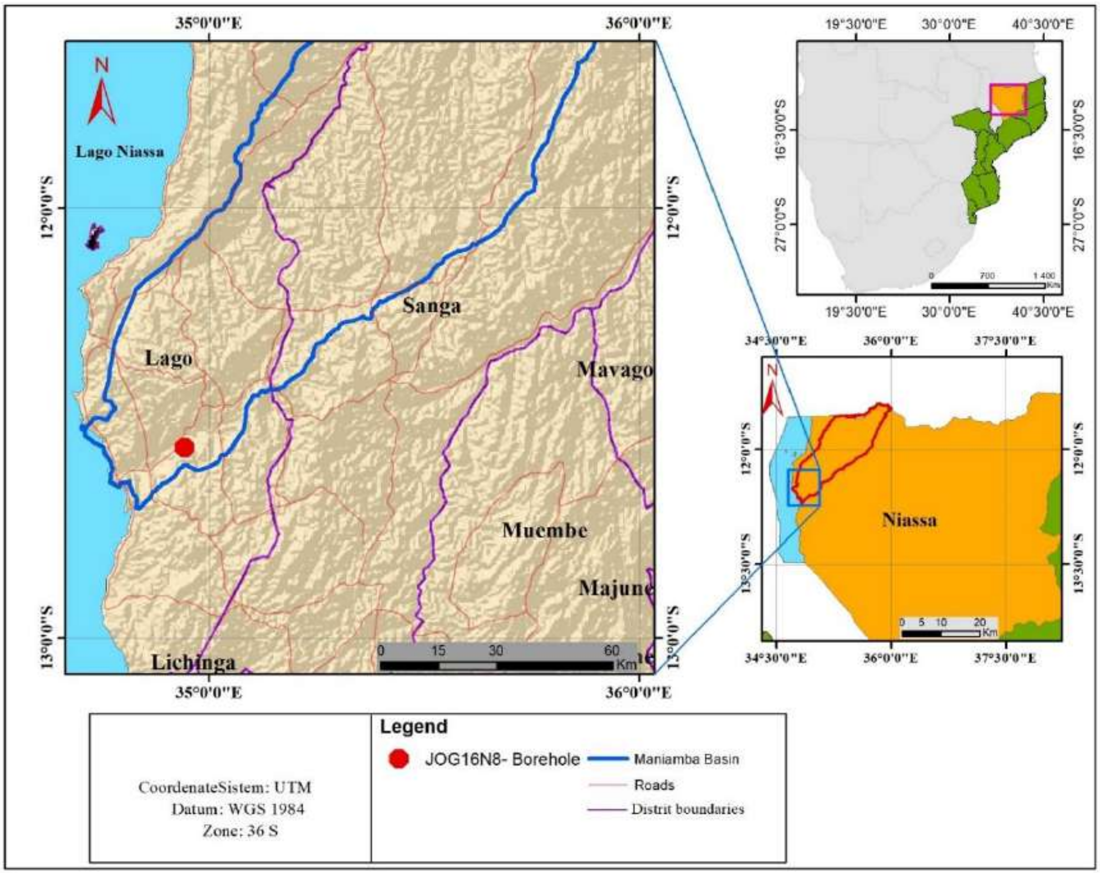

Fig. 1. Geographic map of the studied area.

2. Geographic Location and Geological setting of the Maniamba Basin

For a detailed description regarding geography and geology of the study are, please see section 5.0 and 5.1.

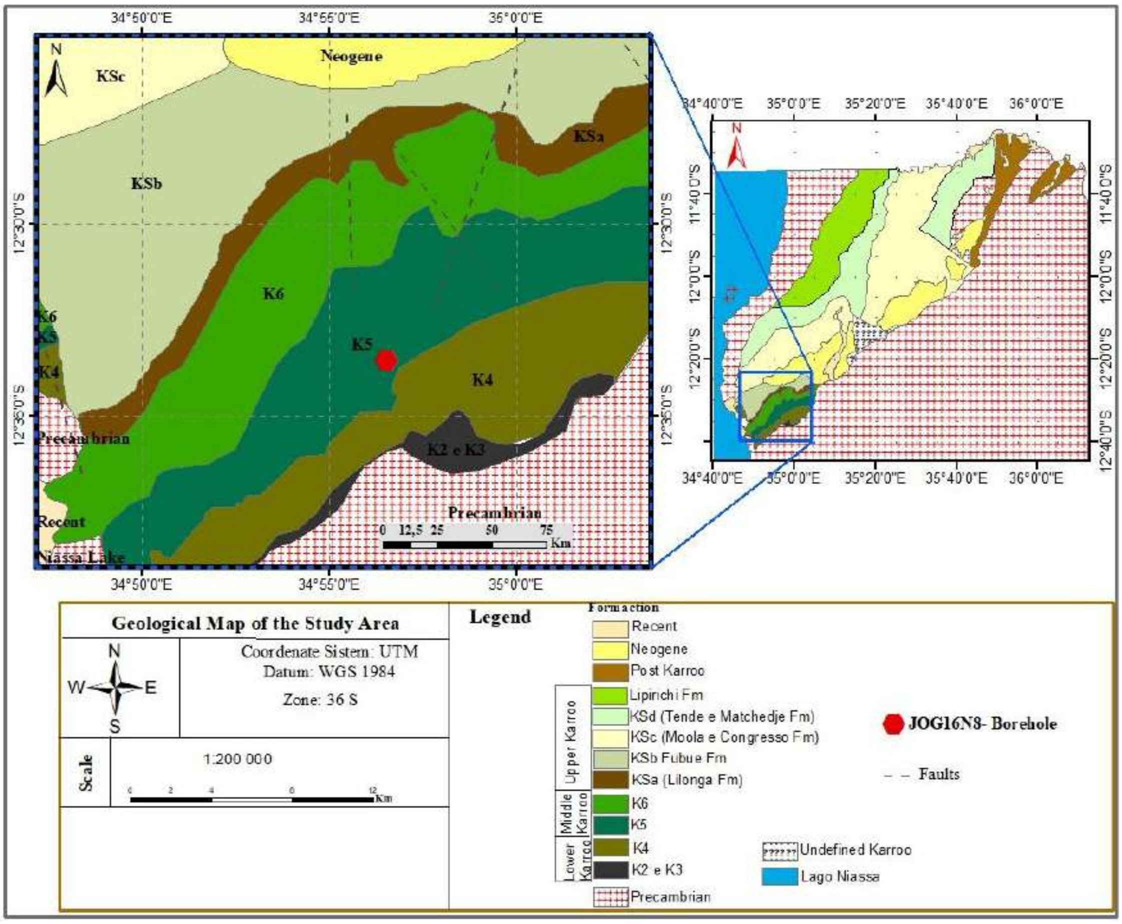

Fig. 2. Geological Map of the Maniamba Basin, Mozambique (Adapted from Verniers et al., 1989).

3. Materials and Methods

3.1 Sampling

This study was carried out on a total of 69 samples collected from a borehole core JOG16N-8 (360 m) from the K5 Formation (Middle Permian) in the Maniamba Basin, Niassa, Northern Mozambique. The drilling was done by JOGMEC (Japanese Oil, Gas, and Metals National Corporation) and permission to sample the core was obtained from Direcção Nacional de Geologia e Minas (Ministry of Mineral Resources and Energy, Mozambique). The procedure used for the study including palynofacies, thermal analysis is found in section 6.2.

Table 1 Palynofacies data of the JOG16N-8borehole, K5 Formation, Maniamba Basin, Mozambique. The barren samples were excluded in the table.

Depth (m)	**% Palynomorphs**					**% Phytoclasts**									**% Amorphous Organic Matter (AOM)**	
	Pollen grains		**Spores**			**Non-opaque phytoclasts (Biost. & non-biost.)**						**Opaque phytoclasts**				
	% Monos.	%Bis.	%Al.	%Monol.	%Tri.	% Biost.	%Non-biost.	%Cut.	%Memb.	%Cort.	%Fungal hyphae	%Eq.	%El.	%Cor.	%Res.	%AOM
106.4	0	0	0	0	0	12.33	0	0	0	0	0	16.0	11.0	55.67	0	5.0
106.62	0	0	0	0	0	20.33	5.67	0	0	0	0	9.67	11.0	43.67	0	9.67
106.96	0	0	0	0	0	14.33	0	0	0	0	0	10.0	13.33	56.33	0	6.0
107.25	0	0	0	0	0	41.0	6.67	0	0	0	0	6.67	9.0	29.33	0	7.33
107.52	0	0	0	0	0	0	0	0	0	0	0	23.0	13.0	51.67	0	12.33
107.77	0	0	0	0	0	2.33	1.67	0	0	0	0	0	17.0	70.0	0	9.0
108.02	0	0	0	0	0	0	0	0	0	0	0	0	9.67	82.33	0	8.0
108.33	0	0.6	0	0	0	4.33	1.33	0	0	0	0	0	8.67	84.67	0	0.33
108.89	1.3	0	0	0	0	13.0	7.0	0	0.33	0.11	0	12.0	12.0	48.67	0	5.67
109.14	1.0	0	0.3	0	0	3.0	0	0	0	0	0	0	15.0	73.67	0	7.0
109.71	0.3	0	0	0	0	16.67	1.0	0.67	0	0	0.3	12.33	10.33	43.0	0	15.0
110.13	0	0	0	0	0	13.67	0	0	0	0	0	15.0	6.67	60.33	0	4.33
110.29	0	0	0	0	0	9.0	0	0	0	0	0	15.0	9.33	63.33	0	3.33
110.8	0	0	0	0	0	0	0	0	0	0	0	0	11.0	86.67	0	2.33
111.33	0	0	0	0	0	5.33	1.0	0.33	0	0	0	8.0	18.0	64.33	0	3.0
118.57	37.3	0	0	0	0.33	3.67	0	0.33	0	0	0	14.0	16.67	15.0	0	12.67
118.79	54.6	0.3	0	0.3	0	3.0	0.33	0	0	0	0	0	3.67	37.67	0	0
119.08	0	0	0	0	0	5.0	1.33	0.33	0	0	0	12.0	37.33	38.33	0	5.67
119.49	0	0	0	0	0.33	5.33	2.0	0	0	0	0	13.0	33.0	42.0	0	4.67
119.8	0	0	0	0	0	0.33	0	0	0	0	0	0	15.0	84.33	0	0.33
120.16	2.3	0	0	0	0	19.33	4.33	0	0	0	0	14.0	13.33	41.33	0	5.33
120.26	4.0	0	0	0	0	20.33	3.67	1.0	0.33	0.11	0	0.67	6.0	58.33	0	5.67
120.51	32.0	0.3	0	0.3	0	4.33	0.33	0.33	0.33	0.11	1.3	0	11.33	47.0	0.33	2.0
120.73	39.0	0.6	0.3	0	0.33	8.67	1.0	0	0	0	1.0	1.0	7.33	39.33	0	1.33
121.11	4.0	0	0.3	0	0	1.0	0	0.33	0.33	0.11	0.7	0	8.0	83.33	0	2.0
130.524	7.0	0	0	0	0	14.33	9.33	2.33	0	0	1.3	1.0	6.67	55.00	0	3.0

131.784	0	0	0	0	0	0	0	0	0	0	0	0	11.0	86.67	0	2.33
142.163	32.3	0	7.3	2.6	3.33	6.67	1.0	0	0	0	0.3	1.67	9.0	30.00	0	5.67
146.243	38.0	0.3	1.3	6.0	1.67	9.33	5.67	0	0	0	0.7	0	17.0	16.33	0	3.67
151.432	33.0	0	0	0	1.0	10.0	4.0	0	0	0	0	1.67	13.0	30.67	0	6.67
163.449	36.3	2.3	0.3	0.3	2.0	6.0	2.33	0	0	0	0.3	1.0	14.0	30.67	0	4.33
168.424	48.6	0.6	0	3.3	0.33	6.33	2.0	0	0	0	1.7	2.0	8.0	23.33	0	3.67
168.964	35.0	0	0	0.3	0	22.0	5.0	1.33	0	0	0	6.67	14.0	11.00	0	4.67
175.424	45.0	0.3	2.0	2.0	0	15.0	0.67	0	0	0	0.7	0.33	8.33	21.67	0	4.0
184.728	3.0	0	0	0	0	10.67	5.67	1.33	0	0	0.3	0.67	7.33	66.33	0	4.67
185.238	1.0	0	0	0	0	18.0	8.33	1.33	0	0	0	3.0	15.0	47.00	0	6.33
190.04	51.6	0	0	0	0	3.67	0	0.33	0	0	2.7	0	7.0	30.00	0	4.67
190.194	34.3	1.0	0	0.3	0.33	13.67	1.33	0.33	0	0	1.0	0.67	6.0	35.67	0	5.33
194.684	2.0	0.3	0	0	0	17.33	2.0	0	0	0	0.3	2.67	9.33	59.67	0	6.33
195.464	59.0	0.3	0	0.3	0	2.67	0	0	0	0	0.7	0	4.67	28.33	0	4.0
199.609	0	0	0	0	0	2.67	0	0	0	0	0	0	9.33	78.00	0	10.0
242.659	11.6	5.3	0	0	0	19.67	8.67	0.33	0	0	0	2.67	13.0	28.00	0	10.67
243.129	0	0	0	0	0	10.67	0.33	0	0	0	0	0	12.33	71.00	0	5.67
248.429	13.6	1.6	0.6	2.6	0	18.67	14.67	0.33	0	0	1.3	2.33	12.0	21.33	0	10.33
249.109	11.6	5.3	0	0	0	19.67	8.67	0.33	0	0	0	2.67	13.0	28.00	0	10.67
249.429	44.3	0.6	0	0	0	2.0	1.67	0	0	0	1.3	1.67	13.0	26.00	4	5.33
250.009	31.0	3.6	0	0	0	15.33	6.67	0	0	0	0.7	0.67	11.0	25.33	0	5.67
251.269	12.6	0	0	0	0	5.67	5.0	0	0	0	0.3	0	12.0	56.33	1	7.0

Biost. =Biostructured; Cut =Cuticles; Memb. =Membrane; Cort. =Cortex; Eq. =Equidimensional; El. =Elongated; Cor. =Corroded; Res. =Resine; pollen +spores = sporomorphs.

4. Results and Discussion

4.1 Features of particulate organic matter

The type of organic matter (Kerogen) has a vital role in the nature of hydrocarbons that can be generated from a given source rock. In the present study, three main constituents of Kerogen have been identified using the classification scheme of Filho *et al*., (2002). The identified kerogen components were phytoclasts, palynomorphs (only sporomorphs) and amorphous organic matter (AOM), as presented in the table 1. In general, phytoclasts are the dominant particles (73.87% of the total assemblages). This abundance is followed by sporomorphs (18.02% of the total assemblages) and AOM (8.11% of the total assemblages). Phytoclasts are plant remains and the observed ones are either translucent or opaque. Translucent phytoclasts are generally brown being structured and structureless (Fig. 3). The observed translucent phytoclasts include cuticles, membranes, cortex and fungal hyphae (Fig. 3) Cuticles are light coloured translucent leaf epidermis and retain their cellular structures (Fig. 3). The cuticles are derived mostly from the leaves of gymnospermous trees (Tyson, 1995). Cuticles cannot be transported very far before they are easily destroyed and, therefore, they are deposited close to their source (Tyson, 1995). Membranes are pale yellow, thin and sheet-like (Tyson, 1995; Filho, 1999). Fungal hyphae are fragments of hyphae generally brown in colour, consisting of individual filaments of the mycelium of the vegetative phase of fungi (Filho, 1999). Opaque phytoclasts are indicators of oxidation and carbonization of wood material and they are completely black (Fig. 3). The observed opaque phytoclasts were subdivided into five subcategories: equidimensional, sharp outline, no internal structure, lath (sharp outline sometimes with pits) and corroded (irregular, diffuse outline and black) (Fig. 3).

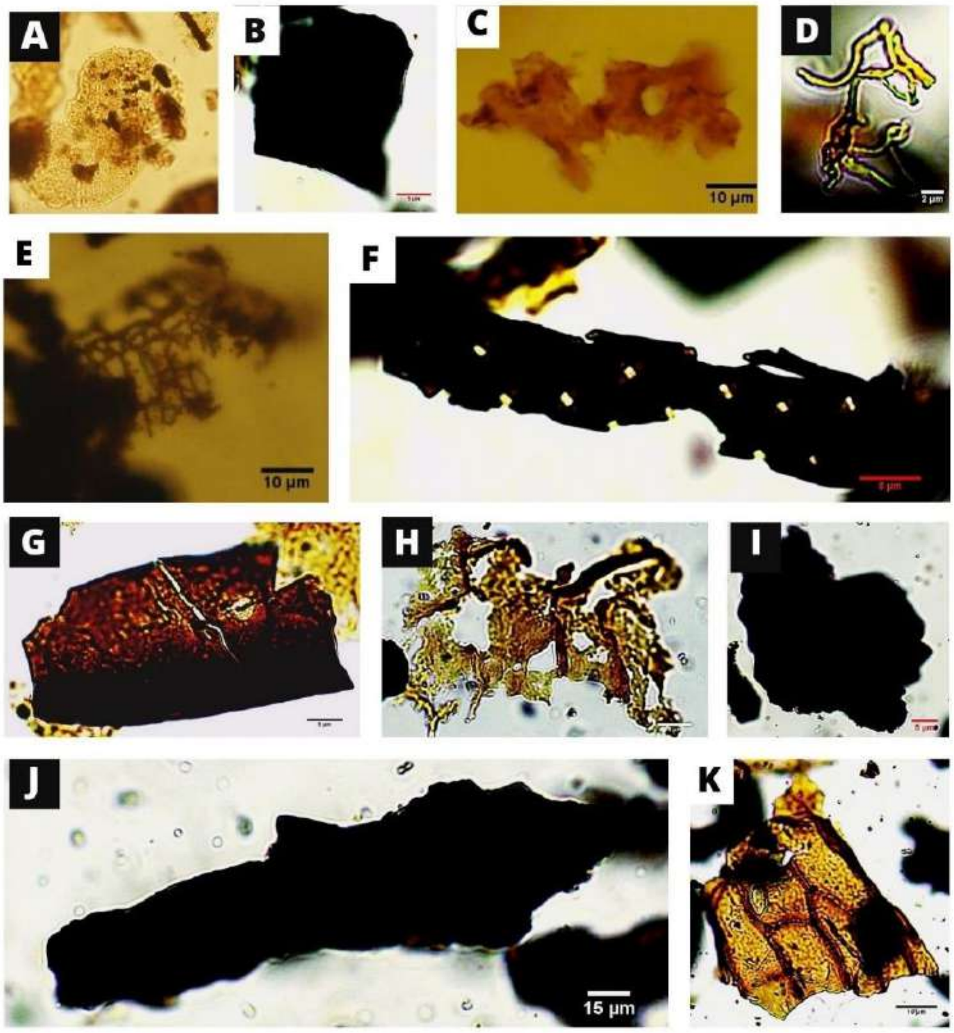

Fig. 3. Selected photomicrographs (under trans mitted light) of the phytoclast groups from the JOG16N-8 borehole, K5 Formation, Maniamba Basin, Mozambique. A) Amorphous organic matter. B) Equidimensional opaque phytoclast. C) Non opaque biostructured organic matter. D) Fungal hyphae. E) Non-opaque phytoclast (cortex). F) Non-opaque phytoclast, biostructured. G) Non opaque phytoclast. H). Membrane. I) Corroded opaque phytoclast. J). Elon gated opaque phytoclast. K) Cuticle.

The sporomorphs represent a considerable proportion in the samples and mainly include monolete spores and monosaccate and bisaccate pollen grains (Figs. 4A- 4F and Fig. 5). Spores and pollen grains display different sizes and shapes, which ranges from oval to triangular and have well-preserved ornamentation, corresponding to a variety of taxa typical of the Permian.

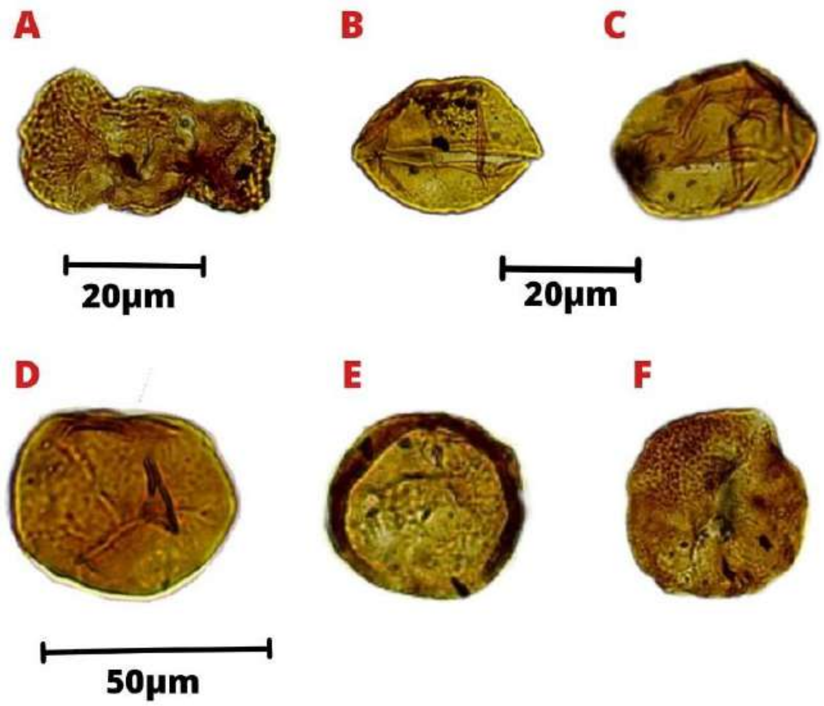

Fig. 4. Photomicrographs of selected sporomorphs (transmitted light micro scope) from the JOG16N-8 borehole, K5 Formation, Maniamba Basin, Mozambique. A) *Hamiapollenites fusiformes.* B) *Laevigatosporites plicatus.* (C) *Laevigatosporites vulgaris*. (D) *Microretaculatisporites* sp. (E) *Marsipipollenites* sp. (F) *Scheuringipollenites ovatus*.

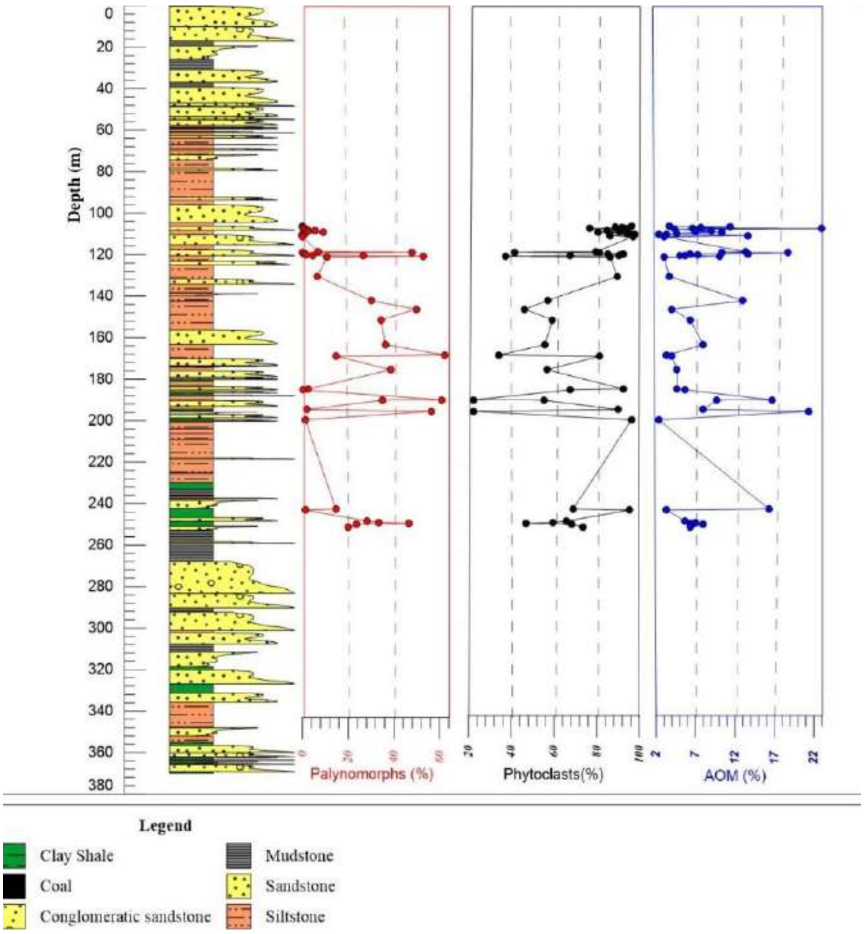

Fig. 5. Variation of the main organic matter compounds over the studied section of the JOG16N-8 borehole, K5 Formation, Maniamba Basin, Mozambique. The amount of palynomorphs stated in the figure are strictly related to sporomorphs.

AOM of these samples are represented by structureless (no morphology) particles of Kerogen, yellowish to brownish (Fig. 3A). The observed AOM is mainly spongy and granular accompanied by amorphous membranous and fibrous phytoclasts (Fig. 3A) associated with biodegradation of higher plants (Tyson, 1995).

4.2 Palynofacies Assemblages

According to the statistical clustering using Euclidian distance and Particulate Organic Matter (POM) (Ward's Method), the samples were classified into three main particle clusters, namely Palynofacies A, B and C (Figs. 6 and 7).

Palynofacies A (phytoclast dominant, opaque): Comprises mainly the lower portion of the productive section of the JOG16N-8 borehole and some middle portions. This palynofacies is represented by eleven samples (Figs. 6 and 7) and is characterized by abundant opaque phytoclasts (64% of total palynofacies A) and a moderate amount of sporomorphs (with a higher percentage of monosaccate pollen grains, 29.4% of the total palynofacies A). Very few AOM particles are observed (6.58% of the total of palynofacies A).

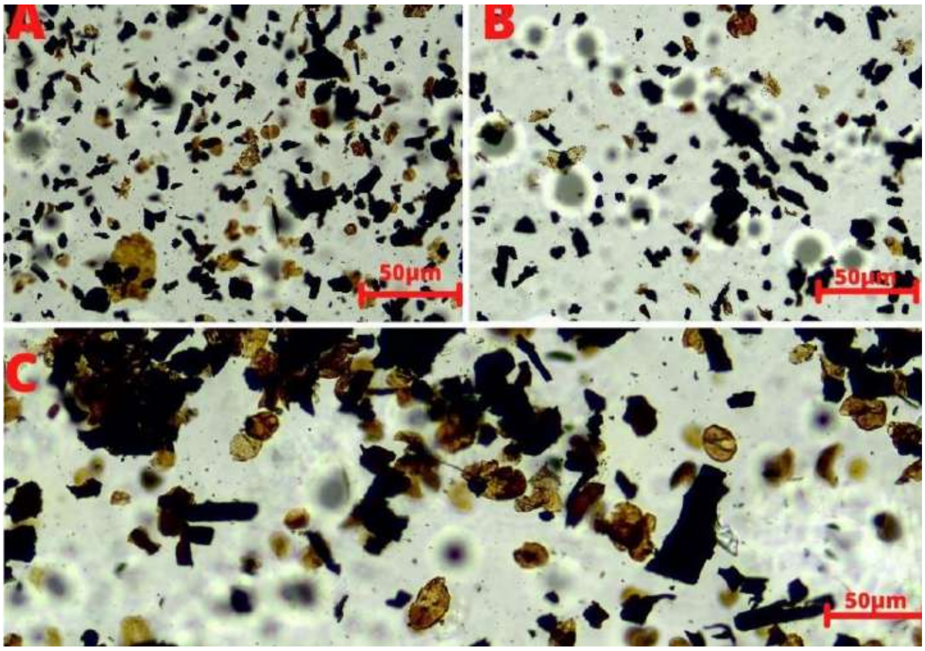

Fig. 6. Photomicrographs (transmitted light microscope) showing the different palynofacies association in the studied section of the JOG16N-8 borehole, K5 Formation, Maniamba Basin, Mozambique. A) Palynofacies A; B) Palynofacies B; C) Palynofacies C.

Palynofacies B (Phytoclast dominant, opaque, Organic Matter): Palynofacies B is restricted to the uppermost part of the productive horizons of the studied borehole. It is characterized by phytoclasts (13.68%, translucent phytoclasts, and 78.8% of opaque phytoclasts) and considerable abundance of AOM (5.23%) if compared to those of palynomorphs (4.26%). The sporomorphs are observed in lower concentration and mainly comprise monosaccate pollen grains. A high supply of phytoclasts in the studied section can dilute all the components and this factor reflects characteristics in which deposition occurs close to the mother flora (Batten, 1983). Also, this palynofacies is characterized by the predominance of non-degraded and biostructured cuticles (fragments of tracheid cells (Fig. 3K)). Large cuticles, as observed in the Fig. 3K, are characteristic of prodelta facies.

Palynofacies C (Palynomorphs dominant: Monosaccate pollen grains, Opaque Phytoclasts): This assemblage covers eight samples. Here, the sporomorphs become the dominant palynofacies group (49.83% of the total palynofacies) with abundant mono- and bisaccate pollen grains (Fig. 6C). In this assemblage, phytoclasts (45.81%) are however more abundant than AOM (4.35%). The higher percentage of sporomorphs identified in the samples is an indicator of depositional environments close to active fluvial-deltaic sources suggesting humid conditions associated with oxygenated environments, where lowered salinities suppress any planktonic production and sporomorph input is high (Tyson, 1995, Filho, 1999).

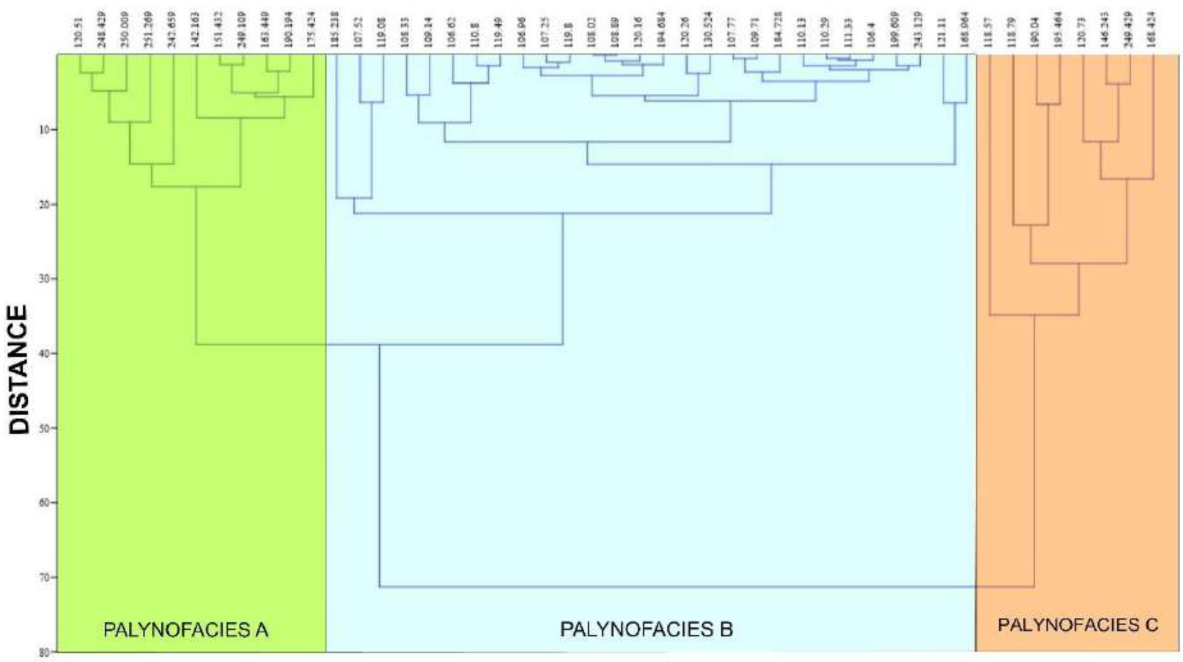

Fig. 7. Cluster diagram for the studied material with related Palynofacies A, B and C of the JOG16N-8 borehole, K5 Formation, Maniamba Basin, Mozambique.

4.3 Paleoenvironmental Interpretations

Palynofacies is a tool that is used widely in several fields of geology aiming at recognizing proximal-distal relationships with regard to source, regressivetransgressive trends in stratigraphic sequences, transportation distance from the source, hydrocarbon source rock potential and in the identification of the various depositional environments (e.g., oxic open marine, dysoxic-anoxic, brackish freshwater, flooded palaeomire, swamps, peats, etc.). For the identification of depositional environments the classic Palynofacies, AOM-Phytoclast-Palynomorph ternary plot of Tyson (1993) (Fig. 8) was used herein. The APP ternary diagram (Fig. 8) shows that the samples of the K5 Formation fall into four fields: Field I: highly proximal, shelf or basin; II: marginal dysoxic-anoxic; III: proximal shelf, V: mud dominated oxic shelf (distal shelf). The Tyson diagram suggests that the K5 Formation was deposited under highly proximal and oxic shelf conditions. These data corroborate with the abundance of opaque phytoclasts over non-opaque phytoclasts suggesting also a general fluvial-deltaic sedimentary environment (Tyson, 1995).

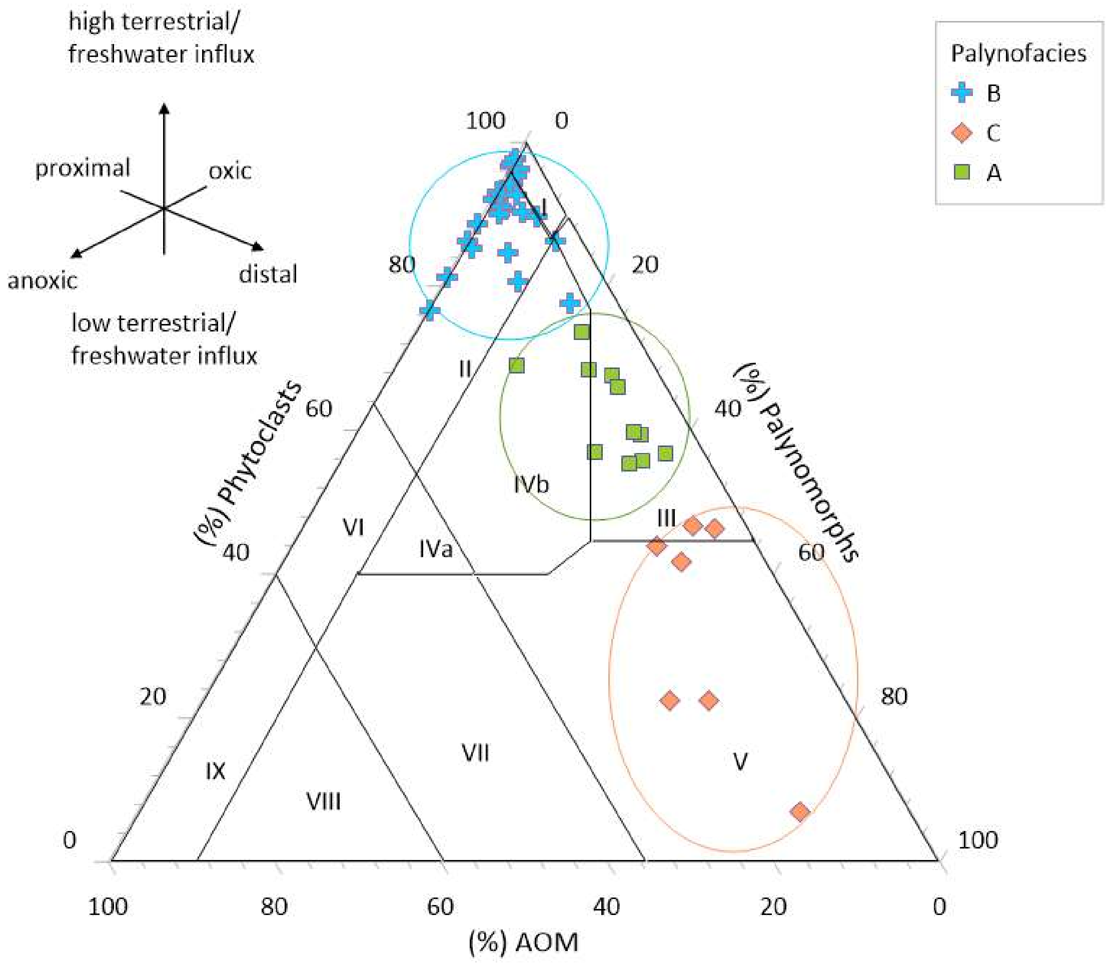

Fields	Environment	Kerogen type
I	Highly proximal shelf or basin	III gas prone
II	Marginal dysoxic-oxic basin	III gas prone
III	Heterolithic oxic shelf (proximal shelf)	III, IV gas prone
IV	Shelf to basin transition	III, II mainly gas prone
V	Distal shelf	III>IV gas prone
VI	Proximal suboxic-anoxic shelf	II oil prone
VII	Distal dysoxic anoxic shelf	II oil prone
VIII	Distal dysoxic anoxic shelf	II>>I oil prone
IX	Distal suboxic anoxic basin	II>I highly oil prone

Fig. 8. Tyson (1995) diagram for paleoenvironmental interpretations and the palynofacies sampling representation (A, B and C) from the studied area (JOG16N-8 borehole, K5 Formation, Maniamba Basin, Mozambique). The amount of palynomorphs stated in the diagram are strictly related to sporomorphs.

This abundance may be a result either of oxidizing conditions in proximity to terrestrial settings (Tyson, 1995) or due to the fact that some wildfires were part of the Middle

Permian ecosystem. Charcoal for instance has been found through some sections of the borehole core, but nothing in this regard has been published yet. However, the presence of charcoal suggests that wildfires were part of the Middle Permian ecosystem. Also, recent studies have revealed that abundance of opaque particles may have been as a result of an increased runoff in the fluvial-delta environment under obliquity cycle-controlled monsoon climate (Li *et al*., 2020). Further, the Tyson ternary diagram, modified by Hacquebard and Donaldson (1969), (Fig. 9), suggests that the sedimentary succession in the K5 Formation occurred in a lacustrine and swampy environment. These findings are in line with the terrestrial alluvial fan-river-braided systems and the delta-shallow lacustrine sedimentary systems for the studied area as identified by De Bock and Verniers (1984), Verniers *et al*., (1989) and Paz, 2018. Lastly, the identified Palynofacies A, B and C, the occurrence of spores (Figs. 4B-4D) are also in accordance with the higher contribution of the continental material in the sedimentary system of the section meaning a more proximal depositional environment (Filho, 1999).

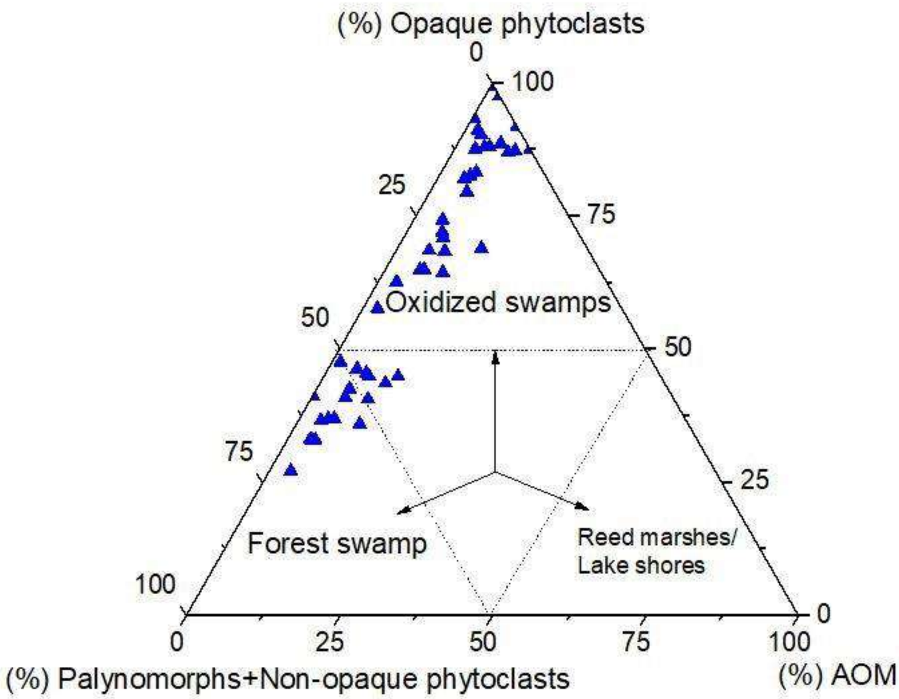

Fig. 9. Tyson (1995) Ternary diagram modified by Hacquebard and Donaldson (1969) for additional palaeoenvironment interpretations in the Maniamba Basin. The amount of palynomorphs stated in the diagram are strictly related to sporomorphs.

4.4 Source rock potential

Rock Eval Hawk pyrolysis analysis integrated with biomarkers, organic petrography and palynofacies are being undertaken in two borehole cores closer to the area presented herein (Nhamutole *et al.* in press). These data will be important to build up full history of the Basin. However, the source rock potential investigated herein has been identified only on the basis of the palynofacies in order to get some inferences whether the kerogen is oil or gas prone and the spore coloration in order to determine levels of thermal maturity. The thermal maturity analysis is considered to be an indispensable tool to assess hydrocarbon generation potential due to the fact it is a key parameter for the conversion of sedimentary organic matter to oil and gas (Tissot and Welte, 1984). The spore colour Index (SCI) assesses the level of maturity and is based on the fact that transmitted colour of spores and pollen in unoxidized organic residue becomes darker with increasing thermal maturity (Staplin, 1969). However, this method can present limitations due to misinterpretation of colours. In the present study, the chosen spore for this analysis was *Laevigatosporites plicatus* (Fig. 10). The SCI range from pale yellow to yellow, indicating an immature phase (Pearson, 1990; Tyson, 1995). Moreover, it indicates little to poor hydrocarbon generation potential (Fig. 10). In addition, there is no clear trend for the SCI values over the stratigraphic section. Coal quality studies have shown vitrinite reflectance (%Ro) ranging from 0.4-0.6 inferring immature to mature phases (JOGMEC, 2015). These values corroborate at some stage with those observed by SCI methods, however more detailed studies using vitrinite measures are needed in the future.

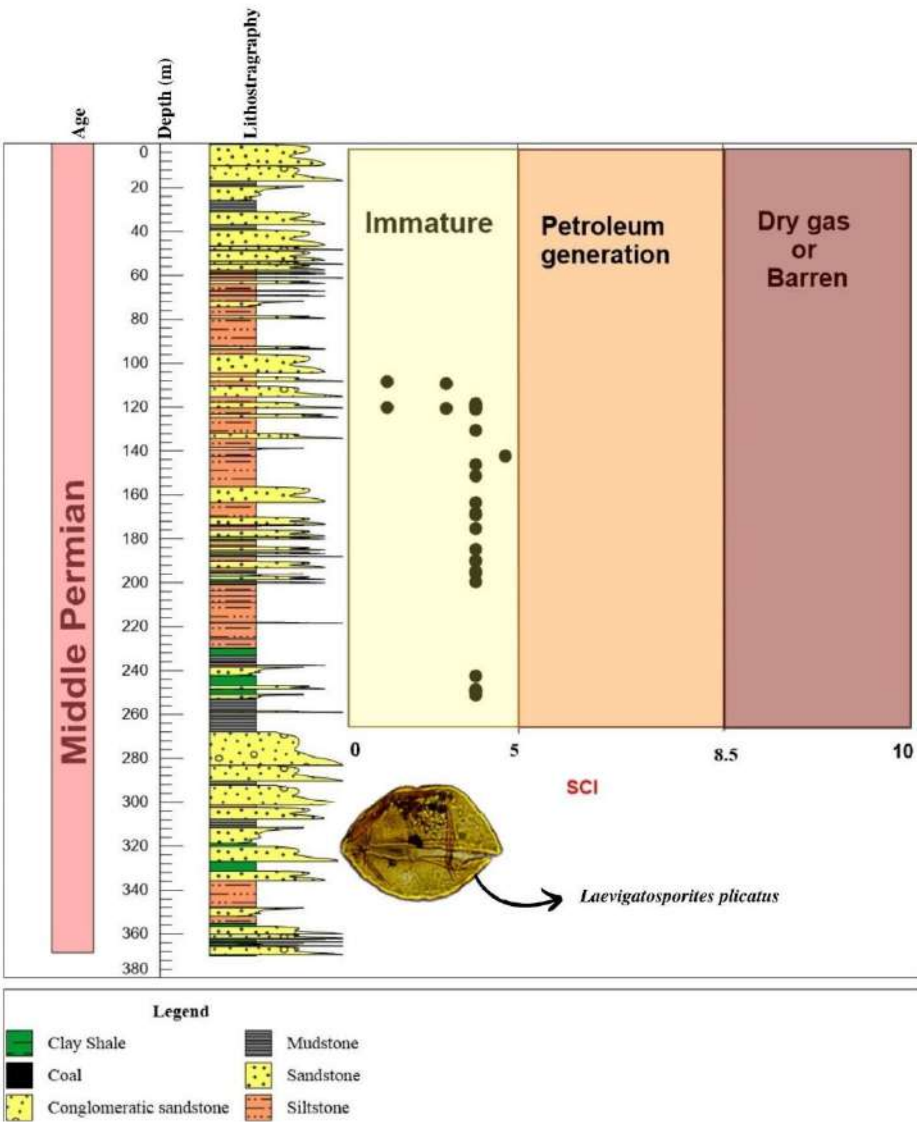

Fig. 10. Spore Colour Index (SCI) illustrating an immature phase for the studied stratigraphic section of the JOG16N-8 borehole, K5 Formation, Maniamba Basin, Mozambique.

The dominant phytoclasts (mostly opaques) represented clearly by oxidized or carbonized material suggests the presence of kerogen Type III and Type IV (with no or very little potential for hydrocarbon in the study area) (Fig. 11). Five samples fall in field IV of the Tyson 1995 diagram (Fig. 8) which represent a type II Kerogen. Samples within this field, however, are considered by Tyson (1995) to be more gas prone. This conclusion was expected due to the high input of continental material (mainly higher plants) that lower the H/C atomic ratio and contribute further to the enrichment in Oxygen derived from the high cellulose and lignin content. However, regarding the phytoclast abundance *versus* hydrocarbon potential, there are horizons with larger amounts of translucent phytoclasts relative to opaque phytoclasts indicating less transportation and gas prone. This scenario is also reported from other Karoo formations in Mozambique (Moatize Minjova and Sanangoé-Mefidezi Basin) which indicate the existence of a potential for oil and wet gas production with transition into dry gas (Fernandes *et al*., 2014; Mahabeer, 2017). Other similar patterns were also reported in the Sichuan Basin, China (Zhenzhuchon Formation, Li *et al*., 2020), Ordos Basin, China (Triassic Yanchang Formation, Zhang *et al*., 2015), Raniganj Sub–basin, India (Barren Measures Formation, Ahmed *et al*., 2018) and others.

In summary, based on the results of palynofacies it can be inferred that the siltstone-sandstone-claystone of the K5 Formation are represented by immature Type II, III, and abundant Type IV kerogen with no or very little potential for hydrocarbon. However, use of integrated proxies in some deeper sections of the Basin is being taken into consideration because it will be important to understand its potential for hydrocarbon and palaeoenvironments.

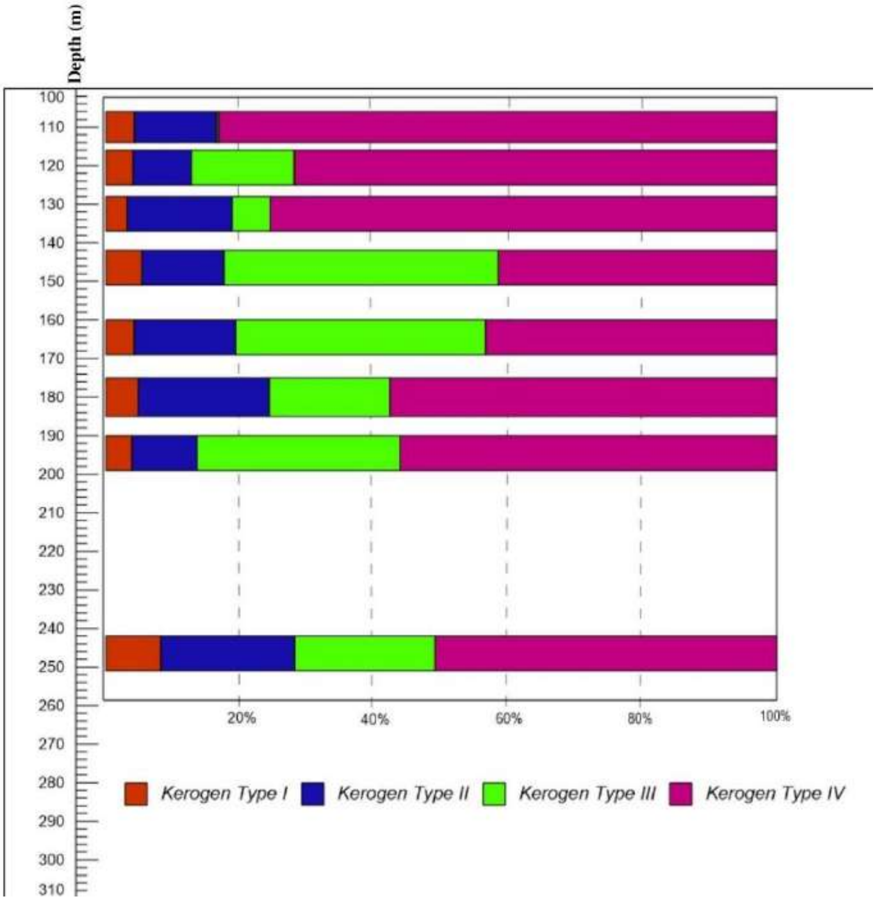

Fig. 11. Kerogen typification based on the relative abundance of different organic matter compounds in the JOG16N-8 borehole, K5 Formation (Middle Permian), Mozambique area.

5. Conclusions

Palynofacies analysis was conducted on 69 samples of the Middle Permian, Maniamba Basin, Mozambique. This is the first palynofacies study carried out so far for source rock evaluation and paleoenvironmental reconstruction in the Maniamba Basin, Northern Mozambique. The main results of this study can be summarized as follows:

Well preserved palynofacies assemblages comprising three palynofacies categories dominated mostly by opaque phytoclasts were identified.

The most predominant kerogen component are phytoclasts with less abundant palynomorphs and sparse AOMs.

The APP ternary plot indicates deposition under highly proximal and oxic shelf conditions. Furthermore, it can also be concluded that the sedimentary succession of the K5 Formation represents an ancient lacustrine-fluvial deposit within an oxidizing regime that alternated according to the climate from dysoxic to an oxic regime.

The predominance of opaque phytoclasts in the sediments from the K5 Formation may be related to wildfire events during the Middle Permian and possible increased runoff in the fluvial-deltaic environment under obliquity cycle-controlled monsoon climate.

Palynofacies analyses indicate type II, III and IV kerogen in immature stage for the rocks of the studied section which in turn provides some vital information regarding the exploration of hydrocarbon in the K5 Formation, Maniamba Basin. However, more powerful techniques are in progress in order for providing a better understanding of the Basin potentiality.

References

Ahmed, W., Bhat, G.M., Mclennan, J., Sinha, H.N., Kanungo, S., Pandita, S.K., Singh, Y., Hakhoo, N., Hafiz, M., Thusu, B., Choudhary, N.H., 2018. Kerogen typing using palynofacies analysis in Permian Barren Measures Formation in Raniganj sub–basin, East India. The Palaeobotanist 67(2), 113–122.

Amaro, D.L ., 1950. Relatório da 1ª Brigada de Fomento Mineiro; (Campo mineiro de Macequece, Lago Niassa). Relatório inédito dos Serviços Geólogicos de Moçambique 198, 24-54.

Araújo, R., Macungo, Z., Smith, R., Tolan, S., Angielczyk, K., Crowley, J., Milisse, D.,Mugabe, J., 2020. The first Lower Triassic tetrapod fossils from Metangula Graben (Niassa Province, Mozambique) and their biostratigraphic significance. Palaeontologia africana 54, 56-58.

Batten, D.J., 1981. Palynofacies, organic maturation and source potential for petroleum. In Brooks, J. (Eds.), Organic maturation studies and fossil fuel exploration. Academic Press, London, pp. 201-223.

Batten, D.J., 1996. Palynofacies and palaeoenvironmental interpretation; in McGregor, D. C. (Eds.), Palynology: principals and applications. Publishers Press, Salt Lake City, pp.1011-1064.

Borges, A., Freitas, F. Nunes, A.F. ,1950. Relatório da campanha da quarta brigada do Fomento Mineiro. Relatório inédito dos Serviços Geólogicos e Mineiros de Lourenço Marques 178, 29 pp.

Castanhinha, R., Araújo, R., Junior, L.C., Angielczyk, K.D., Martins, G.G., Martins, R.M.S., Chaouiya, C., Beckman, F., Wilde, F., 2013. Bringing Dicynodonts back to life: palaeobiology and anatomy of a new Emydopoid Genus from the upper Permian of Mozambique. Plos one, 8 (12):e80974.

De Bock, F., 1983. Estudo palinológico do Karoo inferior nas bacias de Moatize e de Ncondezi e do Karoo na Mancha de Metangula. Aplicação na exploração do carvão. Direcção Nacional do carvão de Maputo, Moçambique, 32 pp. (In Portuguese).

De Bock, F., Verniers, J., 1984. The palynology of the Karoo graben of Metangula, Niassa province, Northern of Mozambique. VIth International Palynology Conference. Calgary, Canada, 32pp.

El Beialy, S.Y., El Atfy, H.S., E.M. El Khoriby, E.M., R.H. Abu-Zied, R.H., 2008. Palynostratigraphy, palynofacies and source rock evaluation of the Cenomanian Bahariya Formation, GPTSW-7 well, north Western Desert. Egyptian Journal of Environmental Sciences, Mansoura University 36, 63–88.

Fernandes, P., Rodrigues, B., Jorge, R., Marques, J., 2014. Potencial gerador de hidrocarbonetos dos argilitos carbonosos das Formações de Vúzi e de Moatize (Karoo Inferior) da Bacia Carbonífera de Moatize–Minjova, Província de Tete, Moçambique. Comunicações Geológicas 101, 433-437.

Filho, J.G.M., 1999. Aplicação de estudos de palinofácies e fácies orgânica em rochas do Paleozóico da Bacia do Paraná, Sul do Brasil. PhD thesis, Universidade Federal do Rio Grande do Sul, 254pp. (in Portuguese).

Filho, J.G.M, Carvalho, M., Menezes, T., 2002. Palinofácies. In: Técnicas e Procedimentos para o Trabalho com Fósseis e Formas Modernas Comparativas, Dutra, T.L. (Eds.), Unisinos, São Leopoldo, pp. 20-24.

Götz, A., Hancox, J., Lloyd, A., 2017. Permian climate change recorded in palynomorph assemblages of Mozambique (Moatize Basin, eastern Tete Province). Acta Palaeobotanica 57, 3-11.

Hacquebard, P. A., Donaldson , J. R., 1969. Carboniferous coal deposition ssociated with floodplain and limnic environments in Nova Scotia. Geological Society of America 114, 143-191.

JOGMEC., 2015. The results of drilling survey III in Mozambique. National Institute of Mines report, 40pp.

Li, L.Q., Wang, Y.D., Vajda, V., Liu, Z.S., 2020. Palynofacies analysis for interpreting paleoenvironment and hydrocarbon potential of Triassic–Jurassic strata in the Sichuan Basin, China. Palaeoworld 30, 126-137.

Macungo, Z., Loide, I., Zunguza, S., Nhamutole, N., Maharaj, I.E.M., Mugabe, J., Angielczyk, K.D., Araújo, R., 2020. Endothiodon (therapsida, anomodontia) specimens from the middle/late permian of the Metangula graben (Niassa

Province, Mozambique) increase complexity to the taxonomy of the genus. Journal of African Earth Sciences 163, 103647.

Mahabeer, K.C., 2017. Palynology of the Permian Sanangoé-Mefidezi Basin, Tete Province, Mozambique and correlations with Gondwanan Microforal assemblages. Unpublished Masters Dissertation, University of the Witwatersrand, 168pp.

Nhamutole, N.E., Bamford, M.K., Araújo, R., 2021. New species of *Protaxodioxylon* (conifer wood) from the Middle Permian of the Metangula Graben (Niassa Province, Mozambique) and their implications. Journal of African Earth Sciences 183, 104323.

Nhamutole, N.E., Bamford, Marion., Souza, P.A., Do Carmo, D.A., Da Silva, T.F., *in press*. Petroleum potential assessment based in the integration of organic geochemistry and organic petrograph in the Metangula graben, Mozambique. Journal of South African Geology. (in press)

Paz, V., 2018. Sistemas Deposicionais e Fácies Sedimentares da Bacia Carbonífera de Maniamba. Bachelor Thesis, Universidade Eduardo Mondlane, 121pp. (in Portuguese).

Pearson, D.L., 1990. Pollen/spore Color "standard". Phillips Petroleum Geology Branch, Bartlesville, Oklahoma, 3pp.

Raafat, A., Tahoun, S.S., Aboul Ela, N.M., 2021. Palynomorph biostratigraphy, palynofacies, thermal maturity and paleoenvironmental interpretation of the Bajocian–Aptian succession in the OBA D-8 Well, Matruh Basin, Egypt. Journal of African Earth Sciences 177,104157.

Staplin, F.L., 1969. Sedimentary organic matter, organic metamorphism and oil and gas occurence. Bulletin of Canadian Petroleum Geology 17, 47-66.

Tissot, B., Welte, D.H., 1984. Petroleum Formation and Occurence (Second Edition). Springer Verlag, Heldelberg, 699 pp.

Tyson, R.V., 1993. Palynofacies analysis. In: Jenkins, D.G. (Eds.), Applied Micropaleontology. Kluwer Academic Publication, Netherlands, pp. 153–191.

Tyson, R.V ., 1995. Sedimentary Organic Matter, Organic facies and palynofacies.

Chapman and Hall, London, 615 pp.

Vale M., 2014. Projecto, desenvolvimentos e avaliação da ocorrência de carvão existente na Bacia Carbonífera de Maniamba, Provincia de Niassa em Moçambique, 100pp. (in Portuguese).

Vaz, M., 2017. Palinologia como ferramenta para a reconstituição da história geológica da Bacia Carbonífera de Moatize-Minjova (Karoo, Moçambique). Master Thesis, Faculdade de Ciência, Universidade do Porto. Portugal, 144pp. (in Portuguese).

Verniers, J., Jourdan, P.P., Paulis, R.V ., Frasca-Spada, L., De Bock, F.R ., 1989. The Karroo Graben of Metangula Northern Mozambique. Journal of African Earth Sciences 9, 137–158.

Vincente, A., Almeida, C., Camarinhas, M., Rocha, D., 1950. Relatório de actividade da 2ª Brigada de Fomento Mineiro para a Região de Maniamba. Relatório inédito dos Serviços Geólogicos de Moçambique, 152 pp. (in Portuguese).

Zhang, M., Ji, L., Wu, Y., He, C., 2015. Palynofacies and geochemical analysis of the Triassic Yanchang Formation, Ordos Basin: Implications for hydrocarbon generation potential and the paleoenvironment of continental source rocks. International Journal of Coal Geology 152, 159–176.

Zobaa, M.K., El Beialy, S.Y., El-Sheikh, H.A, El Beshtawy, M.K., 2013. Jurassic-Cretaceous palynomorphs, palynofacies, and petroleum potential of the Sharib-1X and Ghoroud-1X wells, northWestern Desert. Egypt. Journal of African Earth Sciences 78, 51–65.

Chapter Two

Petroleum potential from Permian-Triassic strata of the Maniamba Basin, Mozambique: A preliminary characterisation.

Adapted from N.E. Nhamutole, M.K. Bamford, P.A. Souza, T.F. Silva, D.A Carmo

Published by South African Journal of Geology

N.E. NHAMUTOLE, M.K. BAMFORD, P.A. SOUZA, T.F. SILVA AND D.A. CARMO

Petroleum potential from Permian-Triassic strata of the Maniamba Basin, Mozambique: A preliminary characterisation.

Abstract

In order to further our understanding regarding the petroleum potential of the Maniamba Basin, Mozambique, organic rich sediments from four outcrops were investigated. Organic-rich shales, claystones, sandstones and siltstones were sampled for geochemical organic analyses that included TOC (Total Organic Carbon), and Rock Eval Pyrolysis. The pyrolysis analysis showed that the TOC ranges from good to excellent, thus indicating a potential for hydrocarbon generation. Based on the hydrogen index (HI) *versus* oxygen index (OI) diagram, most samples were classified as kerogen type III or IV, however, a mixed type II and III was also observed. These data suggest that the Organic Matter (OM) is of terrigenous origin with the occurrence of organofacies C, CD and D. The majority of the studied samples are found to be at mature to overmature stages. The overmaturation of the OM may be associated with tectonic events during the process of basin subsidence, and close proximity to igneous intrusions. Further, an indigenous nature of the hydrocarbon has been identified. Similar organic matter properties of the studied sections are correlatable with those from Moatize Minjova, Sanangoé-Mefidezi (Mozambique), Ruhuhu (Tanzania) and the

Main Karoo Basin in South Africa. Overall, the results of this study suggest a good potential for gas.

Introduction

Organic geochemistry is an important tool to evaluate the hydrocarbon potential of rocks (Van Krevelen, 1993; Hao et al., 2011) using, for instance, the Pyrolysis Rock Eval. The Rock Eval Pyrolysis is the most common and routinely used method in the petroleum industry providing inputs regarding the content, origin and maturity of organic matter in the rocks (Espitalie et al., 1977; Lafargue et al., 1998; Shalaby et al., 2020; Qin et al., 2021).

In Mozambique, organic geochemistry studies on dispersed organic matter are mostly restricted to the southern portion of the country and concern primarily Mesozoic and Cenozoic rocks [(e.g., the Paleogene Cheringoma Formation, and turbidites and shales in the Senonian to Paleocene Grudja Formation (Kihle,1983)]. For the Palaeozoic, recent studies by Mussa et al. (2018) using organic-rich shales from the Nemo-1x well, reported the existence of kerogen type III (gas-prone) and IV (non-productive or residual) for the samples studied from the Mozambique Basin. Another detailed geochemical study was performed by Loegering and Milkov (2017), using data provided by SASOL from Inhassoro, Pande and Temane fields, where a pure thermogenic gas with no evidence of primary microbial or biodegradation was found. Some other reports from sites apart from the Maniamba Basin do exist, but they are part of internal reports of oil companies (Lineback et al., 1986; Salman et al., 1990; ECL, 2000).

Permian fine to coarse-grained sandstones, siltstones, shales and highly carbonaceous shales of four outcrops from the Maniamba Basin, Mozambique are investigated for their petroleum potential herein. The Maniamba Basin is one of the best-known basins in Mozambique extending over an area of 8 000 000 km^2 and comprising Precambrian to Recent sedimentary deposits (Figure 1). This basin has been regarded as a potential area for gas exploration by ECL (2000) because its organic matter is assumed to be of a terrigenous origin; however, no survey regarding organic matter content and the petroleum generation potential have been done so far

(ECL, 2000). Coal quality studies and related research, however, has been reported (JOGMEC, 2015).

This study represents the first of its nature being undertaken in the Maniamba Basin, which will become useful for a better understanding of the source rock quality, type of kerogen, source rock maturation and migration thus, assisting in identifying future exploration targets.

Geology of the Maniamba Basin

The detailed geological information is found in the section 5.1.

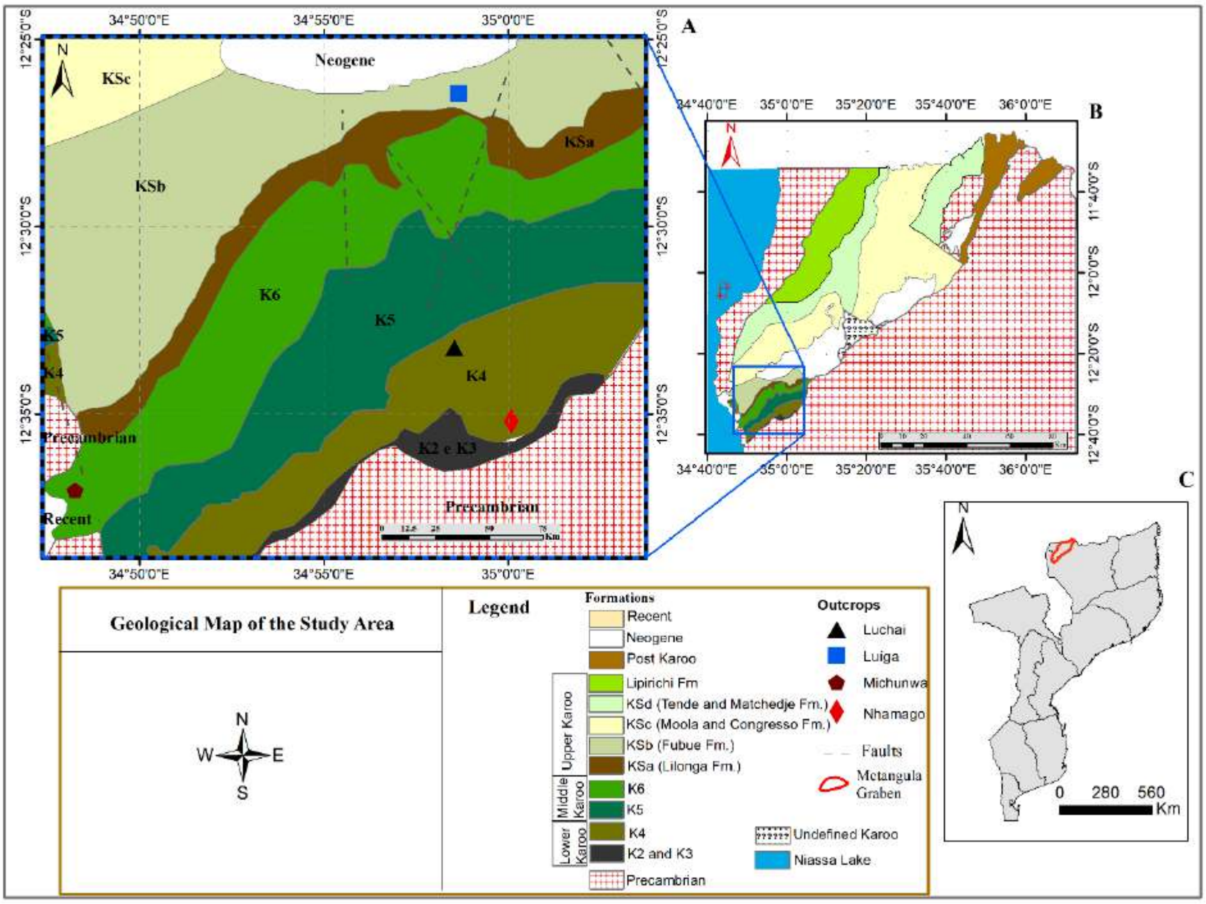

Figure 1. Three map illustrations of the Maniamba Basin with (A) Detailed map of the Maniamba Basin showing the location of the outcrops, (B) General Map of the Maniamba Basin (the rectangle represents an overview of the geological formations studied in the present work), (C) Map of Mozambique with the red polygon in the northern part representing the location of the Maniamba Basin. Maps (A) and (B) were both adapted from Verniers et al. (1989).

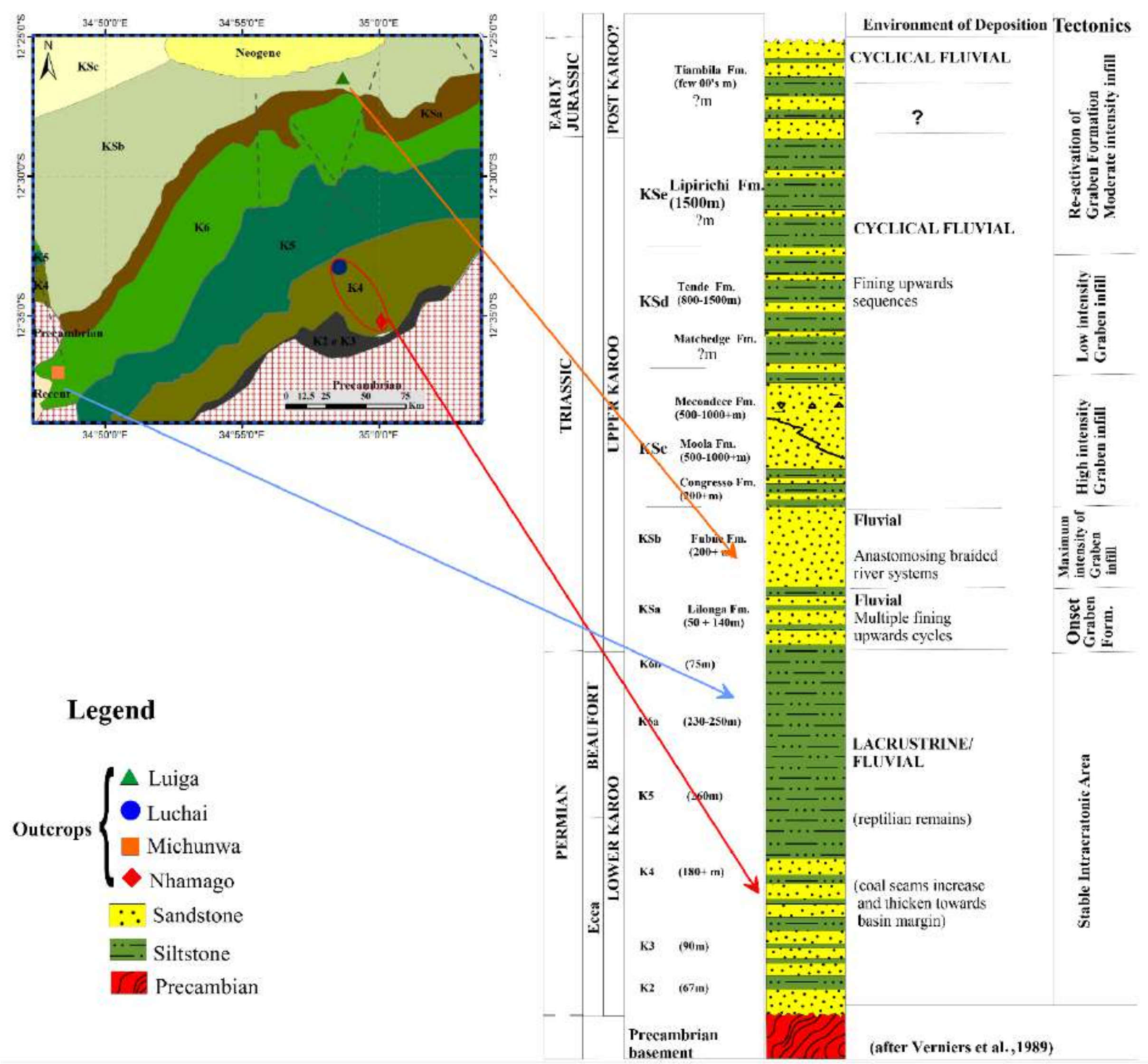

Figure 2. Stratigraphic column showing the lithostratigraphy and palaeoenvironments of the Maniamba Basin adapted from Verniers et al. (1989) and ECL (2000).

Materials and methods

Sampling

Fifteen samples were obtained from four outcrops in the Maniamba Basin during a field campaign in 2021. The sampling sites was Luiga, Michunwa, Luchai and Nhamago (Figures 3A to 3D). For each outcrop 1 kg of samples were collected through a horizontal excavation on the walls of the outcrop in order to avoid weathered and oxidized surfaces. The most preferable sampled rocks were fine-grained siltstone, carbonaceous shale, sandstone and claystone because these are the ones with potential for organic matter preservation. The samples were then submitted to pyrolysis rock eval at the Universidade Federal do Rio Grande Sul (Brazil). Nevertheless, for details regarding pyrolysis rock eval procedures please see section 6.1.1.

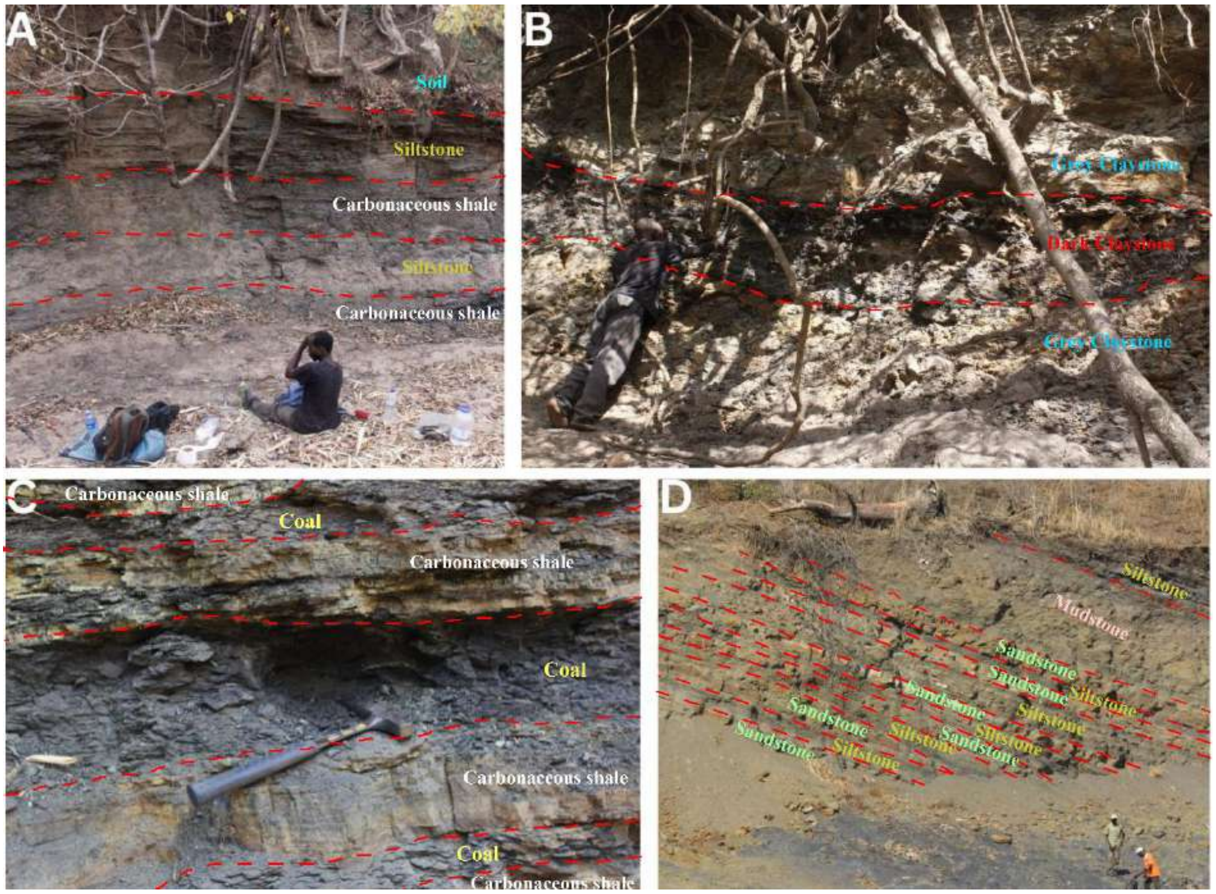

Figure 3. Field illustrations of the studied outcrops showing organic rich units in black: (A) Luiga outcrop (KSb Formation, Early Triassic), (B) Nhamago outcrop (K4 Formation, Middle Permian), (C) Luchai outcrop (K4 Formation, Lower Permian), and (D) Michunwa outcrop (K5 Formation, Middle Permian). The geological age of the sediments from different outcrops in brackets are according to the information given by the geological map (Figure 1) adapted from Verniers et al. (1989).

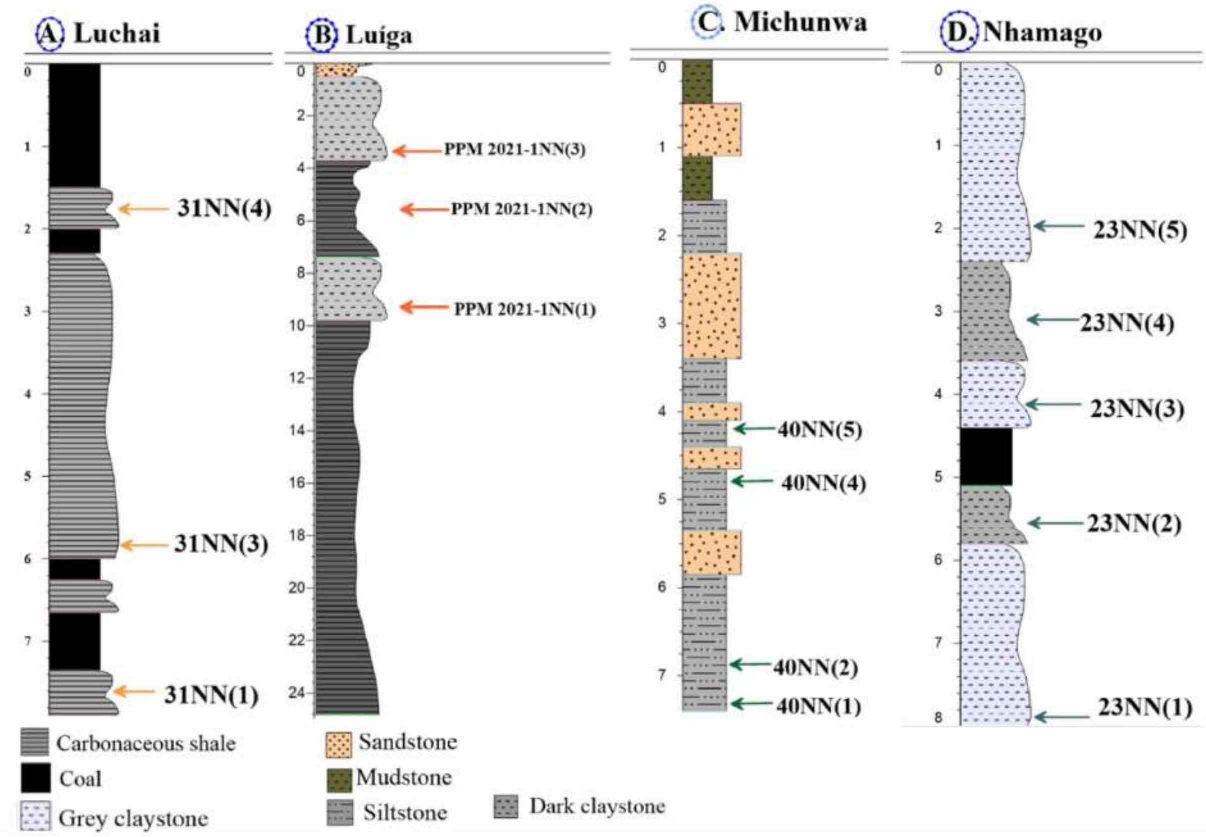

Figure 4. Lithology and sample horizons for the four outcrops from the Maniamba Basin, Niassa, including the collected samples: (A) Luiga, (B) Nhamago, (C) Luchai, and (D) Michunwa.

Results and discussion

All samples were processed under HAWK Pyrolysis to characterise the organic content, kerogen type, thermal maturity, generation potential, nature of hydrocarbons, depositional environment.

Organic richness and source rock quality

The Total Organic Carbon (TOC) measures the organic richness of a rock and it is a qualitative tool to measure the petroleum potential (Peters and Cassa, 1994). Values of 1.0 wt% TOC are considered a minimum value for defining a petroleum source rock (Peters and Cassa, 1994). Additionally, measuring only organic carbon content is not enough for determining the potential of source rocks (Peters and Cassa, 1994). Thus, values of TOC should be regarded with caution because high organic carbon content is not always an indication of a potential oil source due to the fact that reworked organic matter from terrestrial sources within old marine sediments can display high TOC values (Sari and Aliyev, 2006). The results of TOC from the outcrops are presented in the Table 1.

Table 1 Total Organic Carbon (TOC) and Rock Eval pyrolysis results of the outcrop samples from Maniamba Basin.

Outcrops	Lithostratigraphy (Verniers et al., 1989)	Samples	S1 (mg HC/g rock)	S2 (mg HC/g rock)	S3 (mg CO2/g TOC)	PI	S3/S2	GP	Tmax (ºC)	TOC (wt%)	HI	OI
Luíga	KSb (Lower Triassic)	1NN (3)	0	0.04	0.7	0.30	17.5	0.04	537	0.87	4	81
		1NN (2)	0.01	0.47	1.16	0.04	2.46	0.48	452	2.21	21	52
		1NN (1)	0.41	3.83	0.24	0.10	0.06	4.24	434	2.67	143	9
Michunwa	K6 (Middle Permian)	40NN (5)	0.01	0.06	0.75	0.30	12.5	0.061	543	1.88	3	39
		40NN (3)	0.01	1.11	1.47	0.01	1.32	1.12	448	4.70	23	31
		40NN (2)	0	0.3	0.93	0.03	3.1	0.3	450	2.10	14	44
		40NN (1)	0.01	0.25	0.33	0.07	1.32	0.26	537	1.60	15	20
Nhamago	K4 (Lower Permian)	*23NN (5)	0.16	23.5	19.07	0.01	0.81	23.66	428	37.56	62	50
		23NN (4)	0.02	1.27	1.40	0.02	1.10	1.29	435	7.37	17	19
		23NN (3)	0	0.12	0.37	0.01	3.08	0.12	545	1.34	9	27
		23NN (2)	0	0.08	0.66	0.13	8.25	0.08	548	1.16	6	56
		23NN (1)	0.01	0.07	0.94	0.22	13.42	0.08	549	1.82	3	51
Luchai	K4 (Lower Permian)	31NN (4)	0.02	0.95	2.27	0.03	2.38	0.97	437	7.30	12	31
		31NN (3)	0.01	0.57	1.10	0.02	1.92	0.58	436	4.84	11	22
		31NN (1)	0.03	0.54	0.31	0.07	0.57	0.57	439	1.49	36	20

*Abbreviations S1=Free hydrocarbon content, mg HC/g rock; S2 = Remaining hydrocarbon or generative potential, S3=the amount of CO2 from breaking oxygen-containing compounds in kerogen at 300-3900 C, PI=Production Index; GP=Generator Potential; Tmax=Temperature at maximum of S2 peak (℃); TOC=Total organic carbon; HI=Hydrogen Index; OI=Oxygen Index. *Sample 23NN(5) is considered an outlier due to its high value of TOC reaching to 37.56wt%.

The Nhamago outcrop (Figure 5) shows TOC values ranging from 1.1 to 4.8 wt%. This content points to excellent potential for hydrocarbon generation. The values for the Luchai outcrop (Figure 5) range from 1.4 to 7.3 wt%, also suggesting good to excellent organic richness according to Peters and Cassa (1994). In its turn the Michunwa (Figure 5) TOC values range from 1.6 to 4.7 wt% being regarded as good to excellent. The only exception are the samples from the Early Triassic Luiga outcrop (Figure 5), showing values ranging from 0.8 to 2.6 wt%, which are considered fair to very good for hydrocarbon generation. In summary, the variations in TOC content suggest that the carbonaceous shales, siltstones and studied claystone present a good potential for hydrocarbon generation. Further, the majority of TOC values from the studied outcrops are less than 2%.

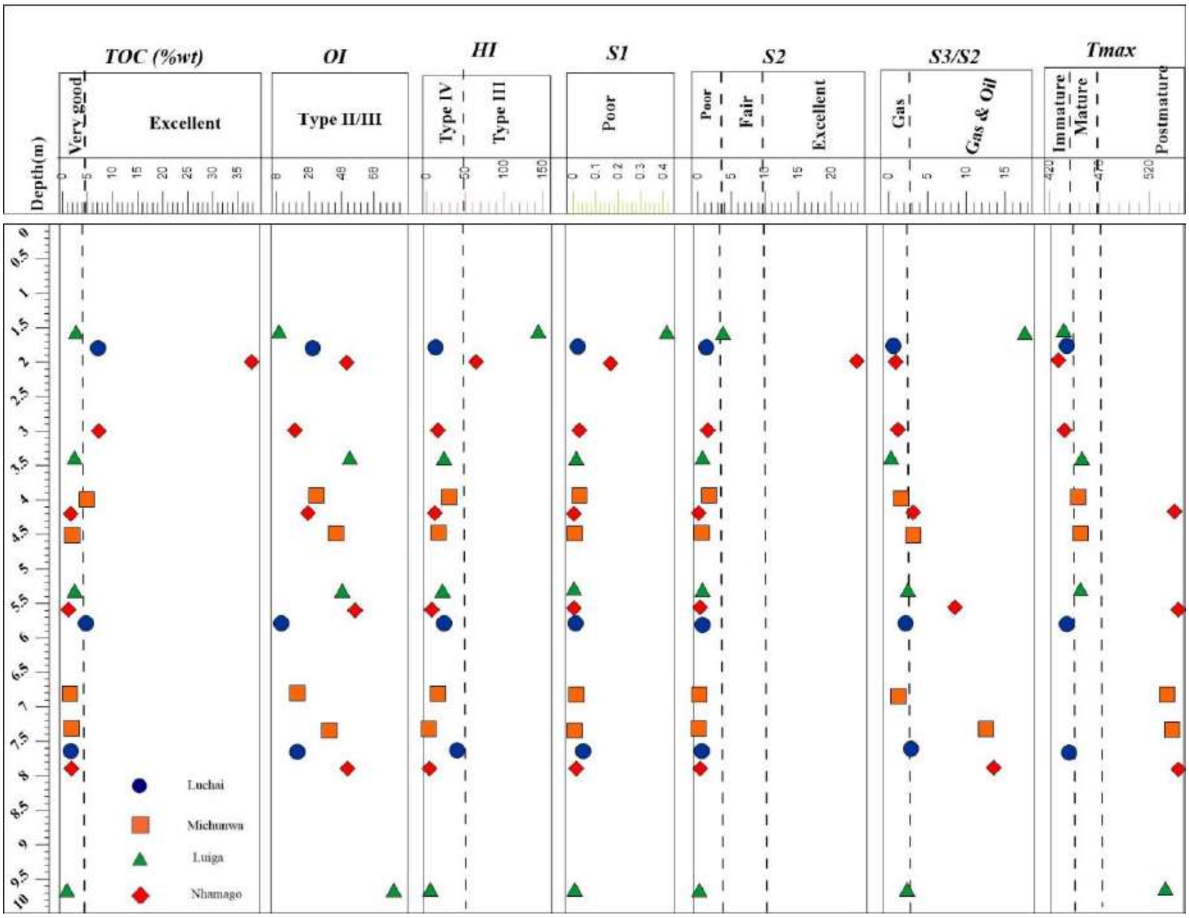

Figure 5. Geochemical log of the four studied outcrops from the Maniamba Basin, Niassa, showing different parameters analysed through Rock Eval pyrolysis data.

Types of kerogen

The types of kerogens (organic matter) are defined by hydrogen and oxygen indices (HI and OI, respectively) (Tissot and Welte, 1978; Waples, 1985; Van Krevelen, 1993). Kerogen types with HI above 600 mg/g rock have an excellent potential for oil generation (Waples, 1985). HI between 150 and 300 mg/g indicates a mixture of kerogen Type III and II, suggesting that the rocks are capable of generating mixed gas and oil, but mainly gas. Kerogen with HI below 150 mg/g indicates mainly type III kerogen, regarded as potential source rock for gas generation. Most of the studied units display low HI values ranging from 1 to 36 (Table 1).

According to Geel et al. (2015), the oil released from kerogen might be adsorbed into the surface of the clay minerals thus lowering the HI values in the Karoo Basin. This fact would reduce the S2 peak and as a consequence reduce the HI values. Further, research performed by Geel et al., 2015 in the Lower Permian Whitehill Formation, Karoo Basin in South Africa indicated that the low HI values in this Karoo Formation has been linked to high clay content, high sulphur content and the presence of solid bitumen. This can be a likely explanation for the Maniamba Basin. In addition, the low HI values for the studied outcrops are indicative of absence of significant amounts of oil-generative lipid materials and the presence of kerogen that is mainly type III or type IV. Additionally, based on the HI versus OI and S2 versus TOC plot diagrams (Figures 6A and 6B), the results show a mix of kerogen type II/III, III and IV.

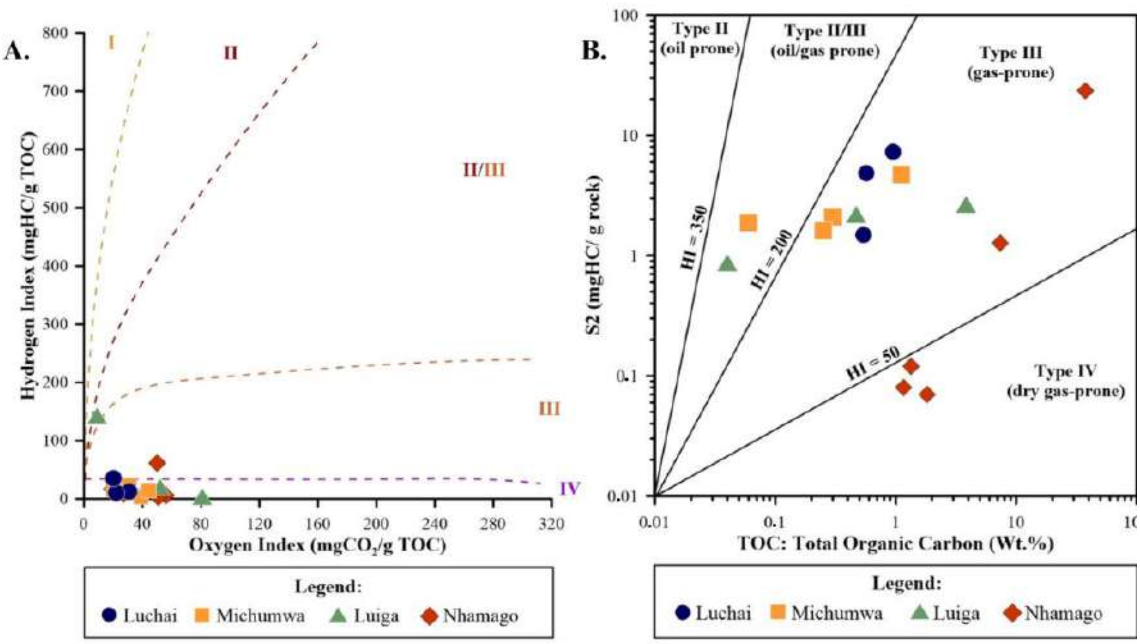

Figure 6. Modified van Krevelen's diagrams illustrating kerogen types of source established from organic geochemical parameters (A) Hydrogen Index (HI) versus Oxygen Index (OI), (B) S2 versus Total Organic Carbon (TOC) plots showing the distribution of different types of kerogen in the outcrop samples modified after Espitalié et al. (1977).

However, the majority is classified as kerogen type III and IV and a few as kerogen type III and type II/III. In the studied area, carbonaceous shales, coal-bearing strata and terrigenous plant materials such as the Permian *Glossopteris* flora have been reported (Araújo et al., 2020) which is consistent with the obtained kerogen types. Moreover, low HI and higher OI values confirm the idea that organic matter is derived mainly from terrestrial sources with non-existent algal content as shown in the organic facies Figure 7.

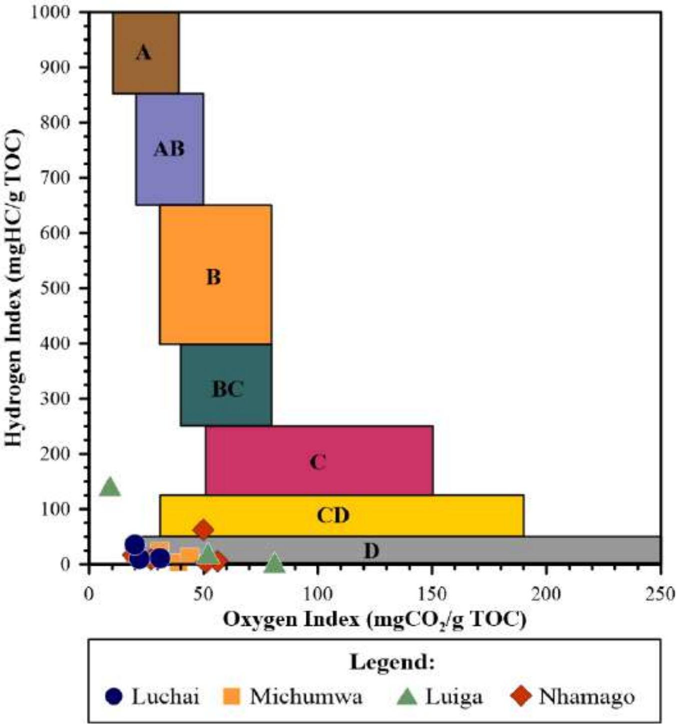

Figure 7. Hydrogen Index (HI) versus Oxygen Index (OI) cross plot indicating the organic facies adapted from Jones (1987).

Thermal maturation and influence of local geology

The composition of the OM changes its properties with increasing pressure and temperature. These conditions can generate either oil or gas. For oil generation a Tmax interval of 435º C to 465º C is necessary (Tissot and Welte, 1978). In regard to gas generation, a minimum Tmax value of 470º C is needed (Espitalie et al., 1997).

In the present study, the Tmax values for the Nhamago samples show immature to postmature rocks (Figure 8). Mature rocks for oil generation are found in the Luchai outcrop (Figure 8). The Michunwa data point to mature to supermature in these samples. Further, the data from the Luiga outcrop show early mature levels to postmature (Figure 8). The large variability of Tmax data can be associated with several effects such as intrusions, oxidation and reworking, alpha irradiation, natural impregnation or contamination by drilling fluids or due to the presence of faults (Peters and Cassa, 1994; Bordenave et al., 1993; Ade, 2000; Sydnes et al., 2019). Additionally, the lack of linear trend in the Tmax values can be associated with the clay mineral content as suggested by Gao et al. 2019. According to Gao et al. (2019), different clay minerals can have different effects on different types of kerogens thus influencing the Tmax values. For instance, with the ratio of kerogen/clay minerals changing, the Tmax can also be affected. The impact of mineral matrix on Rock Eval pyrolysis data has been documented by several researchers (Espitalié et al. 1977; Espitalié, 1986; Peters, 1986; Hazra et al., 2018; and others). Aside from Tmax, other thermal maturity parameter analysed is the Production Index (PI). The PI has been used to interpret the thermal maturity of organic matter (Peters and Cassa, 1994; Nazir and Fazeelat, 2017a, 2017b). According to the aforementioned authors, samples with PI values less than 0.05 might be indicated as immature and as having generated little to no petroleum. Additionally, samples with PI values ranging from 0.05 and 0.10, can be assumed to have yielded very little oil and may have reached the wet gas zone. Finally, if PI values exceed 1.0, then the ability of the kerogen to yield hydrocarbons may have been depleted. For the studied material the Tmax corroborates with PI values indicating mature to postmature source rocks within oil and gas generating zone. Samples at postmature levels cannot generate liquid hydrocarbon, but can act as a potential rock for dry gas (Khan et al., 2022).

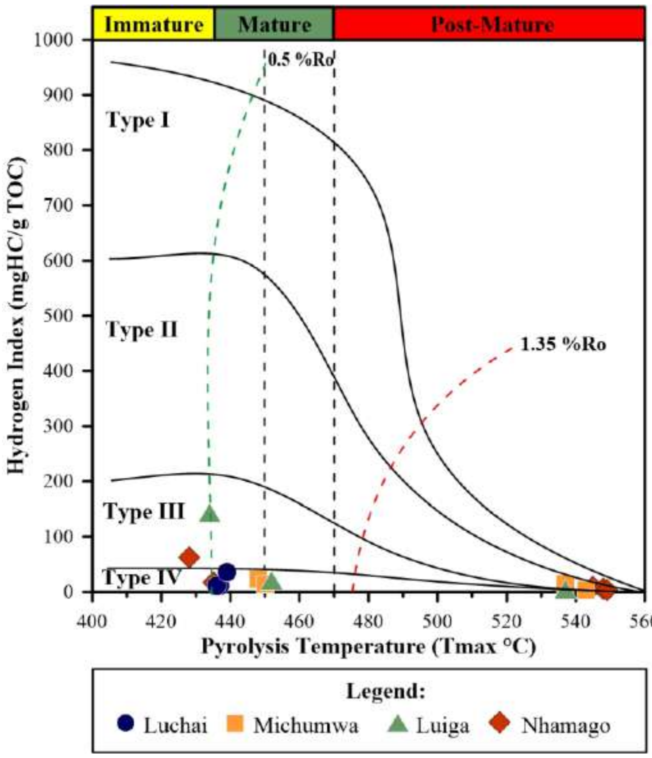

Figure 8. Hydrogen Index (HI) versus Tmax cross plot showing the maturity and type of kerogen in the outcrop samples adapted from Van Krevelen (1993).

In the studied area different geological events may have contributed to the different level of maturation of the sediments in the Maniamba Basin. For instance, the reported kimberlite intrusions that represent the first or second stage of rifting of the Metangula graben (Verniers et al., 1989; Key et al., 2007) (Figure 9). The kimberlite dykes from the Maniamba Basin are reported from Micuela, Tulo and Nhamago sites (Figure 9). The aforementioned kimberlites pipes cut through lower and middle Karoo rocks and consolidated lower Karoo sandstones (Figure 9). In the studied outcrops, only Luchai and Nhamago sites are situated closer to the kimberlite intrusions. The Luchai area present Tmax values representatives of no influence by igneous intrusions. On the other hand, the Nhamago site display greater Tmax values which can represent an influence by the existing kimberlite intrusions in the area. However, further studies based on a large sample size and a systematic approach should be undertaken in order to differentiate reliably the effects of local burial and heating due to the emplacement of the intrusive in the area of study. Additional, should be hypothesised the contribution of the East African rift during the Late Tertiary. The East African rift affected the Metangula area forming the Niassa Lake and a small horst which runs along the Niassa Lake from Metangula over Messumba to near Likoma Island in

Malawi (Verniers et al., 1989). The contribution of the rift system should be further investigated.

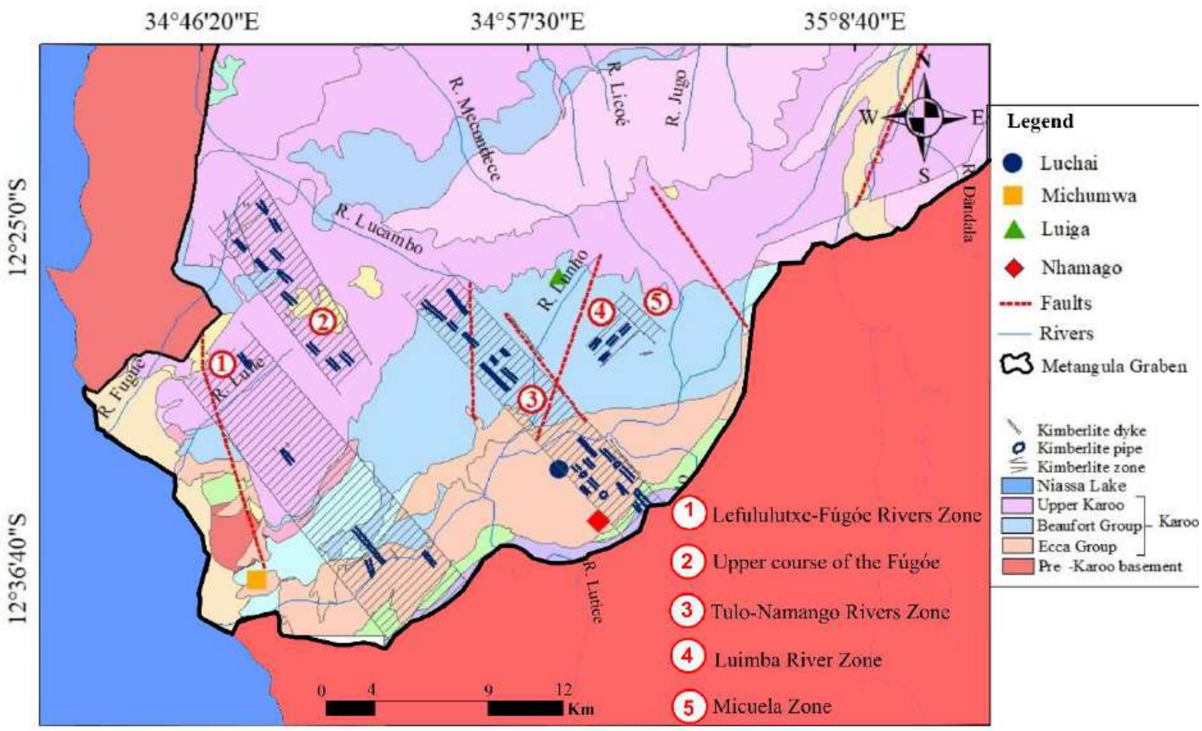

Figure 9. Map showing the influence of kimberlite intrusions in the maturation of the studied samples adapted from Key et al. (2007).

Nature of hydrocarbons and its potential

Regarding migration, the variables S1 versus TOC pointed out to an indigenous nature to the studied samples (Figure 10). This fact can also be supported because all the source rocks contain an expected level of S1 hydrocarbons for their given TOC, and hence, are predominantly indigenous as suggested by Hunt (1995). Moreover, the low values of the S1 yield compared to S2 also suggest the indigenous nature of the hydrocarbon present. On the other hand, the potential for oil production capacity has been plotted using the plot of S1 versus TOC. For the studied samples, only one sample from Luiga (as pointed out above) indicates an oil producible potential as shown in Figure 11. However, more samples will be needed to confirm the oil-generation potential for the studied sites.

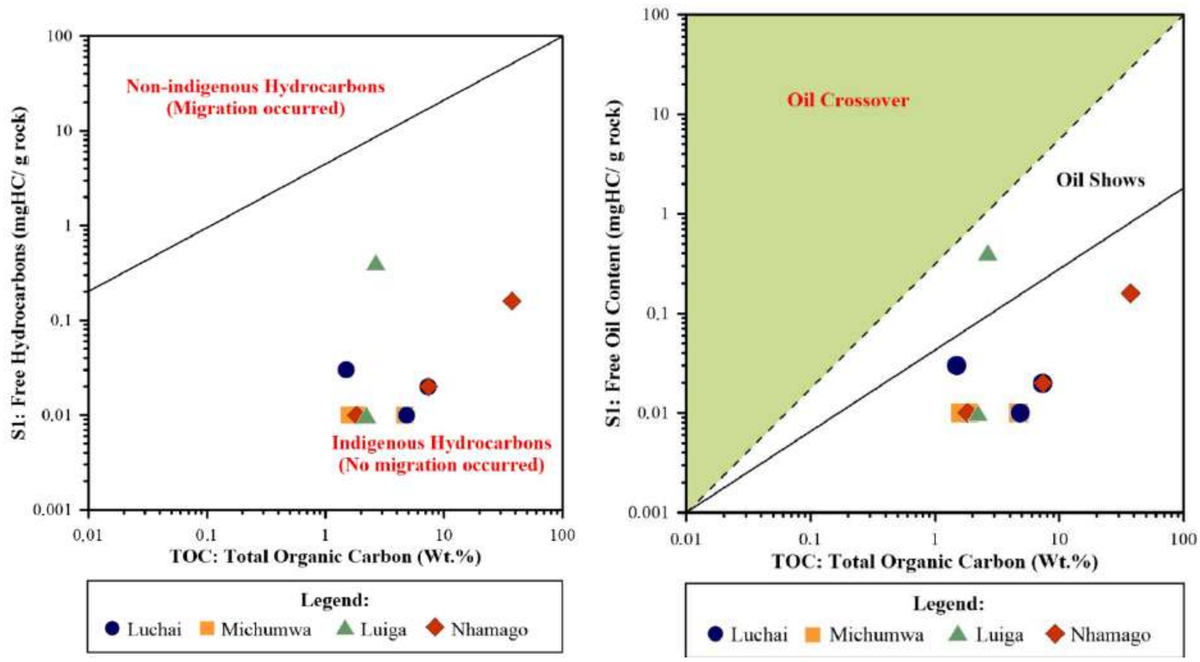

Figure 10. Cross plot S1 versus Total Organic Carbon (TOC) shows the nature of the hydrocarbons within the outcrops adapted from Hunt (1995) and Figure 11 (right side). Free Oil content versus Total Organic Carbon (TOC) showing oil crossover effect from the outcrop samples obtained from Mussa et al. (2018).

Karoo-aged basins with similar organic geochemistry properties

Similar patterns regarding the organic content observed in the studied outcrop are observed in some Gondwana units of similar ages (Figure 12 and Table 2). The first obvious example occurs in the Moatize-Minjova Basin (Karoo Basin of Central Mozambique). In the aforementioned Basin, the target outcrops are from the Lower Permian Vúzi Formation and Moatize Formation. The organic matter of the Lower Permian Vúzi Formation is classified as Type IV Kerogen with low HI suggesting very little potential for gas generation. Some samples from the present study display this scenario. In the same basin, the Moatize Formation (Lower to Middle Permian) according Fernandes et al., 2015, is characterised by having a mixed kerogen type II-III and type III with high TOC values (>4 wt%), moderate values of HI indicating a potential for thermogenic gas generation. The maturation values indicate the end of oil generation and onset of gas generation (Fernandes et al., 2014). The organic matter content in this Formation is similar to some units from the studied sites. All the studied outcrops show a mixed type II-III kerogen. The type II kerogen is only restricted to the Nhamago and Luiga outcrops.

Another surveyed basin, which occurs in the Tete province is the Sanangoé Mefidezi Basin which, according to Mahabeer (2017), shows samples with potential for oil generation, wet gas and dry gas based on the colour of selected sporomorphs. Mahabeer result suggests the occurrence of organic matter type II, mixed type II-III, type III and IV. These results are comparable with the data obtained from the outcrops described herein, however, no type II kerogen is identified for the sites. Regionally, ten Karoo-aged basins have also been surveyed in terms of the organic matter properties, the Ruhuhu and Tenga basins in Tanzania, the Main Karoo and Tuli Basins in from South Africa, the Moatize Minjova and Sanangoé-Mefidezi Basin in Mozambique, the Cahora Bassa and Mid-Zambezi basins in Zimbabwe and the Luangwa Basin in Zambia.

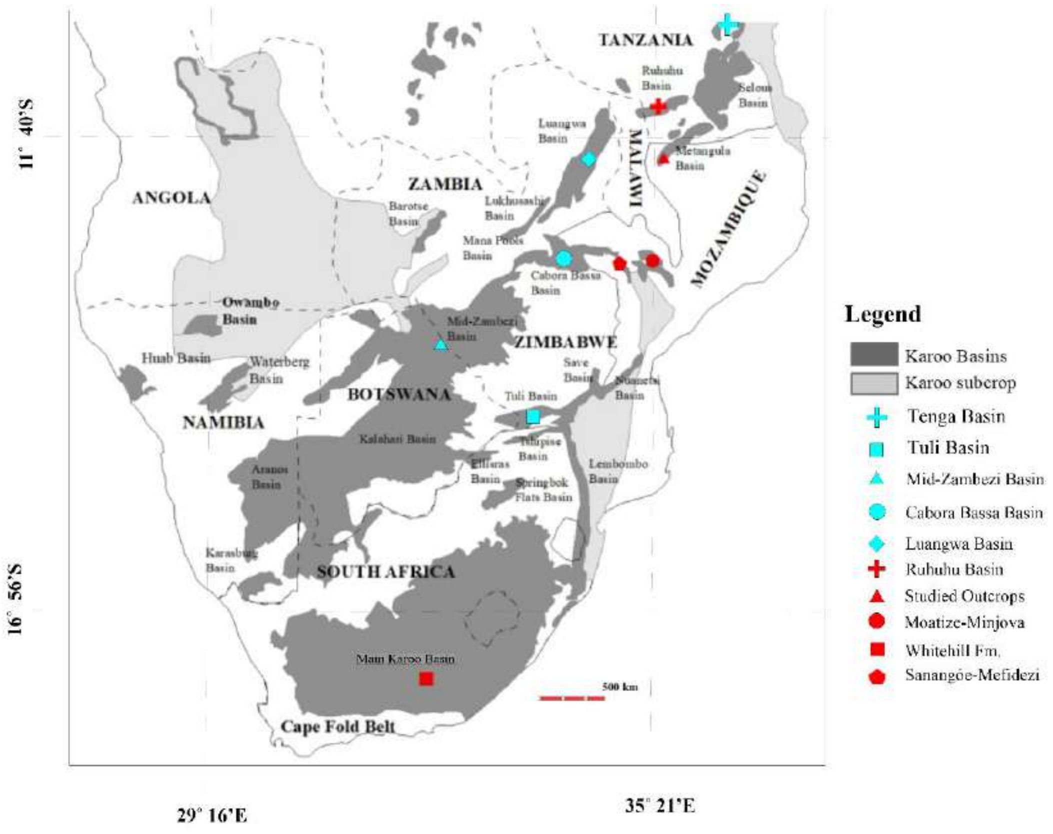

Figure 12. Karoo Basin map illustrating the comparable Karoo sites based on the organic matter properties used in the present study.

The Lower Permian sedimentary rocks from the Ruhuhu Basin in Tanzania display moderate source rock properties (Kreuser et al., 1988). These rocks are mature and placed within the oil window. Kerogen type III is typical for the Ruhuhu Basin. Interestingly, this pattern is observed for the sediments from the Upper Permian in the same basin (Kreuser et al., 1988.). The studied sections in the Ruhuhu Basin display close similarities to those observed from Nhamago and Luiga outcrops. The Karoo sedimentary rocks from the Tenga Basin in Tanzania display type III and mixed type II/III kerogen which is correlatable with the sediments of the studied outcrops because all of the studied show this type of kerogen. Additionally, the black shales of Whitehill Formation in South Africa contain bisaccate pollen of terrestrial origin. An average of 4.5 weight TOC was also observed suggesting that it contains type II kerogen reflecting high level of maturity. The source of OM is of mixed origin (both type II and type III kerogen). The Whitehill Formation (Main Karoo Basin) and the Tuli Basin are rich in TOC being suitable for gas exploration (Geel et al., 2015; Akintola et al., 2023). Because these formations showed a mixed type II and type III kerogen can be correlated with two outcrops of the studied material, Nhamago and Luiga respectively. Other analysed Karoo-age basins such as Cahora Bassa Basin, Mid Zambezi Basin in Zimbabwe, and Luangwa Basin in Zambia have demonstrated close affinities with the studied outcrops, however an exception is observed in the Cahora Bassa Basin (Table 2). In the Cahora Bassa Basin, a type I kerogen is observed and is associated with high latitude lake deposit capable of generating oil (Hiller and Shoko, 1996) (Table 2). In summary, a good correlation within the Karoo Basin can be extrapolated, however more data from some unexplored basins are still needed.

Table 2 The Maniamba Permian outcrops compared with other Karoo sites in terms of organic geochemistry properties

Organic Matter Content	**Whitehill Formation (Lower Permian shale, Karoo Basin) Geel et al., 2015**	**Tuli Basin, South Main Karoo Basin, Akintola et al., 2023**	**Vúzi Formation (Lower Permian) Moatize-Minjova Basin Fernandes et al., 2015**	**Moatize Formation (Lower-Middle Permian) Moatize-Minjova Basin Fernandes et al., 2015**	**Sanangoé Mifedezi Basin Mahabeer, 2017**	**Ruhuhu Basin (Lower and Upper Permian) Kreuser et al., 1988**	**Cahora Bassa Basin, Zimbabwé Hiller and Shoko, 1996**	**Mid Zambezi Basin, Zimbabwe, Hiller and Shoko, 1996**	**Luangwa Basin, Zâmbia Utting and Wielens, 1992**	**Tenga Basin, Tanzânia, Mallah and Sanga, 2022**	**Outcrops (Maniamba Basin) In this paper**
Vitrinite reflectance (%Ro)	4.0	1.19-1.30	1.3-1.69	1.3-1.69	No data	0.5-0.8	<0.5-1.0	<0.5-1.0	0.60-0.94	No data	No data
Tmax (^{0}C)	≥ 563	464–470	≤ 440	≤ 436	No data	No data	430-450??	430-450	No data	No data	428-549
TOC (%t)	07. to 8.15	47.0	0.9 to 2.4	<4.0	No data	No data	> 0.5	>0.5	No data	No data	0.87 to 4.84
Kerogen Types	Mixed of type II and type III	Type III and Mixed type II/III	Type IV kerogen	Mixed of type II-III and type III	Mixed type II-III, type III	Type III kerogen	Mixed type II-III, type I and type III	Type II, Mixed type II/III and type III	Type II, III and IV	Type III and mixed type II/III	Mixed type II-III, type III and type IV

Conclusions

Rock Eval analysis coupled with TOC and kerogen analysis from four outcrops of Permian and Early Triassic ages in the Maniamba Basin were investigated herein. This research was carried out in order to evaluate its source rock potential of the sampled sediments. The main conclusions are as follows:

- The OM within the four outcrops is mainly dominated by kerogen type III, IV with minor mixed II/III kerogen.
- Low values of HI are observed at almost all outcrops.
- The observed kerogen is thermally mature to postmature due to proximity to igneous intrusions (e.g., kimberlite dykes).
- The lower HI and higher OI of OM indicates three organofacies C, CD and D and a kerogen dominated by terrestrial OM within an oxic environment.
- The studied sections revealed to be good to excellent source rocks with regard to organic richness.
- No marine source rock has been identified for the Karoo basins. The Moatize Minjova (Mozambique), Sanangoé-Mefidezi (Mozambique), Ruhuhu Basin, Cahora Bassa Basin (Zimbabwé), Luangwa Basin (Zambia) and Main Karoo Basin (South Africa) have demonstrated close similarities with the sediments from four outcrops of the Maniamba Basin in terms of their organic geochemistry properties. However, an exception is the occurrence of type I kerogen in the Cahora Bassa Basin (Zimbabwe) which is interpreted as high latitude lake deposit capable of generating oil.

All in all, it has been demonstrated herein that the rocks from the Maniamba outcrops possess suitable organic richness and source rock potential, and therefore in the future these sections might be of more interest in terms of hydrocarbon prospectivity. However, more studies are needed in this Basin using other proxies such as vitrinite reflectance, palynofacies, elemental analysis, x-ray diffraction, isotopes and biomarkers in order to improve the data presented herein regarding the determination of the potential for hydrocarbon generation and the contribution of igneous intrusions to the maturation of the studied organic matter.

References

Ade, M., 2000. Caracterização da Matéria Orgânica Dispersa através da técnica de Pirólise “Rock-Eval II” Vantagens e Limitações para a Geologia. Pesquisa em Geociências, 27,43–50.

Akintola, A., Dacosta, F., Rupprecht, S., and Mhlongoa, S.E., 2023. Petrographic, mineralogical, morphological and organic constraints of the Permian shaly-coal in the Tuli Basin of Limpopo-Area Karoo-Aged basin, South Africa: Implication for potential gas generation. Heliyon, 9, e14446, 15pp. doi.org/10.1016/j.heliyon.2023.e14446.

Araújo, R., Macungo, Z., Smith, R., Tolan, S., Angielczyk, K., Crowley, J., Milisse, D. and Mugabe, J., 2020. The first Lower Triassic tetrapod fossils from Metangula Graben (Niassa Province, Mozambique) and their biostratigraphic significance. Palaeontologia africana, 54, 56-68.

Bordenave, ML., Espitálie, J., Leplant, P., Oudin, JL., and Vandenbroucke, M., 1993. Screening techniques for source rock evaluation. In: Bordenave, M.L. (Ed.), Applied Petroleum Geochemistry Editions, Paris, 217–278.

ECL., 2000. The Petroleum Geology and Hydrocarbon Prospectivity of Mozambique. ENH, 144pp. Unpublished report.

Espitálie, J., Madec, M. and Leplat, P., 1977. Source rock characterization method for petroleum exploration: Proceedings of the Ninth Offshore Technology Conference, Houston, 439-442.

Espitalié, J., Deroo, G. and Marquis, F., 1985. La pyrolyse Rock-Eval et ses applications. Revue de l'Institut français du Pétrole 40, 755–784.

Fernandes, P., Rodrigues, B., Jorge, R. and Marques, J., 2015. Potencial gerador de hidrocarbonetos dos argilitos carbonosos das Formações de Vúzi e de Moatize (Karoo Inferior) da Bacia Carbonífera de Moatize–Minjova, Província de Tete, Moçambique. Comunicações Geológicas, 101, 433-437.

Gao, X., Wang, P., Li, J., Wang, M., and Ma, W., 2019. Influencing factors of the Tmax parameter in Rock-Eval pyrolysis, IOP Conf. Series: Earth and Environmental Science, doi:10.1088/1755-1315/360/1/01201.

Geel, C., Booth, P., De Wit, M. and Schultz, H.M., 2015. Palaeoenvironment diagenesis and characteristics of Permian Black Shales in the Lower Karoo Supergroup flanking in the Cape Fold Belt near Jansenville, Eastern Cape, South Africa: Implications for the shale gas potential of the Karoo Basin. South African Journal of Geology, 118, 249-274.

Hao, F., Zhou, X., Zhu, Y. and Yang, Y., 2011. Lacustrine source rock deposition in response to co-evolution of environments and organisms controlled by tectonic subsidence and climate Bohai Bay Basin, China. Organic Geochemistry, 42,323–339.

Hazra, B., Wood, D., Varma, A., Sarkar, B., Tiwari, B., and Singh, A., 2018. Insights into the effects of matrix retention and inert carbon on the petroleum generation potential of Indian Gondwana shales. Marine and Petroleum Geology, 91,125–138.

Hiller, K. and Shoko, U., 1996. Hydrocarbon source rock potential of the Karoo in Zimbabwe. Journal of African Earth Sciences, 23, 31-43.

Hunt, J. M. (1995). Petroleum geochemistry and geology (textbook). Petroleum Geochemistry and Geology, 24, 109–110.

JOGMEC., 2015. The results of drilling survey III in Mozambique. JOGMEC Unpublished report, National Directorate of Geology and Mines, Mozambique. 40pp.

Jones, R.W., 1987. Organic Facies, In: Brook J., Welte D. (Ed.), Advances in petroleum geochemistry. Academic Press, New York,pp.1-90.

Key, R.M., Bingen, B., Barton, E., Daudi, E.X.F., Manuel, S., and Moniz, A., 2007. Kimberlites in a Karoo graben of northern Mozambique: Tectonic setting, mineralogy and Rb-Sr geochronology. South African Journal of Geology, 110, 111–124.

Kihle, R., 1983. Recent surveys outline new potential for offshore Mozambique. Oil and Gas Journal, 28, 126-134.

Khan, N., Ullah, W., Siyar, S., Wadoo, B., Ayyub, T., and Ullah, T., 2022. Hydrocarbon source rock assessment of the shale and coal bearing horizons of the Early Paleocene Hangu Formation in Kala-Chitta Range, Northwest Pakistan. Journal of Petroleum Exploration and Production Technology, 12, 2155–2172, doi.org/10.1007/s13202-021-01433-6.

Kreuser, T., Schramedei, R. and Rullkoter, J., 1988. Gas prone source rocks from Cratogene Karoo Basins in Tanzania. Journal of Petroleum Geology, 11, 169-184.

Lafargue, E., Marquis, F. and Pillot, D., 1998. Rock-Eval 6 applications in hydrocarbon exploration, production and soil contamination studies. Oil and Gas Science Technology, 53, 421-437.

Lineback, J.A., Keal, J. and Burroughs, K., 1986. Source rock potential of East Africa progress report and preliminary geochemical data and interpretation for Mozambique and additional wells in Somalia, Ethiopia and Madagascar. Robertson Research. 400 pp.

Loegering, M.J. and Milkov, A.V., 2017. Geochemistry of Petroleum Gases and Liquids from the Inhassoro, Pande and Temane Fields Onshore Mozambique. Geosciences, 7, 33, doi.org/10.3390/geosciences7020033.

Mahabeer, K.C., 2017. Palynology of the Permian Sanangoé-Mefidezi Basin, Tete Province, Mozambique and correlations with Gondwanan Microforal assemblages. Unpublished master dissertation, University of the Witwatersrand, Johannesburg, South Africa. 168 pp.

Mallah, H. and Sanga, J., 2022. Hydrocarbon source rock potential of the Middle Karoo beds in Tanga Basin. Sixth EAGE Eastern Africa Petroleum Geoscience Forum, 1-3.

Mussa, A., Flores, D., Ribeiro, J., Mizusaki, AMP., Chamussa, M, Filho, J.G.M. and Kalkreuth, W.D., 2018. Characterization of organic matter from a stratigraphic sequence intercepted by Nemo-IX well, Mozambique: Potential for hydrocarbon generation. Energy Exploration and Exploitation, 36,1157-1171.

Nazir, A., and Fazeelat, T., 2017a. Geochemistry of cretaceous rocks, Pakistan: II. Interpretation of source, depositional environment and lithology of organic matter. Petroleum Science and Technology, 35, 93–46.

Nazir, A., and Fazeelat, T., 2017b. Geochemical characterization of cretaceous sediments-Sindh Basin, Pakistan. Energy Sources, Part A: Recovery, Utilization, and Environmental Effects, 39, 406-413.

Peters, K.E., 1986. Guidelines for evaluating petroleum source rock using programmed pyrolysis. Bulletin of American Association for Petroleum Geologists, 70, 318–329.

Peters, K.E. and Cassa, M.R., 1994. Applied source rock geochemistry, in Magoon, L.B., and Dow, W.G., eds., The petroleum system–from source to trap. Bulletin of American Association for Petroleum Geologists, 60, 93-120.

Qin, Z., Zhi, D. and Xi, K., 2021. Organic petrology, geochemistry, and hydrocarbon generation capacity of Permo–Carboniferous source rocks in the Mahu Sag, northwestern Junggar Basin, China. Energy Exploration and Exploitation, doi: 10.1177/0144598721102386.

Salman, G., Sheremetiev, Y. and Koblents, A., 1990. The northern part of Mozambique Basin, a report on the geology and the oil and gas potential of Zambezi Licence Block, Mozambique. ENH, Mozambique.127pp.

Sari, A and Aliyev, S., 2006. Organic geochemical characteristics of the Paleocene–Eocene oil shales in the Nallıhan Region, Ankara, Turkey. Journal of Petroleum Science and Engineering, 53, 123–134.

Shalaby, M., Irwan, M., Liyana, N., Osli, L. and Islam, M., 2020. Geochemical characteristics and depositional environments of the Narimba Formation source rock, Bass Basin, Australia. Journal of Petroleum Exploration and Production Technology, 10, 3207–3225, doi.org/10.1007/s13202-020-00992-4.

Sydnes, M., Fjeldskaar, W., Grunnaleite, I., Løtveit, I. and Mjelde, R., 2019. Transient Thermal Effects in Sedimentary Basins with Normal Faults and Magmatic Sill Intrusions: A Sensitivity Study. Geosciences, 9,160, doi:10.3390/geosciences904016.

Utting, J. and Wielens, H., 1992. Organic petrology, thermal maturity, geology and petroleum source rock potential of the Lower Permian coal Karoo supersystem, Zambia. Energy sources, 14, 337-354.

Van Krevelen, D.W., 1993. Coal: typology–physics–chemistry–constitution. Elsevier Science, Amsterdam.

Verniers, J., Jourdan, P.P., Paulis, R.V., Frasca-Spada, L. and De Bock, F.R., 1989. The Karroo Graben of Metangula Northern Mozambique. Journal of African Earth Sciences, 9, 137–158.

Waples, D.W., 1985. Geochemistry in Petroleum Exploration. International Human Resources Development Corporation, Boston.

Shale-gas potential from the K4 Formation (Permian), Maniamba Basin, Mozambique: Insights from integrated geochemical evaluation, elemental analysis and palynofacies.

Adapted from N.E. Nhamutole, M.K. Bamford, P.A. Souza, T.F. Silva, D.A Carmo, C. M. Félix

Paper submitted to South African Journal of Geology (Under review)

Abstract

A total of 65 samples from a Permian borehole in the Maniamba Basin, Mozambique have been analysed in regard to total organic carbon content, Rock-Eval pyrolysis, elemental composition, vitrinite reflectance and palynofacies. The sediments are mostly composed of quartz, enriched in calcite and clay minerals. The deposition of the peat biomass occurred in a non-marine setting characterised by non-oxygen deficient conditions reinforced by higher input of phytoclast, high C/N and C/S ratios, low V/Cr ratios, low hydrogen index, high oxygen index associated with moderate contribution of palynomorphs and AOM. These data are supported by the identified four grouped palynofacies coupled with organofacies C, CD and D. The sediments display organic richness spanning from very good to excellent and potential for hydrocarbon ranging from fair to excellent. The type of kerogen observed herein are II, III, mixed II/III and IV which represents oil prone, gas, mixed hydrocarbons and is immature to postmature in the anthracite to meta-anthracite bituminous rank. The kimberlite intrusions and the clay mineral content may be the factors that control the thermal maturity trends. In its turn, the content of major element (e.g., log (Fe_2O_3/K_2O) versus log (SiO_2/Al_2O_3) and other ratios have revealed that the K4 Fm is a result of combined iron shale and shale facies. The protolith is attributed to the intermediate and mafic igneous rocks. The paleoclimate conditions are inferred to be humid and are

responsible for paleoweathering. Discriminated functions has allowed to pinpoint the environment of depositional as pertaining to an active continental margin and oceanic island arc under oxic-anoxic conditions. The integrated proxies point out for the existing potential for hydrocarbon generation.

Introduction

Although there is an increase of use of renewable energies in the world, it has been estimated that regardless of this trend there might be an increase of hydrocarbon use by 2030 of up to 41% (Hydrocarbon Processing, 2014). This fact reinforces the need for continued research in new potential sites for hydrocarbon exploration, mainly gas, which is regarded a clean energy resource. This case is applicable for the Maniamba Carboniferous Basin (MCB) in Mozambique. Some of the key studies carried out in the MCB aiming at surveying sources of energy (coal) were done by Verniers et al. (1989), Vale (2014) and JOGMEC (2016). Since these studies, the MCB has been surveyed recently in terms of its hydrocarbon potential, however, the survey was only focused on the use of palynofacies (Nhamutole et al., 2023). Moreover, researchers only analysed the K5 Formation (Middle Permian, Figure 1) justifying the fact that there is a need for the assessment of all the strata of the MCB using combined techniques. Similarly, in another paper (Nhamutole et al., 2023), they completed a pilot study of eight sample sediments from outcrops of the K4 Formation. Their preliminary study on the few samples indicated that a detailed study based on more data is crucial. The present study is aimed at bringing a better interpretation by combining different proxies that include palynofacies, organic geochemistry, elemental analysis and organic petrography in order to get better insights regarding the environment of deposition, thus improving the existing knowledge regarding the hydrocarbon potential in the K4 Formation, Lower Permian from the Maniamba Basin. These combined techniques represent one of the specific aspects of organic facies research technique yet have proven to be efficient in the identification of depositional environments, organic matter's provenance, quality, quantity and type. Other examples using these proxies for establishing the oil and gas source rock characterization can be found in Deaf and Tahoun (2018), Abou Ela et al. (2018), Hunt (1995), Karg and Sauerer (2022), Mussa et al. (2021), Nazir et al. (2020), Peng et al. (2022), Zhang et al. (2015), Zobaa et al. (2011).

According to the existing literature, the current research represents the first organic petrography study of the K4 Formation integrated with petroleum geochemistry and visual kerogen analysis to assess the hydrocarbon potential of this historically neglected basin in Mozambique.

Geology of the Maniamba Basin

The details regarding the geology of the K4 Formation are found in section 5.1.

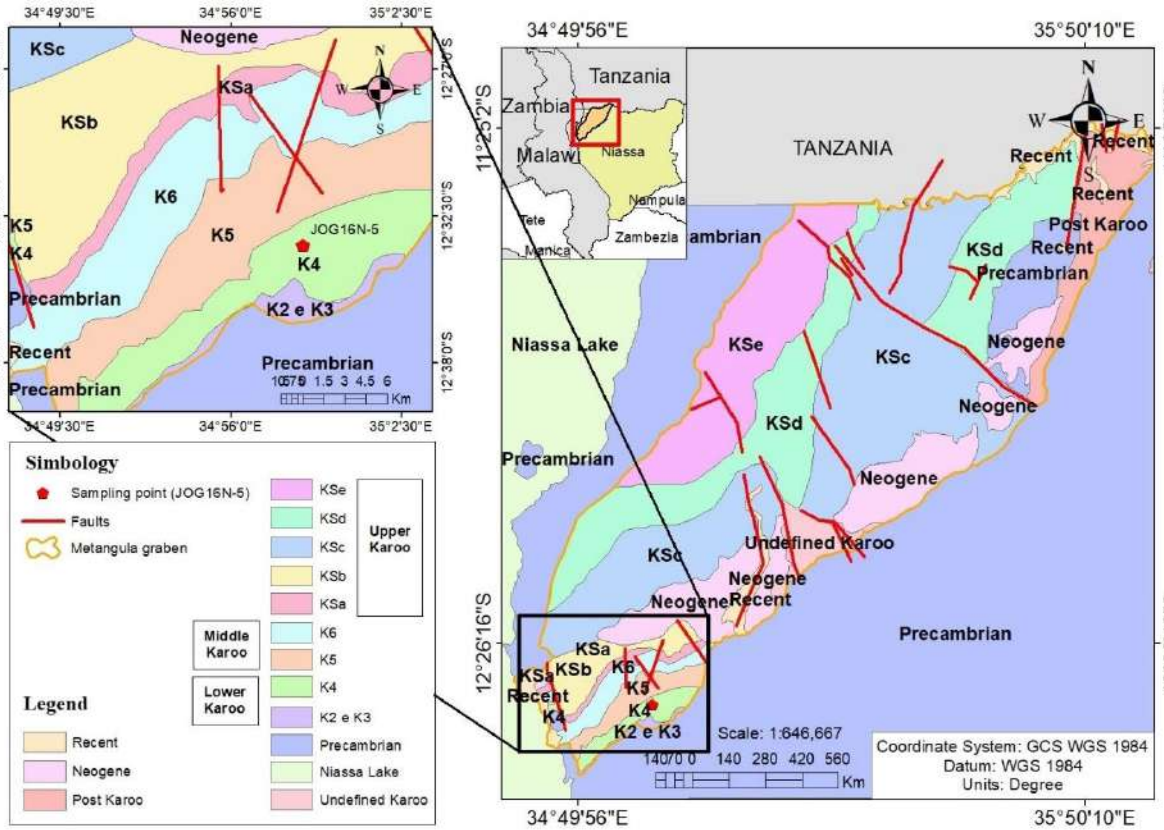

Figure 1. Geology and stratigraphy of the Maniamba Basin adapted from Verniers et al. (1989).

Kimberlite Intrusions

The details regarding the kimberlite intrusions from the Maniamba Basin are found in section 5.1.4.

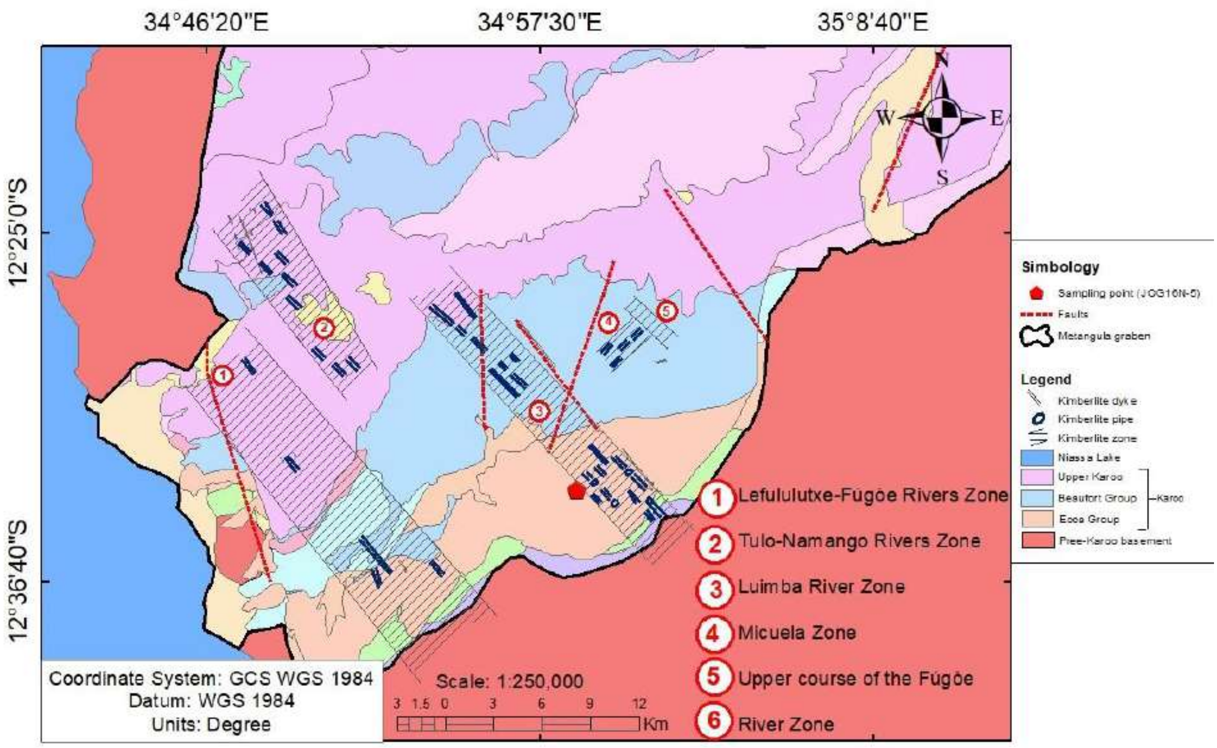

Figure 2. Map of Kimberlite intrusions in the Maniamba Basin adapted from Key et al. (2007).

Methods and Materials

The research described herein consists of 65 samples subsampled from one borehole core drilled by JOGMEC (Japan Oil, Gas and Metal National Corporation) in the Maniamba Basin (MB), K4 Formation (Figure 3). Total organic carbon (TOC), Rock Eval, vitrinite reflectance, palynofacies and elemental composition were used herein. Each method is described in the following section. Laboratory analysis regarding Rock eval, palynofacies, vitrinite reflectance, and elemental analysis are found in sections 6.1.1, 6.2, 6.3.1, 6.4.

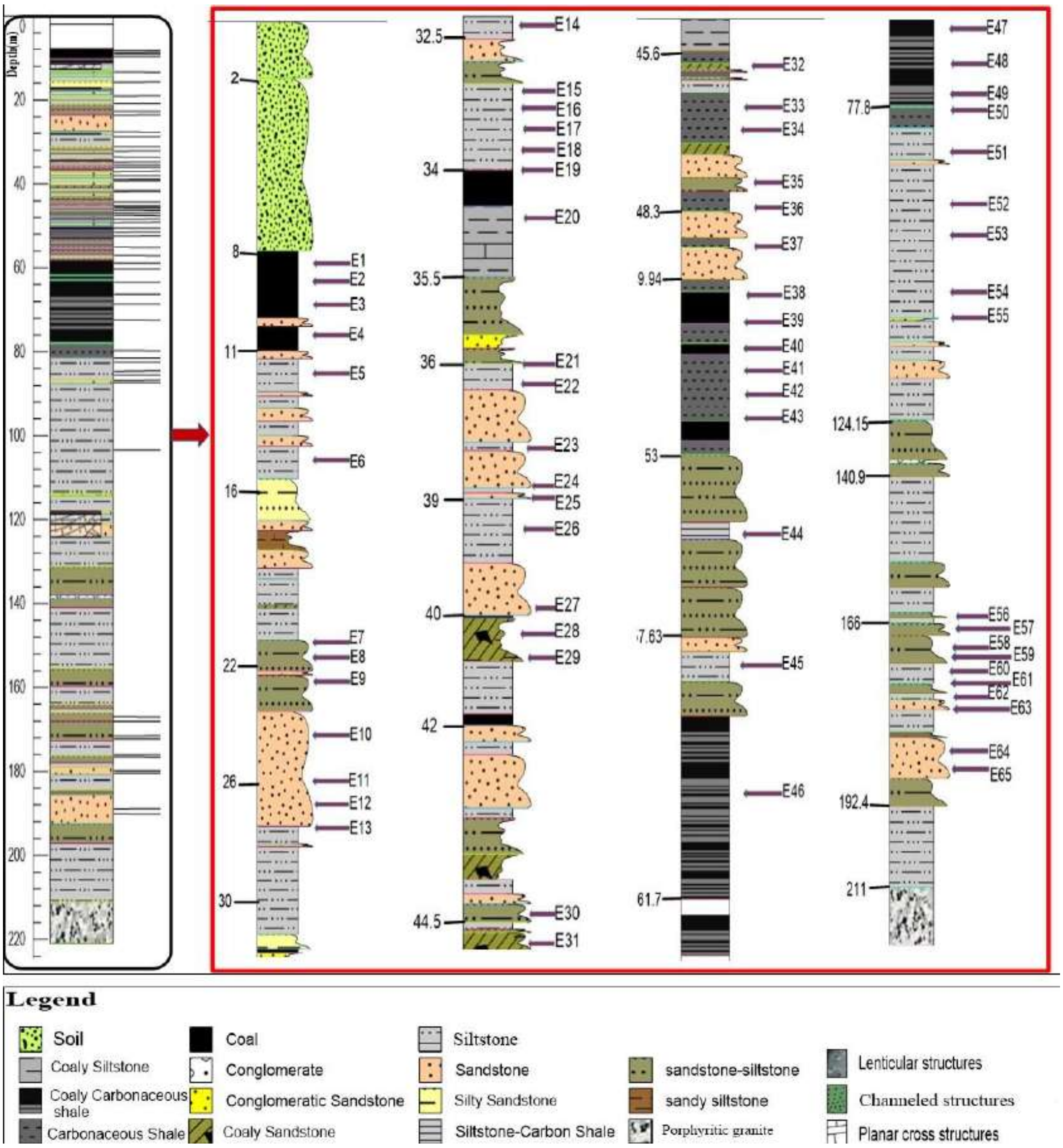

Figure 3. Lithological profile of the studied area indicating the sampling points.

Results

TOC and Rock eval pyrolysis

The obtained results have demonstrated considerable distribution with regard to TOC content, spanning from 0.26 to 21.5 wt% (Table 1 and Figure 4). The highest values of TOC are observed at the top of the sequence and lowest at the bottom (Table 1). The S1 varies from 0 to 0.21 (Table 1 and Figure 4). The S2 values are higher than the S1 values in all samples. The T_{max} of the samples vary from 354 to 586°C indicating stages ranging from immature to postmature rocks with no linear trend with depth.

Similarly, data from organic petrography have showed vitrinite reflectance measurements ranging from 0.54 to 1.57% Rrandom as observed in the Table 1.

Table 1. Results of the TOC, Rock Eval pyrolysis and vitrinite reflectance of the JOG16N-5 borehole.

Depth (m)	S1 (mg HC/g rock)	S2 (mg HC/g rock)	S3 (mg CO2/g TOC)	PI	Tmax (^{0}C)	TOC (Wt%)	HI (mg HC/g rock)	OI (mg CO2/g rock)	Ro (%)
8.55	0.07	31.91	2.11	0.002	430	21.5	148	9	0.62
9.17	0.03	12.42	0.65	0.003	431	11.41	108	5	
9.5	0.04	8.13	0.68	0.005	432	7.28	111	9	
13.2	0.07	18.99	0.61	0.004	431	9.21	206	6	
15.67	0.01	0.08	0.31	0.143	509	1.36	6	23	
18.8	0.01	0.21	0.28	0.075	516	1.5	14	18	
20.67	0.08	17.6	0.9	0.006	431	14.79	118	6	
22.6	0.02	0.77	0.37	0.037	445	2.21	34	16	
23.4	0.02	0.44	0.46	0.057	457	1.73	25	26	
23.58	0.1	5.31	0.53	0.019	438	4.91	108	10	
28.6	0.06	1.84	0.36	0.033	445	3.83	48	9	
30.93	0.02	0.33	0.41	0.06	508	1.78	18	23	
33.18	0.03	1.83	0.59	0.019	451	4.7	38	12	0.71
33.46	0.02	0.26	0.33	0.107	438	1.67	15	19	
33.75	0.06	20.5	0.61	0.004	429	8.96	228	6	
34.6	0.01	0.82	0.36	0.024	438	1.87	43	19	
35.65	0.01	0.7	0.37	0.025	452	2.48	28	15	
36	0.15	12.13	0.87	0.014	427	7.41	163	11	
36.9	0.05	4.21	0.62	0.012	437	4.19	100	14	
37.96	0.03	1.3	0.64	0.027	442	2.85	45	22	
38.9	0.02	0.71	1.06	0.026	444	2.14	33	49	
39.24	0.02	1.04	0.7	0.029	434	2.33	44	29	
41.44	0.03	1.04	1.77	0.029	435	2.29	45	77	
41.82	0.14	28.02	0.87	0.005	428	16.62	168	5	
44.23	0.21	15.59	1.04	0.014	434	18.67	83	5	0.62
45.2	0.12	12.71	0.78	0.01	431	9.9	128	7	
45.8	0.07	3.89	0.79	0.02	447	6.84	56	11	
46.1	0.04	4.47	0.27	0.011	436	3.35	133	8	
46.89	0.08	31.16	1.03	0.003	428	14.94	208	6	0.54
47.3	0.13	14.7	0.74	0.01	431	8.99	163	8	
48.37	0.03	0.89	0.32	0.038	449	2.72	32	11	
49.18	0.04	2.9	0.38	0.015	435	3.07	94	12	
50	0.04	4.48	0.63	0.01	436	4.78	93	13	
50.1	0.04	5.09	0.59	0.008	434	5.58	91	10	0.72
50.83	0.07	36.42	1.6	0.002	426	15.63	233	10	
51.15	0.03	4.91	0.45	0.007	435	4.83	101	9	
51.73	0.06	7.39	0.81	0.008	437	7.8	94	10	
52.32	0.03	4.21	0.63	0.009	440	5.36	78	11	

55.08	0.03	1.13	0.75	0.036	442	3.03	37	24	
57	0.04	3.6	0.37	0.012	436	4.04	89	9	
58.88	0.07	12.57	0.75	0.006	432	13.83	90	5	0.61
60.23	0.01	0.38	0.2	0.037	433	1.46	26	13	1.57
63.27	0.03	8.52	0.52	0.004	433	6.17	138	8	
66.36	0.01	0.24	0.21	0.057	433	0.84	28	25	
68.54	0.05	14.84	0.71	0.004	425	10.76	137	6	
72.32	0.03	7.1	0.43	0.006	432	5.84	121	7	1.6
79.73	0.01	0.03	0.27	0.433	428	0.54	5	49	
81.37	0.03	2.84	0.68	0.012	448	6.68	42	10	
82.3	0.01	0.1	0.33	0.168	441	1.79	5	18	
84.49	0	0.03	0.19	0.26	371	0.25	10	74	
85.38	0	0.02	0.32	0.438	380	0.54	3	58	
103.32	0.01	0.02	0.29	0.432	354	0.28	8	105	
171.47	0.01	0.23	0.34	0.069	576	3.23	7	10	
172.12	0	0.08	0.24	0.146	586	1.33	5	18	1.48
175.2	0	0.21	0.22	0.047	577	2.36	8	9	1.44
175.9	0	0.32	0.27	0.042	440	2.29	13	11	1.21
176.36	0	0.02	0.2	0.259	371	0.26	7	75	1.33
178.84	0	0.08	0.33	0.151	436	0.95	8	34	1.44
179.82	0.01	0.18	0.41	0.092	566	2.27	7	18	1.43
180.23	0.03	1.32	0.44	0.031	442	4.91	26	9	0.89
188.83	0.01	0.02	0.29	0.519	356	0.84	2	34	1.28
189.94	0.09	1.75	0.44	0.054	509	8.91	19	4	1.38

Abbreviations: S1=free hydrocarbon content; S2 = remaining hydrocarbon or generative potential, S3=the amount of CO2 from breaking oxygen-containing compounds in kerogen at 300-3900; TOC: total organic carbon content; HI: hydrogen index; OI: oxygen index; PI: production index; Ro: vitrinite reflectance.

In regard to other pyrolysis data, the HI ranges from 2 to 206 mg HC/gTOC and the OI ranges from 4 to 105mg/TOC (Table 1). The highest percentage of HI is found at the top of the section and decreases towards the bottom of the studied section. The OI shows a completely different trend (Figure 4). This result corroborates with the obtained parameters such as TOC and S2 values. The HI versus OI figure shows the existence of type III, mixed type II/III and type IV kerogens.

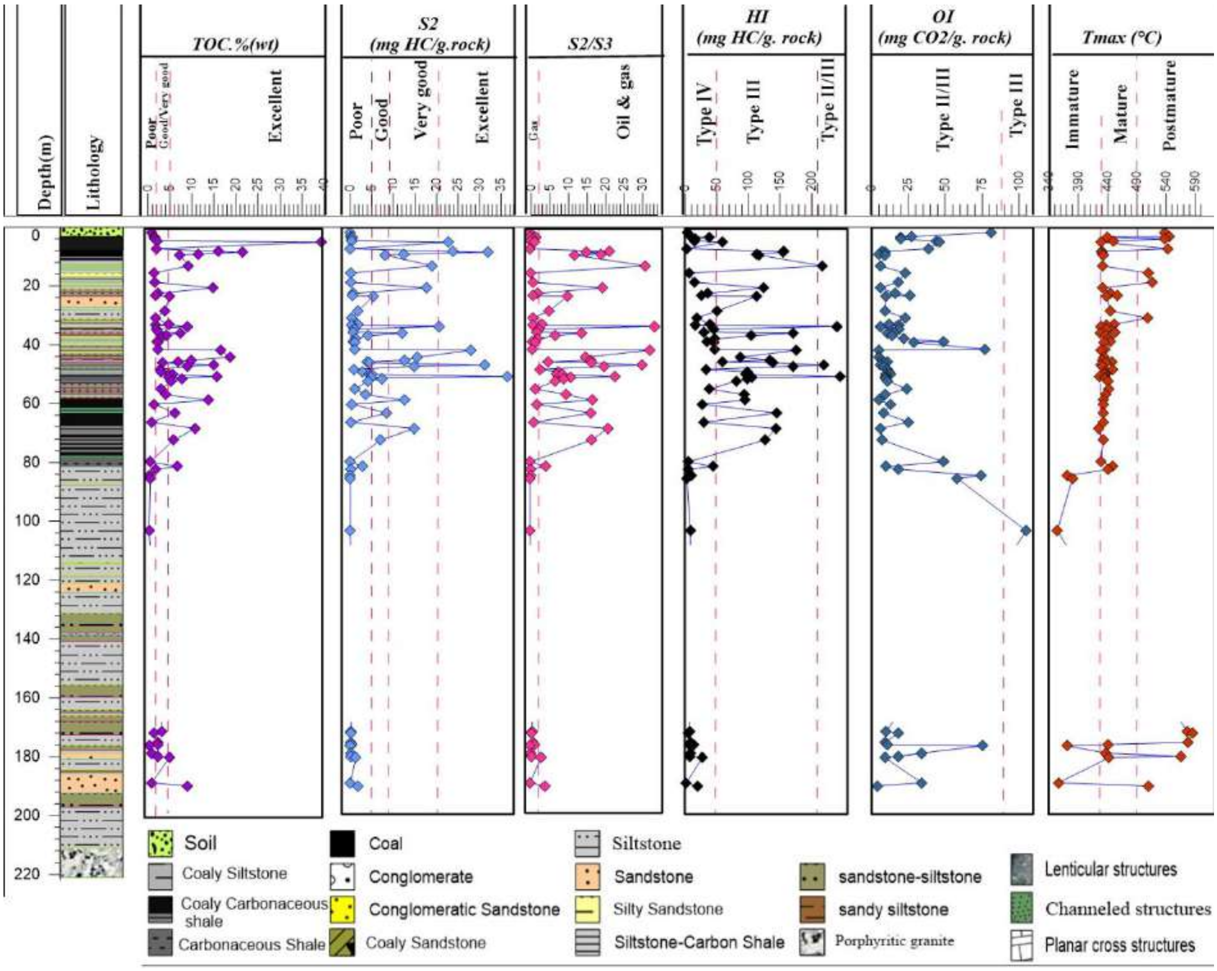

Figure 4. Organic geochemistry log illustrating the variation of the pyrolysis rock eval parameters.

Elemental analysis and provenance

The ash content in the analysed samples varies from 31.3 to 50.8% (Table 2) contributing to the types of kerogens identified herein. The H/C ranges from 0.07 to 0.08 and O/C ranges from 0.03 to 0.20. The number of samples analysed herein is considerably small and the aforementioned interpretation may somehow be misleading as suggested by Durand and Monin (1980). The values of quartz are relatively higher suggesting siliciclastic provenance (Basu et al., 1975). Overall, the abundant major oxides in the studied sedimentary rocks are SiO_2, Al_2O_3, and Fe_2O_3 as shown in Table 2. The lithological variation observed along the K4 Formation corroborates with the common occurrence of quartz and other minerals which is consistent with data from Verniers et al. (1989). The range of the main ratios analysed consist of Al_2O_3/TiO_2 (18.08-22.78%), K_2O/Al_2O_3 (0.07-0.09%), and Ca/Mg>1.

Table 2. Results of elemental analysis of the JOG16N-5 borehole.

Data	Major Oxides and Elements (%)																					
	SiO_2	Al_2O_3	CaO	Cr_2O_3	Fe_2O_3	K_2O	MgO	MnO	Na_2O	P_2O_5	TiO_2	V_2O_5	ZrO_2	BaO	SrO	ZnO	SO_3	Ash (%)	S (%)	O (%)	C (%)	H (%)
16N501	60.99	19.82	0.74	0.02	12.16	2.54	1.13	0.02	0.55	0.08	0.9	0.03	0.05	0.04	0.01	0.04	0.43	37.9	3.2	1.42	49.4	3.8
16N502	53.23	16.86	11.23	0.02	7.38	2.13	1.27	0.06	0.67	0.16	0.74	0.02	0.04	0.03	0.03	0.03	5.52	41.9	2.02	7.33	41.8	3.15
16N503	62.4	19.2	3.53	0.02	6.4	2.34	1.28	0.05	0.82	0.15	0.96	0.02	0.05	0.05	0.03	0.03	2.42	44.6	0.68	7.48	40.1	3.09
16N504	59.11	18.9	2.57	0.02	11.17	2.32	1.6	0.08	0.7	0.29	0.86	0.02	0.04	0.05	0.02	0.03	1.45	50.8	1.81	6.28	34.8	2.73
16N505	50.14	14.44	14.19	0.03	10.12	1.85	1.42	0.09	0.63	0.37	0.69	0.02	0.04	0.03	0.03	0.02	5.08	43.1	1.84	8.25	40.3	3
16N506	50.13	16.05	14.77	0.03	11.17	1.87	1.27	0.08	0.58	0.06	0.75	0.02	0.04	0.05	0.03	0.02	2.555	31.3	2.31	7.23	51.2	3.77
16N507	51.58	16.24	18.1	0.02	4.45	1.91	1.2	0.08	0.6	0.04	0.85	0.03	0.04	0.04	0.03	0.03	4.54	33.5	1.01	9.57	48.1	3.48
16N508	46.96	15.73	22.99	0.01	5.21	1.41	0.85	0.17	0.44	0.06	0.87	0.02	0.04	0.03	0.03	0.02	4.6	31.3	1.25	9.57	49.8	3.46
	H/C	**O/C**	**C/S**	**S/C**	**N/C**	**V/Cr**	**(1)**	**(2)**	**(3)**	**(4)**	**ICV**	**CIA**	**DF1**	**DF2**								
16N501	0.08	0.03	15.0	0.06	0.05	1.5	7.8	22.0	0.7	0.3	0.9	83.0	6.5	-4.6								
16N502	0.08	0.18	20.0	0.04	0.02	1.0	8.0	23.0	8.8	0.7	1.3	55.0	8.0	0.3								
16N503	0.08	0.19	59.0	0.02	0.00	1.0	8.0	20.0	2.8	0.18	0.7	74.0	3.5	-2.0								
16N504	0.08	0.18	19.0	0.02	0.02	1.0	8.0	22.0	1.6	0.14	1.0	77.0	6.0	-4.3								
16N505	0.07	0.20	22.0	0.03	0.02	0.7	7.8	21.0	10.0	0.9	2.0	46.0	11.0	0.09								
16N506	0.07	0.14	22.0	0.05	0.02	0.7	8.6	21.0	12.0	0.9	1.9	48.0	13.0	0.30								
16N507	0.07	0.20	48.0	0.02	0.02	1.5	8.5	19.0	15.0	1.0	1.7	44.0	10.0	3.7								
16N508	0.07	0.19	40.0	0.03	0.01	2.0	11.0	18.0	27.0	1.5	2.0	39.0	14.0	5.0								
Average	**0.39**	**0.16**	**31.0**	**0.03**	**0.02**	**1.0**	**8.4**	**21.0**	**9.8**	**0.70**	**1.4**	**58.0**	**9.0**	**-1.51**								

Chemical Index of Alteration (CIA) =(Al2O3 /(Al2O3+CaO +Na2O + K2O)*100; Maturity Index of Precipitation (ICV) =(Fe2O3+ K2O + Na2O + CaO + MgO + TiO2)/Al2O3)., CN =(Na2O + CaO); Discriminant Function F1 (DF1) = (− 1.773 TiO2 + 0.607 Al2O3 + 0.76 Fe2O3 -1.5 MgO + 0.616 CaO + 0.509 Na2O − 1.224 K2O)-9.09; Discriminant Function F2 (DF2) = (0.445 TiO2 + 0.07 Al2O3-0.25 Fe2O3 -1.142 MgO + 0.438 CaO + 1.475 Na2O + 1.426 K2O)-6.861. (1) =Al_2O_3/K_2O; (2) =Al_2O_3/TiO_2; (3) =CaO/MgO; (4) =CaO/Al_2O_3.

Palynofacies

The palynofacies analysis (Table 3) has shown three different categories of dispersed organic matter namely phytoclast, palynomorphs and AOM. The phytoclast category is the most predominant at almost all the studied slides. The phytoclast group consists of two subdivisions which are non-opaque (translucent) and opaque phytoclasts. The translucent phytoclasts display a slightly dark brown colour and are represented by cuticles, membranes and fungal hyphae with some pronounced irregular contours (Figures 5a-5d).

Table 3. Quantitative distribution of organic matter in the JOG16N-5 borehole.

Depth (m)	**Phytoclasts (%)**	**Palynomorphs (%)**	**AOM (%)**	**Palynofacies**	**SCI[a]**
8.3	49.67	26	24.33	C	X
8.55	70.33	20.67	10	C	
9.17	61.33	31.67	7	C	
9.5	36.33	57.33	6.33	D	
13.2	46.67	31	22.33	C	
15.67	100	0	0	CD	
20.67	51.67	26.34	20	C	
22.6	82.67	31	6.33	CD	
28.6	72	22	6	C	
30.93	87	6	7	CD	
33.18	75	15.33	9.67	C	Pale Yellow
33.46	59.67	28.67	10	C	
35.65	88	5.33	6.67	CD	
36	53.33	26	20	C	
36.9	45.67	42.67	11.67	D	
37.96	83	4.67	12.33	CD	
38.9	83.33	9.33	7.67	CD	
39.24	40.67	42	15	C	
41.44	48.67	47	4.33	D	
41.82	64.67	31.33	4	C	
44.23	51.33	32	16.67	C	Pale Yellow
45.2	58.67	22.33	19	C	
45.8	74.67	16.34	9	C	
46.1	48.67	46	4	D	
46.89	40.67	45.67	13.67	D	Dark Orange
48.37	87.67	5.67	6.67	CD	
49.18	42.67	49.33	8	C	
50	82.67	10.33	7	CD	
50.1	65.67	21.33	13	C	Dark Orange

51.15	47.33	46	6.67	D	
51.73	65	20	14	C	
52.32	44.67	41.33	14	C	
58.88	76	16.33	7.67	C	Pale Yellow
60.23	37.33	55.67	8	D	Dark
63.27	34.67	59	6.33	D	
63.36	75.33	13.67	11	C	
68.54	45.33	47.67	7	D	
72.32	40.33	31.33	14	C	X
79.73	73.67	18.66	7.67	C	
171.47	88.67	6	5.33	CD	
172.12	97.33	0	2.67	CD	Dark
175.2	92.67	6.33	1	CD	Dark
175.9	97.33	0	2.67	CD	Brown
178.84	86.33	9	4.67	CD	Dark
179.82	100	0	0	CD	X
188.83	94.33	0.33	5.33	CD	X
189.94	86	6.67	7.33	CD	Dark

[a]SCI=Spore Colour Index: The Spore Colour Index (SCI) has been carried out at levels in which vitrinite reflectances were measured, X=No data available.

The most prominent characteristic of the observed cuticles is therefore the presence epidermal cell walls characterised by sinuosity (Figures 5a-5c) pertaining to the genus *Trizygia* as reported by Maheshwari, 1968. More importantly in few samples is noted the occurrence of *B. braunii* like material which represents the chlorophyte group. The occurrence of *B. braunii* like material is characterized by its colonial forms of apparent algal origin (Zavattieri et al., 2017).

The sporomorphs were the second most abundant organic matter in the studied assemblage (Figure 5g-5L). The spores are oval to triangular exhibiting ornamentations and well-preserved trilete structure (Figure 5I). On the other hand, the pollen exhibits several ornamentations, form, with varied sizes and colours. The colours are mostly pale yellow to black (Figure 5f). The occurrence of bisaccate pollen grains (glossopterid) either striate, non-striate or taeniates (Figure 5h, 5J, 5K and 5L) is higher in comparison with the monosaccate ones (Figure 5g), which are related to the closeness of the area of provenance. The observed AOM, is slightly dark yellow characteristic of materials derived from terrestrial source as suggested by Tyson (1995). Cluster data based on the relative abundance of kerogen components indicate that samples from the K4 Formation are distributed into four clusters defining four different palynofacies assemblages (Palynofacies-a, Palynofacies-b, Palynofacies-c and Palynofacies -d).

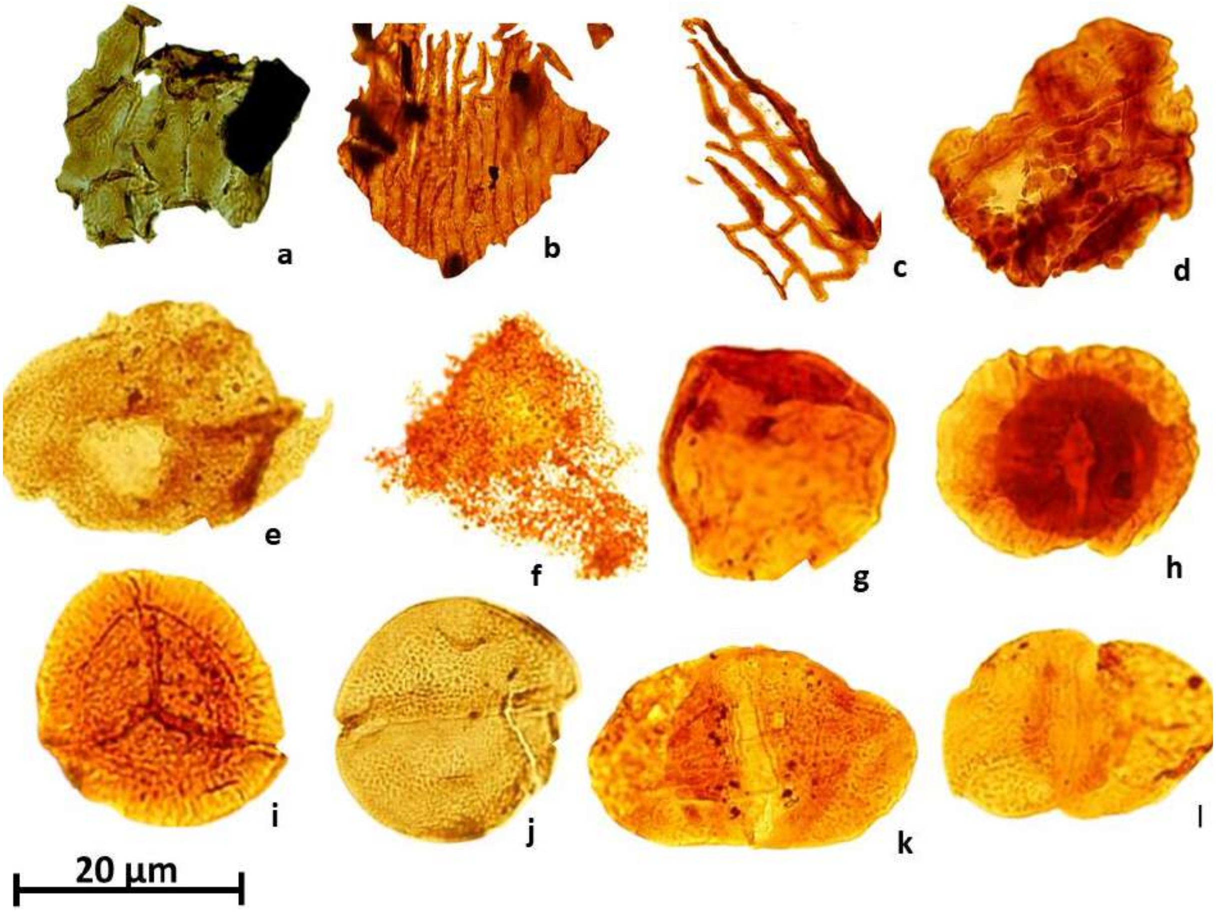

Figure 5. Representation of palynomorphs, AOM and phytoclasts from the JOG16N-5 samples: (**a**) Cuticule and opaque phytoclast (dark woody material); (**b**), Cuticle, (**c**) Cuticle; (d) *Botryococcus braunii* Kutzing (1849); (**e**) unidentified pollen; (**f**) Amorphous Organic Matter (AOM); (**g**) *Marsupipollenites triradiatus* (Balme and Hennelly, 1956); (**h**) unidentified pollen; (**i**) *Cirratriradites* sp., (**j**) *Scheuringipollenites maximus* (Hart) Tiwari (1973); (**k**) *Protohaploxypinus limpidus* (Balme and Hennelly) Balme and Playford 1967; and (**l**) *Falcisporites* sp.

Paleoredox conditions and sediment maturity

Paleoredox variables used in the present study has demonstrated V/Cr values spanning from 0.7 to 2.0 (average = 1.0), high TS content (> 2 wt%) in some samples, Carbon/Sulphur ratios greater than 3 and the Nitrogen/Carbon ratio in low concentration. In regard to sediment maturity the chemical alteration index (CIA) ranges from 39 to 83, whereas de compositional variability index (ICV) values were mostly less than 1.4 in average.

Discussion

Source rock potential

In the pyrolysis data presented herein, the S1 values suggest that the studied sediments present very little free organic compounds and thus indicating that no hydrocarbons have migrated into the sediments from other hydrocarbon source beds (Tissot and Welte, 1984; Peters, 1986). Additionally, it is likely that minor content of highly volatile organic compounds originally were contained in the samples but due to process of samples handling they were lost to the atmosphere (Tissot and Welte, 1984; Peters, 1986). Moreover, those obtained S1 values can be linked to adsorption process onto clay minerals obtained through Rock Eval pyrolysis. The samples have S2 suggesting poor to excellent source rocks (Peters, 1986; Tissot and Welte, 1984). The S2 versus TOC plot (Figure 6a) shows that the samples fall into the type II kerogen (oil prone), type III kerogen (gas prone), mixed type II/III kerogen (oil and gas) and type IV (dry gas). However, the majority of the samples display a type III kerogen indicating that the OM of the samples was sourced primarily from terrigenous plants. According to (Tissot and Welte, 1984), this type of kerogen presents a low potential for hydrocarbon generation however gas generation is excepted at sufficient depth. The relationship between TOC (wt%) and S1 (Figure 6b) can determine the origin and type of the hydrocarbons. The type of the hydrocarbons can be identified as indigenous or non-indigenous. Figure 6b, shows that the S1 hydrocarbons in the JOG16N-5 borehole core samples are of an indigenous nature.

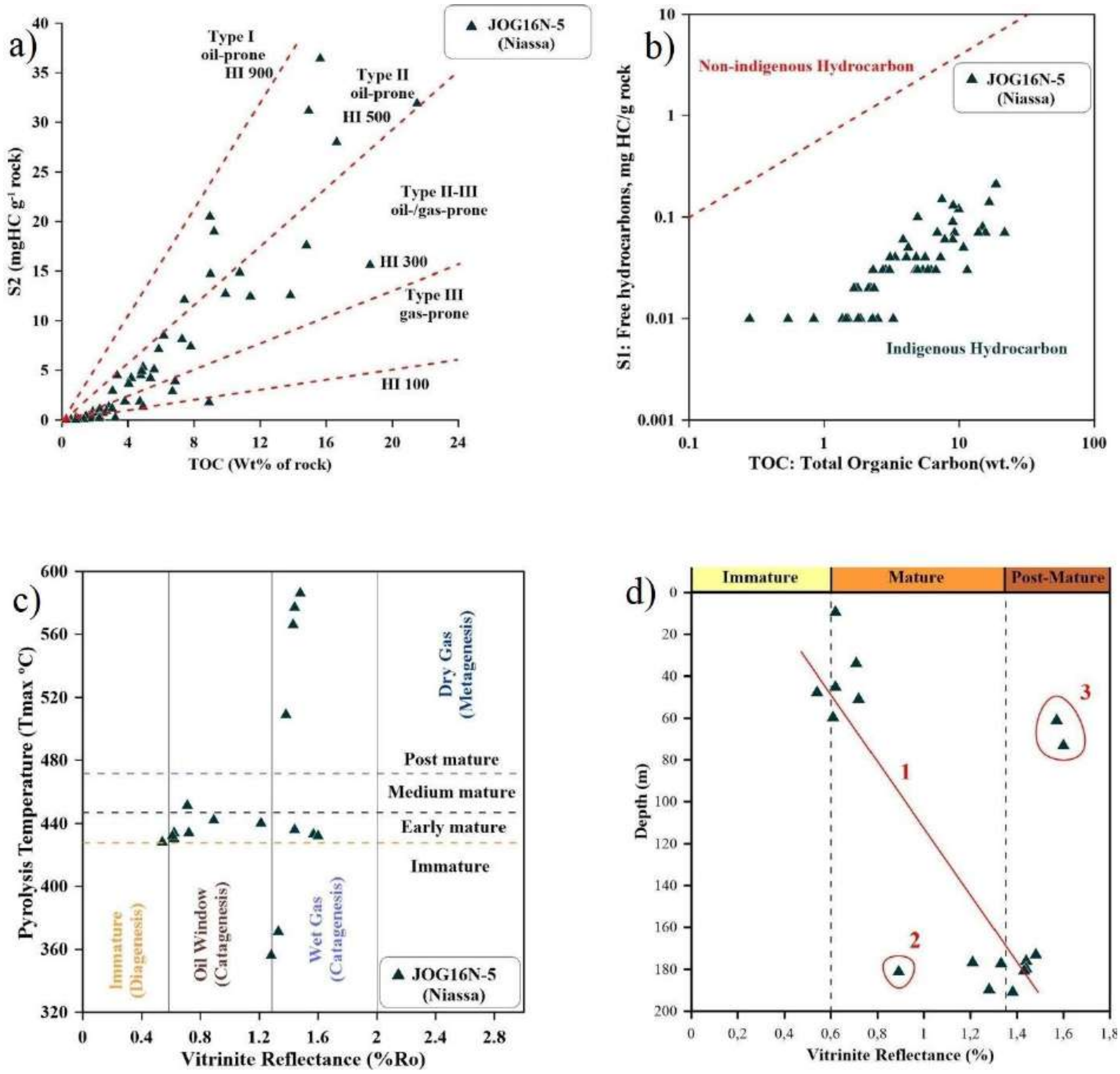

Figure 6. (**a**) S2 versus TOC illustrating the type of kerogen for the samples of the JOG16N-5, (b) S1 versus TOC showing the type of the hydrocarbon products, (**c** and **d**) Maturation of the samples indicating trends that are influenced by external factors (where 1-samples following the normal trend, 2-samples influenced by inconformity or fault and 3-samples showing a strong influence of kimberlite intrusions).

Maturation

The T_{max} variation in the samples through depth shows nonexistence of a linear trend which can in part be influenced by the clay mineral content, as suggested by (Gao et al., 2019). They argue that different clay minerals have different effects on different types of kerogens. For instance, if the ratio of kerogen/clay minerals alter, the T_{max} will also alter. The effect of mineral matrix on Rock Eval pyrolysis has been described by several researchers (Espitalie et al., 1977; Hazra et al., 2018; 2022; Peters, 1986).

Twenty-two samples show T_{max} less than 435^{o}C indicating immature conditions. Eight samples display values greater than 435^{o}C which are postmature, and the remaining majority are matured source rocks according to (Peters and Cassa, 1994). The matured sediments indicate that they may have already generated hydrocarbons. The post-maturity level of the samples easily can be associated with the occurrence of kimberlite intrusions in the NE of the K4 Formation as suggested by Key et al. (2007) (Figure 2). These igneous bodies can alter the Rock- Eval pyrolysis parameters as reported by Ade (2000) and others. The vitrinite reflectance is displaying the expected effect of influence by kimberlite intrusions due to its greater values. The vitrinite values are higher indicating that the vitrinite reflectance is displaying the expected effect of influence by kimberlite intrusions (Figure 6d). Three populations of data are observed within the vitrinite profile (Figure 6d). The population indicated by number 3 represents a rapid increase in vitrinite reflectance within certain depths which can also be linked with an unconformity that can occur in the area as suggested by (Ramachandran et al., 2015). Anyway, more data would be needed needed to confirm that conclusion.

The SCI based on the analysis of *Cycadopites cymbatus, Densosporites complicatus* (Figure 7) display spores with pale yellow colour to dark indicative of immature to postmature level of thermal maturation. On the other hand, the values of Production Index that relies on the S1 and S2 parameters is greater than 0.4 in only four samples although not considered as the most reliable parameter to identify the maturity of the rocks. Furthermore, as suggested by Neville et al. (2015), on their study in the Beaufort-Mackenzie Basin, Canada, these PI values are more likely to be influenced by contamination.

The low T_{max} and vitrinite values of the deeper zones in the borehole core are likely to be influenced by drilling fluids (e.g., natural impregnation or contamination) or due to the presence of faults. Similarly, Ade (2000), Bordenave et al. (1993), Chen et al. (1999), Peters and Cassa (1994) have also observed the same patterns in Rock-Eval data.

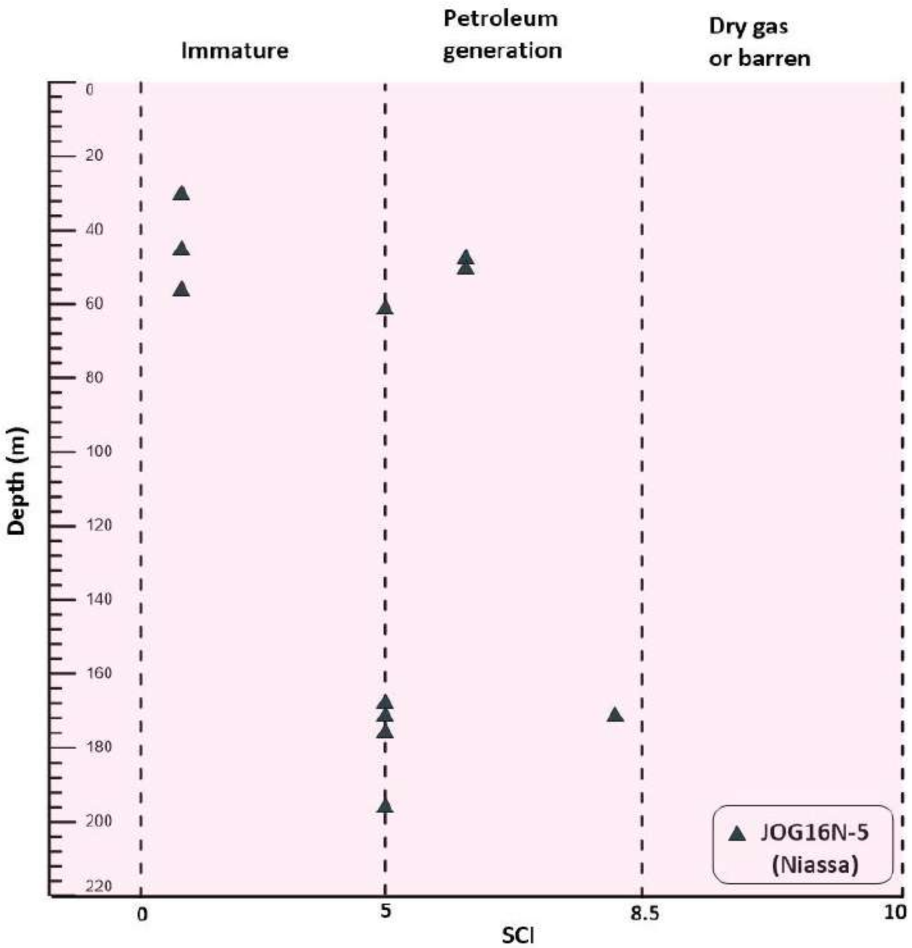

Figure 7. Spore colour index (SCI) versus Depth(m) plot showing maturation variability.

Organic Matter Quality

The most dominant types of observed organic matter are type III and IV (wet gas and dry gas) respectively. The type III kerogen (gas prone) has been reported in several proliferous systems worldwide such as Parnaiba Basin, Brazil (Mussa et al., 2021), Tuli Basin, South Africa (Akintola et al., 2023), Cahora Bassa Basin, Zimbabwé (Hiller and Shoko, 1996) and others. This kerogen type is linked with its common occurrence in siltstones and sandstones as observed herein. In its turn, the type IV kerogen, considered a dead carbon, is linked to reworked or oxidized sources, and also may be originated from other types of kerogens that were reworked and oxidized. The both kerogen type III and type IV both kerogen types are derived from higher plants. The trend observed for the HI is influenced by cracking process of insoluble OM as a result of heating of the samples located closer to kimberlite dykes. Additionally, such variation may be attributed to subaerial exposure of the strata or source of the organic matter. The potential of producible oil has been inferred based on the oil crossover effect diagram (Figure 8a) (Jarvie, 2012). The crossover effect plot showed that 19 studied samples have capacity for oil production (Figure 8a), according to (Jarvie, 2012). However, this parameter can be influenced by factors such as handling preparation before the analysis, and natural impregnation that can alter the high free hydrocarbon values (Jarvie, 2012). The thermal maturity plot (HI versus T_{max}) indicates that the samples are immature to mature, with a notable predominance of type III, mixed type II/III and IV kerogens (Figure 8b).

Three organic facies were obtained following the standard facies postulated by (Jones, 1987) (Figure 8c). The identified organic facies are: C which is potential gas, where the OM is mostly of woody nature, terrestrial and constituent of majority of the coals. Another identified organic facies is CD which represents transported, recycled, eroded and oxidized nature of the organic matter. Lastly, organic facies D representing very little or barren potential for hydrocarbon generation, with the OM being highly oxidized and thermally postmature. These results corroborate with the presence of oxidized or marsh vegetation and forest swamp with preserved structures obtained from palynofacies data.

The identified kerogen types support the palynofacies data outlined below. The type of kerogen obtained corroborates with the elemental analysis data, however, it should be highlighted that only 8 samples were considered for elemental analysis herein.

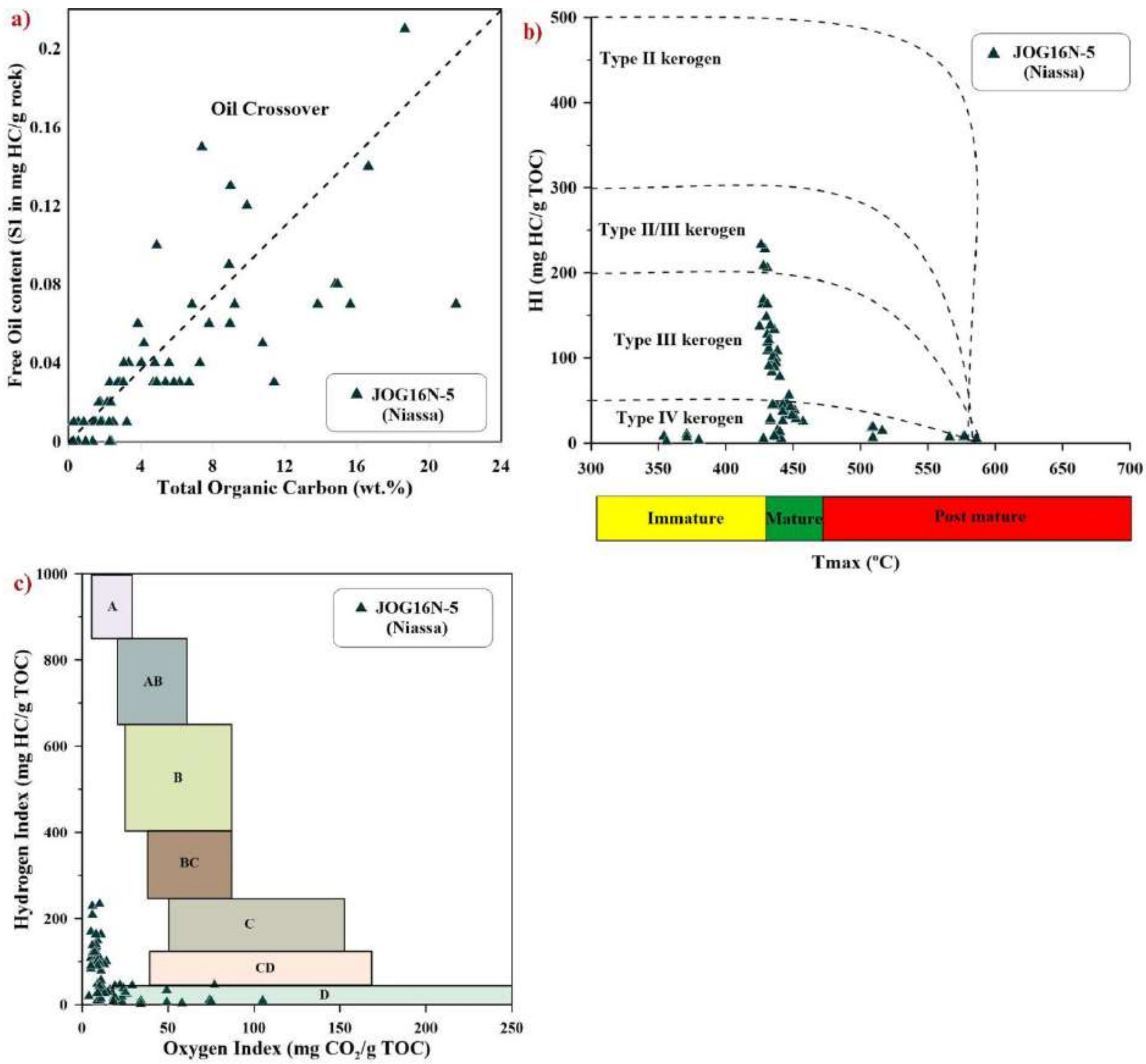

Figure 8. (**a**) Free oil content (S1 in mg/grock versus TOC) content showing oil crossover effect (**b**) Hydrogen index content versus T_{max} of the samples in regard to HI and maturity of the samples, and (**c**) Modified Van Krevelen diagram showing the depositional environment of the organic matter found in the JOG16N-5 samples.

Elemental analysis

Through this analysis, high ash content has been identified fact that has an influence in the observed higher values for the ratio O/C than to the ratio H/C, thus contributing to the abundance of kerogen type III and IV. Nevertheless, the type of kerogen in the studied material obtained through the Rock-Eval pyrolysis and palynofacies proxies pointed out to the existence of type II, III, mixed type II/III and type IV kerogens with a potential hydrocarbon generation and mostly gas. However, the H/C and O/C diagram based on small sample size has shown the occurrence of the process of coalification with samples reaching the catagenesis and metagenesis stages thus falling in the stage of anthracite and bituminous coals (Figure 9).

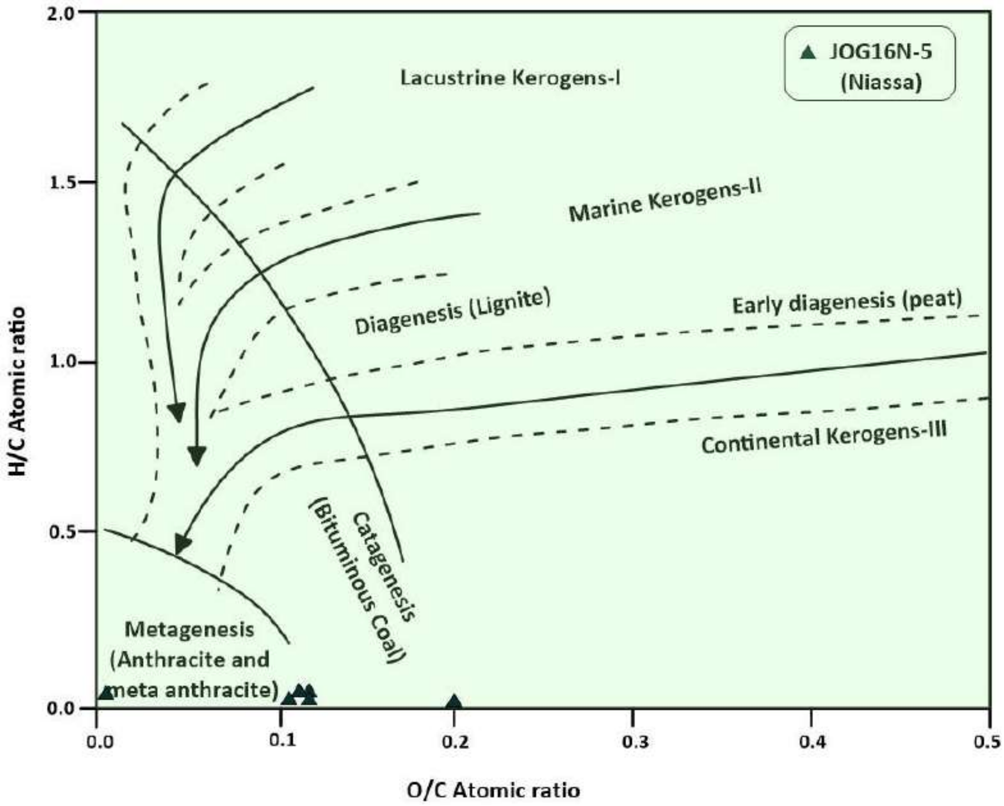

Figure 9. H/C and O/C indicating the process of coalification for some samples of the K4 Formation, Maniamba Basin, Mozambique.

Provenance

In the studied sediments, the Al_2O_3/TiO_2 ratio has been used as parameter for provenance inference as suggested by Hayashi et al. (1997). For the study samples, the Al_2O_3/TiO_2 ratio suggests a provenance from intermediate and felsic igneous rocks as observed in Figure 10a (Hayashi et al., 1997). Similarly, the discrimination function diagrams (Figure 10b) corroborates with the obtained results. The aforementioned relative abundance of the oxides strongly supports the existence of clay and quartz as the principal mineral components. The low values of the K_2O/Al_2O_3 ratio reinforce the existence of kaolinite (Figure 11a). The likely occurrence of illite in the studied sediments may be linked to thermal event associated with kimberlite emplacement observed in the study area (Figure 2). Additionally, the strong presence of smectite is also observed in the selected samples (Figure 11). In regard to Ca/Mg content, most of the analysed samples are enriched in calcite corroborating with the lithologies observed in the studied section which includes carbonaceous shale, coaly carbonaceous shale, carbonaceous siltstone (Figure 3).

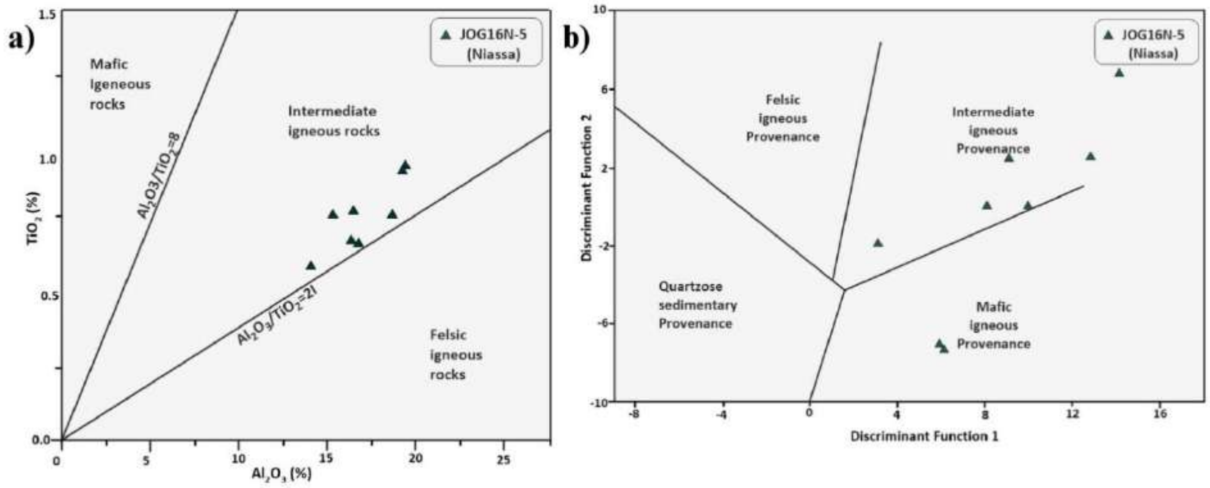

Figure 10. (**a**) TiO_2 versus Al_2O_3 for the K4 Formation borehole cores showing the sediment provenance, and (**b**) Discriminant functions diagram adapted from Roser and Korsch (1988).

Cox et al. (1995), emphasized that the K_2O/Al_2O_3 ratio can be interpreted as defining the original composition of sediments. For the studied sediments, the K_2O/Al_2O_3 ratio indicates the presence of traces of K-feldspars as suggested by Cox et al. (1995).

The facies of the the investigated K4 Fm are iron shale and shale. The iron oxide is present in the form of hematite (Fig. 11b). The source of iron can unveil important information regarding depositional environment (Einsele, 2000). Overall, the hematite's origin in seawater is associated with hydrothermal activity which can be in the form of volcanic activity or linked to sedimentary source derived from river systems (Einsele, 2000). For the purpose of getting further information regarding the source of iron in the studied K4 Formation, the Al-Mn-Fe diagram proposed by Adachi et al. (1986) was used (Figure 10c). The proposed diagram confirms that the iron is originated from in sedimentary source linked to river system.

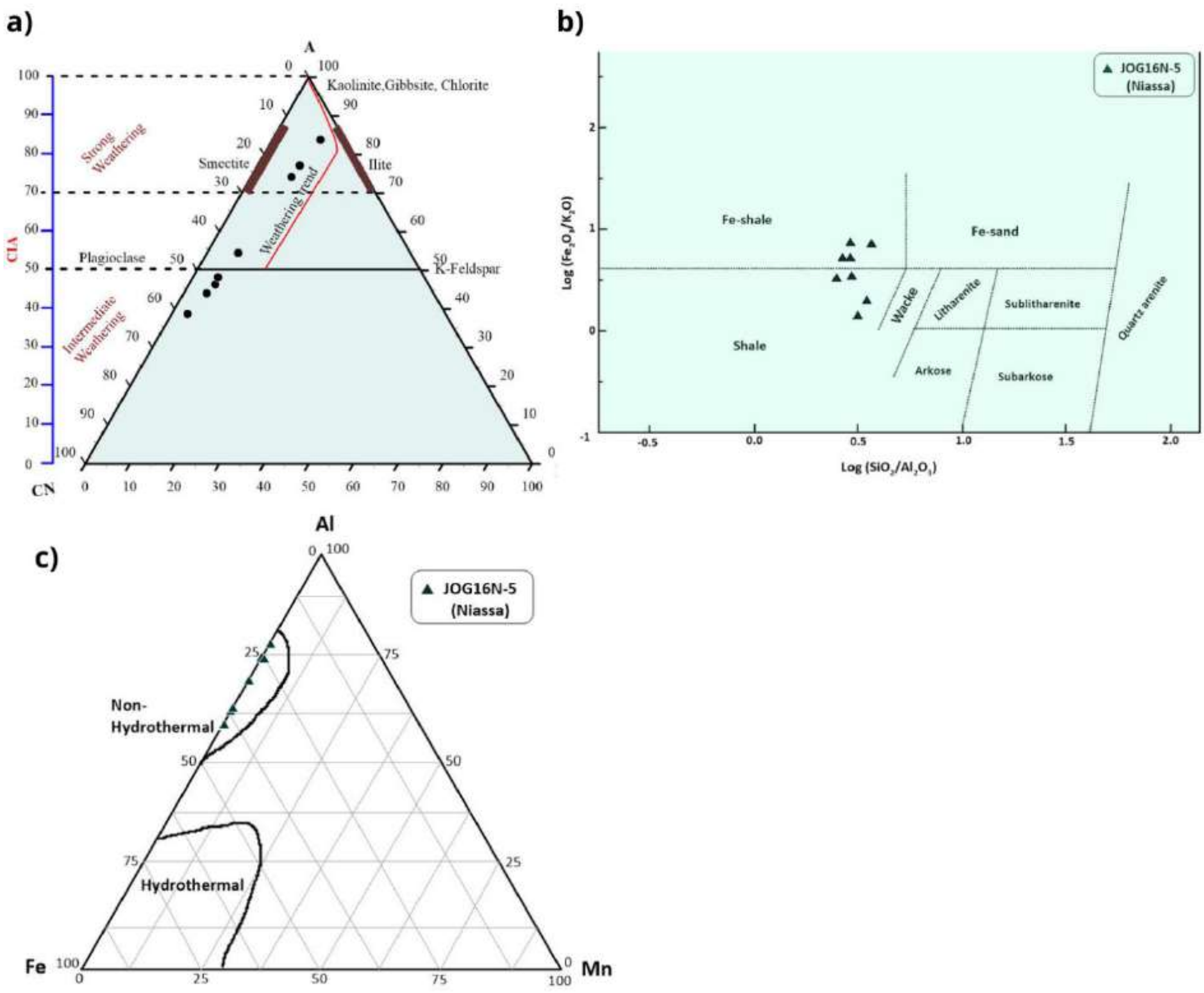

Figure 11. (a) Ternary diagrams of A–CN–K for the sample set from the JOG 16N-5 borehole core, (**b**) Geochemical classification of the shales, K4 Formation (after Herron, 1988), and (**c**) Provenance of the sediments from the K4 Formation based on: A. Al–Mn–Fe ternary diagram adapted from Adachi et al. (1986).

Palynofacies

The palynological data has demonstrated the major abundance of phytoclasts over palynomorphs and amorphous organic matter. The quantity of opaque phytoclasts is up to 75% suggesting oxic conditions, reworking and a likely subaerial exposure of the particulate organic matter. According to Tyson (1995), the predominance of the aforementioned type of organic matter is typical of fluvio-deltaic areas (proximal environments). In its turn, the opaque phytoclasts are dark being elongated, equidimensional with some diffuse outlines (Figure 5a). Interestingly, a freshwater algae *Botryococcus braunii* is found in the sequence. The occurrence of this green algae could represent coal swamp and typical fluvial-lacustrine system. Other important component are the palynomorphs represented by pollen and spores. The abundance of pollen grains characteristic of an arborescent vegetation indicates hygrophilous to the mesophilous environment (Ruckwied et al., 2014) in the retrieved palynofloral assemblages. Lastly, the identified AOM group (Figure 5f) is structureless, slightly diffuse displaying varied sizes under transmitted microscopy. According to Tyson (1995), the aforementioned fields suggest highly proximal shelf basin (type III-gas prone), heterolithic oxic shelf (types III and IV) and shelf to basin transition (types II and III-oil and gas) (Figure 12a), deposits corroborating with the data obtained from the swamp diagram (Figure 12b) modified after Mukhopadhyay (1986).

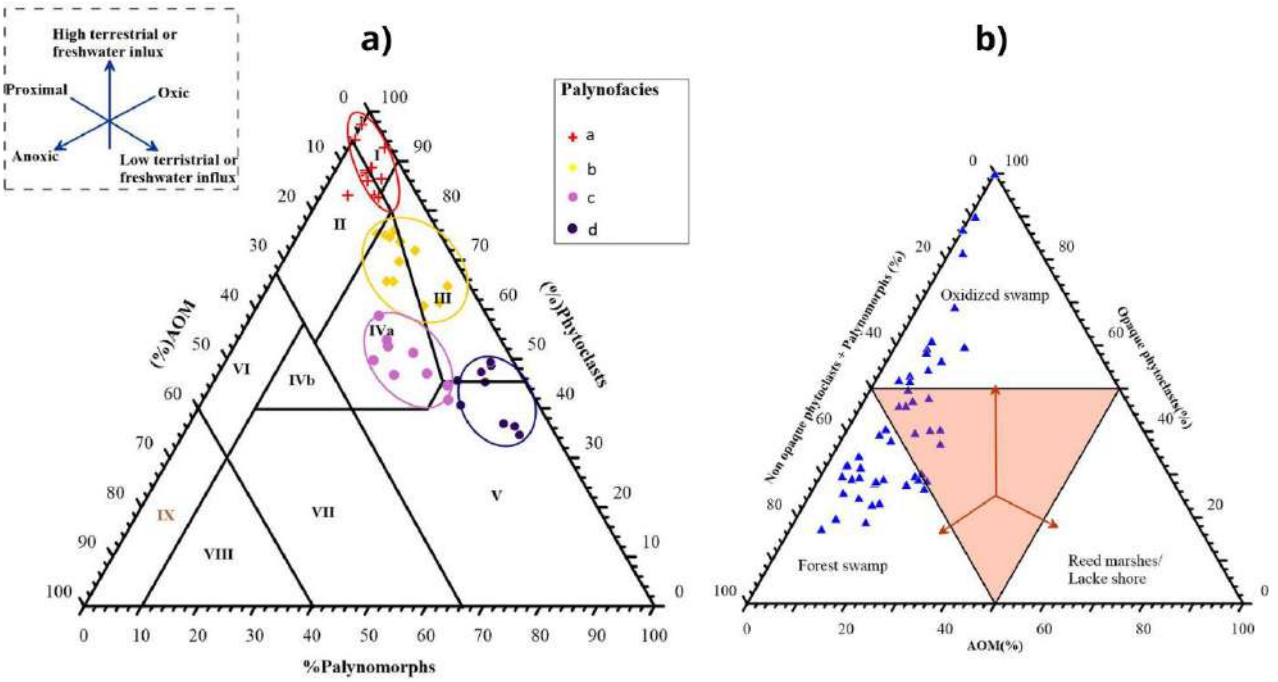

Figure 12. (**a**) Tyson ternary diagram for JOG16N-5 samples, and (**b**) Paleoenvironmental diagram adapted after Mukhopadhyay (1986) indicates deposition under swampy conditions.

Palynofacies associations

In this study, palynofacies associations (Figure 13), were established for a better understanding of depositional environments as it follows:

Palynofacies (PFa): The phytoclast group almost dilute all the other components. In some sections the content of phytoclast reaches up to 100%. There is a balance between the content of palynomorphs and amorphous organic matter which at some sections both components reach the same percentage. A total of nine samples of this succession are represented by palynofacies a (PFa) (Figure 12a). The greater proportion of opaque phytoclasts and the low occurrence of other OM types in PFa suggest that exposed sections of deposited sediments undergone extremely oxidizing conditions due to the fact that black wood particles are very common in proximal, high–energy settings that influence the deposition of coarse–grained sediments of fluvial to delta–systems (Fisher, 1980).

Palynofacies (PFb): The decrease of phytoclast content compared to palynofacies a is observed herein. Phytoclast content is less than 60%. On the other hand, palynomorphs and amorphous organic matter are increasing considerably. The palynomorphs in this palynofacies reaches up to 30% whereas amorphous organic matter (AOM) reaches up to 24% suggesting deposition under less oxidizing conditions than PFa. Additionally, the concurrence of the lithological data coupled with organic matter (OM) elements for PFb reveals mixed environmental settings, which is mainly characterized by the oxic swamps displaying low to medium energy levels.

Palynofacies (PFc): The content of phytoclast increases with compared to PFb but not reaching the amount observed in palynofacies a. The phytoclast reaches up to 70%. The palynomorphs and AOM decreases as the amount of palynomorphs increases indicating swampy settings in a dysoxic to anoxic environment. (Figure 12a).

Palynofacies (PFd): Phytoclast group decreases drastically displaying values less than 40%. The other organic matter components increase with the palynomorphs displaying greater values in almost all the grouped horizons. The increase of palynomorphs in the PFd compared to other organic matter components combined with the concurrence of sediments comprising carbonaceous shale, shale, fine–grained siltstones, suggest low–energy environmental settings through the deposition of PFd. Thus, in summary, the swampy environments are considered for the PFa as demonstrated by plotted diagram (Figure 12b).

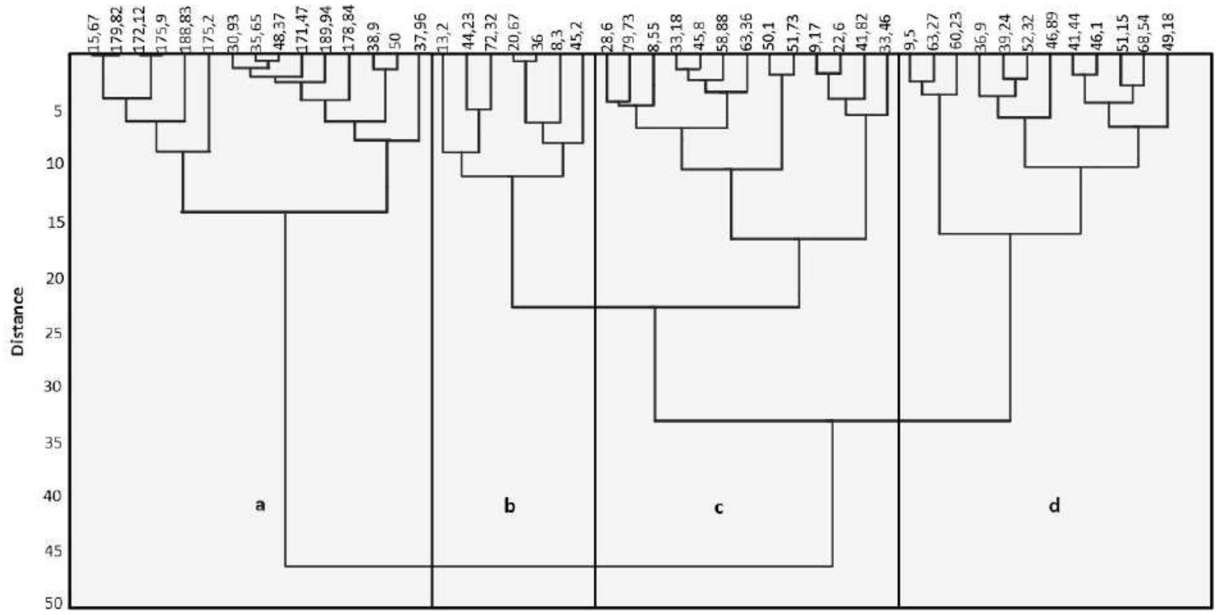

Figure 13. Dendrogram using Q-mode showing four palynofacies assemblages for the K4 Formation samples.

Palaeoclimate inferences

The plot of SiO_2 versus (Al_2O_3+K_2O+Na_2O) has been used to determine the paleoclimate conditions that prevailed during the process of deposition as suggested by Suttner and Dutta (1986). Unfortunately, crucial elements such as Rb, Ni and Cu were not measured which would have given significant inputs regarding the paleoclimate of the area (Chen et al., 1999). The plot of investigated samples on the proposed diagram adapted from Suttner and Dutta (1986), suggest that humid conditions prevail in the K4 Formation (Figure 14). The aforementioned conclusion is supported by the observed scarcity of rock fragments and feldspars as also argued by Sallam and Wanas (2019) in their geochemistry study of the Jurassic rocks from Gulf of Suez, Egypt. The occurrence of carbonaceous sediments in the K4 Fm in lacustrine or fluvial environments according to Verniers et al. (1989), support the idea of prevailing humid periods during its deposition. Additionally, based on Gondwana reconstruction, the studied area displayed humid conditions during early to Late Permian with shift to more arid environment at the end of the Triassic (Verniers et al., 1989). Aside from that, the occurrence of silicified wood pertaining to varied species (Nhamutole et al., 2021), the reasonable amount of fungal remains observed under the microscope, and the well-known *Glossopteris* sites identified from the studied K4 Formation sustain the obtained paleoclimate inferences (Nhamutole et al., 2021). The humid climate is also supported by the diversified palynotaxa that is retrieved along the studied according to ongoing research.

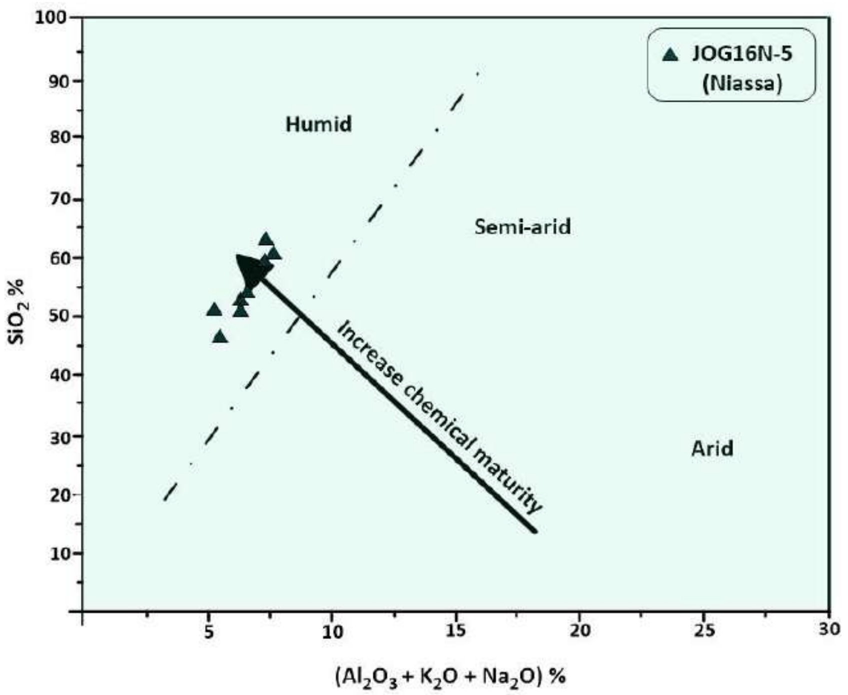

Figure 14. Paleoclimate inference of the study samples based on SiO_2 versus $Al_2O3+K_2O+Na_2O$ diagram (Suttner and Dutta, 1986).

Paleoredox and relationship with depositional environments

Murray and Boreham (1992), proposed the Fe_2O_3/TiO_2 and $Al_2O_3/(Al_2O_3+Fe_2O_3)$ diagram for deepening the investigation regarding environment of deposition. The studied sediments indicate continental margin and a combination of continental margin with pelagic sedimentary environment (Figure 15a). The pelagic sedimentary environment is observed due to the presence of terrigenous debris. Furthermore, Vanadium and Chromium was used for environment deposition inferences since Vanadium is deposited under reducing conditions, while Cr is mainly accompanied only with the detrital fraction and is not affected by paleoredox conditions (Jones and Manning, 1994). The results of the aforementioned ratio are summarized in Table 2. This result corroborates with the data yielded by the plotted Fe, TS and TOC diagram (Figure 15b). However, these results should be taken in caution because were based on small sample size. Redox conditions were also inferred based on the plot between Carbonate (wt%) versus TOC (wt%) based on Ricken (1993) (Figure 15c). Based on the TOC versus Carbonate three paleoredox environment conditions have been identified which are aerobic, dysaerobic and anaerobic respectively.

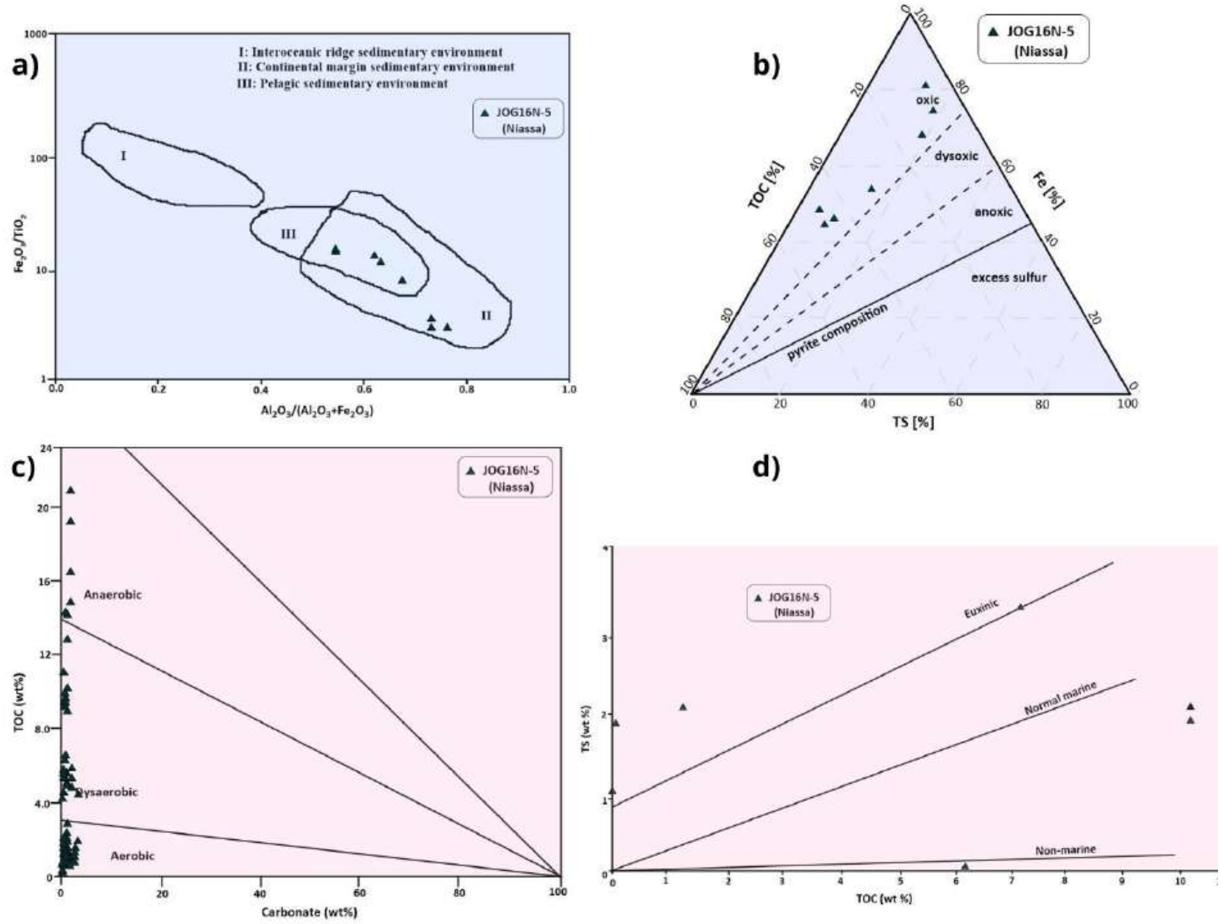

Figure 15. (**a**) Provenance of the sediments based Fe_2O_3/TiO_2 versus $Al_2O_3/(Al_2O_3+Fe_2O_3)$, (**b**) Ternary plot containing relative proportions of TOC, TS, and Fe. The proposed normal-marine line adapted from Berner and Raiswell (1983), (c) TOC versus $CaCO_3$ indicating the paleoredox conditions, and (**d**) Diagram of TS versus TOC indicating the prevailing oxic-anoxic conditions during the K4 Formation deposition. The normal-marine line is taken from Berner and Raiswell (1983).

Additionally, based on the plot between TS and TOC (Figure 15d), the samples are found scattered either below or above the normal marine line (Berner, 1984). The samples are located above the normal marine line (Figures 15d and 16) indicate euxinic conditions suggesting that the deposition was controlled by more reduced conditions (dysoxic-suboxic) (Berner, 1984). In contrast, the samples that are plotted below the normal marine line (Figure 15d and 16) suggest high paleoproductivity and suboxic-oxic conditions (Berner, 1984). In the study area, some sample has high TS content (> 2 wt%). However, in the lack of marine influence the presence of such high sulphur content may be stipulated as derived from volcanic sources [(e.g., kimberlite intrusions (Figure 2)] as observed in the study area.

Furthermore, the carbon (C)/sulphur (S) ratio is useful for the identification of the existence of sulphate reduction as proposed by Berner and Raiswell (1983). Here, more oxygenated conditions are inferred based on the aforementioned ratio. Also, deposition under freshwater conditions is inferred using the relation between C and S Berner (1984). This conclusion corroborates with the wet forest swamp depositional environment of the studied samples as shown by the ternary plot adapted after Mukhopadhyay (1986) (Figure 12).

Lastly, the Nitrogen/Carbon ratio has also been investigated for paleoredox inferences. According to this ratio, values less than 0.05 are representative of land plants whereas those greater than 0.08 are related to planktonic organisms (Vandenbroucke and Largeau, 2007). Thus, in alignment to low concentration observed in the studied samples can be inferred that the OM is derived from terrestrial plants.

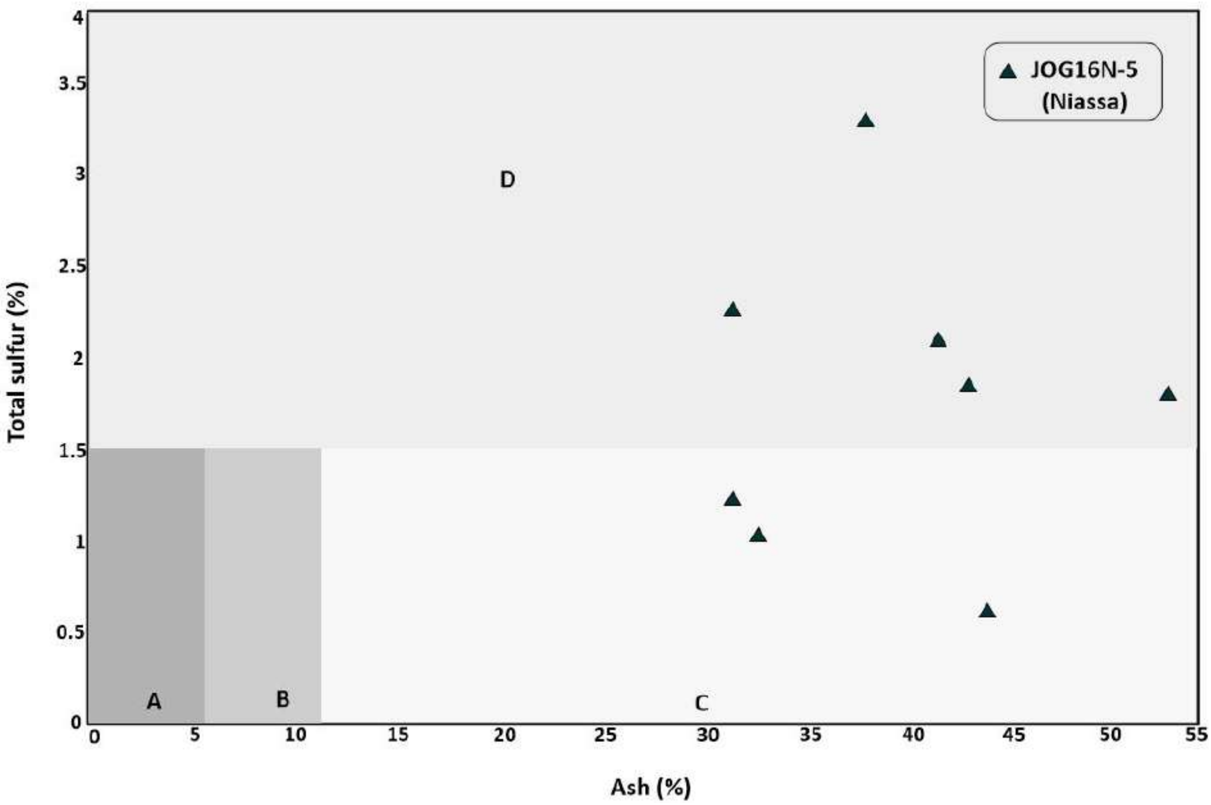

Figure 16. Plot of ash versus sulphur used for plot critical interpretation environment of deposition. A=Ombrogenous peat; B=Transition area; C=Topogenous peat; D=Marine influenced peat.

Sediment maturity

Sediment maturity is determined by the degree of chemical weathering (Nesbit and Young, 1984). Several indices, variables and parameters are used to analyse the level of weathering and maturity. The most used variables are as follows: plagioclase alteration index (PIA) (Fedo et al., 1995), the index of chemical alteration (CIA) (Nesbitt and Young, 1984), and the compositional variability index (ICV) (Cox et al. 1995) (Table 3). The CIA is responsible to define the level of weathering (Nesbitt and Young, 1984). On the other hand, ICV indicates the maturity of the sediment and tectonic activity (Cox et al., 1995). CIA in the range of 50 and 60 indicates weak chemical weathering. In its turn, CIA spanning from 60 to 80 and those higher than 80, suggest moderate and strong weathering respectively. Accordingly, the CIA values of the investigated K4 Formation indicate weak to strong weathering (Figure 17). The ICV values proposed by Cox et al. (1995), indicate maturity of sediments related to tectonism, while the ICV values greater than 1 indicate immature sediments formed in environment influenced by an active tectonism. In contrast, ICV values less than 1 suggest mature sediments formed in passive tectonic environments. The comparison of both parameters (ICV and CIA values) of the studied K4 Formation samples indicates immature to mature sediments with incipient to strong weathering (Figure 17).

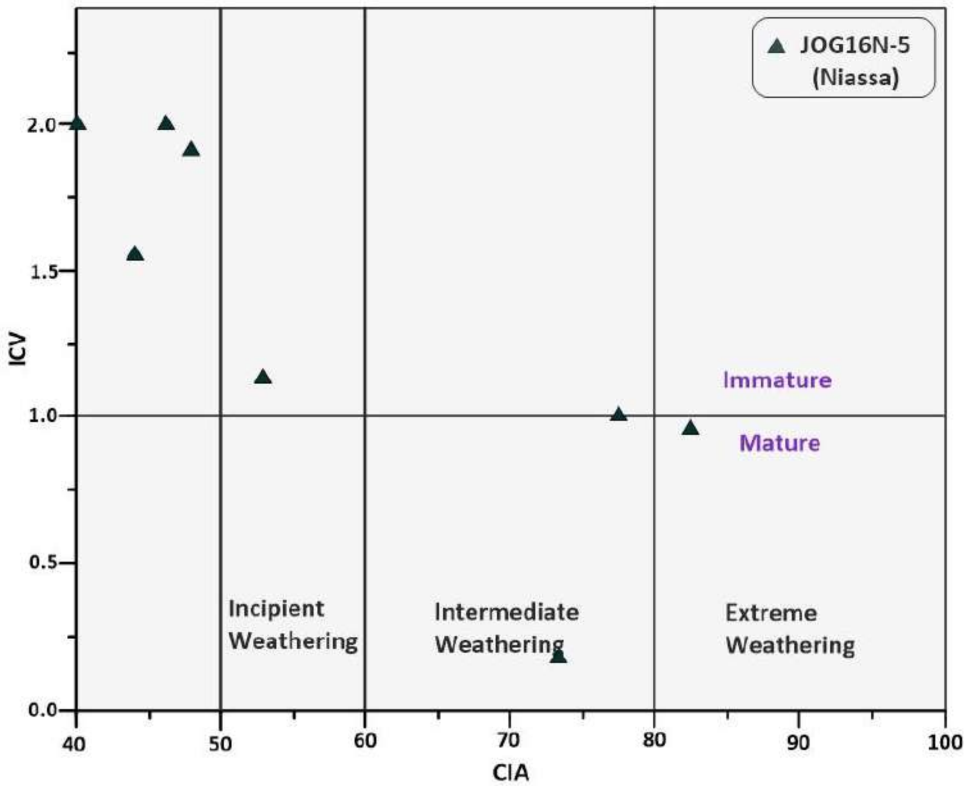

Figure 17. Index of Compositional Variability (ICV) versus Chemical Index of Alteration (CIA) adapted from Cox et al. (1995) and Nesbitt and Young (1984).

Tectonic settings

Two model of diagrams are used to identify the main tectonic settings of the surveyed K4 Formation in the Maniamba Basin following Roser and Korsch (1986). The aforementioned diagram based on elemental analysis (K_2O/Na_2O vs. SiO_2) are crucial to infer the tectonic settings due to the fact that plate tectonics may have an influence in chemistry content of the rocks (Peters et al., 2005). For the studied material, the bivariate diagram of K_2O/Na_2O ratio versus SiO_2 proposed by Roser and Korsch (1986), indicates that the oceanic island arc is predominant in the majority of the Maniamba samples, however any exception was observed for three samples which are indicative of an active continental margin (Figures 18a and 18b).

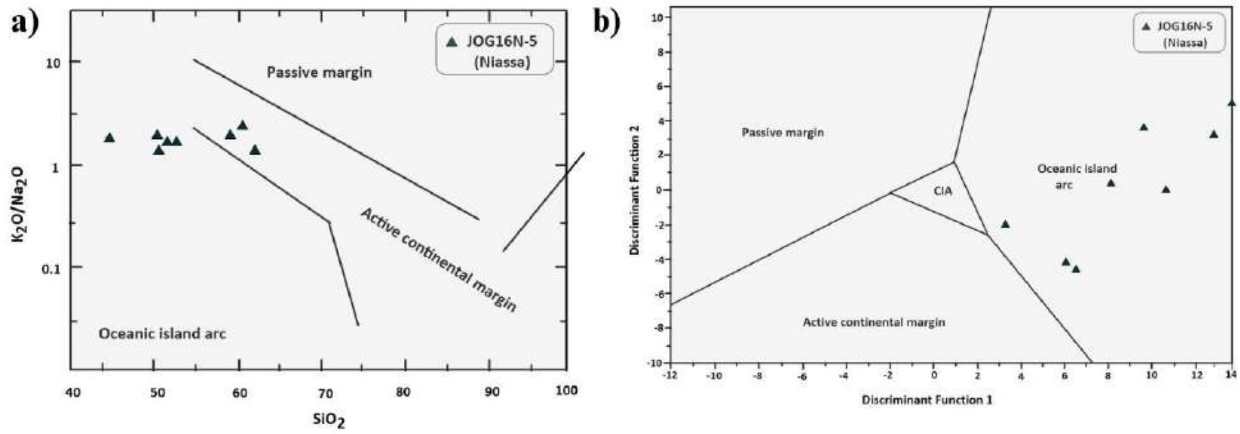

Figure 18. (**a**) Bivariate plot of K_2O/Na_2O versus SiO_2 showing tectonic setting of K4 Formation, Maniamba Basin based on investigated sediments adapted after Roser and Korsch (1986), and (**b**) Tectonic setting based on discrimination function for samples of the K4 Formation, Maniamba Basin.

Conclusions

An integration of palynofacies, Rock Eval pyrolysis, TOC, vitrinite reflectance and elemental analysis was used for further characterisation of the OM content, assessment of the potential source rock as well as better understanding of the depositional environment of the sedimentary strata intercepted by the JOG16N-5 borehole core from the Maniamba Basin, Niassa, Mozambique. The conclusion is as it follows below:

- The samples have demonstrated organic richness ranging from very good to excellent organic richness with regard to TOC (wt%).
- The sequence has low HI values and higher OI values linked to kerogen type III and IV. However, a mixed type II/III and type II was also observed. Most samples are gas prone.
- Thermal maturity parameters based on SCI, T_{max} and vitrinite reflectance have demonstrated immature to postmature phases. The majority of the samples are within the oil and gas generative potential. Additionally, T_{max}, vitrinite reflectance and SCI values displayed the expected kimberlite effect, associated with the likely presence of faults.

- Elemental analyses show a greater contribution of ash content (31.3-50.8%) in the samples, a fact that can be associated with the existence of type III and IV kerogen. The studied samples are in the catagenesis and metagenesis phase as shown by the diagram of O/C and H/C. High sulphur content was observed in some samples and the volcanism activity (e.g., kimberlite intrusions) has been inferred as the main source.
- The mineralogical content of the studied sediments includes calcite, quartz, illite, kaolinite, smectite clay minerals and traces of K-feldspars. The mineralogical content is responsible for the occurrence of Fe-shale and shale facies. The both facies are a combination of mafic and intermediate igneous rocks in the studied formation. The existence of these facies may suggest that the K4 Formation can act as unconventional source rock.
- The obtained palynofacies suggest: (PFa) indicates oxidized swamp settings, (PFb) indicates mixed environmental settings which is mostly characterized by the oxic swamps exhibiting energy levels ranging from low to medium, (PFc and PFd) represent dense vegetation in swampy settings with the latter displaying more oxic conditions.
- The deposition of sediments occurred in a proximal-distal setting under highly oxygenated environment; however, some anoxic conditions were also observed. These environmental conditions were influenced by higher supply of opaque and non-opaque phytoclast that diluted the other OM components. These results agree with other proxies used in this study.
- The paleoclimate that prevailed in the time of the deposition of the K4 Formation time was typical humid which enabled the existence of incipient, moderate and strong paleo weathering. The humid climate could be a demonstration of once existing luxuriant glossopterid vegetation which characterized most of the Lower Gondwana sequences. In addition, the sediments source rocks are considered active continental margin and oceanic island arc for the K4 Fm.

All in all, this study highlights that the K4 Formation has a potential for hydrocarbon, mainly gas.

References

Adachi, M., Yamamoto, K. and Sugisaki, R., 1986. Hydrothermal cherts and associated silicious rocks from northern Pacific: their geological significance as indication of ocean ridge activity. Sedimentology Geology, 47, 125–148.

Ade, M., 2000. Caracterização da Matéria Orgânica Dispersa através da técnica de Pirólise “Rock-Eval II” Vantagens e Limitações para a Geologia. Pesquisa em Geociências, 27, 43–50.

Akintola, A., Dacosta, F., Rupprecht, S. and Mhlongoa, S.E., 2023. Petrographic, mineralogical, morphological and organic constraints of the Permian shaly coal in the Tuli Basin of Limpopo-Area Karoo-Aged basin, South Africa: Implication for potential gas generation. Heliyon, 9, e14446, 15pp, doi.org/10.1016/j.heliyon.2023.e14446

Basu, A., Young, S., Suttner, L., James, W. and Mack, G., 1975. Re-evaluation of the use of undulatory extinction and cristalinity in detrital quartz for provenance. Journal of Sedimentology and Petroleum, 45, 873-882.

Berner, R.A., 1984. Sedimentary pyrite formation: an update. Geochimica et Cosmochimica Acta, 48, 605–615.

Berner, R.A. and Raiswell, R., 1983. Burial of organic carbon and pyrite sulfur in sediments over Phanerozoic time: a new theory. Geochimica et Cosmochimica Acta, 47, 855–862.

Bordenave, M., Espitálie, J., Leplant, P., Oudin, J. and Vandenbroucke, M., 1993. Screening techniques for source rock evaluation. In: Bordenave, M.L. (Ed.), Applied Petroleum Geochemistry. Editions Technip, Paris, 217–278.

Cox, R., Lowe, D. and Cullers, R., 1995. The influence of sediment recycling and basement composition on evolution of mudrock chemistry in the southwestern United States. Geochimica et Cosmochimica Acta, 59, 2919–2940.

Chen, J., An, Z. and Head, J., 1999. Variation of Rb/Sr ratios in the loess-paleosol sequences of Central China during the last 130,000 years and their implications for monsoon paleoclimatology. Quaternary Research, 51, 215–219.

Deaf, A. and Tahoun, S., 2018. Integrated palynological, organic geochemical, and sequence stratigraphic analyses of the middle to upper Cenomanian hydrocarbon reservoir/source Abu Roash "G" Member: a depositional model in northwestern Egypt. Marine and Petroleum Geology, 92, 372–402.

Durand, B. and Monin, J., 1980. Elemental Analysis of Kerogens (C, H, O, N, S, Fe). Institut Français du Petrole, Rueil-malmaison, France. Geochimica and Cosmochimica Acta, 46, 1193–1202.

Einsele, G., 2000. Sedimentary Basins: Evolution, Facies, and Sediment Budget. Springer Verlag, Berlin. 792pp.

Espitálie, J., Madec, M. and Leplat, P., 1977. Source rock characterization method for petroleum exploration: Proceedings of the Ninth Offshore Technology Conference, Houston, 439–442.

Fedo, C., Wayne, N. and Young, G., 1995. Unravelling the effects of potassium metasomatism in sedimentary rocks and paleosols, with implications for paleoweathering conditions and provenance. Geology, 23, 921–924.

Fisher, M., 1980. Kerogen distribution and depositional environments in the Middle Jurassic of Yorkshire UK. In: Singh BD, Singh HP and Tiwari RS (Editors)-4th International Palynological Conference, Lucknow, 1976–1977.

Gao, X., Wang, P., Li, J., Wang, M. and Ma, W., 2019. Influencing factors of the Tmax parameter in Rock-Eval pyrolysis, IOP Conf. Series: Earth and Environmental Science, doi.org/10.1088/1755-1315/360/1/01201.

Hayashi, K., Fujisawa, H., Holland, H. and Ohmoto, H., 1997. Geochemistry of 1.9Ga sedimentary rocks from northeastern Labrador, Canada. Geochimica et Cosmochimica Acta, 61, 4115–4137.

Hazra, B., Wood, D., Varma, A., Sarkar, B., Tiwari, B. and Singh, A., 2018. Insights into the effects of matrix retention and inert carbon on the petroleum generation potential of Indian Gondwana shales. Marine and Petroleum Geology, 91, 125–138.

Hazra, B., Katz, B., Singh, D. and Singh, P., 2022. Impact of siderite on Rock-Eval S3 and oxygen index. Marine and Petroleum Geology, 143, doi.org/10.1016/j.marpetgeo.2022.105804.

Herron, M., 1988. Geochemical classification of terrigenous sands and shales from core or log data. Journal of Sedimentary Petrology, 58, 820–829, doi.org/10.1306/212F8E77-2B24-11D7-8648000102 C1865D.

Hiller, K. and Shoko, U., 1996. Hydrocarbon source rock potential of the Karoo in Zimbabwe. Journal of African Earth Sciences, 23, 31–43.

Hunt, J., 1995. Petroleum geochemistry and geology, 2nd ed; W. H. Freeman and Company, New York. 743pp.

Hydrocarbon Processing., 2014. http://www.hydrocarbonprocessing.com/article/BP predicts-slowdown-in-global-energy-demand.html.

Jarvie, D., 2012. Shale resource systems for oil and gas: Part 1-Shale-gas resource systems. In: Breyer, J.A. (Ed.), Shale Reservoirs-Giant Resources for the 21st Century; Bulletin of the American Association for Petroleum Geologist, 69–87.

JOGMEC., 2016. The results of drilling survey III in Mozambique. Unpublished report, National Directorate of Geology and Mines, Mozambique.

Jones, R., 1987. Organic Facies, In: Brook J., Welte D. (Ed.), Advances in petroleum geochemistry. Academic Press, New York, 1–90.

Jones, B. and Manning, D.A.C. 1994. Comparison of Geochemical Indices Used for the Interpretation of Palaeoredox Conditions in Ancient Mudstones. Chemical Geology, 111, 111–129.

Karg, H. and Sauerer, B., 2022. Thermal maturity assessment of marine source rocks integrating Raman spectroscopy, organic geochemistry and petroleum systems modelling. International Journal of Coal Geology, 264,104131, doi.org/10.1016/j.coal.2022.104131.

Key, R., Bingen, B., Barton, E., Daudi, E., Manuel, S. and Moniz, A., 2007. Kimberlites in a Karoo graben of northern Mozambique: Tectonic setting, mineralogy and Rb-Sr geochronology. South African Journal of Geology, 110, 111–124, doi.org/10.2113/gssajg.110.1.111.

Maheshwari, H.K., 1968. Studies in the *Glossopteris* flora of India. Remarks on *Trizygia* speciosa Royle with reference to the genus *Sphenophyllum*. Palaeobotanist, 38, 283–287.

Menezes, T., Mendonça, J., Araújo, C., Souza, P. and Mendonça, J. 2008. Fácies Orgânicas: conceitos, métodos e estudos de casos na indústria de petróleo. Revista Brasileira de Geociências, 38, 80–96.

Mukhopadhyay, P., 1986. Petrography of selected Wilcox and Jackson Group fignites from the Tertiary of Texas. In Geology of Gulf Coast Lignites (Edited by Finkelman R. and Casagrande D.). The 1986 annual meeting of the Geological Society of America, Coal Geology Division, Field Trip, 126–145.

Murray, A.P. and Boreham, C.J., 1992. Organic Geochemistry in Petroleum Exploration. Australian Geological Survey Organization, Canberra. 230 pp.

Mussa, A., Kalkreuth, W., Mizusaki, A., Bicca, M. and Koefoed, J., 2021. Geochemical characterization of the organic matter in the Devonian Pimenteiras Formation, Parnaiba Basin, Brazil–Implications for depositional environment and the potential of hydrocarbon generation. Journal of Petroleum Science and Engineering, 206, doi.org/10.1016/j.petrol.2021.108461.

Nazir, A. and Fazeelat, T., 2016. The geochemical characterization of crude oils reservoirs in Cretaceous sequences, Lower Indus Basin, Pakistan. Energy Sources, Part A: Recovery, Utilization, and Environmental Effects. Petroleum Science and Technology, 38, 744–751.

Nesbitt, H. and Young, G., 1984. Prediction of some weathering trends of plutonic and volcanic rocks based upon thermodynamic and kinetic consideration. Geochimica et Cosmochimica Acta, 48, 1523–1534.

Nhamutole, N., Bamford, M. and Araújo, R., 2021. New species of *Protaxodioxylon* (conifer wood) from the Middle Permian of the Metangula Graben (Niassa Province, Mozambique) and their implications. Journal of African Earth Sciences, 183, 104323, doi.org/10.1016/j.jafrearsci.2021.104323.

Nhamutole, N., Bamford, M., Souza, P., and Do Carmo, D., 2023. Palynofacies analysis of the JOG16N-8 borehole, K5 formation from the Maniamba Basin (middle Permian), Mozambique: A contribution for hydrocarbon exploration. Journal of African Earth Sciences, 205, 104997, doi.org/10.1016/j.jafrearsci.2023.104997.

Neville, L., McNeil, D., Grasby, S., Galloway, J., Sanei, H. and Dewing, K., 2015. Rock-Eval Pyrolysis Results for Cuttings Samples from the Natsek E-56 Well, Beaufort-Mackenzie Basin, Canada. Geological Survey of Canada, 76, doi.org/10.4095/297341.

Peng, J., Xu, C., Dai, B., Sun, L., Feng, J. and Huang, Q., 2022. Numerical Investigation of Brittleness Effect on Strength and Microcracking Behaviour of Crystalline Rock. International Journal of Geomathematics, doi.org/10.1061/(ASCE)GM.1943-5622.0002529.

Peters, K., 1986. Guidelines for evaluating petroleum source rock using programmed pyrolysis. Bull. American Association for Petroleum Geology, 70, 318–329.

Peters, K. and Cassa, M., 1994. Applied source rock geochemistry, in Magoon, L.B., and Dow, W.G., eds., The petroleum system–from source to trap. American Association for Petroleum Geology, 60, 93-120.

Peters, K.E., Walters, C.C. and Moldovan, J.M., 2005. The Biomarker Guide. Biomarkers and Isotopes in the Environment and Human History. Cambridge University.

Ramachandran, K., Babu, V., Behera, B. and Harinarayana, T., 2015. Source rock analysis, thermal maturation and hydrocarbon generation using rock-eval pyrolysis in parts of Krishna–Godavari basin, India: a case study. Journal of Petroleum Exploration and Production Technology, 3, 11–20.

Ricken, W., 1993. Sedimentation as a Three-Component System: Organic Carbon, Carbonate, Noncarbonate. Springer -Verlag, Berlin; New York.

Roser, B. and Korsch, R., 1986. Determination of tectonic setting of sandstone mudstone suites using SiO_2 content and K_2O/Na_2O. Journal of Geology, 91, 611–627.

Ruckwied, K., Götz, A.E. and Jones, P., 2014. Palynological records of the Permian ecca Group (South Africa): Utilizing climatic icehouse–greenhouse signals for cross–basin correlations. Palaeogeography, Palaeoclimate and Palaeoecology, 413, 167–172.

Sallam, E. and Wanas, H., 2019. Petrography and geochemistry of the Jurassic siliciclastic rocks in the Khasm El-Galala area (NW Gulf of Suez, Egypt): Implications for provenance, tectonic setting and source area paleoweathering. Journal of African Earth Sciences, 160, 103607.

Suttner, L. and Dutta, P., 1986. Alluvial sandstone composition and paleoclimate. Framework mineralogy. Journal of Sedimentology and Petroleum, 56, 329–345.

Tissot, B. and Welte, D., 1984. Petroleum Formation and Occurrence, second ed. Springer Verlag, Heidelberg.

Tyson, R., 1995. Sedimentary Organic Matter Organic Facies and Palynofacies. Chapman and Hall, London, UK.

Vale, M., 2014. Projecto, desenvolvimentos e avaliação da ocorrência de carvão existente na Bacia Carbonífera de Maniamba. Provincia de Niassa em Moçambique. 100pp. Unpublished report.

Vandenbroucke, M. and Largeau, C., 2007. Kerogen origin, evolution and structure. Organic Geochemistry, 38, 719–833.

Verniers, J., Jourdan, P., Paulis, R., Frasca-Spada, L. and De Bock, F., 1989. The Karroo Graben of Metangula Northern Mozambique. Journal of African Earth Sciences, 9,137–158.

Zavattieri, A.M., Gutiérrez, P.R. and Ezpeleta, M., 2017. *Syndesmorion stellatum* (Fijałkowska) Foster et Afonin chlorophycean algae and associated microphytoplankton from lacustrine successions of the La Veteada Formation (late Permian), Paganzo Basin, Argentina. Paleoenvironmental interpretations and stratigraphic implications. Review of Palaeobotany and Palynology, 242, 1–20, doi.org:10.1016/j.revpalbo.2017.02.011

Zhang, M., Ji, Li., Wu, Y., He. And C., 2015. Palynofacies and geochemical analysis of the Triassic Yanchang Formation, Ordos Basin: Implications for hydrocarbon generation potential and the paleoenvironment of continental source rocks. International Journal of Coal Geology, 152, 59–176.

Zobaa, M., Oboh-Ikuenobe, F. and Ibrahim, M., 2011. The Cenomanian/Turonian oceanic anoxic event in the Razzak Field, north Western Desert, Egypt: source rock potential and paleoenvironmental association. Marine and Petroleum Geology, 28,1475–1482.

Reconstructing the Late Permian-Early Triassic environment of a coal-bearing succession in the Maniamba Basin, Mozambique (Central Gondwana): A multiproxy palynological and geochemical approach.

Adapted from Nhamutole, N; Bamford, M; Souza, P.A; Felix, C.M; Pereira, E; Bastos, L; Mendes, L; Deus, O; Nopeia, M; Carmo, D.A

Published by International Journal of Coal Geology

Contents lists available at ScienceDirect

International Journal of Coal Geology

journal homepage: www.elsevier.com/locate/coal

ELSEVIER

Check for updates

Reconstructing the late Permian-early Triassic environment of a coal-bearing succession in the Maniamba Basin, Mozambique (Central Gondwana): A multiproxy palynological and geochemical approach

N. Nhamutole[a,b,*], M.K. Bamford[a], P.A. Souza[c], C.M. Felix[c], E. Pereira[d], L. Bastos[d], L. Mendes[e,f], O. Deus[g], M. Nopeia[h], D.A. Carmo[h]

Abstract

The Maniamba Basin is an intracratonic, Karoo-aged basin located in northern Mozambique. Newly published studies have indicated the occurrence of organic-rich units in the Maniamba Basin, based on Rock Eval data. However, detailed characterization of the palaeoenvironments in the basin is still lacking. In this study, detailed palynological, palynofaciological, XRD and organic geochemical techniques (TOC, total sulphur, and biomarkers) were performed in order to understand past environments that prevailed in the basin. The palynological data reveal the dominance of gymnosperm taxa (striate and non-striate bisaccate, and praecolpate pollen grains) followed by lycopsids, sphenopsids and ferns suggesting hypautochthonous sedimentation characterized by warm and humid palaeoclimate. The palynological results indicate a Permian and Triassic age for the strata. The organic-rich units unveiled a dominance of phytoclasts and palynomorphs, and to a lesser extent by terrestrial and bacterially derived organic matter with no fluorescence, indicating high maturity. Swamp, river and lake dominated environments with oxic-suboxic-anoxic

conditions, reflecting shifting of depositional conditions overtime, are inferred in the Maniamba Basin. The deposition and accumulation of organic-rich units were mainly controlled by palaeoredox conditions linked to basin infill during different rifting episodes. The biomarkers mainly consist of saturated compounds that suggest terrestrial organic matter with freshwater algal contribution.

Overall, the integration of mineralogical composition with palynofacies, biomarkers and palynology indicate the presence of potential source rocks that were thermally influenced. Additionally, the petroleum fluids known from younger strata in the Rovuma and Mozambique basins did not show any link with the source rock reported previously.

1. Introduction

The Maniamba Basin, located in Niassa Province, Northern Mozambique, is well-known as an intracratonic basin of Karroo equivalent age in Mozambique, that comprises a complete succession of the Permian deposits (Verniers et al., 1989). A recent study by Nhamutole et al. (2024) on the outcropping strata from the Maniamba Basin, highlighted the presence of organic-rich intervals made up of black to grey claystones, siltstones and black shales, that are prospective hydrocarbon source rocks based on the interpretation of pyrolysis Rock-Eval data. That study represented only a preliminary characterization, which should be complemented with a multiproxy study in order to strengthen the current state of knowledge regarding the stratigraphy, palaeoenvironments as well as palaeoredox conditions that controlled the organic matter preservation and enrichment in the basin. Amongst these multiproxy methods are palynological, petrographical and geochemical analyses that have a widespread application in the understanding of the earth’s past record, and have not yet been applied to strata in the Maniamba Basin (central Gondwana). In this basin, most of the stratigraphic work was based on lithostratigraphic inferences, which raise some ambiguities and misinterpretation regarding the ages of the different sections. To address these limitations, in this study we used palynology to constrain the age and to understand the palaeovegetation and geodynamics of this part of Gondwana. Additionally, since biomarkers are regarded as an essential tool for tracking biodiversity, paleoenvironmental reconstruction and its change through geological time (Peters et al., 2005), we have used biomarkers to show whether or not the light oil from the Mozambique and Rovuma Basins that lie unconformably over the Karoo aged strata are sourced from the Maniamba Basin formations. Lastly, the organic rich units have been be evaluated for their mineralogical composition in order to assess their potential for unconventional or conventional resources, as well as for future projects on carbon storage and sequestration.

The understanding of palaeoenvironments will add important information in light of the transition to cleaner energy, since the world is currently shifting to a focus on the so-called “advantaged” hydrocarbons (Davies and Simmons, 2021).

2. Geology of the Maniamba Basin

The geology details of the Maniamba basin are included in the section 5.1.

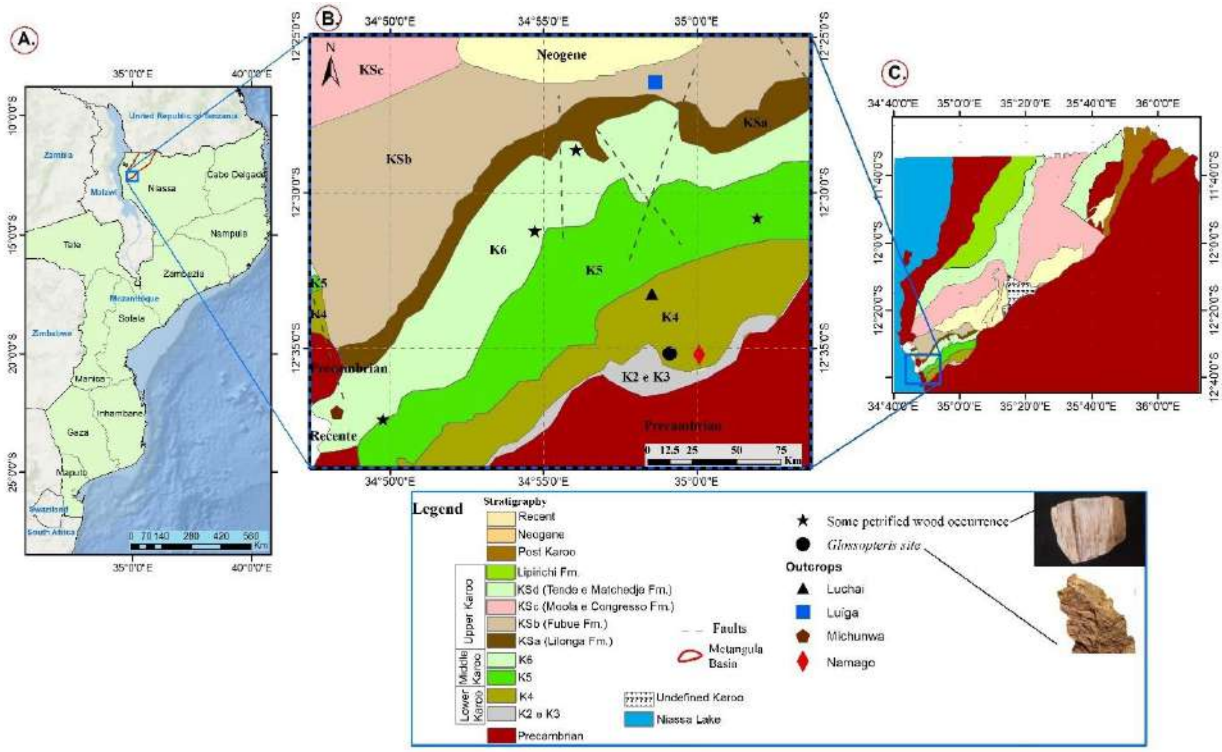

Figure 1. Basin, modified from Verniers et al. (1989). A: Geographic location of the studied area within Mozambique; B-C: schematic representation of the geological settings of the Maniamba Basin.

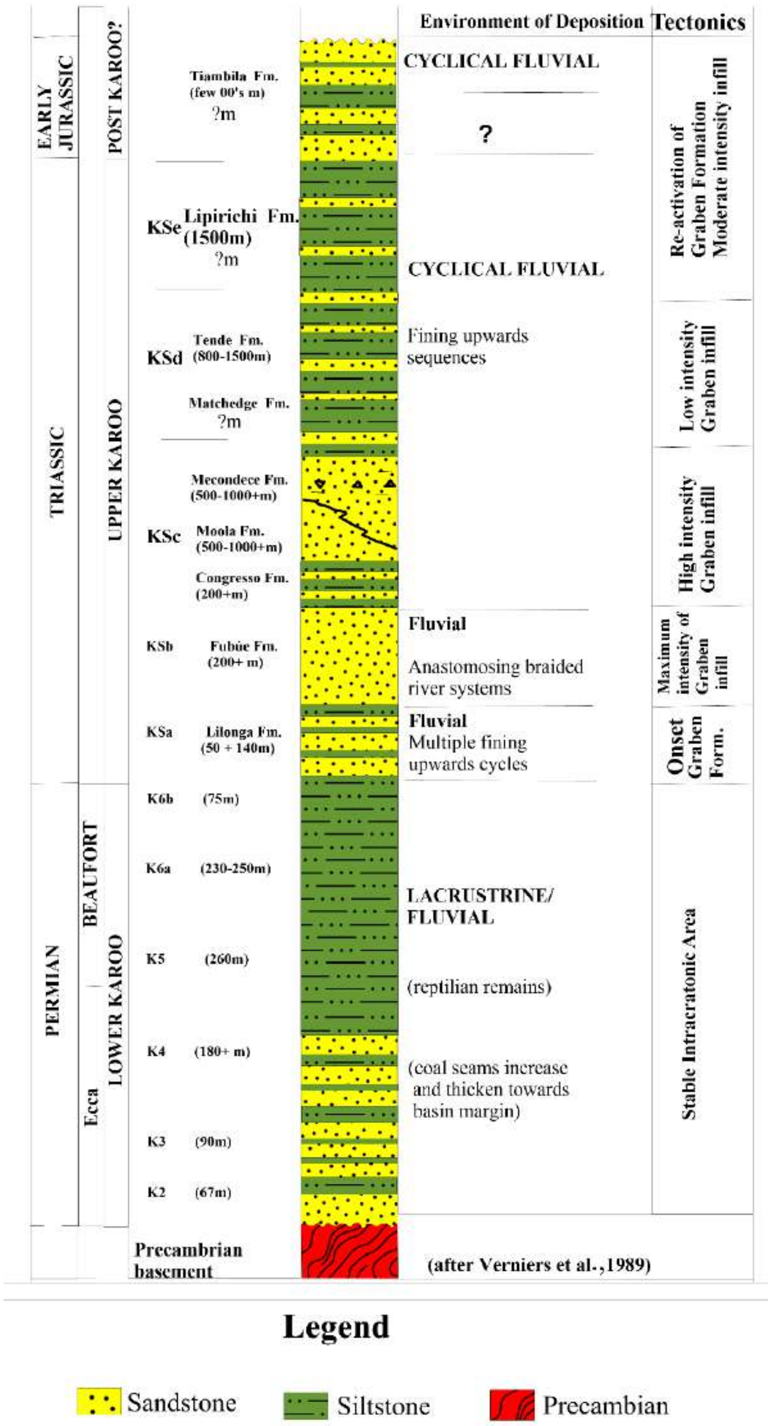

Figure 2. Lithostratigraphic overview of the studied Basin highlighting palaeoenvironments and tectonism (after Verniers et al., 1989).

3. Methods and Materials

3.1. Lithological description

Amongst the studied outcrops, the Luiga site represents the deepest deposit with a total depth of *ca.* 24m with carbonaceous shales dominating the profile. Sandstones and claystones are also observed in this succession. The Luchai outcrop is dominated by carbonaceous shale with varied thickness being intercalated by coal layers. The siltstone occurs as a predominant lithology in the Michunwa outcrop; however, sandstone horizons and mudstone intercalate towards the top of the sequence. Lastly, the Nhamago section consists of grey claystone at the bottom as well as in the top of the succession. However, an intercalation of dark claystone with coal is identified in the middle portion of this succession.

3.2. Sampling

Ten (10) samples were subsampled from outcropping in the Maniamba Basin (Figs 3 and 4). The selection of the outcrops was based on previous recognition and characterization, and they present some vertical and lateral variations. Palynology, palynofacies, biomarkers, and XRD laboratory procedures are described in sections 5.1, 6.1.2, 6.4 respectively.

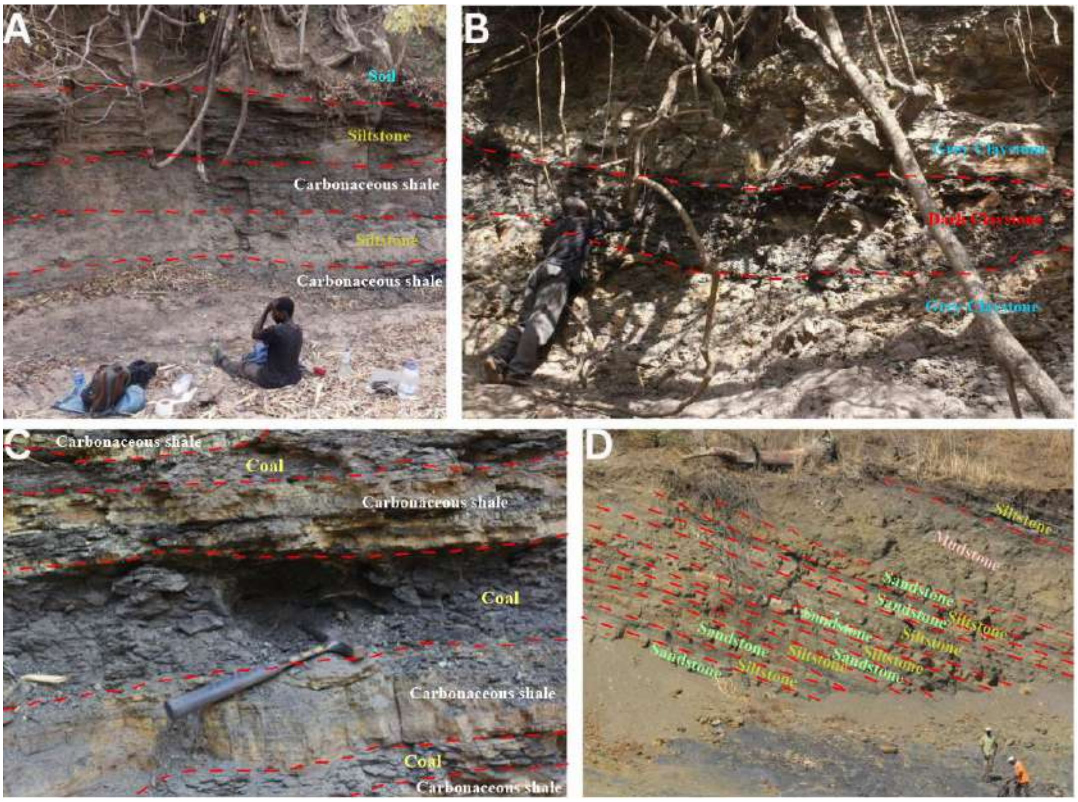

Figure 3. Field illustrations of the studied outcrops displaying sampled units: A: Luiga outcrop; B: Nhamago outcrop; C: Luchai outcrop; D: Michunwa outcrop.

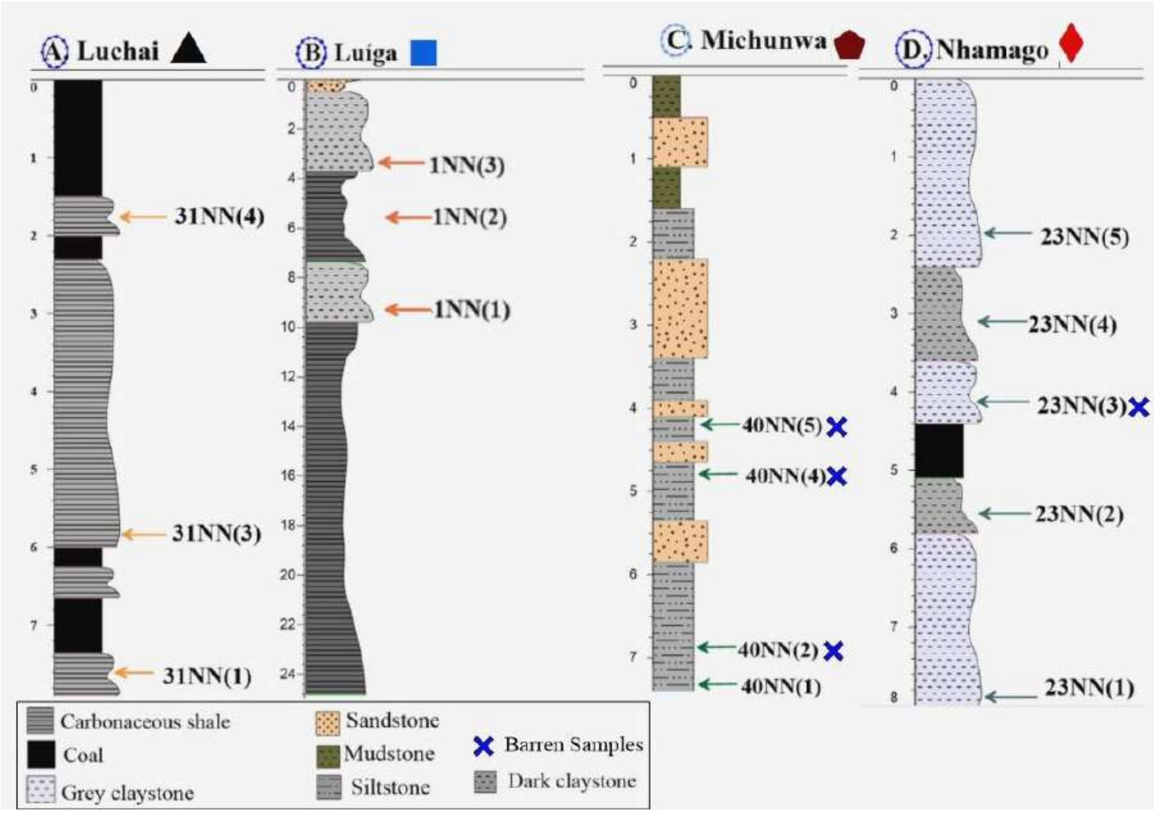

Figure 4. Lithology and sample horizons for the four outcrops from the Maniamba Basin, including the collected samples A: Luiga, B: Nhamago, C: Luchai, and D: Michunwa.

4. Results and Discussions

4.1. Palynology

4.1.1. Luchai and Nhamago outcrops

The Luchai outcrop is characterised by a low content of spores and dominance of bisaccate pollen which comprise striate and non-striate forms. Twenty-four species distributed in seventy genera of pollen and spores were identified (Table 1 and Fig. 5). The occurrence and abundance of taxa such as *Lueckisporites virkkiae*, *Striatopodocarpites gondwanensis*, *Striatopodocarpites fusus*, alongside *Platysaccus papilionis* suggest a Lower-Middle Permian age (Guadalupian) for the sediments from the Luchai outcrop (Modie, 2007; Lopes et al., 2014; Pereira et al., 2016). In contrast, the strata from the Nhamago outcrop are characterized by a smaller number of recovered sporomorphs. Seven different species of palynomorphs were retrieved (Table 1 and Figs. 5 and 6). Most of the identified sporomorphs were also found in the Luchai strata which can suggest a similar age.

Table 1 Vertical distribution of palynomorphs recovered from the outcrop samples.

Lithostratigraphy		Outcrops (Maniamba Basin)										
		Luchai		Nhamago		Michunwa				Luiga		
		31NN		23NN		40NN				1NN		
Depth (m)/samples number		(1)	(3)	(2)	(4)	(1)	(2)	(4)	(5)	(3)	(4)	5B
Laevigatosporites colliensis	Spores		X						X			x
Laevigatosporites vulgaris									X		x	
Baculatisporites sp.			X									
Converrucosisporites micronodosus		X										
Apiculatisporis sp.		X										
Polypodiisporites mutabilis												x
Horriditriletes tereteangulatus		X		X							x	x
Horriditriletes filiformis		X									x	x
Horriditriletes ramosus											x	
Leiotriletes directus		X										
Microbaculispora tentula		X								X	x	
Calamospora spp.			X									
Calamospora sp.											x	
Procoronaspora spinosa										X		
Potonieisporites brasiliensis	Pollen	X										
Lueckisporites virkkiae		X										
Platysaccus leschikii		X										
Platysaccus papilionis		X										
Protohaploxypinus limpidus		X		X	x							x
Protohaploxypinus goraiensis											x	x
Protohaploxypinus diagonalis												x
Striatopodocarpites fusus		X										
Striatopodocarpites cancellatus					x				X	X	x	
Striatopodocarpites gondwanensis		X										
Lunatisporites variesectus		X										
Scheuringipollenites medius			X		x		x					x
Scheuringipollenites ovatus		X	X	X	x							x
Scheuringipollenites maximus			X		x							
Weylandites magmus		X										x
Weylandites lucifer		X							X		x	x
Vittatina sp.												
Vittatina subsaccata											x	
Vittatina fasciolata												x
Cycadopites cymbatus				X		x					x	x
Cycadopites follicularis		X										
Guttulapollenites hannonicus												x
Staurosaccites cordubensis												x

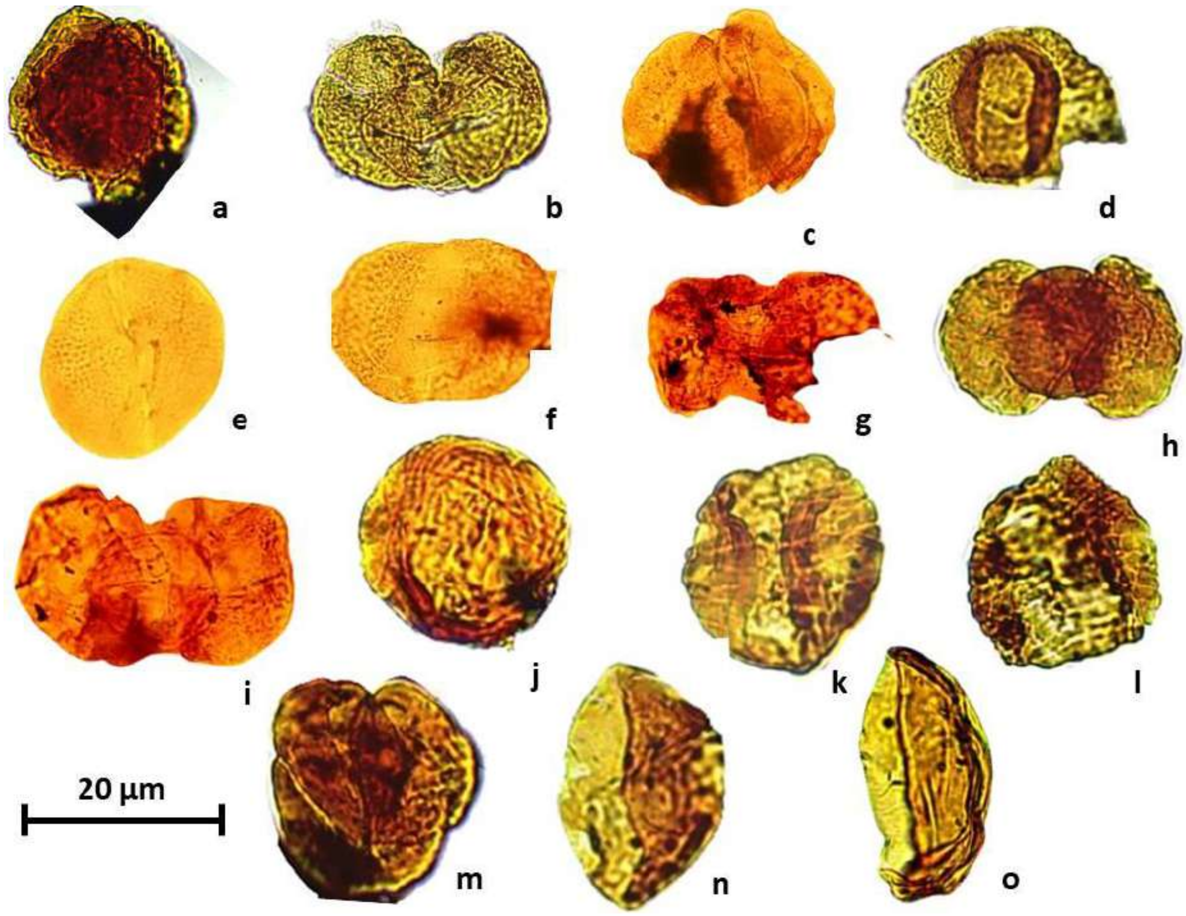

Figure 5. A: Unidentified pollen grain; B: *Lueckisporites virkkiae* (Potonié and Klaus, 1954); C: *Striatopodocarpites* spp; D: *Potonieisporites magnus* Lele and Karim (1971); E: *Scheuringipollenites ovatus* (Tiwari, 1973); F: *Protohaploxypinus goraiensis* (Potonié 691 and Lele; Hart, 1964); G: *Protohaploxypinus limpidus* (Balme and Hennelly), Balme 692 and Playford (1967); H: *Striatopodocarpites cancellatus* (Balme and Hennelly), Hart (1963); I: *Striatopodocarpites fusus* (Balme and Hennelly) Potonie; J: *Weylandites magmus* (Bose and Kar), Backhouse (1991); K: *Weylandites* spp.; L: *Vittatina* spp.; M: *Gutulapollenites hannonicus* (Goubin, 1965); N: *Cycadopites cymbatus* (Segroves, 1970); O: *Cycadopites follicularis* (Wilson and Webster, 1946).

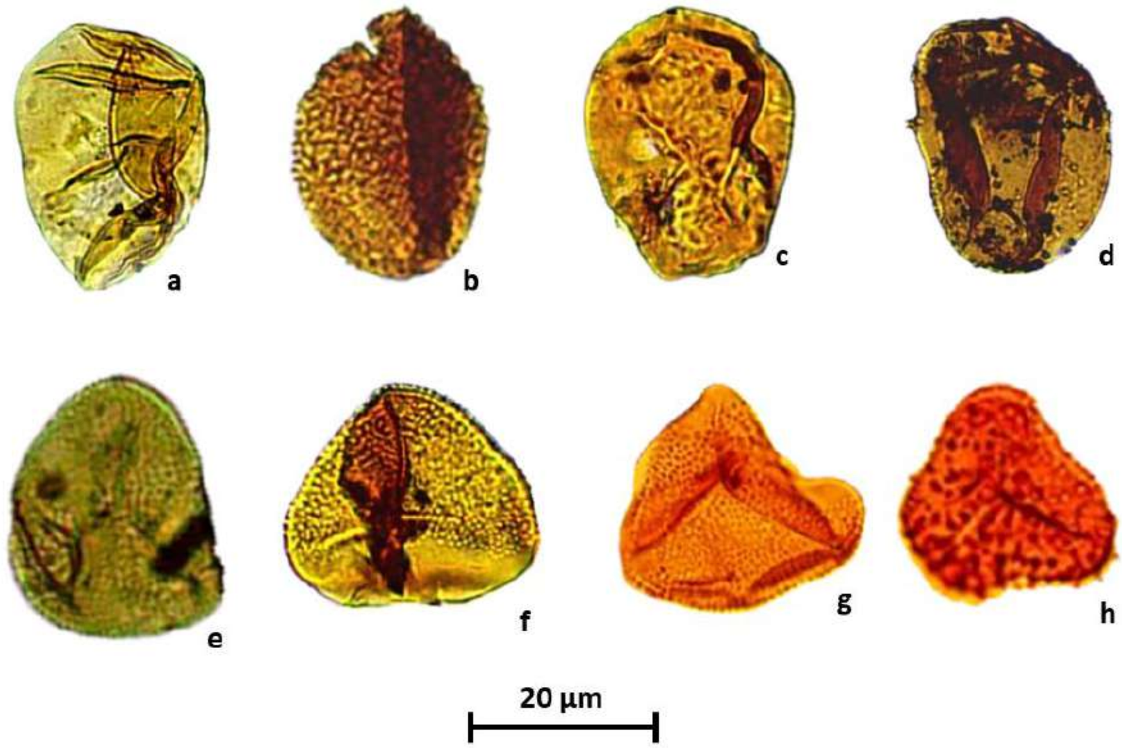

Figure 6. A: *Calamospora* spp.; B: *Polypodiisporites* spp., C: *Laevigatopsorires colliensis* (Balme and Hennelly), Venkatachala and Kar (1968); D: *Laevigatosporires vulgaris* Ibrahim), Alpern and Doubinger (1973); E: *Converrucosisporites confluens* (Playford and Dino, 2002); F: *Converrucosisporites confluensis* (Balme and Hennelly) Playford y Dino (2002); G: *Converrucosisporites micronodosus* (Balme and Hennelly), Playford y Dino (2002); H: *Horriditriletes tereteangulatus* (Balme and Hennelly), Backhouse (1991).

4.1.2. Michunwa outcrop

The Michunwa strata display a low level of preservation and as a result only nine species and eight genera were identified (Table 1). Typical Permian sporomorphs were observed; however, their long stratigraphical range hinders a precise age assignment.

4.1.3. Luiga outcrop

The Luiga strata are made up by an assemblage dominated by striate bisaccate pollens and low concentration of spores. Here, typical Changhsingian aged sediments are identified based on the abundance of *Guttulapollenites hannonicus*; *Striatopodocarpites cancellatus*, *Protohaploxypinus limpidus*, *Protohaploxypinus* *goraiensis*, *Weylandites lucifer* and *Calamospora* sp. (Pereira et al., 2016; Lopes et al., 2014; Barbolini et al., 2018; Aggarwal et al., 2019). Additionally, the palynoassemblage is characterized by the presence of stratigraphically significant genera such as *Polypodiisporites* reported from Late Permian strata from Salt Range in Pakistan (Pereira et al., 2016). A remarkable and prominent feature in the Early Triassic assemblage is the occurence of the spore tetrads (Table 1) of lycopsids (*Lundbladispora*) and pteridophytes (*Calamospora*). The Triassic palynoflora from the Maniamba Basin (central Gondwana) is discussed in Nhamutole et al. (2024b).

4.1.4. Paleoenvironmental based on palynoflora and lithofacies

The palynological study has shown well-preserved forms characterized by an abundance of gymnospermous pollen assigned to glossopterids that consist of non-striate and striate bisaccate pollens (Table 1). The spore group is the least dominant group in the studied outcrop and is represented by filicopsids such as *Horriditriletes*, *Leiotriletes*, *Converrucosisporites* and lycopsids (Table 1). The abundance of arborescent vegetation indicates a development in a forest swamp located in a small distal marginal part of the mire. Interestingly, the studied flora is made up by the dominance of glossopterids (e.g., *Protohaploxypinus*, *Striatopodocarpites, Scheuringipollenites*) and conifers *(e.g., Platysaccus, Potonieisporites)* co-existing with filicopsids *(e.g., Horriditriletes, Leiotriletes, Apiculatisporis)*, sphenopsids (*e.g., Calamospora, Laevigatosporites),* voltziales *(Lueckisporites, Lunatisporites,* which are indicative of a typical hypautochthonous sedimentation as reported by Birks and Birks (1980). The conifer occurrence in the Maniamba Basin is shown by the presence of Permian fossil woods assigned to *Australoxylon teixeirae*, *Agathoxylon africanum* and *Agathoxylon karooensis* (Nhamutole et al., 2024b). Most of the identified palynotaxa described above they do occur either commonly and abundantly representing a typical palynoflora typical of humid and warm lowland areas, in which the upland vegetation's influence is rare (Lopes et al., 2021). The greater proportion of pollen grains compared to spores as well as the high content of opaque compared to translucent phytoclasts in the outcrop strata suggest a swampy environment in the proximal settings (e.g., Mendonça Filho et al., 2010a). Furthermore, the luxuriant vegetation could be linked to a prevailing warm and humid climate that favoured their growth during Permian (Middle and Late) as seen in most Gondwana sequences (McLoughlin, 2001; Aggarwal et al., 2019). Similar paleoclimate patterns have been described by Nhamutole et al. (2021) in the analysis of *Protaxodioxylon* fossil woods from Maniamba Basin. In this study, they suggest that conifer woods have thrived in a typical environment influenced by abundant water supply and that the growth of plants were mainly controlled by variation in climate. Moreover, climate variation models during the studied period in the Maniamba Basin are found in Verniers et al. (1989). Yet, the paleoredox conditions observed in the water column coupled with high primary production has resulted in the organic matter enrichment representing the main factor that led to the organic matter accumulation homogeneity. The dominance of non-translucent phytoclasts over translucent phytoclasts could be attributed to palaeofires and existing conditions of oxidation either before or post deposition in proximity to high energy settings (Tyson, 1995). The observed non-opaque phytoclasts in most cases display a large size which could be linked to the short distance of transport (Tyson, 1995). Similar results have reported by Nhamutole et al. (2023) in their palynofacies study based on borehole core from the Maniamba Basin, Mozambique. In summary, based in the present data, a swampy environment combined with lacustrine settings influenced by fluvio-alluvial conditions with intercalations of finer and coarser sediments characterize the studied strata. Furthermore, the observed lithologies in all the studied successions are quite similar and generally the sandstone units depict channel-fill successions. Those sandstones may represent crevasse splay deposits which were formed by the rupture of natural levees in the onset stages of flooding events (Collinson, 1996; Miall, 2010; Bicca et al., 2017).

The mudstone and carbonaceous shale horizons indicate overbank deposits with environmental settings prone to formation and accumulation of coal seams. Yet, the presence of black mudstones may suggest variation in water levels, with consequent subaerial exposure of organic matter (Mendonça et al., 2017). The thin siltstone units interbedded with sandstone layers (e.g., Michunwa strata) represent clastic deposition in the over banks at the time of flooding episodes. Here, the flood peaks might have been followed by sedimentation of particles of the size of silt and mud as suggested by Collinson (1996) and Bicca et al. (2017).

4.2. Palynofacies

The OM is subdivided into three distinct categories, namely phytoclasts, sporomorphs (pollen and spores) and AOM derived from bacteria and resin as defined by Tyson (1995) and later updated by Mendonça et al. (2017) (Table S1-Supplementar Material). The phytoclasts were identified as opaque phytoclasts, and non-opaque phytoclasts (cuticles, membranes, and fungal hyphae). The identified cuticles are typical of different plant groups as shown in the Figs. 7A-I, however, the cuticles observed under incident blue light have shown dark or no fluorescence (Figs. S1 and S2-Supplementary Material).

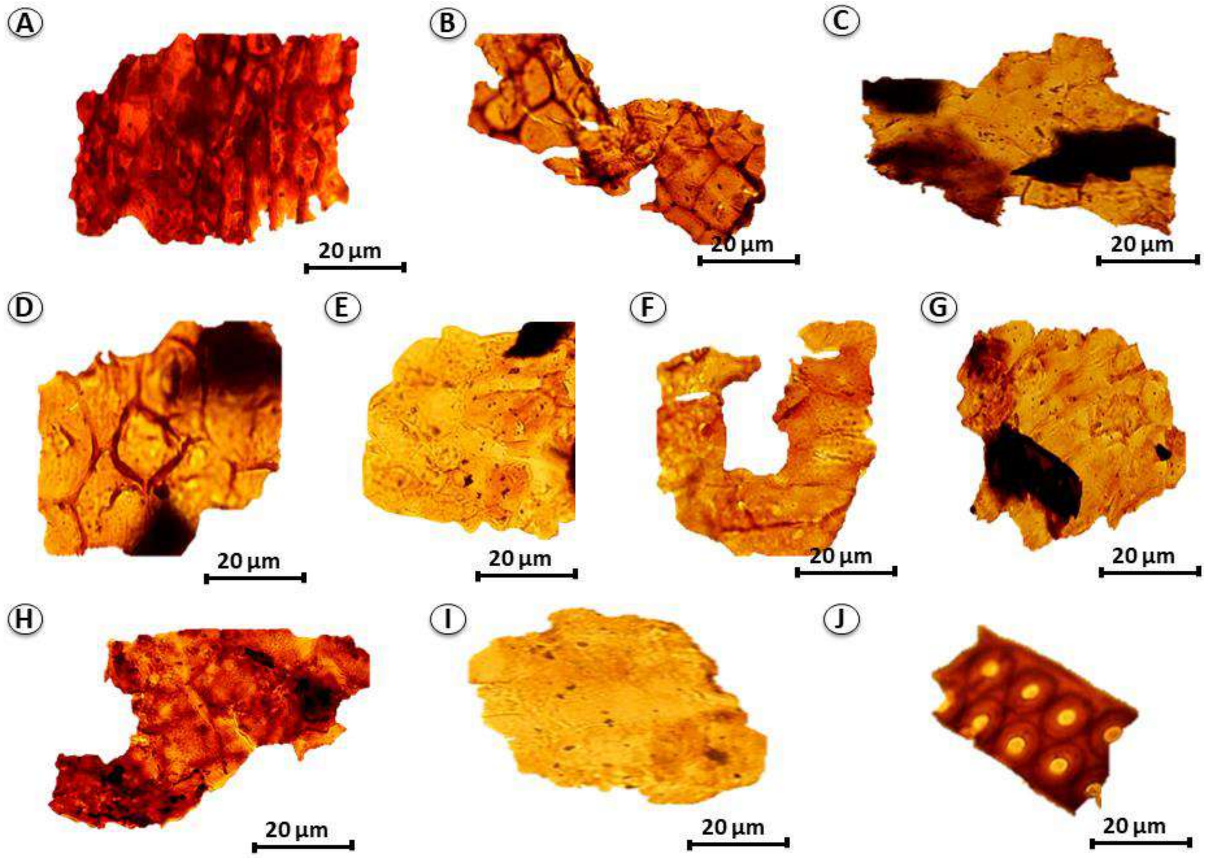

Figure 7. Microfotographs showing different types of cuticles from selected samples from studied outcrops. A: Glossopteris conifer type; B: Plant cuticle; C-D: Conifer cuticle; E: Unidentified cuticle type; F: Conifer cuticle; G-H: Glossopteris conifer; E-Unidentified. cuticle type; J: Biostructured non-opaque phytoclast (a tracheid of a gymnosperm wood with bordered pitting in an alternate pattern, possibly *Agathoxylon* sp.).

Membranes which are organic particles derived from leaves of plants are also observed and they generally pale yellow and sheet-like particle (Tyson, 1995). These membranes are poorly preserved and are in low quantity (Table S1-Supplementary

Material). Fungal remains which represented by fungal hyphae (Tyson, 1995; Fonseca et al., 2020), are found in low quantity through the studied units (Fig. 8E). These fungal remains display orange to dark brown colour in transmitted white light microscope and do not show fluorescence (Fonseca et a., 2020). The palynomorph groups follow the phytoclasts and are represented by organic compounds which belong to the sporomorph category. Diversified subgroups of pollen were observed under transmitted light microscopy ranging from monosaccate, striate and non-striate to colpate. Pollen grains observed under blue light have shown yellow to orange colour fluorescence (Fig. 8F-G). Additionally, the observed spores display varied ornamentations, shapes and sizes with no observed fluorescence (Fig. 8H). They are characterized as monoletes and triletes; however, they do not show diversification when compared with the pollen group. In generally, the numbers of recovered palynomorphs are considerably low and their state of degradation may have resulted from subaerial exposure during the periodic drop in water levels, triggering arid deposition conditions. Another hypothesis for their scarcity and the poor preservation of these elements could be related to the reduced quantity of plants at the site of deposition (Mendonça et al., 2017). The amorphous category consists of AOM derived from terrestrial sources, resins and bacterially derived AOM (Figs. 8A-D). The terrestrial AOM exhibits structureless, homogeneous, rounded to subangular patterns with colours ranging from orange to dark brown (Figs. 8A-B). The AOM is terrestrially derived with no fluorescence, indicating that it was influenced by maturity and the amorphization patterns (Figs. S3 and S4-Supplementary Material) as defined by Suárez-Ruiz et al. (2012) and Fonseca et al. (2020). The observed resins are structureless, with homogeneous particles, and orange to light brown in colour. The resins are associated with gymnosperms (Tyson, 1995; Suárez-Ruiz et al., 2012). The AOM derived from bacteria is characterized by a huge density of tiny particles displaying orange colour with different outlines (Fig. 8D). This bacterial-like material did not show fluorescence. Yet, fungal remains are present and therefore reflect the proximity to the terrestrial source area (Suárez-Ruiz et al., 2012; Mendonça et al., 2017) and are orange-brown in colour (Fig. 8E).

Based on the statistic estimations of recovered organic matter, three palynofacies are identified in the coal-bearing sequences as follows:

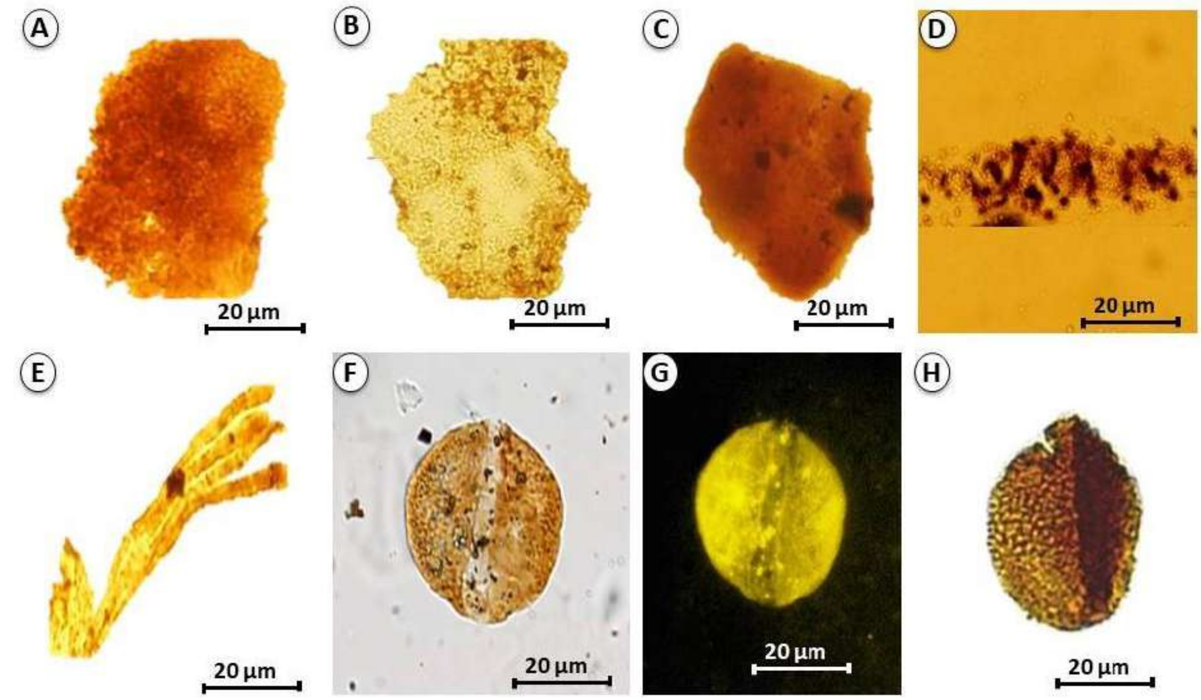

Figure 8. Microphotographs of the organic components from the outcrop strata in the Maniamba Basin. A and B: Terrestrially derived AOM; C: Higher plant resin; D: Plate-like bacterial-derived AOM; E: Fungal hyphae; F: Non-striate bisaccate pollen in Transmitted light microscope; G: Non-striate bisaccate pollen in fluorescence mode; H: Trilete spore.

4.2.1. Palynofacies I

The high concentration of well-preserved pollen and spores reinforcing the concept of the growth of conifers, glossopterids and ferns in the swamp environment at the time of the deposition of the sediments, indicate that the luxuriant vegetation thrived and was sustained by local climate. However, beside the contribution of lowland vegetation, upland contributors are also observed albeit being in minor quantities as mentioned above. Yet, the abundance of sporomorphs followed by only amorphous organic matter indicates periods of restriction characterised by the development of reducing conditions (Mendonça Filho et al., 2017; Tyson, 1995). This restriction may have triggered the stagnation of the water body as well as the development of a low oxygen layer and stratification in the water column (Tyson, 1995; Mendonça Filho et al., 2010a, 2017a; Marques-Lima et al., 2023) as also demonstrated by the ternary diagram proposed by Mukhopadhyay (1986) (Fig. 9). In this palynofacies a decrease in water level could be linked to the relative increase of the space of accommodation which is possibly triggered by rifting activity.

Moreover, the phytoclasts are observed in lower concentrations. The palynofacies I is observed in samples 40NN (2), 31NN (4) and 23NN (4). Here, the highest TOC content in the succession is observed (7.96%) which could be linked with high occurrence of bacterially-derived AOM (Manga et al., 2024). No lithology-controlled facies observed herein.

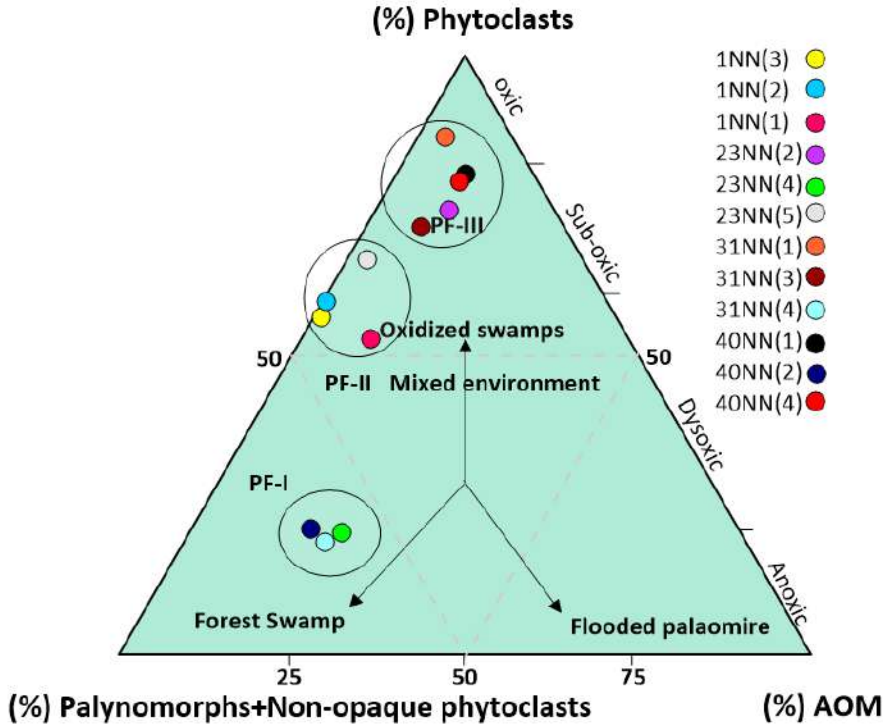

Figure 9. Ternary diagram linked with paleoredox conditions proposed by Mukhopadhyay (1986) adapted by Marchionni (1980); Sing and Sing (1996); Aggarwal et al. (2019).

4.2.2. Palynofacies II

The palynofacies II is characterized by suboxic palaeoredox conditions (Fig. 9). The palynofacies association consists of a high frequency of opaque phytoclasts with a sub-dominance of palynomorphs. This interval is, generally, characterized by a fluvial runoff, in a less oxic environment if compared to palynofacies III Tyson, 1995; Mendonça Filho et al., 2010a, 2017a; Marques-Lima et al., 2023). The palynofacies II is observed in samples 1NN (1), 1NN (2), 1NN (3). Here, there is no lithology-controlled facies.

4.2.3. Palynofacies III

Palynofacies III is found in samples 23NN (2), 31NN (1), 31NN (3), 40NN (1) and is dominated by opaque phytoclasts with lesser abundance of palynomorphs and amorphous organic matter (Table 2).

Table 2 Relative percentage of different organic matter components linked to mineralogical composition.

Samples	Phytoclasts (%)	Palynomorphs (%)	AOM (%)	Mineral phases (XRD
1NN (2)	56.3	42.6	1.0	Calcite+quartz
1NN (2)	59.4	40.3	0.3	Quartz+kaolinite+montmorillonite+ortoclasse
1NN (1)	52.6	37.4	10.0	Quartz+kaolinite
23NN (2)	74.0	15.3	10.7	Quartz+kaolinite+chlorite+orthoclase
23NN (4)	20.8	58.2	22.0	Kaolinite+quartz+montmorillonite
31NN (1)	65.8	31.0	3.2	Quartz+kaolinite+montmorillonite+chlorite
31NN (3)	86.3	9.7	4.0	Quartz+kaolinite+vaterite
40NN (1)	71.4	20.0	8.6	Quartz+kaolinite+muscovite+orthoclase
40NN (2)	19.1	60.4	20.5	Quartz+microcline+anorthite
40NN (4)	80.3	9.7	10	Quartz+kaolinite+montmorillonite+anorthite

*AOM=Amorphous organic matter

The opaque phytoclasts could have originated from oxidation of organic matter with structural shapes such as cuticle, tracheids and translucent brown coloured wood. The oxidation can occur during transportation or as a result of depositional variations (Cincotta et al., 2015; Mendonça Filho et al., 2017, 2023). The studied samples are characterised by high quantity of elongated phytoclast over its equidimensional counterpart (Table S1-Supplementary Material), fact that corroborates with deposition close to the sources which is regarded being the proximal (Aggarwal, 2021). Moreover, the high concentration of opaque phytoclasts suggests oxidizing conditions, increasing of water column, and deposition under moderately higher energy conditions in the proximity of terrestrial sources, or degradation of terrestrial organic matter as indicated by oxic to suboxic conditions as shown in the ternary diagram modified from Mukhopadhyay (1986). Here, the amorphous group is completely represented by palynomorphs terrestrially derived OM including higher plants resin albeit some bacterial-derived AOM is also identified (Fonseca et al., 2021; Manga et al., 2024). Similar scenarios have been documented in oxic swamps, prodelta, and river sediments. Furthermore, the high abundance of opaque phytoclasts in the palynofacies III could reflect the existence of fire during the deposition of the sediments, as reported by Nhamutole et al. (2023). All the palynofacies record the occurrence of proportion of siltstone and carbonaceous shale. However, only the palynofacies III is marked by their dominance. In summary, the palynofacies data agree with the information from the TOC and sulphur diagrams (Figs. 10 and 11). All the information is substantiated by the schematic palaeovironmental reconstruction of the study area which corroborates with the scheme proposed by Paz (2018), based on lithostratigraphic descriptions (Fig. 12).

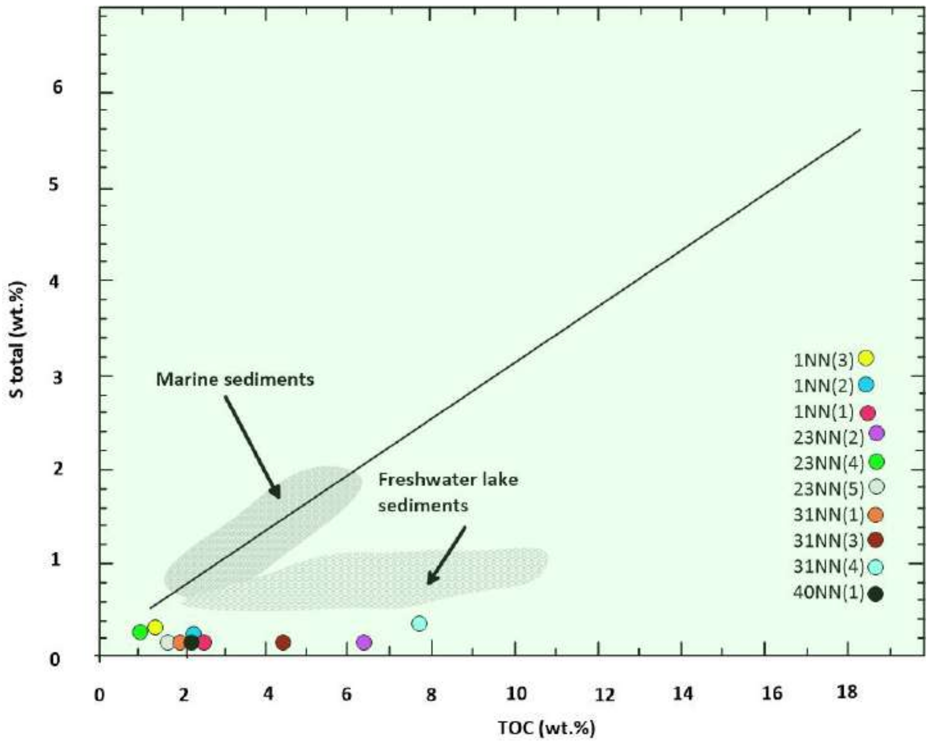

Figure 10. TOC (wt%) vs. Sulphur (%) diagram showing paleoenvironmental conditions.

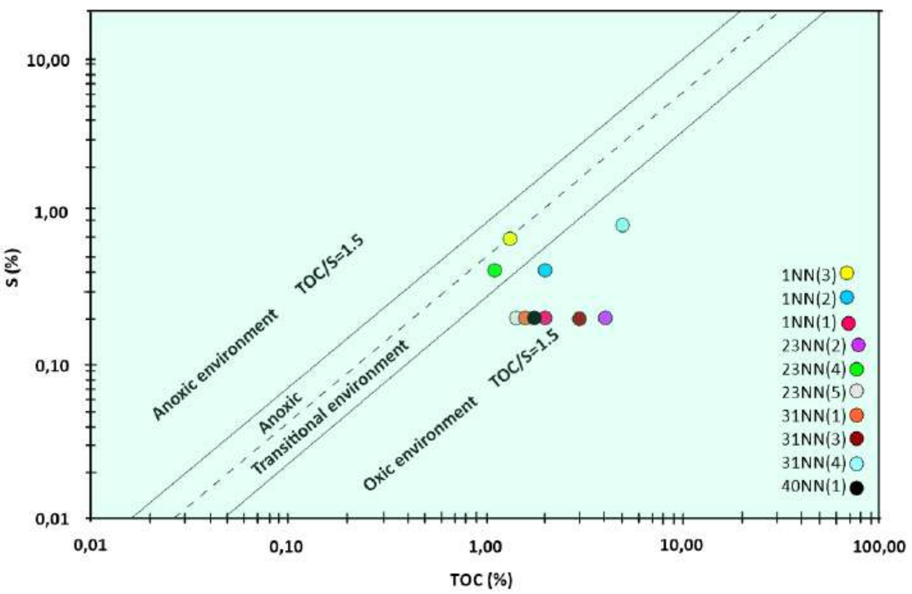

Figure 11. TOC (wt%) versus Sulphur (%) diagram demonstrating paleoredox conditions of the studied outcrop strata.

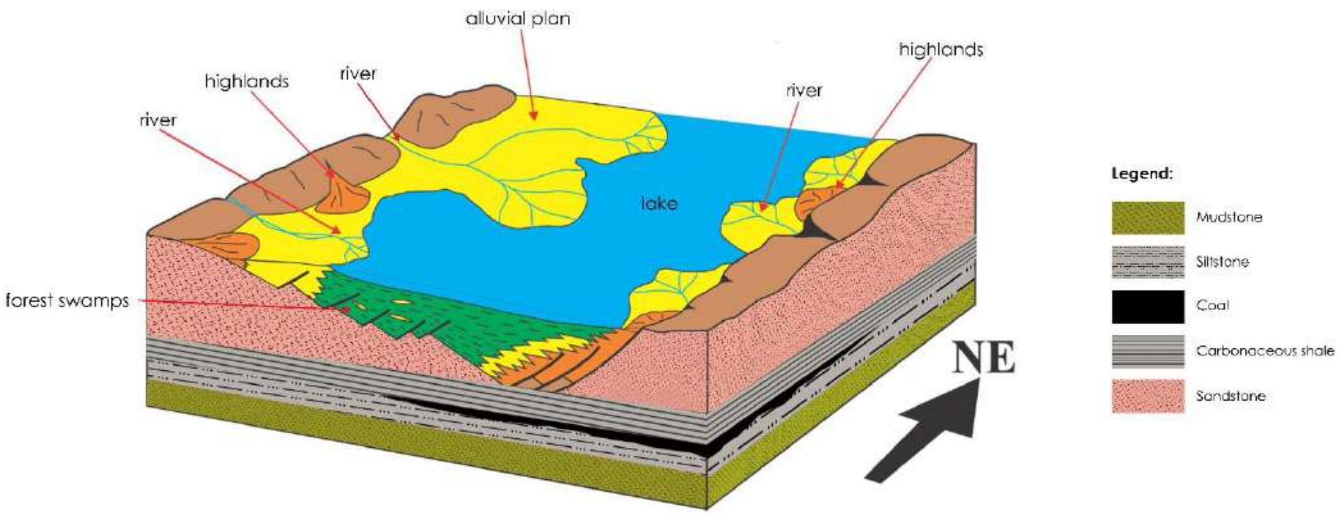

Figure 12. Paleoenvironmental reconstruction of the study area adapted from Paz (2018). Fig 14. Ternary plot (saturated vs. aromatic vs. asphaltenes) displaying the relative abundance and thermal maturity of the outcrop samples.

4.3. Rock Extract

The highest concentration of extractable organic matter (EOM) was observed in sample 40NN (1) (13.3%) and sample 23NN (2) (10.7%) (Table 3 and Fig. 13). These contents suggest that the samples display bitumen in large amounts, which corroborates with the data from palynofacies. Liquid chromatography has unveiled that the EOM is mainly represented by saturated compounds (11.1%-92.2%) followed by the asphaltenes fraction (1.2%-74.6%). Lastly, the aromatic fractions are in smaller amounts, ranging from 0.3% to 1.9%. The EOM composition is typical of terrestrial mature organic matter (Tissot and Welte, 1984).

Table 3 Relative percentages of extract organic matter (EOM), Hydrocarbons fractions, TOC and sulphur (S).

Samples	EOM (mg)	Saturated mg)	%	Aromatic (mg)	%	Asphaltens (mg)	%	TOC (Wt%)	S (%)
1NN (3)	7.7	7.1	92.20	0.5	6.49	0.1	1.29	1.4	0.18
1NN (2)	6.4	2.8	43.75	0.5	7.85	3.1	48.43	2.11	0.17
1NN(1)	8.8	5.3	60.22	1.3	14.77	2.2	25.0	2.29	0.13
23 NN (2)	10.7	5.4	50.46	1.1	10.28	4.2	39.25	6.34	0.13
23NN (4)	5.2	0.7	13.46	1	19.23	3.5	67.30	1.1	0.17
23NN (5)	4.1	2.5	60.97	0.4	9.75	1.2	29.26	1.67	0.13
31 NN (1)	3.2	0.4	12.5	0.3	9.37	2.5	78.12	1.98	0.13
31 NN (3)	3.6	0.8	22.22	0.6	16.66	2.2	61.11	4.33	0.13
31 NN (4)	6.3	0.7	11.11	0.9	14.28	4.7	74.60	7.96	0.19
40 NN (1)	13.1	9.5	72.51	1.9	14.50	1.7	12.97	2.0	0.13

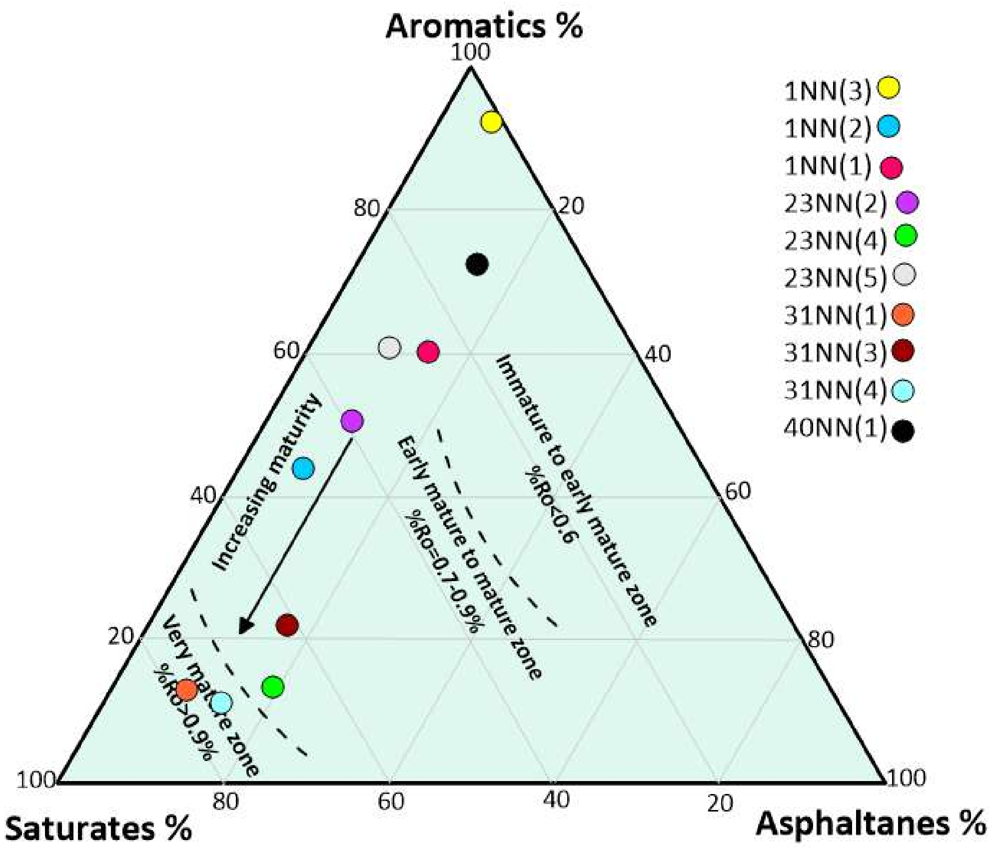

Figure 13. Ternary plot (saturated vs. aromatic vs. asphaltenes) displaying the relative abundance and thermal maturity of the outcrop samples.

4.4. Hydrocarbon biomarkers

Hydrocarbon biomarkers are organic compounds encased in sedimentary rocks, with molecular structures directly related to their precursor compounds, revealing information about past groups of organisms (Brocks and Grice., 2011). Therefore, hydrocarbon biomarkers provide robust information of past ecosystems, hence their use as palaeoenvironmental indicators. Here, biomarkers corroborate with palynological data in order to provide a molecular perspective of the analysed organic matter, assessing the palaeoenvironment, vertical heterogeneity, and source of organic-rich units from outcrop in the Maniamba Basin. The distribution and critical information obtained from them are interpreted for each outcrop as follows:

4.4.1. Luchai outcrop

For the Luchai outcrop, the liquid chromatography revealed the recovery of a low amount of soluble organic matter (bitumen), despite the occurrence of preserved organic matter (TOC=1.98%). This is reflected in the occurrence of some aromatic compounds (methyl-phenantrenes) in the terpane chromatograms, as seen in figure 14.

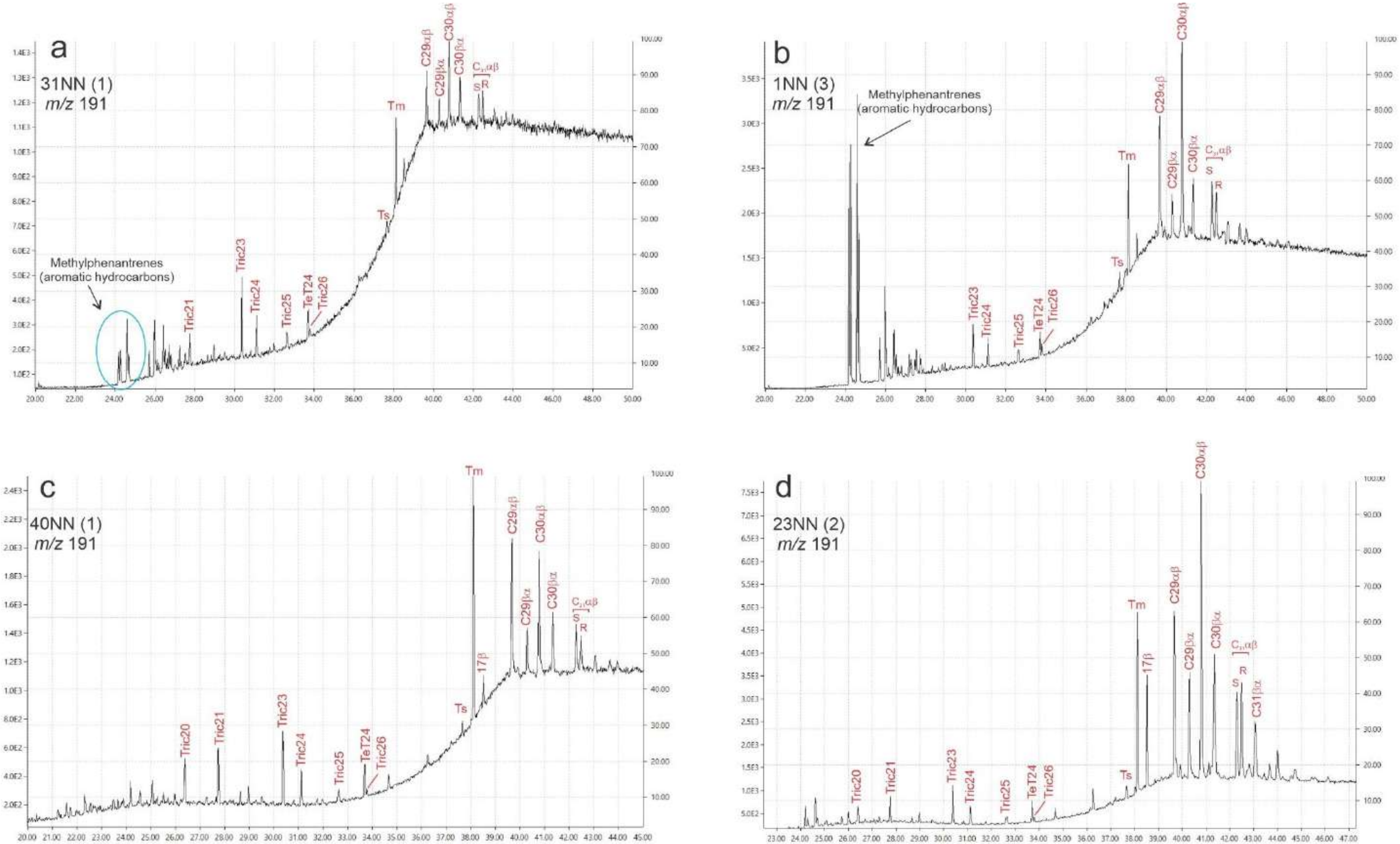

Figure 14. Tricyclic, tetracyclic and pentacyclic in mass chromatograms (*m/z* 191) from the outcropping strata in the Maniamba Basin.

The significant low amount of bitumen, even with a TOC around 2%, may be related to elevated thermal evolution (residual TOC). Indeed, the assessment of thermal maturity through the methyl-phenantrene index (Radke et al., 1982) suggests the onset of oil generation window (MPI-1=0.84) (Fig. 15). The same degree of maturity is not indicated by the saturated biomarkers, as noticed in the terpane and sterane profiles. Specifically, predominance of the C_{27} 17aTrisnorhopane (Tm), low degree of isomerization in the homohopanes (e.g. C_{31}S/R ratio), and the predominance of the less stable configuration of the steranes (αααR) are not in agreement with the MPI-1 index. An explanation for this discrepancy could be related the process of maturation. Saturated biomarkers may not respond well to rapid maturation as observed by Farrimond et al. (1996) and a context of rapid heating (igneous emplacement) is, therefore, raised to explain the contrast in the aromatic and saturated proxies. It should be noted that the influence of kimberlite intrusions has been reported by Nhamutole et al. (2024a) in their study of Rock data from this locality. Their emplacement was probably connected to the first or second graben faulting phase (Verniers et al., 1989). Here, should be highlighted the potential detection of 2-methylanthracene in the sample 31NN (1) (Fig. 16). The 2-methylanthracene indicates high temperature thermal processes and is generally observed in oils/rocks that experienced high thermal stress (Zhang et al., 2016), such as the influence of igneous intrusions (George, 1992). In terms of organic matter sources, the samples from the Luchai outcrop show the predominance of odd over even alkanes with high molecular weight characteristic of input from higher plants since the precursor molecules are found in resins of plants (Peters et al., 2005). The predominance of C_{29} sterane ($C_{29} > C_{28} > C_{27}$) is also indicative of input of terrestrial organic matter (Volkman, 1986) (Fig. 17).

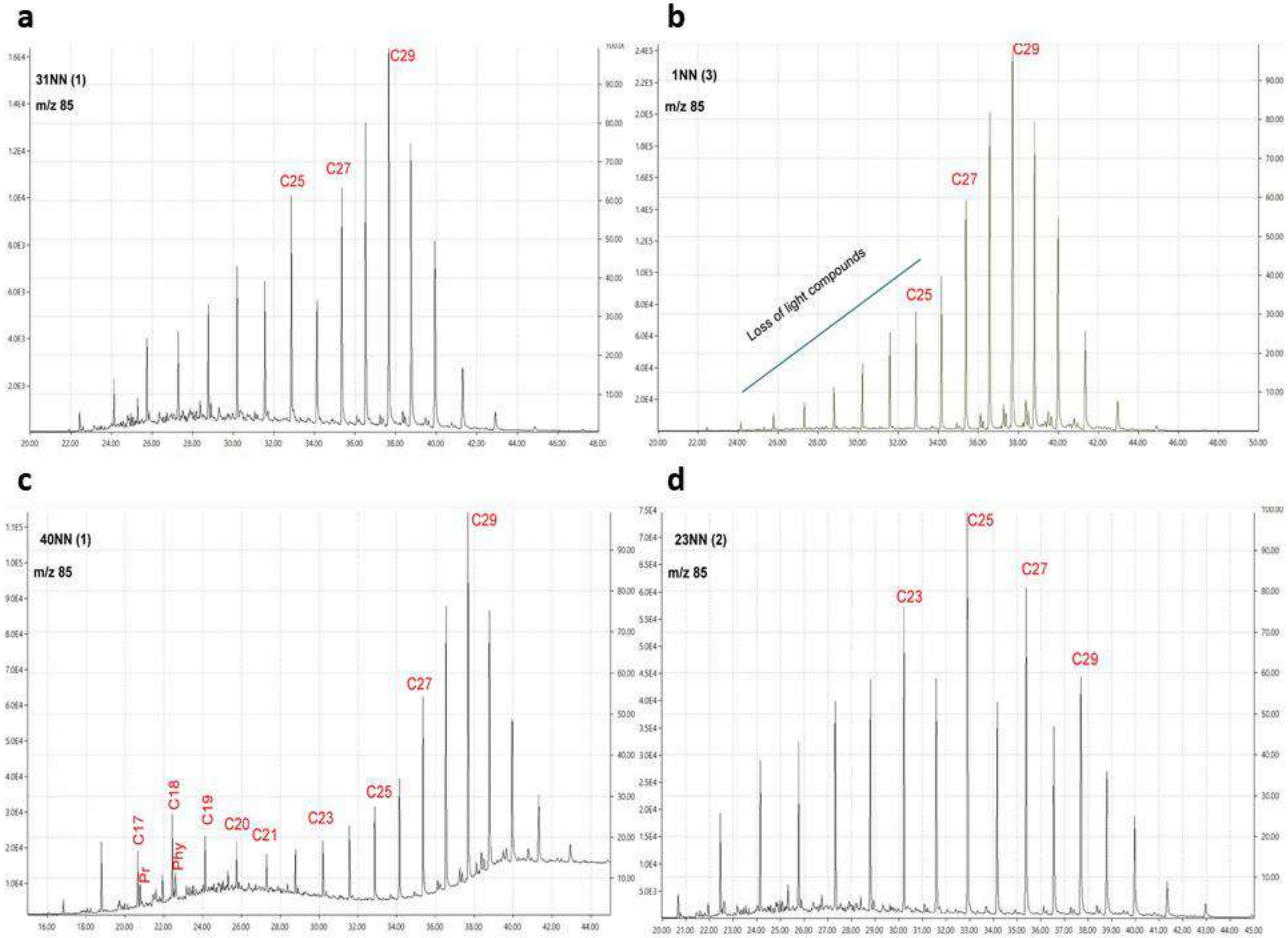

Figure 15. Mass chromatogram (*m/z* 85) of saturated hydrocarbons from the outcrop strata.

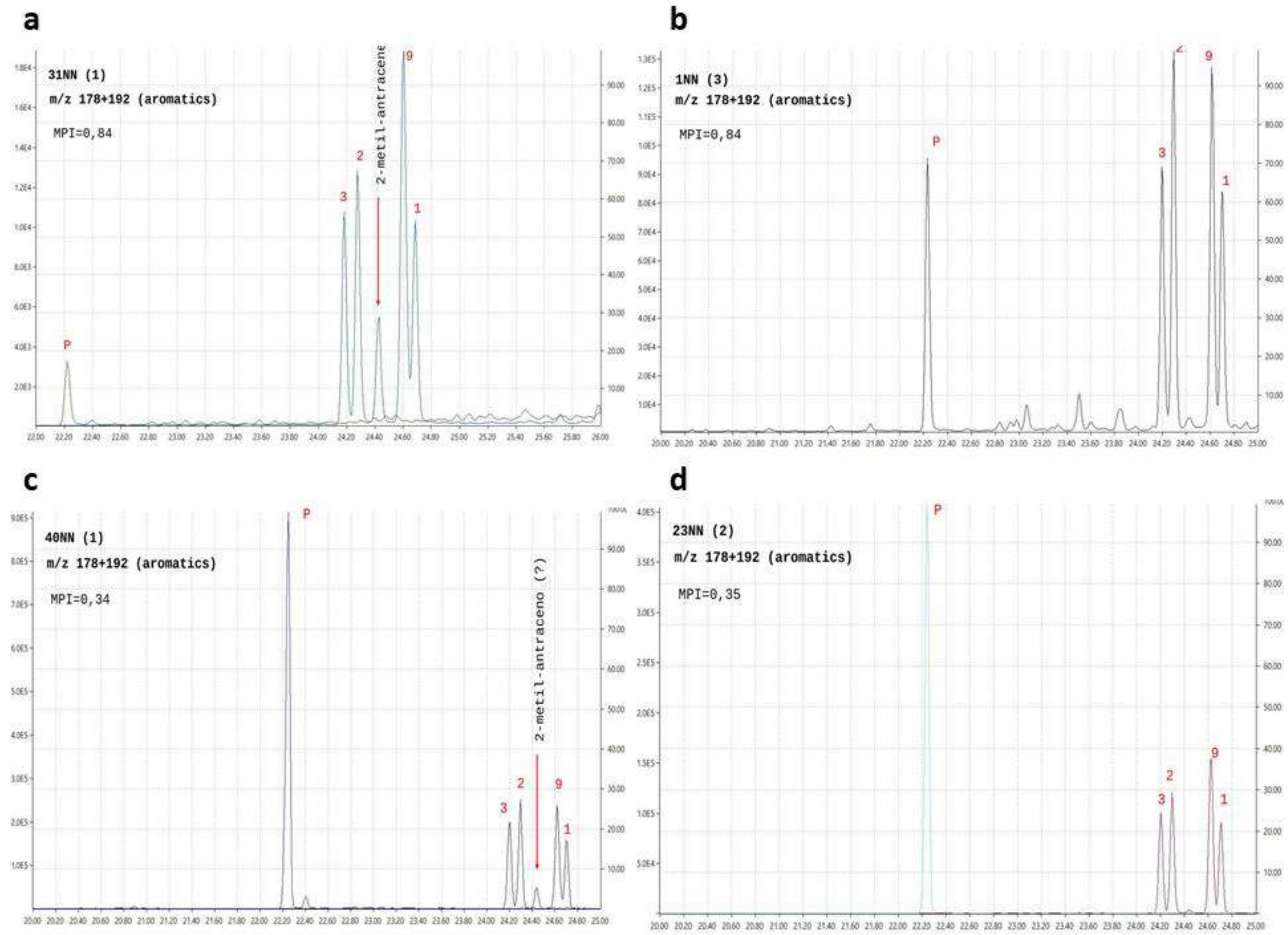

Figure 16. Mass chromatogram (*m/z* 178+192) of aromatic hydrocarbons of the outcrop strata.

4.4.2. Luiga outcrop

The biomarker assessment for the profiles of this section is quite similar to the Luchai section with respect to the predominance of odd *n*-alkanes and terpane distribution. Furthermore, the observed predominance of a much more stable configuration αααS of C_{27} steranes could indicate a further contribution of organic matter such as a type of algae (Koodner et al., 2008) (Fig. 17). Freshwater algae *Botryococcus braunii* were reported in samples from analysed borehole cores in the Maniamba Basin by Nhamutole et al. (2025) although they were not detected in the palynological analysis performed herein. These algae can occur in lagoonal and lacustrine facies and have the ability to adapt to different salinity conditions (Mendonça Filho et al., 2011b; Tyson, 1995).

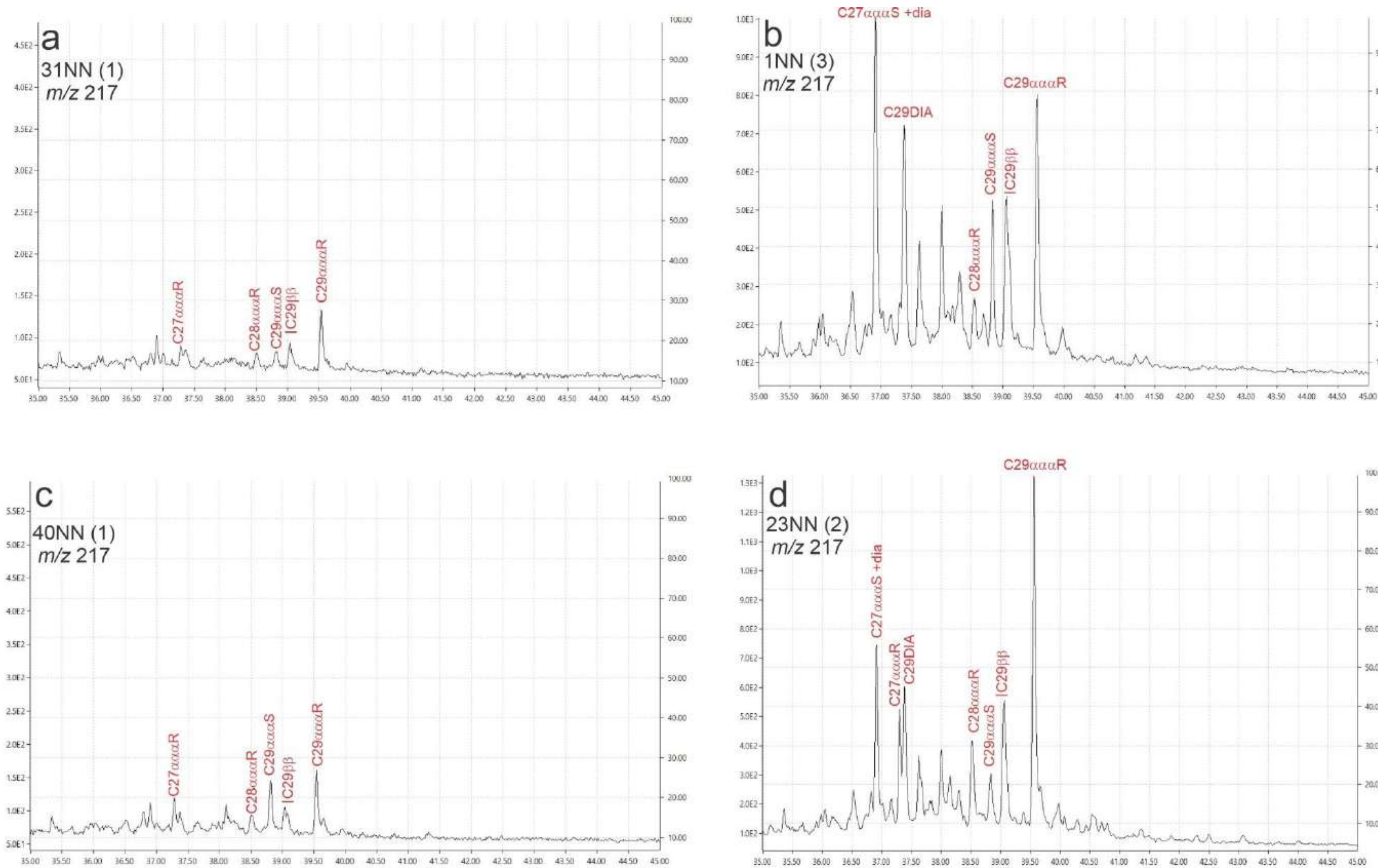

Figure 17. Representative 217 mass chromatograms showing the sterane distributions in selected samples from the studied samples.

4.4.3. Michunwa outcrop

The Michunwa strata depict the same scenario as reported from the above two sections. However, for these samples the presence of n-alkanes of low molecular weight was observed, suggesting low thermal evolution. This indicates that these compounds are either not well developed or have not yet been formed. Generally, the Phytane component is greater than Pristane, however such proxies should be analysed with caution since the samples might have been influenced by thermal activity, homohopane isomerization and source input (Ten Haven et al., 1987; Peters et al., 2005). The relative abundance of hopanes over steranes typifies organic matter derived from terrestrial settings (Tissot and Welte, 1984). The methyl-phenantrene index was low (0.35) likely reflecting low thermal evolution. The influence of igneous activity is not considered for these strata since no igneous intrusions were observed nearby (Nhamutole et al., 2024a).

4.4.4. Nhamago outcrop

The Nhamago strata corroborate with the interpretation from the above sections. The relative abundance of hopanes over steranes indicate organic matter from terrigenous sources (Tissot and Welte, 1984) as well as the predominance of C_{29} αααR steranes (Kodner et al., 2008). The methyl-phenantrene was too low suggesting low thermal evolution. Albeit the Nhamago site is located closer to igneous intrusions, however no influence was identified.

Overall, the distributions of terpanes display high content of H30 hopane, followed by H29 hopane, across most samples. The Low Ts over Tm represents a low thermal evolution history for most of the samples; however, these results agree with the previous results published based on pyrolysis data performed by Nhamutole et al. (2024a) from the same strata. The identified biomarkers suggest a freshwater lacustrine depositional setting for the studied samples with no marine influence at the time of the deposition of the sediments. The occurrence of membranes co-occurring with the presence of sporomorphs and resins (Table S1-Supplementar Material) strengthen the idea of terrestrial source area, as suggested by Marques-Lima et al. (2023), and Manga et al. (2024).

The molecular data also unveiled that the organic-rich sediments were deposited mostly in oxidized conditions; however, reducing conditions were also observed. These conditions were triggered by local and regional tectonic framework related to different rifting phases as reported by Verniers et al. (1989) and Key et al. (2007). Organic matter accumulation, production and production in African continental basins has been associated with stage of active rifting, in cases where basins and rift lakes were found in their highest depths (Manga et al., 2024 and references therein). Additionally, according to Verniers et al. (1989), the Maniamba Basin was located in an embryonic rift during the Permian-Triassic boundary to the end of Gondwana uplift and erosion cycle. It was filled with sediments as it progressively sank, influencing organic matter deposition and existing palaeoredox conditions. Thus, other factors such as palaeoclimate and palaeogeography could have played an important role for the dominant palaeoredox conditions observed for the Maniamba Basin. However, broader sampling is needed to confirm the influence of those variables. Nonetheless, the data analysed herein represent an important contribution for the understanding of the Maniamba Basin evolution as well as its potential for hydrocarbon. Interestingly, the biomarker data regarding thermal maturity of the samples corroborates with the information provided by the interpretation of the spore coloration index (SCI) as stated in the Table S1-Supplementar Material. Lastly, it should be highlighted that the general assemblage of biomarkers is consistent with previous studies that have addressed a scenario of continentalization for the Gondwana in the middle to late Permian transition (Bastos et al., 2021).

4.5. Mineralogy of the strata

The outcrop strata of all four sites were investigated for their mineralogical composition based on XRD patterns. The mineral content provides a qualitative and quantitative assessment as well as relevant information such as petrophysical properties. The XRD data revealed the presence of nine minerals in which quartz is the most dominant. Quartz is present in all studied samples and is followed by clay minerals in terms of abundance (Fig. 18~~9~~, Table 2). Clay minerals are represented by montmorillonite, kaolinite, smectite and minor chlorite and illite. In addition, there are moderate amounts of feldspar (e.g., orthoclase, microcline) and carbonates represented by aragonite, calcite and vaterite. The dominance of quartz and occurrence of some carbonates point to the hardness and brittleness of the studied fine-grained samples. Similar results have been observed in the Main Karoo Basin, Whitehill Formation (Chabalala et al., 2020). These properties could have allowed the rocks to expel hydrocarbons thus acting as good source rocks. Yet, the studied organic units, due to their mineralogical composition, can be suitable for hydraulic fractures as well as possible utilization in carbon capture and sequestration (CCS) following the current energy policies. Furthermore, it is worth noting that clay minerals are derived from the active weathering process of parent source rocks, hence their content is influenced by climate and environmental conditions. Fagel (2007) suggested that a high concentration of kaolinite and smectite indicate prevailing warm and humid climates. In contrast, high concentration of chlorite and illite corroborate with arid climate. Within the outcrop strata, the samples display a high abundance of quartz and kaolinite in comparison to an absence of illite, suggesting that these units were deposited under a prevailing warm humid climate. The mineral composition agrees with the palynology assessment that favour the existence of luxuriant vegetation linked to a prevailing warm and humid climate during the middle and late Permian in most Gondwana sequences (McLoughlin, 2001; Aggarwal et al., 2019; Nhamutole et al., 2021, 2024).

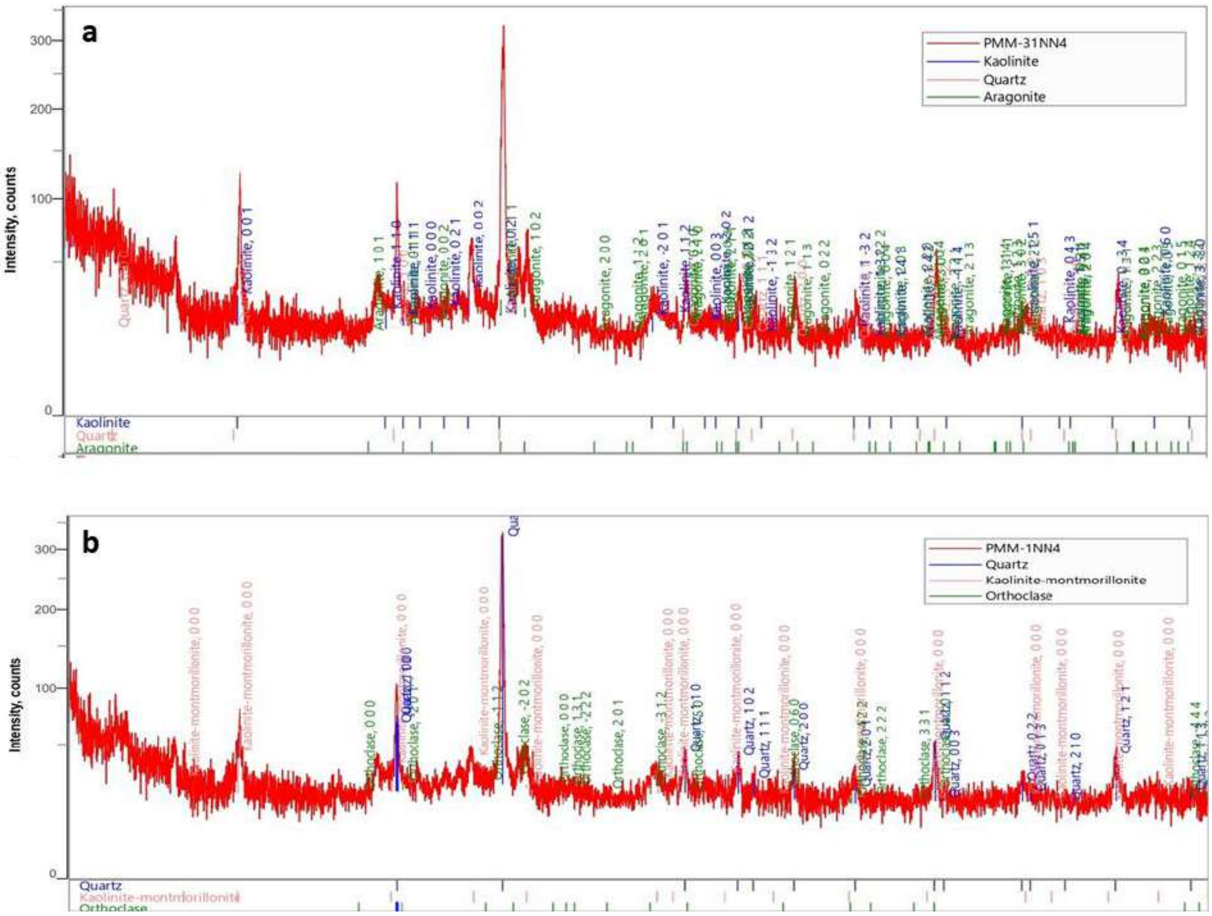

Figure 19. XRD diagrams of the selected samples showing some of the identified mineral phase.

4.6. Hydrocarbon prospectivity

Based on molecular data from the current research and other available works (Loegering and Milkov, 2017; ECL, 2000), a comparative analysis was undertaken (Table 4). The main aim was to identify the existing similarities or dissimilarities in the petroleum geochemistry signatures amongst the source rocks from the Maniamba Basin with petroleum fluids from either Rovuma and Mozambique basins since the pre-rift section of these two basins is by extrapolation considered to be equivalent to the Karoo rocks (ECL, 2000). In fact, should be highlighted that all those basins pertain to the same tectonic framework despite the fact that Karoo rocks such as the one from the Maniamba Basin have never been targeted during petroleum drillings. Even though the formations from the Maniamba Basin have been therefore suggested as the potential source for petroleum fluids in the Rovuma Basin as well as in the Mozambique Basin (ECL, 2000; Norconsult, 2007). Nevertheless, the comparative analysis carried out herein has considered three main factors such as source input, depositional environment and thermal evolution (Table 4). Biomarkers from the Maniamba Basin indicates terrestrial sourced organic matter influencing hydrocarbon generation potential. In contrast, data from Loegering and Milkov, 2017 and ECL, 2000) suggest marine sourced organic matter for the Rovuma and Mozambique basins respectively. In regard to depositional environment, molecular ratio data suggest that the Maniamba Basin hydrocarbons originated from suboxic-oxic terrigenous fluvio-lacustrine environments of Permian age. In its turn, biomarkers in the light oil from Mozambique and Rovuma basins are derived from hypersaline, sub-oxic marine shales of Cretaceous age. Those data stress that the dynamics and different paleoredox conditions prevailed over geological time during the formation of oil in Central Gondwana. Furthermore, the light oils from the Mozambique and Rovuma basins as well as the source rock from the Maniamba Basin show quite similar maturation phases however is quite common in the latter Basin to find overmature rocks that were influenced by the emplacement of igneous intrusions (Nhamutole et al., 2023; 2024a).

In overall, the comparative analysis suggests that the light oil from the Mozambique and Rovuma basins could not be sourced from the source rocks in the Maniamba Basin due to the fact that they completely depict a distinct petroleum geochemistry signature as previously inferred by Loegering and Milkov (2017) albeit the fact that the data from Karoo biomarkers were not available at that moment for a precise correlation.

Table 4 Comparative analysis of source rocks (Maniamba Basin) with fluids from Mozambique e Rovuma Basin.

Petroleum basins	Source input	Depositional environment	Paleoredox conditions	Thermal maturity
Maniamba Basin (This study)	Higher plants	Fluvio-Lacustrine (Terrestrial)	Suboxic-oxic	Mostly late mature and overmature
Rovuma Basin (ECL, 2000)	Lower organisms	Marine shales	Hypersaline, suboxic-oxic-anoxic	Early mature
Mozambique Basin (Loegering and Milkov, 2017)	Lower organisms	Marine shales	Hypersaline, suboxic-oxic	Early mature

5. Conclusions

1-The palynomorph occurrences presented in this study allowed the constraint of the outcrop strata to Guadalupian (Luchai and Nhamago) and latest Lopingian-Lower Triassic (Luiga) based on biostratigraphic affinities with existing Gondwana schemes from the Moatize-Minjova Basin, Mozambique (Pereira et al., 2016), Salt Range Basin, Pakistan (Balme, 1980) and Main Karoo Basin, South Africa (Barbolini et al., 2018).

2-The dominance of long chain *n*-alkanes with a minor concentration of short chain hydrocarbons corroborates with deposition of organic matter from terrestrial sources

3-The studied samples are immature to overmature as demonstrated by Ts/Tm ratio, methyl-phenantrene, and the occurrence of 2-methlylantracene linked to the influence of kimberlite emplacement in the Lower and Middle units of the Maniamba Basin.

4-Three palynofacies were identified in the strata with the extrapolation of an APP plot (ternary diagram) indicating a shift towards proximal-distal oxic-suboxic-anoxic conditions reflecting shifting of environment conditions over time. The environmental shifting is further supported by Pr/Ph ratios.

5-The peat-forming palynoflora consists of the dominance of gymnosperm pollen assigned to glossopterids that includes striate and non-striate bisaccate pollen. Subordinate occurrence of trilete spores is represented by lycopsids, sphenopsids and filicopsids. The high proportion of arborescent vegetation indicates a development in a forest swamp. Additionally, the dominance of glossopterids with moderate representation of conifers co-existing with lycopsids, filicopsids and sphenopsids are an indication of a sedimentation of hypautocthonous type.

6-The abundance of phytoclasts indicates the existence of a dense vegetation cover nearby to the site of deposition. Yet, the high content of opaque phytoclasts suggests that palaeo-wildfires occurred during the deposition.

7-The mineral composition is characterised by the dominance of quartz and clay, together with moderate contribution of carbonates and feldspars that created ideal conditions for source rock expulsion of hydrocarbons.

8-Hydrocarbon fingerprints suggest that the light oils from the Mozambique and Rovuma Basins were not sourced from the Karoo formations of the Maniamba Basin.

Overall, this study using a number of proxies together provides pivotal information for a better understanding of the geodynamics of the Maniamba Basin.

References

Aggarwal, N., Agrawal, S., Thaku, B., 2019. Palynofloral, palynofacies and carbon isotope of Permian coal deposits from the Godavari Valley Coalfield, South India: Insights into the age, palaeovegetation and palaeoclimate. Inter. J. Coal Geol. https://doi.org/10.1016/j.coal.2019.103285.

Aggarwal, N., 2021. Sedimentary organic matter as proficient tool for the palaeoenvironmental and palaeodepositional settings on Gondwana coal deposits. J. Petr.Explor. Techn. 12, 257-278.

Araújo, R., Macungo, Z., Smith, R., Tolan, S., Angielczyk, K., Crowley, J., Milisse, D., Mugabe, J., 2020. The first Lower Triassic tetrapod fossils from Metangula Graben (Niassa Province, Mozambique) and their biostratigraphic significance. Palaeontol. Afr. 54, 56–58.

Balme, J., 1980. Palynology, and the Carboniferous-Permian boundary in Australia and other Gondwana continent. Palynol. 4, 43–55.

Barbolini, N., Rubidge, B., Bamford, M.K., 2018. A new approach to biostratigraphy in the Karoo retroarc foreland system: Utilising restricted-range palynomorphs and their first appearance datums for correlation. J. Afr. Earth Sci. 140, 114–133.

Bastos, L.P.H., Rodrigues, R., Pereira, E., Bergamaschi, S., Alferes, C.L.F., Augland, L.E., Svensen, H.H., 2021. The birth and demise of the vast epicontinental Permian Irati-Whitehill sea: evidence from organic geochemistry, geochronology, and paleogeography. Palaeog. Palaeclimat. Palaeoecol. 562, 110103.

Bicca, M.M., Philipp, R.P., Jelinek, A.R., Ketzer, J.M.M., dos Santos Scherer, C.M., Jamal, D.L., Domingos dos Reis, A., 2017. Permian-Early triassic tectonics and stratigraphy of the Karoo Supergroup in northwestern Mozambique. J. Afr. Earth Sci. 130, 8–27.

Birks, H.J.B. and Birks, H.H., 1980. Quaternary Palaeoecology. Edward Arnold, London, 289 pp.

Brocks, J.J., Grice, K., 2011. Biomarkers (ancient biomolecules, evolution) Encyclopaedia of Geobiology. In: Encyclopedia of Earth Science Series. Springer, Netherlands, pp. 167–182.

Catuneanu, O., Hancox, P.J. and Rubidge, B.S. (1998). Reciprocal flexural behaviour and contrasting stratigraphies: a new basin development model for the Karoo retroarc foreland system, South Africa. Basin Res. 10, 417–439.

Chabalala, V.P., Wagner, N., Malumbazo, N., Eble, C.F., 2020. Geochemistry and Organic Petrology of the Permian Whitehill Formation, Karoo Basin (RSA) and the Devonian/Carboniferous shale of the Appalachian Basin (USA). Int. J. Coal Geol. 232, 1–18.

Cincotta, A., Yans, J., Godefroit, P., Garcia, G., Dejax, J., Benammi, M., Amico, S., Valentin, X., 2015. Integrated palaeoenvironmental reconstruction and taphonomy of a unique upper cretaceous vertebrate-bearing locality (Velaux, Southeastern France). PLoS ONE 10,1–20. https://doi.org/10.1371/journal.pone.013423.

Collinson, J.D., 1996. Alluvial sediments. In: Reading, H.G. (Ed.), Sedimentary Environments: Processes, Facies and Stratigraphy. Blackwell Science, Oxford, pp. 37–82.

Davies, A., Simmons, M., 2021. Demand for 'advantaged' hydrocarbons during the 21st century energy transition. Energy reports 7, 4483–4497.

ECL (Exploration Consultants Ltd)., 2000. The Petroleum Geology and Hydrocarbon Prospectivity of Mozambique. Unpublished report, Empresa Nacional de Hidrocarbonetos (ENH), pp.144.

Fagel, N., 2007. Clay minerals, deep circulation and climate. In: Hillaire, C., de Vernal, A. (Eds.), Proxies in Late Cenozoic Paleoceanography. Develop. Mar. Geol. 1, 139–184.

Farrimond, P.; Bevan, J.C.; Bishop, A.N., 1996. Hopanoid hydrocarbon maturation by an igneous intrusion. Org. Geochem. 25, 149–164.

Fonseca, C., Mendonça Filho, J.G., Lézin, C., Duarte, L.V., 2020. Organic facies variability and paleoenvironmental changes on the Moroccan Atlantic coast across the Cenomanian-Turonian oceanic anoxic event (OAE2). Int. J. Coal Geol. 230, 103587 https://doi.org/10.1016/j.coal.2020.103587.

Fonseca, C., Mendonça Filho, J.G., Lézin, C., Baudin, F., de Oliveira, A.D., Souza, J.T., Duarte, L.V., 2021. Boosted microbial productivity during the Toarcian oceanic anoxic event in the Paris Basin, France: new evidence from organic geochemistry and petrographic analysis. Geological Society Special Publications 514, 309–334. https://doi.org/10.1144/SP514-2020-167.

Galasso, F., Pereira, Z., Fernandes, P., Spina, A., Marques, J., 2019. First record of Permo-Triassic palynomorphs of the N'Condédzi sub-basin, Moatize-Minjova Coal Basin, Karoo Supergroup, Mozambique. Rev. Micropal. 64, 100357. https://doi.org/10.1016/j.revmic.2019.05.001.

George, S.C.,1992. Effect of igneous intrusion on the organic geochemistry of a siltstone and an oil shale horizon in the Midland Valley of Scotland. Org. Geochem. 18, 705–723.

Key, R.M., Bingen, B., Barton, E., Daudi, E.X.F., Manuel, S. and Moniz, A., 2007. Kimberlites in a Karoo graben of northern Mozambique: Tectonic setting, mineralogy and Rb-Sr geochronology. S. Afr. J. Geol. 110, 111–124.

Kodner, R.B., Pearson, A., Summons, R.E., Knoll, A.H., 2008. Sterols in red and green algae: quantification, phylogeny, and relevance for the interpretation of geologic steranes. Geobiol. 6(4), 411–420.

Lindström, S., McLoughlin, S., 2007. Synchronous palynofloristic extinction and recovery after the end-Permian event in the Prince Charles Mountains, Antarctica: implications for palynofloristic turnover across Gondwana. Rev. Palaeobot. Palynol. 145, 89–122.

Loegering, M.J., Milkov, A.V., 2017. Geochemistry of Petroleum Gases and Liquids from the Inhassoro, Pande and Temane Fields Onshore Mozambique. Geosci., 7, 33, doi.org/10.3390/geosciences7020033.

Lopes, G., Pereira, Z., Fernandes, P., Marques, J., 2014. Datação Palinológica dos Sedimentos Glaciogénicos da Formação (Tilítica) de Vúzi, sondagem ETA 65, Bacia Carbonífera de Moatize–Minjova, Moçambique—Resultados Preliminares. Actas do IX Congresso Nacional de Geologia. 2º Congresso de Geologia dos Países de Língua Portuguesa, Porto, Portugal, pp. 7.

Lopes, G., Pereira, Z., Fernandes, P., Mendes, M., Marques, J., Jorge, R., 2021. Late Permian palaeoenvironmental evolution of the Matinde Formation in the Muar´adzi

Sub-basin, Moatize-Minjova Basin, Mozambique. J. Afr. Earth Sci. 176, 104138. https://doi.org/ 10.1016/j.jafrearsci.2021.104138.

Makled, W., Tahoun, S., 2015. Digital quantification of the miospore coloration to assess the thermal maturity: Novel RGB-based measuring technique. Mar. Petrol. Geol. 67, 1–15.

Manga, W.G.O., Fonseca, C., Bessong, M., Franco, N., Oliveira, A.D., Meying, A., Tonye, M.D., Mendonça Filho, J.G., 2024. Paleoenvironmental factors controlling organic-rich formations deposition in the Babouri-Figuil Basin (Northern Cameroon). Internat J. Coal Geol. 292, 104589. https://doi.org/10.1016/j.coal.2024.104589.

Marchionni, D.L., 1980. Petrography and depositional environments of the Liddel seam, Upper Hunter Valley, New South Wales. Int. J. Coal Geol. 1,36–61. https://doi.org/10.1016/0166-5162(80) 90005-1.

Marques-Lima, D., Mendonça Filho, J.G., Fonseca, C., Oliveira, A.D., Mendonça, J.O., Gonçalves, P.A., 2023. Organic facies variability and paleoenvironmental characterization of the Codó and Itapecuru formations (Aptian-Albian) of Parnaíba Basin, Brazil. Inter. J. Coal Geol. 277, 104337. https://doi.org/10.1016/j.coal.2023.104337.

Mendonça Filho, J.G., Chagas, R.B.A., Menezes, T.R., Mendonça, J.O., Silva, F.S., Sabadini-Santos, E., 2010. Organic facies of the Oligocene lacustrine system in the Cenozoic Taubate basin, Southern Brazil. Int. J. Coal Geol. 84, 166–178.

Mendonça Filho, J.G, Menezes, T. Filho, J., 2011b. Organic composition (palynofacies) (chapter 5). In: ICCP Training course on dispersed organic matter, 33–81.

Mendonça Filho, J.G., Gonçalves, P.A., 2017. Organic Matter: Concepts and Definitions, Chapter 1, in: Suárez-Ruiz, I., Graciano Mendonça Filho, J. (Eds.), Geology: Current and Future Developments. The Role of Organic Petrology in the Exploration of Conventional and Unconventional Hydrocarbon Systems. Bentham Science Publishers, United Arab Emirates, pp. 1–33.

Mendonça Filho, J.G., Menezes, T.R., Mendonça, J.O., 2023. Chapter 18: Palynofacies - trends and parameters. In: Mendonça Filho, J.G., Borrego, A.G. (Eds.), 15th ICCP Training Course on Dispersed Organic Matter. JCCP, University of Patras, Patras, Greece, pp. 209–230. ISBN 978-84-09-53900-0.

McLoughlin, S., 2001. The breakup history of Gondwana and its impact on pre-Cenozoic floristic provincialism. Austral. J. Bot. 49, 271–300.

Miall, A.D., 2010. Alluvial deposits. In: James, N.P., Dalrymple, R.W. (Eds.), Facies Models 4. Geological Association of Canada, Newfoundland, pp. 105–138.

Modie, B.N., 2007. The Palaeozoic Palynostratigraphy of the Karoo Supergroup and Palynofacies: Insights into Palaoenvironmental Interpretations, Kalahari Karoo Basin, Botswana. PhD thesis, University of Bretagne Occidentale, pp.316.

Mukhopadhyay, P., 1986. Petrography of selected Wilcox and Jackson Group fignites from the Tertiary of Texas. In Geology of Gulf Coast Lignites (Edited by Finkelman R. and Casagrande D.). The 1986 annual meeting of the Geological Society of America, Coal Geology Division, Field Trip, 126-145.

Nhamutole, N.E., Bamford, M.K., Araújo, R., 2021. New species of *Protaxodioxylon* (conifer wood) from the middle permian of the Metangula graben (Niassa province, Mozambique) and their implications. J. Afr. Earth Sci. 183, 104323.

Nhamutole, N., Bamford, M., Souza, P., Carmo, D., 2023. Palynofacies analysis of the JOG16N-8 borehole, K5 formation from the Maniamba Basin (middle Permian), Mozambique: A contribution for hydrocarbon exploration. J. Afr. Earth Sci. 205pp. https://doi.org/10.1016/j.jafrearsci.2023.104997.

Nhamutole, N., Bamford, M., Souza, P., Silva, T.F., Carmo, D., 2024a. Petroleum potential from Permian-Triassic strata of the Maniamba Basin, Mozambique: A preliminary characterisation. S. Afr. J. Geol. 127, 117–130.

Nhamutole, N., Bamford, M., Souza, P., Félix, C.M., Carmo, D.A., Peu, J., 2024b. Palynology of two drilling cores from the Maniamba Basin, Mozambique (central Gondwana): Insights on age and palaeoenvironments. Rev. Palaeob. Palynol. 334, 105271. https://doi.org/10.1016/j.revpalbo.2024.105271.

Nhamutole, N., Bamford, M., Souza, P., Félix, C.M., Carmo, D.A., Zimba, A., Bande, P., 2025. New palynological data from Maniamba Basin, Mozambique (Karoo): Correlations and implications for Lopingian floristic ecosystem reconstruction. Rev. Palaeob. Paly. 336, 105310. https://doi.org/10.1016/j.revpalbo.2025.105310.

Paz, V., 2018. Sistemas Deposicionais e Fácies Sedimentares da Bacia Carbonífera de Maniamba. Bachelor dissertation, Eduardo Mondlane University, p. 121.

Peters, K.E., Walters, C.C., Moldovan, J.M., 2005. The Biomarker Guide. Biomarkers and Isotopes in the Environment and Human History. Cambridge University.

Pereira, Z., Fernandes, P., Lopes, G., Marques, J., Vasconcelos, L., 2016. The Permian– 685 Triassic transition in the Moatize–Minjova Basin, Karoo Supergroup, Mozambique: A 686 palynological perspective. Rev. Palaeobot. Palynol. 226, 1–19.

Radke, M., Welte, D.H., Willsch, H.,1982. Geochemical study on a well in the Western Canada Basin: relation of the aromatic distribution pattern to maturity of organic matter. Geochim. Cosmochim. Acta 46,1–10. https://doi.org/10.1016/0016-7037(82)90285-X.

Singh, MP., Singh, PK., 1996. Petrographic characterization and evolution of the Permian coal deposits of the Rajmahal basin, Bihar, India. Int. J. Coal Geol. 29,93–118. https://doi.org/10. 1016/0166-5162(95)00005-4.

Suárez-Ruiz, I.; Flores, D.; Mendonça Filho, J.G., Hackley, P.C., 2012. Review and update of the applications of organic petrology: Part 1, Geological Applications. Inter. J. Coal Geol. 99, 54–112.

Ten Haven, H.L., Leeuw, J.W., Rullkotter, J., Sinninghe, J.S., 1987. Restricted utility of the pristane/phytane ratio as a palaeoenvironmental indicator? Nature 330, 641–643.

Tissot, B.P., Welte, D.H., 1984. Petroleum Formation and Occurrence. (second ed). Springer Verlag, Heidelberg.

Tyson, R.V., 1995. Sedimentary Organic Matter, Organic Facies and Palynofacies. Chapman and Hall, London, pp.615.

Volkman, J.K., 1986. A review of sterol markers for marine and terrigenous organic matter. Org. Geochem. 9 (2), 83–99. https://doi.org/10.1016/0146-6380(86) 90089-6.

Verniers, J., Jourdan, P.P., Paulis, R.V., Frasca-Spada, L. and De Bock, F.R., 1989. The Karroo Graben of Metangula Northern Mozambique. J. Afr. Earth Sci. 9, 137–158.

Zhang, H., Wang, C., Zhao, R., Yin, X., Zhou, H., Tan, L., Wang, J., 2016. New diagnostic ratios based on phenanthrenes and anthracenes for effective distinguishing heavy fuel oils from crude oils. Mar. Pol. Bul. 106, 58–61.

Saturated hydrocarbons in source rocks from Maniamba Basin, Mozambique*:* A contribution for a better understanding of past environments.

Adapted from Nelson Nhamutole N, Marion Bamford, Sidney de Lima, Artur Barros, Lorena de Almeida, Jardel Peu.

Submitted to the South African Journal of Chemistry

Abstract

Karoo Palaeozoic sediments from the Maniamba basin, Mozambique were analyzed by integrating the molecular composition of biomarkers, inorganic chemistry, and palynofacies proxies to further understand their origin. Unimodal distribution is revealed through Gas chromatography-mass spectrometry for *n-alkanes* coupled with the abundance of compounds of medium and high molecular weight. The dominance of stigmastane over cholestane and ergostane, Terrigenous Aqueous Ratio (TAR>1), and high concentration of C_{19} and C_{20} tricyclic terpenes are indicative of non-marine influence. The Preferential Index of Carbon, the Odd over Even Preference for the distrubtion of *n*-alkanes, the low values for the ratio 18α(H)-trisneohopane over 17α(H)-trisnorhopane, the C_{29} ααα S/(S+R) isomerization ratios in C_{29} steranes, C_{30} βα/(βα+αβ), C_{31} αβ S/(S+R) and C_{32}αβ S/(S+R) isomerization ratios suggest organic matter (OM) with low thermal evolution. These data are supported the Spore Color Index and vitrinite reflectance. The nature of the OM is supported by isoprenoids Pristane/Phytane ratios, palynofacies, and high contribution derived from an ecosystem dominated by ancient Glossopterid and conifer flora. Finally, data from studied proxies indicate weak to strong palaeoweathering, highly proximal, marginal oxic-anoxic Basin characterized by kerogens associated with weakly and strongly oxidized swamps suggesting an existing potential for gas.

1. Introduction

Biomarkers are the remnants of molecules that have been synthesized by organisms and display chemical structures related to the biological precursor.[35] Biomarkers have proven to be essential tools for a better understanding of critical aspects in evolutionary biology, palaeobiology, palaeoecology, petroleum geoscience, and environmental science[18]. Similarly, palynofacies are a crucial technique for the study of organic matter whose distributions reflect palaeoenvironment changes. Both biomarkers (molecular fossils) and palynofacies are key disciplines used to develop a geological model for interpreting the complexities of sedimentary basins in the petroleum system as stated by Wood and Miller,[46] and others. Additionally, in the petroleum industry, major elements, and trace elements are also used in the interpretation of the provenance of the organic matter, tectonic framework together with the possible pathways for hydrocarbon migration. [21, 2]

To our knowledge and according to the available literature, there are no focused studies that have attempted to identify biomarkers in Palaeozoic Karoo rocks from the Maniamba Basin, Mozambique. In the same way, no biomarker study has been performed for aged Karoo organic-rich sediments. In Mozambique, the only known published biomarker study belongs to Loegering and Milkov.[23] This study was based on data provided by SASOL regarding the hydrocarbon oil field from Inhassoro, Pande, and Temane localities. However, other biomarker laboratory data performed in the Rovuma and Mozambique Basin do exist but are restricted to oil companies.[22, 37,12] Additionally, palynofacies and Rock-Eval pyrolysis analysis from outcrops and one of the existing drilled borehole cores in the Maniamba Basin were recently undertaken.[32,33]Despite the preliminary characterization mentioned above, more information needs to be unveiled regarding the content of organic matter (OM) and its link with past environments.

The crucial key aspects that have guided the present research has to deal with the need of organic matter characterization, identification, assessment of its paleotemperature and paleodepositional conditions. Hence, biomarkers, kerogen visual analysis and inorganic chemistry were integrated for these purposes.

2. Geology

The geological description is found in section 5.1.

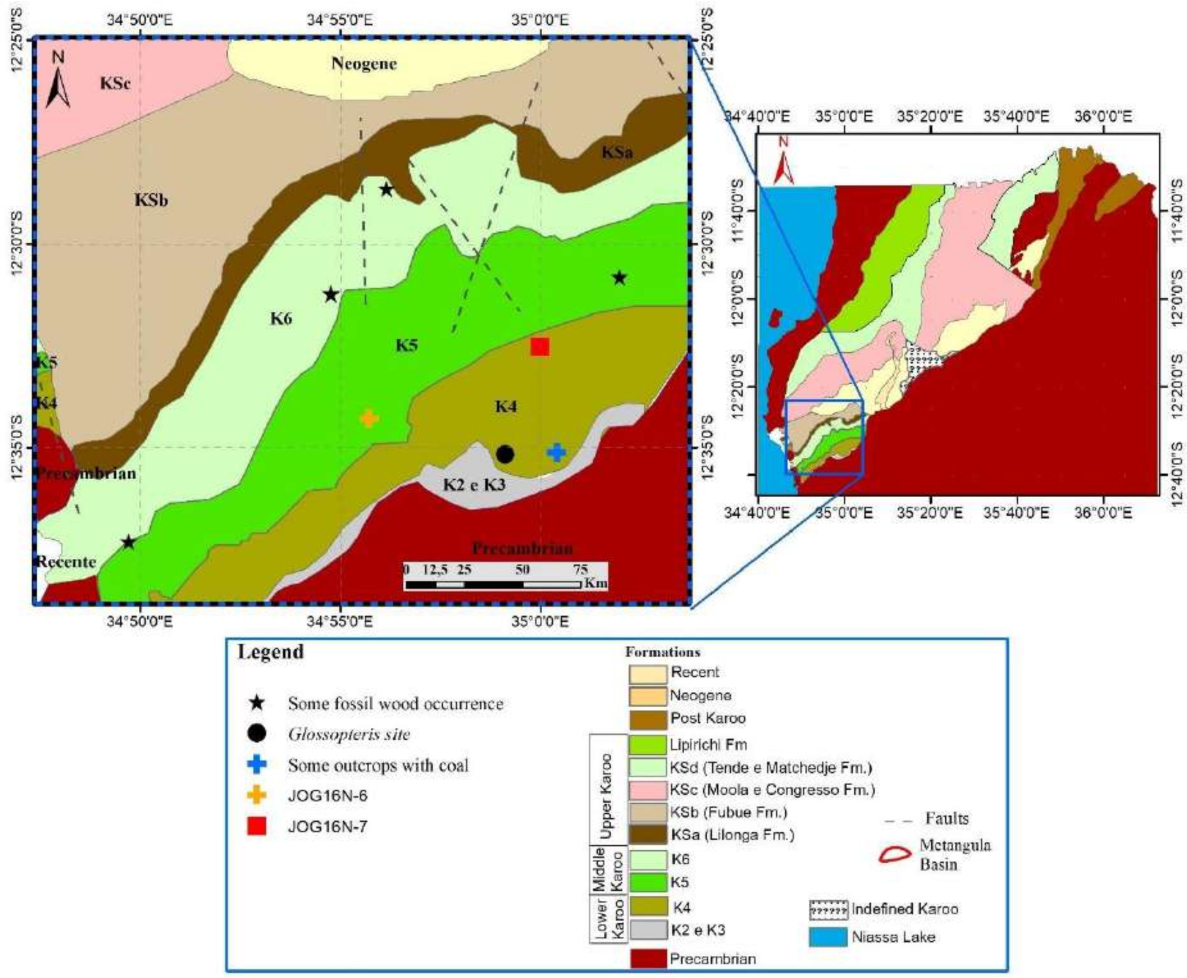

Figure 1. Geology of the investigated area.

3. Materials and Methods

Fifteen sediments enriched in the organic matter were analysed for biomarkers at the Federal University of Piaui, Brazil (Organic Geochemistry laboratory-LAGO). They were subsampled considering those with TOC higher than 1wt%. The interpretation of Pyrolysis Rock-Eval data coupled with Raman Spectroscopy, carbon and sulphur Isotopes, and palynostratigraphy are not part of the present manuscript, however, those data have been submitted elsewhere for publication (Nhamutole et al., *in press*). For inorganic geochemistry, twenty-one samples were used. Additionally, for palynofacies analyses 39 samples were collected from the JOG16N-6 (320 m) borehole while sixty-four samples were analyzed from the JOG16N-7 (280 m) borehole from MB, Mozambique (Figure 2). The palynofacies analyses were performed at the Wits University. The permission to use the cores was given by the government of Mozambique. The analytical procedures undertaken herein includes biomarkers, palynology, and XRD are described in sections 6.1.2, 6.2, 6.4.

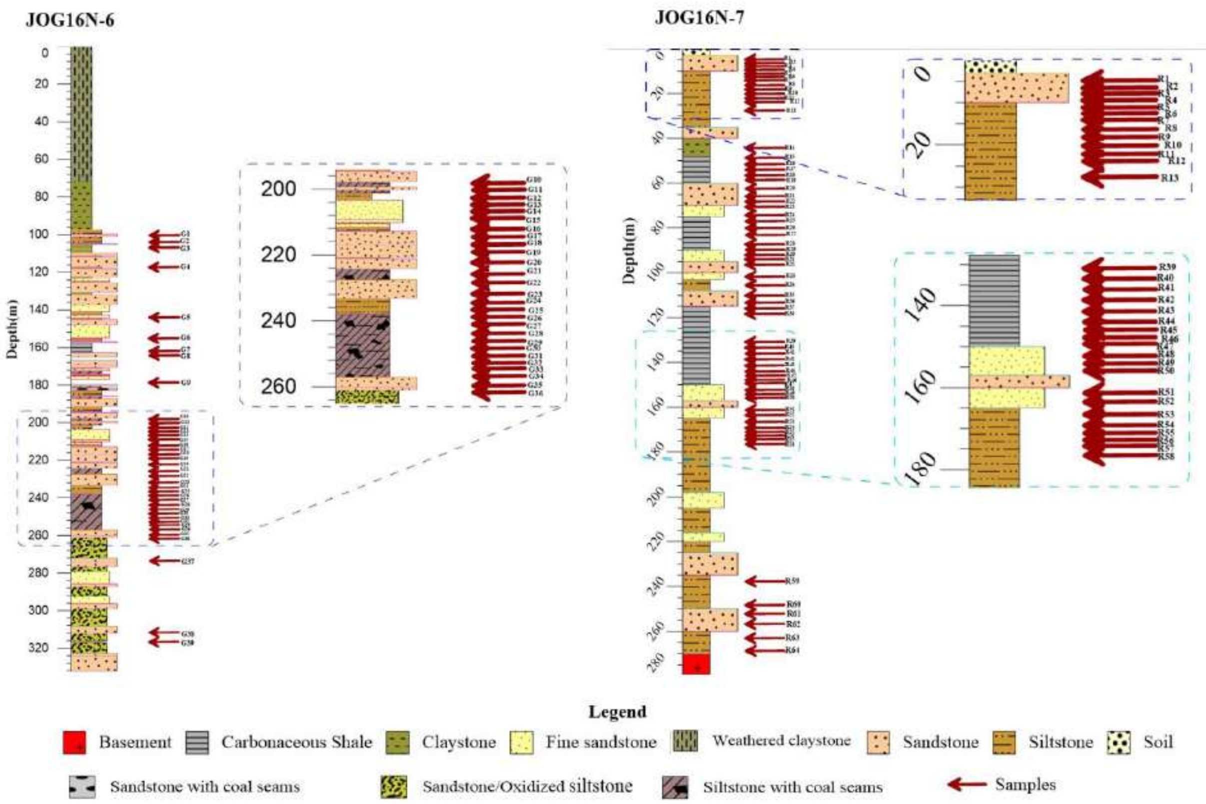

Figure 2. Lithological profile showing the lithologies and sampled points for both borehole cores.

4. Results and discussions

For this study, 15 rock samples from JOG-16N-6 and JOG-16N-7 boreholes were subjected to extraction under reflux. The reflux was made up of an azeotropic mixture of either dichloromethane or methanol. The extract yields ranged from 0.03 to 1.12% for JOG-16N-6 and 0.03 to 3.10 for JOG-16N-7, respectively. The neutral fraction was obtained by a fractionation with column chromatography using silica, and hexane for classic biomarkers analysis.

4.1 Maturity based on hydrocarbon biomarkers

Saturated hydrocarbons-based chromatograms (*m/z* 85) that have been extracted from rocks are shown in Figures 3 and 4. However, calculated biomarkers parameters are demonstrated in Table 1.

Table 1: Biomarkers of a saturated nature.

Parameters	Samples														
	G2	G24	G28	G29	G31	G32	G34	R15	R17	R19	R29	R30	R49	R60	R63
SOM	0.03	0.14	0.22	0.06	0.41	0.13	1.12	1.90	3.10	0.85	2.90	2.80	1.52	0.02	0.81
%Sat.	10.00	0.39	0.76	0.77	1.45	0.35	6.28	0.20	2.42	0.46	0.79	4.95	0.81	2.5	0.83
%Aro.	18.57	17.97	9.85	6.93	22.83	12.01	30.43	4.49	14.55	0.93	12.75	15.72	28.46	30	14.17
%Polars.	44.29	23.83	16.67	5.38	23.55	36.75	34.78	23.47	41.21	30.23	39.04	44.88	59.35	32.5	45.83
$\Sigma(C_{13-18})$	17.85	7.53	6.70	11.34	14.55	14.45	9.34	7.38	12.65	14.68	9.20	11.50	13.22	2.12	5.10
$\Sigma(C_{19-24})$	49.64	41.61	62.46	58.81	57.33	55.12	53.02	39.86	46.28	47.70	41.44	41.63	49.47	35.16	45.91
$\Sigma(C_{25-35})$	32.52	50.86	30.83	29.85	28.12	30.44	37.64	52.76	41.07	37.62	49.37	46.87	37.31	62.72	48.99
CPI	1.60	1.88	1.77	1.33	1.99	1.87	2.37	2.59	2.50	1.84	2.08	2.20	2.98	1.15	2.05
CPI-1	1.32	1.61	1.48	1.22	1.57	1.49	1.79	2.00	1.90	1.39	1.71	1.81	2.27	0.77	1.57
OEP-1	1.06	1.08	1.29	1.19	1.31	1.23	1.36	1.19	1.34	1.11	1.23	1.33	1.55	0.64	1.14
OEP-2	1.70	1.90	1.69	1.02	1.83	1.68	2.20	2.58	2.33	1.64	1.96	2.13	2.54	0.80	2.02
TAR	0.75	2.75	1.04	0.63	0.63	0.72	1.29	2.80	1.19	1.13	1.90	1.66	8.94	4.32	1.12
Pr/Ph	3.28	0.64	1.72	0.68	4.08	2.91	4.53	6.76	4.66	2.19	4.46	6.36	6.02	0.04	7.94
Pr/(Pr+Ph)	0.77	0.39	0.63	0.40	0.80	0.74	0.82	0.87	0.82	0.69	0.82	0.86	0.86	0.04	0.89
Pr/C_{17}	0.58	0.17	0.75	0.21	0.62	0.50	1.97	12.84	2.62	1.72	3.34	2.37	1.52	0.07	5.29
Ph/C_{18}	0.14	0.16	0.16	0.19	0.12	0.14	0.33	0.96	0.45	0.58	0.73	0.29	0.22	0.41	0.50
Ts/Tm	-	0.07	0.02	0.01	0.02	-	-	-	-	-	-	-	-	-	-
C_{30} βα/(αβ+βα)	0.40	0.36	0.36	0.33	0.33	0.34	0.34	0.39	0.41	0.36	0.36	0.37	0.37	0.11	0.37
C_{31} αβ S/(S+R)	0.54	0.50	0.58	0.58	0.56	0.57	0.57	0.50	0.49	0.50	0.54	0.57	0.56	0.65	0.57
C_{32} αβ S/(S+R)	0.46	0.49	0.53	0.58	0.50	0.52	0.53	0.39	0.38	0.40	0.44	0.49	0.49	0.63	0.55
C_{33} αβ S/(S+R)	0.56	0.48	0.56	0.61	0.52	0.56	0.56	0.36	0.43	0.41	0.44	0.49	0.51	0.53	0.53
C_{34} αβ S/(S+R)	0.56	0.46	0.62	0.87	0.57	0.57	0.63	0.38	0.40	0.44	0.44	0.48	0.51	-	0.53
C_{27} S/(S+R)	0.26	0.18	-	-	0.41	-	-	-	-	-	-	-	0.37	0.44	0.31
C_{29} S/(S+R)	0.09	0.22	0.31	0.04	0.28	0.11	0.35	0.17	0.13	0.10	0.16	0.19	0.20	0.03	0.25

SOM - Soluble Organic Matter; **%Sat.:** percentage distribution of the class, based on gravimetric data; **%Aro.:** percentage distribution of the class, based on gravimetric data; **%Polars.:** percentage distribution of the class, based on gravimetric data; **CPI:** $0.5x(C_{23}+C_{25}+C_{27}+C_{29})/[C_{22}+2(C_{24}+C_{26}+C_{28})+C_{30}]$ in *m/z* 85; **CPI-1:** $2x(C_{23}+C_{25}+C_{27}+C_{29})/[C_{22}+2(C_{24}+C_{26}+C_{28})+C_{30}]$ in *m/z* 85; **OEP-1:** $(C_{21}+6C_{23}+C_{25})/(4C_{22}+4C_{24})$ in *m/z* 85; **OEP-2:** $(C_{25}+6C_{27}+C_{29})/(4C_{26}+4C_{28})$ in *m/z* 85; **TAR:** $(C_{27}+C_{29}+C_{31})/(C_{15}+C_{17}+C_{19})$ in *m/z* 85; **Pr/Ph:** Pristane/Phytane in *m/z* 85; **Pr/(Pr+Ph):** Pristane/(Pristane + Phytane) in *m/z* 85; **Pr/C_{17}:** Pristane/C_{17} *n*-alkane in *m/z* 85; **Ph/C_{18}:** Phytane/C_{18} *n*-alkane in *m/z* 85; **T_s/T_m:** C_{27} 18α(H)-22,29,30-trisnorneohopane/C_{27} 17α(H)-22,29,30-trisnorhopane in *m/z* 191; **$T_s/(T_s+T_m)$:** C_{27} 18α(H)-22,29,30-trisnorneohopane/(C_{27} 18α(H)-22,29,30-trisnorneohopane + C_{27} 17α(H)-22,29,30-trisnorhopane) in *m/z* 191; **C_{30} βα/(αβ+βα):** C_{30}-17β(H),21α(H)- moretane/(C_{30}-17α(H),21β(H)-hopane + C_{30}-17β(H),21α(H)- moretane) in *m/z* 191; **C_{31} αβ S/(S+R):** C_{31}- 17α(H),21β(H)-homohopane 22S/(C_{31}- 17α(H),21β(H)-homohopane 22S + C_{32}- 17α(H),21β(H)-homohopane 22R) in *m/z* 191; **C_{32} αβ S/(S+R):** C_{32}- 17α(H),21β(H)-bishomohopane 22S/(C_{32}- 17α(H),21β(H)-bishomohopane 22S + C_{32}- 17α(H),21β(H)-bishomohopane 22R) in *m/z* 191; **C_{34} αβ S/(S+R):** C_{34}- 17α(H),21β(H)- tetrakishomohopane 22S/(C_{34}- 17α(H),21β(H)- tetrakishomohopane 22S + C_{34}- 17α(H),21β(H)- tetrakishomohopane 22R) in *m/z* 191; **C_{27} S/(S+R):** C_{27} 5α(H),14α(H),17α(H)-cholestane S/(C_{27} 5α(H),14α(H),17α(H)-cholestane S + C_{27} 5α(H),14α(H),17α(H)-cholestane R) in *m/z* 217; **C_{29} S/(S+R):** C_{29} 5α(H),14α(H),17α(H)-stigmastane S/(C_{29} 5α(H),14α(H),17α(H)-stigmastane S + C_{29} 5α(H),14α(H),17α(H)-stigmastane R) in *m/z* 217.

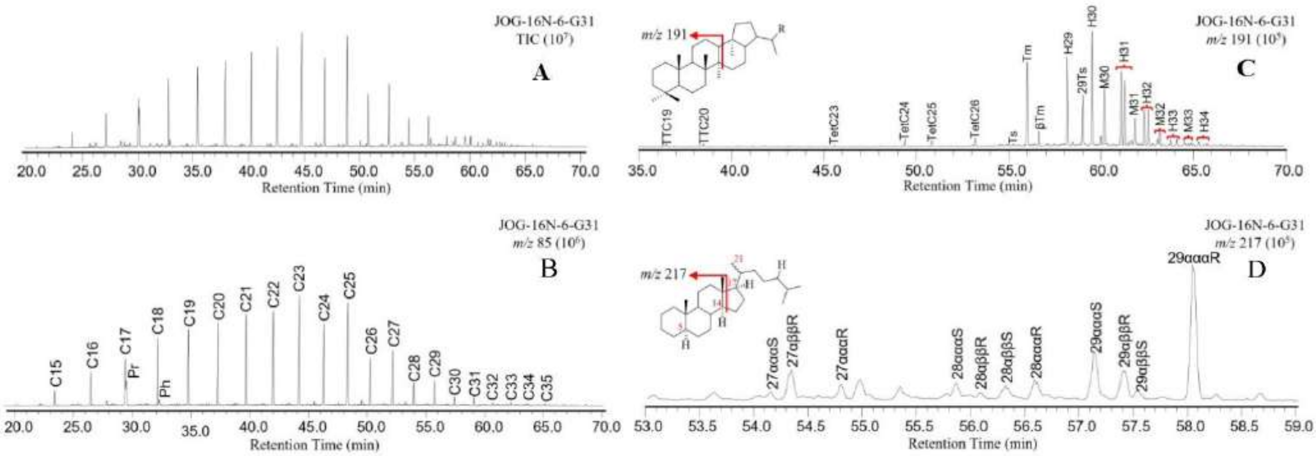

Figure 3. A. Total ion chromatogram (TIC) of saturated hydrocarbons from JOG16N-6 borehole. B. Mass chromatogram (*m/z* 85) of saturated hydrocarbons from JOG16N-6. C. Tricyclic, tetracyclic, and pentacyclic in mass chromatograms (m/z 191) from JOG16N-6 borehole. D. Pentacyclic terpenes in mass chromatograms (m/z 217) from JOG16N-6 borehole.

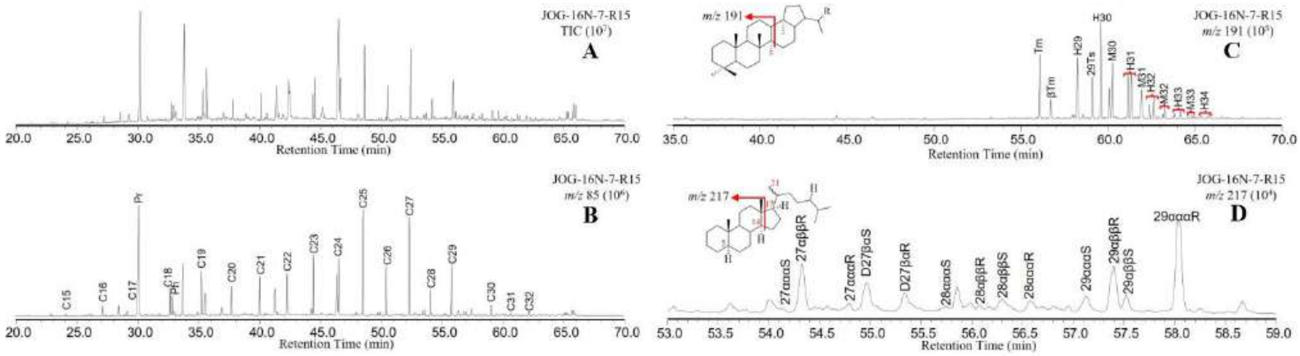

Figure 4. A. Total ion chromatogram (TIC) of saturated hydrocarbons from JOG16N-7 borehole. B. Mass chromatogram (m/z 85) of sutured hydrocarbons from JOG16N-7. C. Trycyclic, tetracyclic and pentacyclic in mass chromatograms (m/z 191) from JOG16N-7 borehole. D. Pentacyclic terpanes in mass chromatograms (m/z 217) from JOG16N-7 borehole.

Preferential Index of Carbon (CPI) and Odd-to-Even Predominance (OEP) values range from 1.06-2.37 and 0.64-2.98 for JOG-16N-6 and JOG-16N-7, showing odd over even preference suggesting low thermal evolution for the organic matter (Figure 5).[41]

Terpenes are shown in Figures 3 and 4. The stability of terpenes compounds through thermal degradation is quite different with 8α(H)-trisneohopane (Ts) being more stable if compared to 17α(H)-trisneohopane (Tm). Nevertheless, due to different stability, the Ts/Tm ratio tends to be greater in oils of high thermal (Moldovan et.)[27,39]. The Ts is significantly low in the studied samples fact that hindered the calculation of the ratio Ts/Tm (Table 4).

Nonetheless, the maturity has been tested analyzing the values of C_{27} 17β(H)-22,29,30-trinorhopane (βTm). This isomer characterized the samples as being immature, however should be emphasized that βTm is not stable under thermal degradation even if in comparison to Ts and Tm as reported by Hong et al.[17].

C_{30} βα/(βα+αβ) hopane relationship relies on moretanes compared to isomers of 17α,21β. Values of this relationship decrease with the advancement of thermal evolution. Samples with C_{30} βα/(βα+αβ) values greater than 0.8 are considered immature whereas those less than 0.15 are in the mature stage.[35] All the isomers including C_{31} αβ S/(S+R) and C_{32} αβ S/(S+R) ratios have demonstrated that the samples are of low thermal evolution.[38]

The ratio C_{29} ααα S/(S+R) ratio based on the distribution of steranes (Figures 3 and 4) is widely tested in thermal assessment. Thus, with increasing maturation, isomerization of regular steranes in C_{20}-5α(H),14α(H),17α (H) of R configuration is observed, resulting in a combination of R (biological epimer) together with S (geological epimer) configurations. It is expected that the C_{29} 20S/(20S+20R) values will reach balanced values between 0.52 and 0.55. Here this ratio presented values between 0.03 and 0.31 corroborating with the other maturity parameters. The steranes shows the dominance of the biologically derived 20R-a(H), 14a(H), 17a (H)-steranes, which is typical of sediments that are less evolved thermally. These results corroborate with the palynofacies data described in section 4.3.

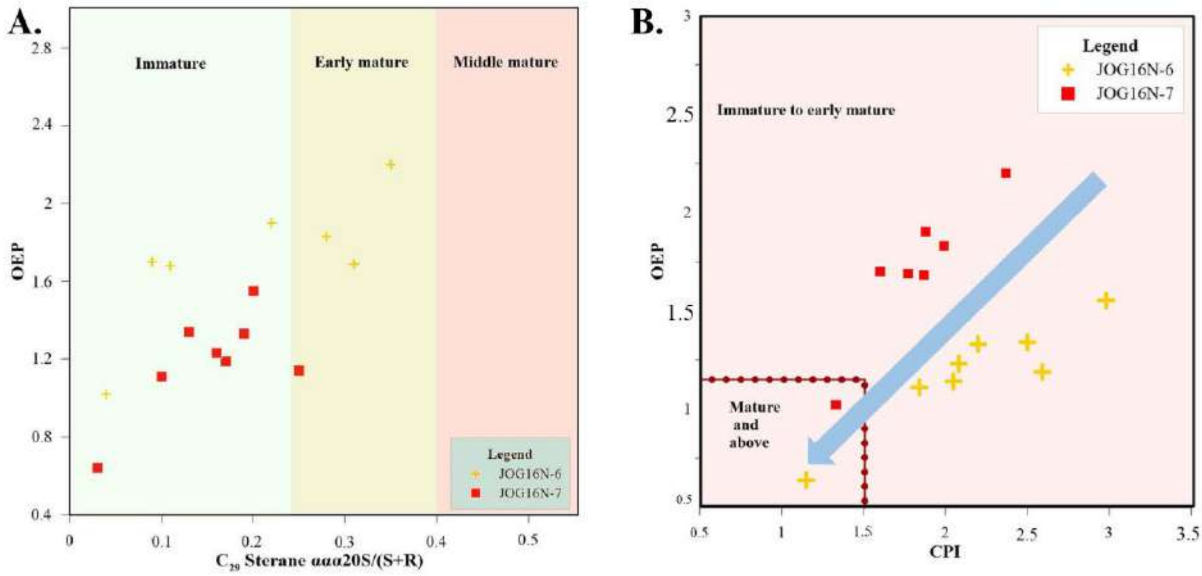

Figure 5. Maturity of sediments from JOG16N-6 and JOG16N-7 borehole. A. OEP vs. C_{29} ααα20S/(S+R). B. OEP vs. CPI. and **Figure 6 (right)**. OM source and its associated biomarker from studied Basin. A. Ph/n-C_{18} vs. Pr/n-C17. B. C_{27} /C_{29} regular steranes vs. Pr/Ph.

4.2 Depositional environment based on biomarkers and palaeobotanical evidence

The environment of depositional has been investigated based on molecular fossils. Normal alkanes and isoprenoids have been obtained through chromatogram *m/z* 85. Terpenes were obtained from *m/z* 191 whereas steranes were obtained from m/*z* 217 and *m/z* 218 (Figures 3C-D and 4C-D).

The *n*-alkanes distributions ranged from C_{14} to C_{35}, showing unimodal distribution (same source of organic matter origin) with a high relative abundance of compounds of medium and high molar mass (C_{19} to C_{35}), with a predominance of C_{27-31} (TAR>1) and odd over even preference (CPI>1) suggesting terrigenous OM (Bray and Evans, 1961). The Pristane/Phytane (Pr/Ph) ratio is generally applied to get pivotal insights regarding paleo redox condition despite its many limitations. Pr/Ph ratio > 3.0 indicates contributions from terrigenous OM in which deposition occurred in non-deficient oxygen conditions. In contrast, the Pr/Ph ratio with values less than 0.8 indicates reduced conditions as identified by Didyk et al.[9,27]The aforementioned ratio generally decreases with thermal maturation and increases with biological decomposition.[41] In general, JOG-16N-6 and JOG-16N-7 samples showed Pr/Ph ratios ranging from 0.04

to 7.94 (Figure 6) suggesting that during the sedimentation period at the same stage, the oxygen content decreased, indicating a transitional environment ranging from oxic-anoxic (Figure 6).

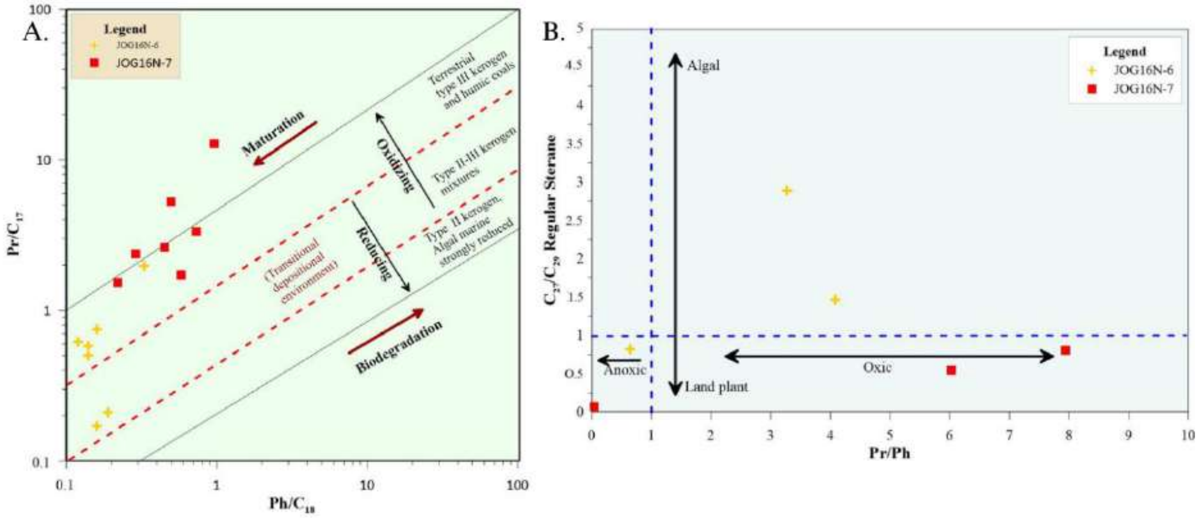

Figure 6. OM source and its associated biomarker from studied Basin. A. Ph/n-C_{18} vs. Pr/n-C17. B. C_{27} /C_{29} regular steranes vs. Pr/Ph.

Gallegos (1971), is considered as the first to identify the cheilantanes (*m/z* 191, Figures 5 and 6) and these compounds are widespread in lacustrine and marine source rocks. The series of cheilantanes or terpenes can extend at least up to C_{54}. Only C_{19} and C_{20} terpenes were identified. The absence or low relative abundance of C_{23} to C_{26} homologs is expected in samples with organic matter of terrestrial origin. In general, steranes and diasteranes were detected in elevated concentrations, with C_{27} and C_{28} steranes exhibiting comparatively lower abundance. The predominance of C_{29} sterane (stigmastane), attributed to terrestrial plant sources,[35] is consistent with TAR, CPI, and Pr/Ph parameters, along with other measured variables as shown in Figure 7. In Figure 7, a marine contribution is observed, it may be because on those sites an increase of sporomorphs (pollen and spores) content is observed. Additionally, no marine palynomorph (e.g., dinoflagellates, prasinophytes, and others) have been identified under the microscope analysis associated with the fact that the amount of AOM is lower in all studied sections. The ratio observed in steranes $C_{27/C29}$ was less than 1 indicating a predominance of continental OM as observed in palynofacies analysis in section 4.3. Our data corroborates with the previous assumptions reported from the Permian Gondwana sequence from Brazil, India, and Australia.

These above conclusions are quite supported by palaeobotanical data. For instance, during the Permian *glossopterid* remains dominate the floras at almost all Gondwana sites. The success of *Glossopteris* is largely attributed to their deciduous habit and specialized root systems which allowed them to colonize the extensive diversified ecosystems such as high-latitude, lowland, lake-margin, and mire environments.[29]Nevertheless, is well-known that buried plant remains such as the ones observed in the K5 and K4 sites comprise principally wood, spores, pollen and leaf material that were buried as peats and eventually converted to III or IV kerogens from which hydrocarbons are obtained.[13] This is the likely case for the Maniamba Carboniferous Basin where *Glossopteris* leaves have been found (Figure 1 and Figure 8).[44] Four species have been recognized so far, *Glossopteris indica, G. browniana, G. ampla, Glossopteris aff. retifera and G. cf. communis.*[44] Additionally, the diversified palynological assemblages that include *Scheuringipollenites ovatus, Laevigatosporites plicatus, Cycadopites cymbatus, Gutullappolenites hannonicus*, *Horridriletes tereatengulatus*, *brevitriletes levis*,[34] and abundance of conifer fossil woods endemic to Karoo and Gondwana formations such as *Agathoxylon africanum, A. karooensis, Australoxylon teixeirae*, *A. zambesiensis*, *Protaxodioxylon metangulense,* and *P. verniersii* corroborate with the provenance and type of OM identified in the present study (Figure 1 and Figure 8).[31,34] The abundance of the primitive conifer woods has been associated with increasing C_{29} and the occurrence of C_{20} (diterpenes) as the latter constitute the main part of resins in conifers as suggested by Schwark et al.[40] Hence, the amount of the dominant gymnosperms inputs linked to different rifting episodes in the Basin is thought as the principal factor controlling the terrigenous-dominated organic matter enrichment in the study area.

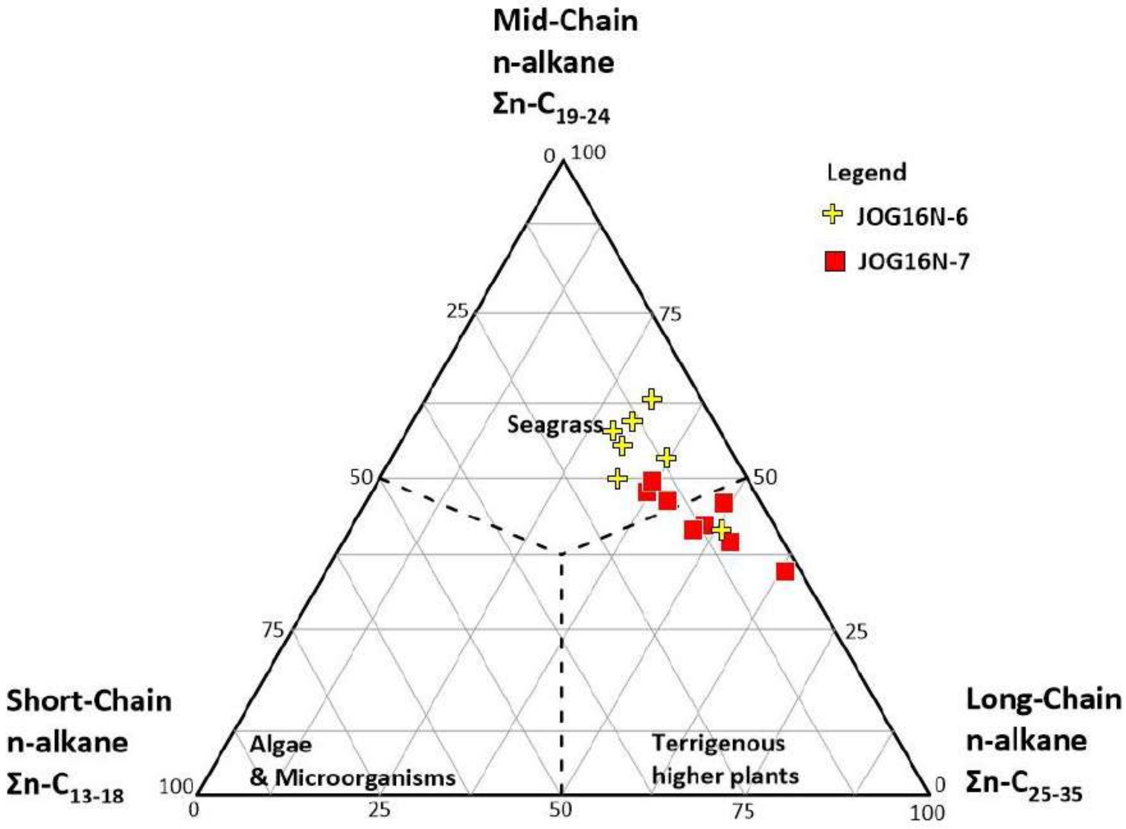

Figure 7. n-alkanes chain illustrated in the ternary diagram.

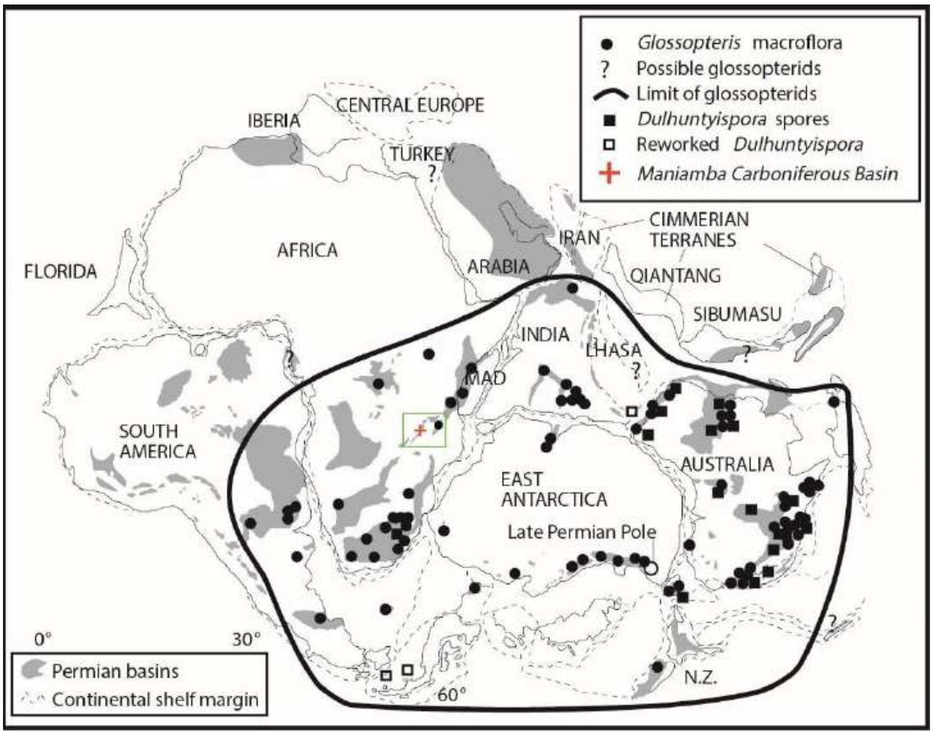

Figure 8. Distribution of Paleoflora bearing Glossopteris in the Gondwana map. The Maniamba basin is indicated in red adapted from McLoughlin (2001).

4.3. Palynofacies

The OM components observed in the MB were grouped into phytoclasts, palynomorphs and AOM (Table 2 and 3, Figure 9). This classification was based on standard schemes proposed by[10,42] and others. Most of the observed phytoclasts are opaque, however some are translucent (brown and pale yellow). Opaque phytoclasts include corroded and equidimensional forms (Figure 10). Translucent phytoclasts include cuticles, membranes, fungal hyphae biostructured and non-biostructured phytoclasts (Mendonça Filho et al.[25]). Phytoclasts of opaque nature are related to III and IV types of kerogens which are more gas prone (Zoba et al.[47]) while the translucent phytoclasts can somehow be linked to kerogen type II which generates gas and oil.[10,41,42] Palynomorphs can be of varied forms, origins and types which include marine and terrestrial (sporomorphs) forms are lipid-rich organic matter being oil-prone (Mendonça Filho et al.[25]).

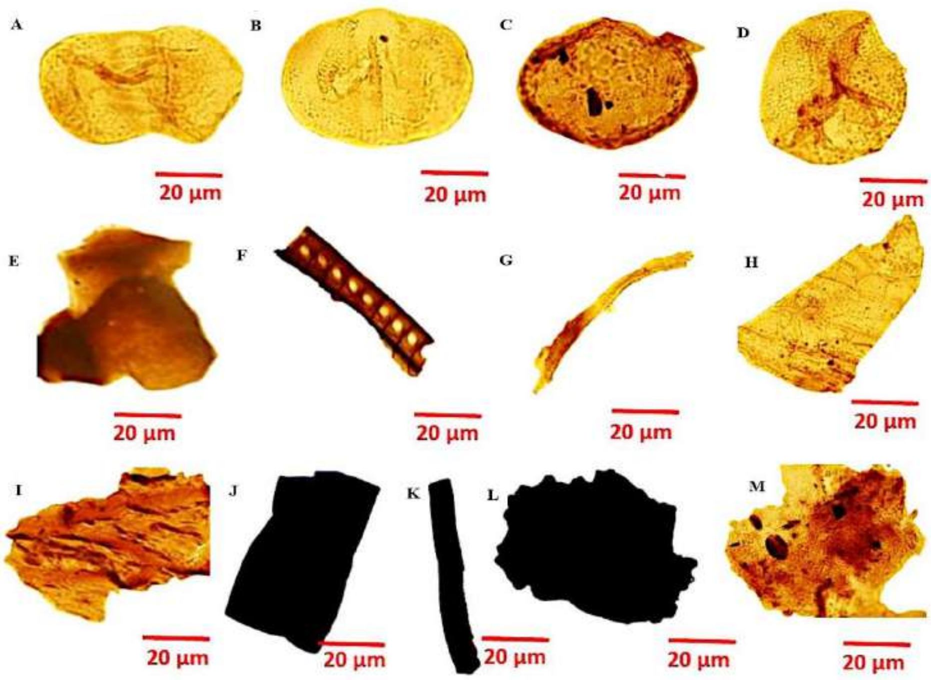

Figure 9. Selected organic matter components from the JOG16N-7 borehole. A. *Protohaploxypinus goraiensis*. B. *Scheuringipollenites ovatus*. C. *Marsupipollenites triradiatus*. D. *Verucosisporites* sp. E. Translucent phytoclast. F. Biostructured phytoclast. G. Fungal hyphae. H. Cuticle. I. Translucent phytoclast. J, K, L-Opaque phytoclast. M. AOM.

The AOM in the Basin is mostly granular and therefore could be associated with generation of liquid hydrocarbon (Figure 10).[42] The type of palynofacies described below suggested from the studied samples were obtained from cluster data (Q-mode) according to the types, abundance and distribution of OM (Table 2 and 3, Figure 11).

Table 2: Palynofacies data for the JOG16N-6 borehole.

101.63	G1	1.33	98.67	0.0
104.58	G2	28.33	67.34	4.33
106.245	G3	21.33	76.34	2.33
117.55	G4	0.67	99.33	0.0
144.77	G5	1.33	98	0.67
156.13	G6	19.67	76	6.0
163.06	G7	1.33	98.67	0.0
163.58	G8	1.0	98.33	0.67
178.20	G9	0.0	100	0.0
200.90	G10	3.33	96.67	0.0
201.80	G11	23.33	73.0	3.67
201.92	G12	12.0	83.0	5.0
202.92	G13	4.0	95.67	0.33
203.12	G14	11.0	89.0	0.0
203.35	G15	5.33	89.67	5.0
210.40	G16	33.33	61.67	5.0
211.73	G17	23.67	69.0	7.33
212.12	G18	13.0	84.67	2.33
220.93	G19	46.67	50.0	3.33
221.17	G20	30.67	67.33	1.67
223.60	G21	27.33	71.67	1.0
225.30	G22	15.34	81.33	3.33
233.40	G23	8.33	89.67	2.0
234.92	G24	6.67	93.33	0.0
237.82	G25	1.33	95.67	3.0
240.57	G26	31.0	64.0	5.0
242.74	G27	49.67	49.0	1.33
244.10	G28	46.0	51.0	3.0
245.57	G29	8.0	82.0	10.0
247.41	G30	30.33	63.0	6.67
250.51	G31	38.67	60.0	1.33
251.53	G32	31.33	67.67	1.0
251.83	G33	29.33	69.0	1.67
253.30	G34	28.33	70.67	1.0
255.13	G35	35.0	62.33	2.67
255.48	G36	41.66	56.67	1.67
275.06	G37	11.0	83.0	6.0
311.36	G38	3.0	94.67	2.33

316.44	G39	3.67	92.33	4.0

Table 2: Palynofacies data for the JOG16N-7 borehole.

Depth (m)	Samples	Palynomorphs (%)	Phytoclasts (%)	AOM (%)
9.65	R3	0.0	100	0.0
16.47	R8	3.33	96.67	0.0
19.105	R9	0.0	99.33	0.67
27.615	R12	35.0	62.66	2.34
46.77	R14	46.33	49.67	4.0
57.79	R18	8.0	90.0	2.0
75.65	R24	8.0	90.33	1.67
82.86	R25	15.0	85.0	0.0
88.385	R26	53.67	44.0	2.33
90.15	R27	39.33	55.67	5.0
91.86	R28	31.67	66.66	1.67
95.44	R30	3.33	96.67	0.0
104.4	R31	3.67	96.33	0.0
108.26	R32	55.33	42.0	2.67
115.46	R33	4.67	95.33	0.0
116.93	R34	38.0	61.0	1.0
118.23	R35	26.0	73.67	0.33
128.55	R38	34.33	65.67	0.0
133.62	R40	35.67	63.0	1.33
140.29	R43	34.67	65.33	
143.3	R46	45.33	50.0	4.67
144.64	R47	6.67	85.67	7.66
145.22	R48	23.67	74.33	2.0
150.66	R50	14.67	81.0	4.33
155.68	R52	53.0	47.0	0.0
156.5	R53	10.33	87.33	2.33
157.22	R54	37.0	61.67	1.33
159.18	R56	20.67	77.66	1.67
163.92	R57	0.0	100	0.0
168.49	R58	44.33	55.67	0.0
238.67	R59	0.0	100	0.0
255.18	R60	0.0	100	0.0
256.4	R61	1.0	98.33	0.67
272.84	R64	33.67	64.0	2.33

4.3.1 Palynofacies Associations

Palynofacies A (both boreholes): These palynofacies is characterized by high phytoclast input (up to 70%), moderate palynomorphs content (30%), and very low AOM quantity. Some horizons are completely barren of AOM.

Palynofacies B (both boreholes)**:** An increase in palynomorphs from bottom to top is observed reaching up to 50% in some horizons. A steady decrease of phytoclast is verified in which some sections display a difference between palynomorphs and phytoclasts of less than 3% suggesting anoxic. A slight recovery of AOM is observed for the JOG16N-7 borehole, core while in the JOG16N-6 borehole a decrease of AOM compared to the Palynofacies A is observed.

Palynofacies C (both boreholes): The phytoclast content reach up to 95%. The palynomorphs decrease significantly with some horizons exhibiting values below 10%. At some horizons the AOM and palynomorphs are completely diluted by the phytoclast content which reaches 100%.

Palynofacies D (both boreholes): The content of phytoclasts reaches up to 80%. The palynomorphs in the majority of sections are less than 10%. However, the AOM increases slightly reaching up to 10.

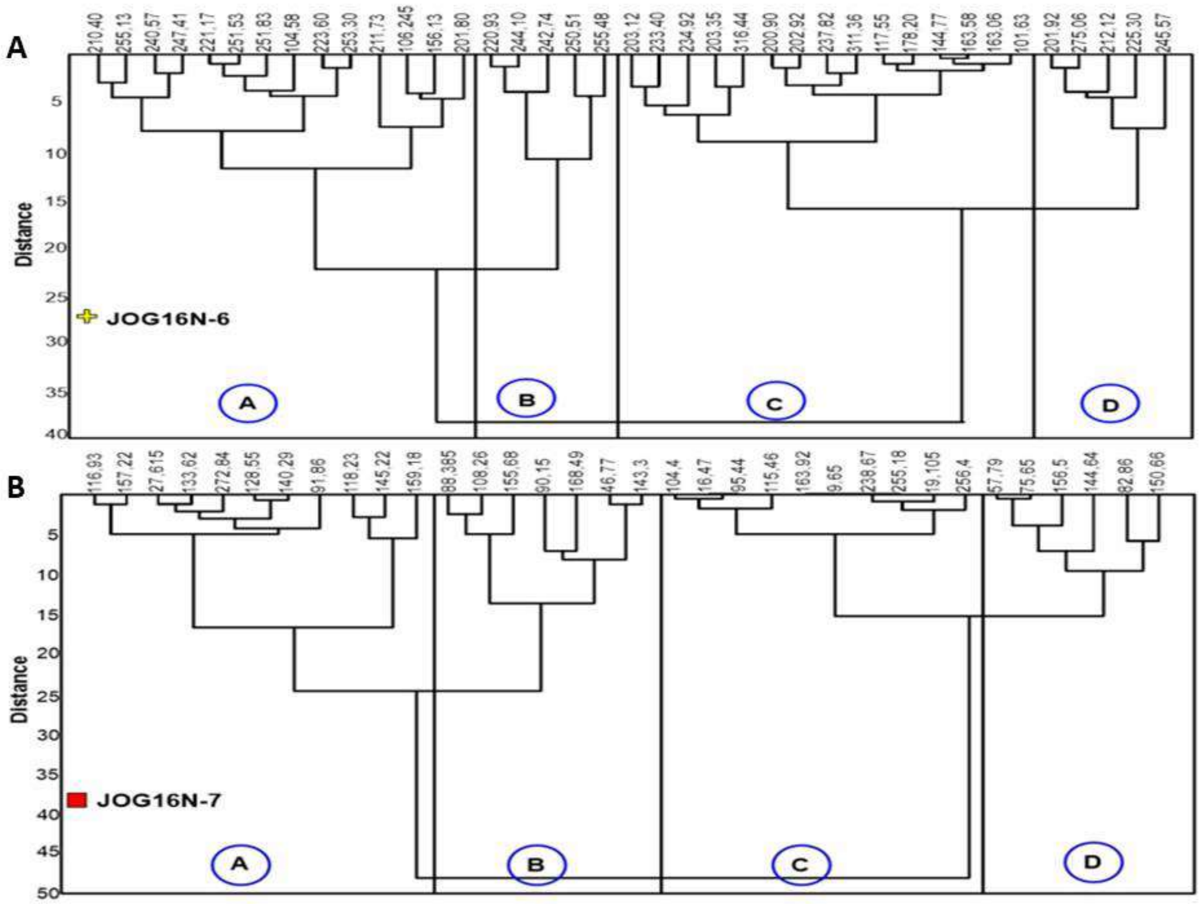

Figure 10. Dendrogram using Q-mode showing four palynofacies assemblages for both studied boreholes.

In general, the observed palynofacies indicate that the OM is mostly terrigenous in origin without marine influence since no marine palynomorphs were identified for both boreholes. The slight variation of OM types is linked to different preservation conditions. An abundance of kerogen type III and IV in the organic-rich sediments from the two boreholes corroborates the fact that the studied OM is derived from a terrestrial source as argued above. Additionally, is well-known that Permian continental sediments, mainly the ones enriched in coal are important natural gas source rocks across the pan-Gondwanan rift.[19,20] It was possible to evaluate the paleotemperature using the spore color index (SCI) and the results showed values that suggests low thermal evolution for all the samples (Figure 12). All the samples were considered immature. In addition, vitrinite values suggested that the studied samples are mostly under low maturity stages displaying a linear trend with increasing depth (Figure 12).

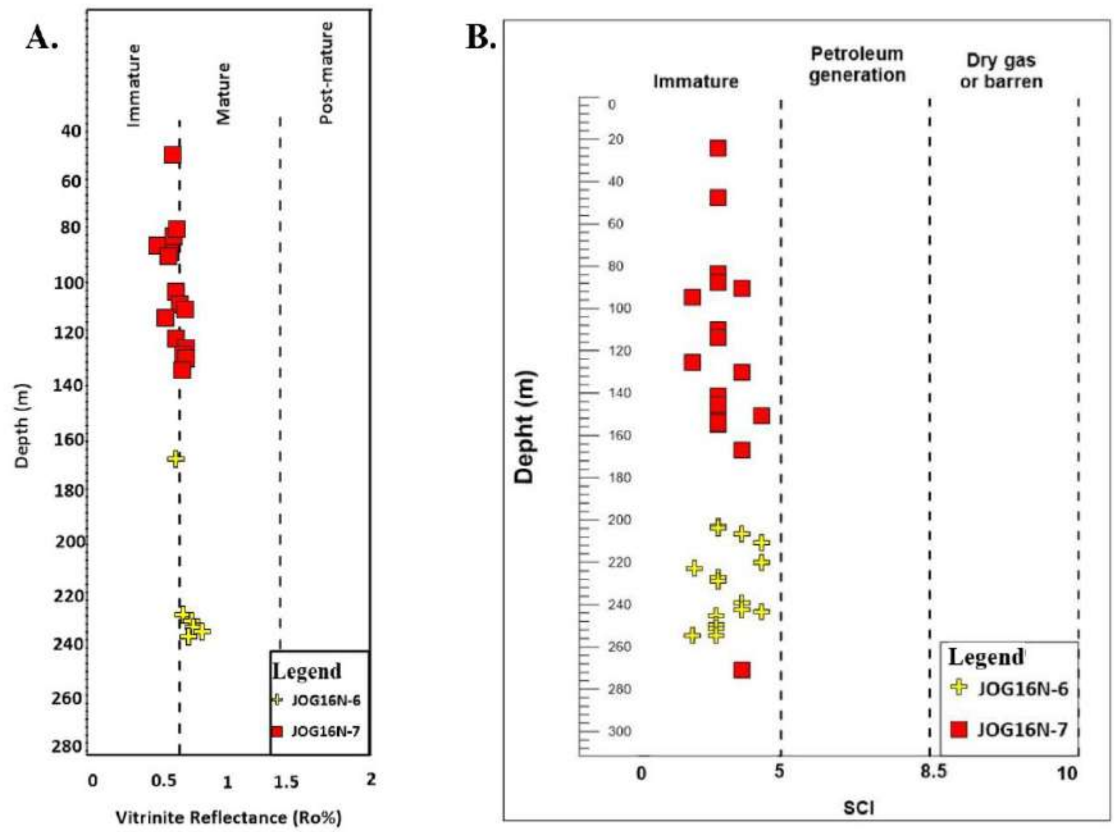

Figure 11. A. Thermal characterization based on VR (vitrinite reflectance) vs. Depth (m). B. Thermal maturity estimation based on spore/pollen color vs. Depth (m).

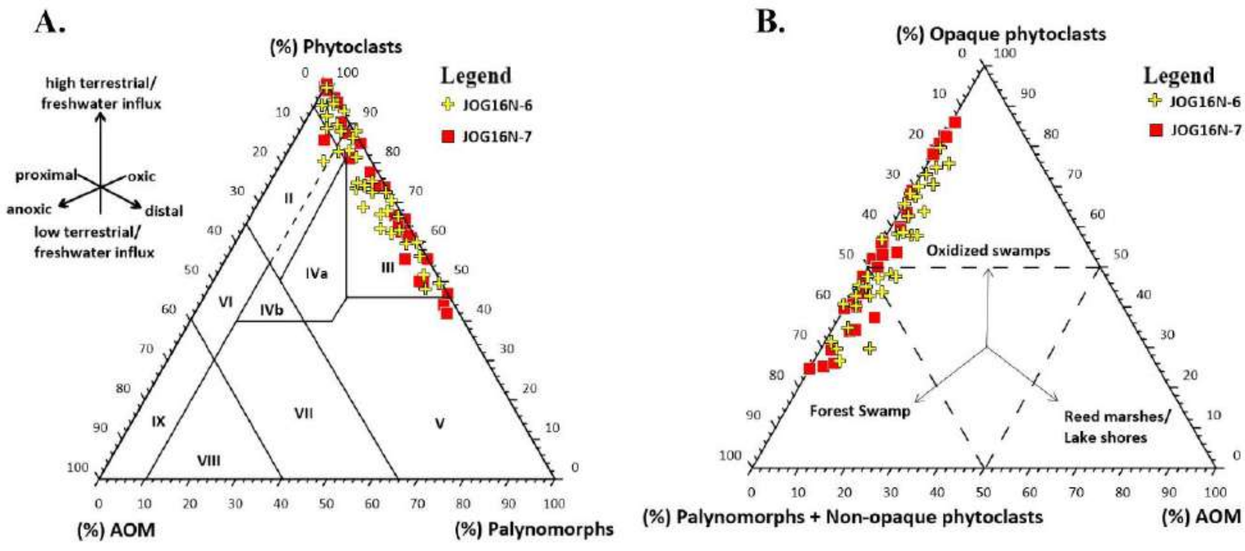

Figure 12. Tyson diagram showing paleoenvironmental inferences. B. Paleo conditions based on swamp diagram adapted from Haecquebard and Donalson (1969).

4.3.2 Depositional environment based on palynofacies

The abundance of opaque phytoclast in the samples suggest a non-oxygen deficient environment that could have affected the OM preservation as also observed through molecular fossils in the Pr/Ph ratios. This scenario is also supported by the identified types of palynofacies. The observed woody material, coaly material, phytoclast and, sporomorphs suggest the continental origin of the OM.[43] Previous studies show that the K4 and K5 Formations are characterized by varied lithofacies which include sandstone, siltstone, coal, and shales (Figure 2). The sandstones are interpreted as an indicator of fluvial settings. In contrast, organic-rich shales enriched on organic matter, and siltstone are representative of swampy terrestrial depositional (Figure 13B). The diagrams proposed by[15,43] have shown that the sediments have been deposited in I, II, III, and IV different fields. The fields represent deposition in proximal to marginal basins with fluctuated paleoredox conditions spanning from oxic-dysoxic to anoxic conditions which is an indicative of gas generation potential. (Figure 13A and B).

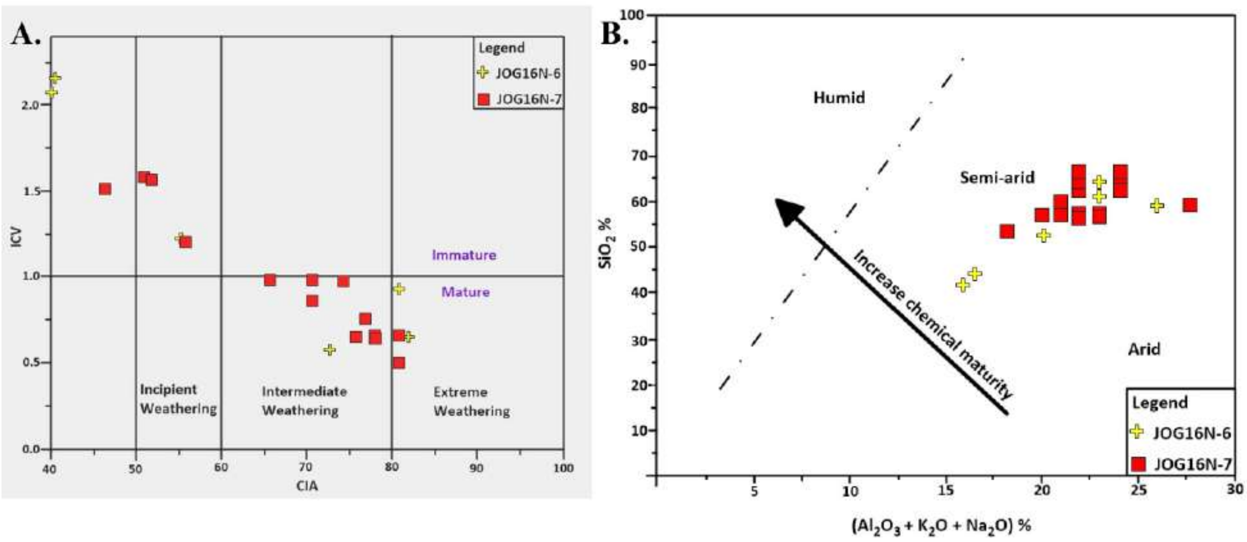

Figure 13. A. Index of Compositional Variability (ICV) vs. Chemical Index of Alteration (CIA) adapted from Cox et al. (1995) and Nesbitt and Young (1984). B. Paleoclimate inference of the study area adapted from Suttner and Dutta, 1986.

Provenance, Paleoclimate and Tectonic settings

The geochemistry of major elements commonly has been applied to further our understanding about the provenance of sediments because sediment composition is associated with the source area from which they originated.

The major elements of the Maniamba sections indicated higher SiO_2 suggesting a considerably higher enrichment of this oxide if compared to other elements as expected in siliciclastic deposits. The high proportion of silica and other major components in the investigated fine-grained black samples, allows them to be harder and brittle, helping them to expel hydrocarbons. The 30-norhopane is lower in content in comparison with the relatively higher content of hopane thus influencing the nature of the samples which is silica according to Connan et al.[6] (Table 1). The same sections are also enriched in Al_2O_3 and TiO_2 (Table 4). The Al_2O_3/Na_2O ratio is useful for delineating the intensity of the weathering process. These sediments display high Al_2O_3/Na_2O content suggesting at some point high weathering intensity. According to Nesbitt and Young,[30] the most important feasible variable used to measure the paleoweathering is the Chemical Alteration Index (CIA). The Chemical Alteration Index in the Maniamba samples is ranged from 40.0 to 81.63 suggesting weak to strong weathering (Figure 14 and Table 4).

Another important parameter is the SiO_2/Al_2O_3 ratio for which values above 10 represent higher maturity of the sediments associated with high recycling. The sediments from the present research have shown low composition maturity. Similarly, for a better interpretation the Index of Compositional Variability (ICV) proposed by Cox et al.[7], has been tested. According to this index, sediments displaying an immature nature have values of ICV greater than 1, and is originated from active tectonic conditions. In its turn, ICV<1, indicates sediments originate from passive tectonic settings. Regarding the ICV parameter, the studied borehole cores display values ranging from 0.52 to 2.53 suggesting non-mature to early phases of maturation (Figure 14 and Table 4). The Al_2O_3/TiO_2 ratio has been regarded as a climatic indicator. Values less than 20 represent humid conditions whereas those above 30 are indicative of an arid environment. The data of the study have demonstrated a high Al_2O_3/TiO_2 ratio suggesting that the provenance site had periods of humid to semi-humid climate. Yet, the occurrence of carbonaceous sediments at different horizons in the MB derived from either fluvial or lacustrine settings is indicative of a past paleoflora characterized by paleoclimate of humid nature. However, Verniers et al.[44] in their study on the MB have identified a shift from arid to humid paleoclimate. The aforementioned conclusion corroborates with the fact that red-coloured fine sediments do occur in some horizons from Lower and Middle Karroo in the studied basin and the occurrence of concretions of calcilutite and calcrete which are considered to be formed favourably under a semi-arid climate according to Verniers et al.[44] as shown in the Figure 14B.

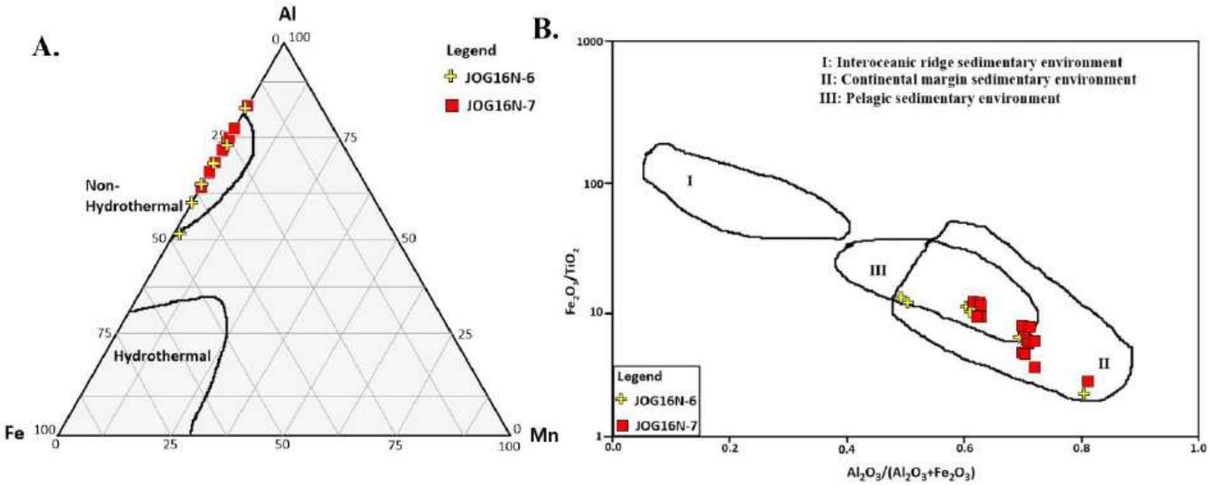

Figure 14. A. Source of the fine rocks from Maniamba obtained from: A. Plot modified from Adachi et al. (1986). B. Fe_2O_3/TiO_2 vs. $Al_2O_3/(Al_2O_3+Fe_2O_3)$.

Table 4: Some obtained major oxides data for the studied borehole cores and paleoweathering indexes.

SiO_2(%)	Al_2O_3(%)	TiO_2(%)	K_2O(%)	Na_2O(%)	Fe_2O_3(%)	CaO(%)	MgO(%)	CIA	ICV	
42.91	13.23	0.60	1.98	0.66	12.35	17.08	0.85	40.15	2.53	
61.06	19.98	0.85	2.96	0.86	11.26	0.78	1.28	81.28	0.90	**JOG16N-6** Borehole core
59.12	22.94	0.99	2.59	0.75	10.20	1.41	1.26	82.84	0.74	
64.09	19.94	1.0	2.95	0.89	3.82	3.37	1.12	73.44	0.65	
53.75	17.43	0.77	2.54	0.68	6.06	11.0	1.12	55.07	1.27	
44.84	14.03	0.68	1.97	0.57	9.67	18.50	1.05	40.0	2.3	
59.01	16.65	0.69	9.66	0.99	9.66	5.12	1.21	51.35	1.64	
58.46	15.6	0.71	5.14	0.79	5.14	11.12	1.14	47.77	1.54	
66.0	18.75	0.84	2.82	0.87	7.12	1.48	1.26	78.38	0.76	
57.82	18.85	0.78	2.6	0.78	6.91	6.17	1.27	66.37	0.98	
64.48	19.15	0.90	2.77	0.89	6.92	1.54	1.12	78.64	0.73	**JOG16N-7** Borehole core
63.31	20.23	0.87	2.9	0.87	6.79	1.75	1.39	78.56	0.72	
65.49	20.09	0.90	3.11	0.91	7.51	0.50	1.46	81.63	0.71	
66.88	20.58	0.92	2.83	0.77	3.92	1.13	1.19	81.31	0.52	
58.35	19.99	0.89	2.52	0.67	5.71	4.93	1.62	71.11	0.81	
57.62	20.72	0.99	2.26	0.61	10.23	3.25	1.17	77.19	0.89	
60.22	18.44	0.85	2.24	0.71	9.12	3.23	1.49	74.89	0.95	
58.86	19.05	0.89	2.27	0.69	8.36	4.81	1.88	71.02	0.99	
58.52	17.28	0.84	2.09	0.63	5.48	10.45	2.06	56.74	1.24	
54.01	15.73	0.78	1.96	0.56	7.66	13.07	2.05	50.22	1.65	
63.54	19.82	0.95	2.46	0.61	5.53	2.99	1.35	76.58	0.70	

***Chemical Index of Alteration** (CIA) =(Al_2O_3 /(Al_2O_3+CaO* +Na_2O + K_2O)*100; **Maturity Index of Precipitation** (ICV) =(Fe_2O_3+ K_2O + Na_2O + CaO + MgO + TiO_2)/Al_2O_3)., **CN** =(Na_2O + CaO); **Discriminant Function F1** = (− 1.773 TiO_2 + 0.607 Al_2O_3 + 0.76 Fe_2O_3 -1.5 MgO + 0.616 CaO + 0.509 Na_2O − 1.224 K_2O)-9.09; **Discriminant Function F2** = (0.445 TiO_2 + 0.07 Al_2O_3-0.25 Fe_2O_3 -1.142 MgO + 0.438 CaO + 1.475 Na_2O + 1.426 K_2O)-6.861

Paleoclimate inferences obtained through the study of fossil woods in the Basin were also reported by Nhamutole et al.[31] Another important oxide used herein to define the paleoenvironment and depositional setting was iron oxide. According to the iron oxide content, two sources can be determined. The hydrothermal activity source indicates that the iron has been originated in seawater and non-hydrothermal source (sedimentary derivation source) which indicates that the iron has been originated from the river system.[11] Yet, the data were plotted in the Adachi et al.[1] diagram based on the percentage of Aluminium, Iron, and Manganese. The plotted data unveil that the iron is derived from fluvial settings adding substantial insights regarding the depositional environment (Figure 15A and B).

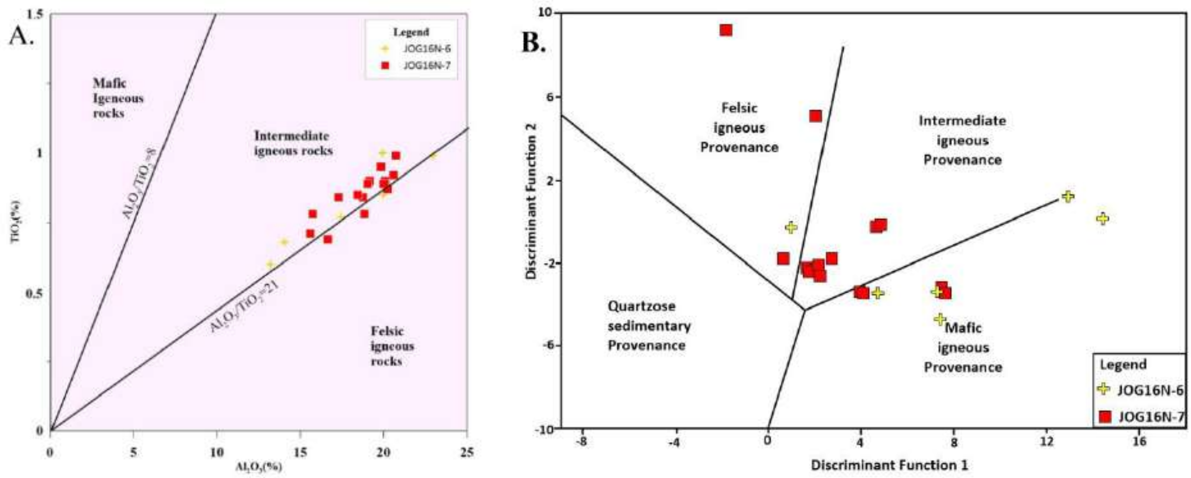

Figure 15. A. TiO_2 vs. Al_2O_3 for the Maniamba borehole cores showing the sediment provenance. B. Discriminant functions indicating more inputs regarding sediment provenance adapted from Hayashi et al. (1997).

Additionally, intermediate igneous rocks are regarded the source rock provenance based on the Al_2O_3/TiO_2 herein (Fig. 15A). However, a minor contribution from felsic and mafic igneous rocks is also observed (Figure 15B).

All in all, an important factor to be considered is the fact that sedimentary rock provenance can rely on the tectonic setting. One of the most used tectonic classifications are obtained from plotting values of K_2O/Na_2O versus SiO_2 as well as a plot of discriminant factor 1 versus discriminant factor 2.[36] The plot of the aforementioned variables indicated the dominance of samples from the continental active margin (Figure 16).

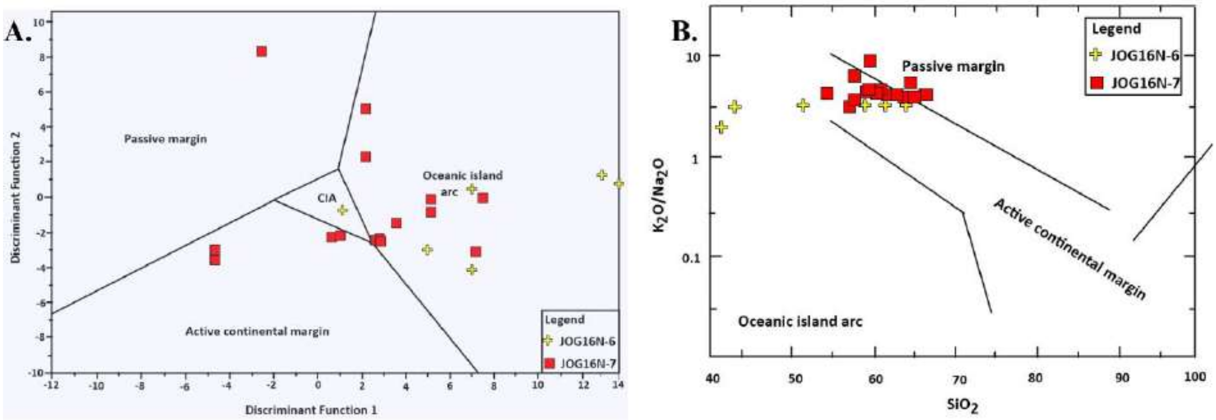

Figure 16. A. Tectonic provinces of the Maniamba sediments inferred by two discriminant functions. B. Tectonic setting of the Maniamba Basin demonstrated by inorganic ratios (obtained from Bhatia, 1983).

5. Conclusions

A combination of molecular fossils, inorganic geochemistry, and palynofacies have allowed the study of OM content, hydrocarbon potential, and determination of the prevailed depositional environments of the sediments intercepted by JOG16N-6 and JOG16N-7 borehole cores. Palynology has revealed the non-marine origin of the OM characterized by kerogen types III, II/III and IV. These data are substantiated by four clustered palynofacies assemblages dominated by phytoclast, and moderate contribution of well-preserved spores, pollen, and AOM. The presence of an ancient ecosystem dominated by the Glossopterid and conifer flora, and palynological associations support the above conclusion. Aside from that, the distribution of *n*-alkanes has demonstrated an unimodal pattern with predominance of C_{27-31} and a preference for odd over even molecules indicating terrigenous OM. The type of the OM is also substantiated by the abundance of molecular compounds such as stigmastane if compared to colestane and ergostane, TAR>1, and the high concentration of tricyclic terpenes. The spore color index (SCI) integrated with vitrinite reflectance indicates samples with low thermal evolution. The CPI and OEP values ranging from 1.06-2.37 and 0.64-2.98 suggest OM with low thermal evolution. These findings are further supported by the values of 18α(H)-trisneohopane (Ts) over 17α(H)-trisnorhopane (Tm), the C_{29} ααα S/(S+R) isomerization ratios in C_{29} steranes and C_{30} βα/(βα+αβ), C_{31} αβ S/(S+R) and C_{32}αβ S/(S+R). The high Al_2O_3/TiO_2 ratio coupled with the occurrence of sporomorphs suggests that a semi-arid to humid paleoclimate prevailed in the Basin.

Additionally, regarding mineral content, the fine-grained sediments pertain to intermediate rocks with a minor contribution from felsic rocks that have experienced incipiently to strong paleoweathering as indicated by Chemical Alteration Index (CIA) and Al_2O_3/TiO_2 diagram. The provenance of the sediments constituted mostly a part of active continental margin. Biomarkers (pristane/phytane ratios) and major elements showed that the OM is typical from proximal-distal conditions linked to variations in paleoredox. Furthermore, the rock samples did not show signs of considerable migration of hydrocarbons since the observed longer-chained molecules are still unbroken according to the gas chromatograms. Here, we have shown that the combined proxies have produced a more robust interpretation of the data from the JOG16N-6 and JOG16N-7 borehole core (Karoo) from the Maniamba Basin, northern Mozambique.

References

1. Adachi M, Yamamoto K, Sugisaki R. Hydrothermal cherts and associated siliceous rocks from northern Pacific: their geological significance as an indication of ocean ridge activity. Sediment. Geol. 1986; 47:125–148.https://doi.org/10.1016/0037-0738(86)90075-8.
2. Akinlua A, Adekola SA, Adeyemi AK. Rare earth and trace element geochemistry of Cretaceous kerogens. Arab. J. Geosci. 2018; https://doi.org/10.1007/s12517-018-3900-0.
3. Araújo R, Macungo Z, Smith R, Tolan S, Angielczyk K, Crowley J, Milisse D, Mugabe J. The first Lower Triassic tetrapod fossils from Metangula Graben (Niassa Province, Mozambique) and their biostratigraphic significance. Palaeontol. Afr. 2020; 54: 56–58.
4. Bhatia MR. Plate-tectonics and geochemical composition of sandstones. J. Geol. 1983; 91: 611–627.
5. Bray EE, Evans ED. Distribution of n-paraffins as a clue to recognition of source beds. Geoch. Cosmoch. Acta 1961; 22: 2–15. https://doi.org/10.1016/0016-7037(61)90069-2.
6. Connan J, Bouroullec J, Dessort D, Albrecht P. The microbial input in carbonate–anhydrite facies of a sabkha palaeoenvironment from Guatemala: A molecular approach. Org. Geoch. 1986; 10:29-50. https://doi.org/10.1016/0146-6380(86)90007-0.
7. Cox R, Lowe DR, Cullers RL. The influence of sediment recycling and basement composition on the evolution of mudrock chemistry in the southwestern United States. Geochim. Cosmochim. Acta 1995; 59: 2919–2940.https://doi.org/10.1016/0016-7037(95)00185-9.
8. De Grande SMB, Aquino FR, Mello MR. Extended tricyclic terpenes in sediments and petroleum. Org. Geoch. 1993; 20:1039.
9. Didyk BM, Simoneit BRT, Brassell SC, Eglinton G. Organic geochemical indicators of paleoenvironmental conditions of sedimentation. Nature. 1978; 272:216–22. https://doi.org/10.1038/272216a0.
10. Dow WG, O’Connor DI. Kerogen maturity and type by reflected light microscopy applied to petroleum exploration, in: Staplin, F.L. et al. (Eds.) How to Assess Maturation and Palaeotemperatures. Palaeontols Mineralogs. 1982; 133-157.

11. Einsele G. Sedimentary Basins: Evolution, Facies, and Sediment Budget. SpringerVerlag, Berlin, 1992; 628. https://doi.org/10.1007/978-3-662-04029-4.
12. Exploration Consultants Ltd (ECL). The Petroleum Geology and Hydrocarbon Prospectivity of Mozambique. Empresa Nacional de Hidrocarbonetos (ENH), Unpublished report. 2000; 144.
13. Flores RM. Coal and Coalbed Gas: Fueling the Future. Waltham, MA, Elsevier, 2014;127:1–2. DOI: *https://* 10.1016/j.coal.2014.02.001.
14. Gallegos EJ. Identification of new steranes, terpenes, and branched paraffin in Green River shale by combined capillary gas chromatography and mass spectrometry. Anal. Chem. 1971; 43: 1151.
15. Hacquebard PA, Donaldson JR. Carboniferous coal deposition associated with Floodplain and Limnic Environments in Nova Scotia. Geological Society of America, 1969; 143–19.
16. Hayashi KI, Fujisawa H, Holland HD, Ohmoto H. Geochemistry of 1.9 Ga sedimentary rocks from northeastern Labrador, Canada. Geochem. Cosmochim. Acta 1997;61, 4115–4137. https://doi.org/10.1016/S0016-7037(97)00214-7.
17. Hong ZH, Li HX, Rullkötter J, Mackenzie AS. Geochemical application of sterane and triterpene biological marker compounds in the Linyi Basin. Org. Geochem. 1986;10:433-439. https://doi.org/10.1016/0146-6380(86)90043-4.
18. Inglis G, Bhattacharya T, Hemingway J, Hollingsworth E, Feakins S, Tierney J. 2022. Biomarker Approaches for Reconstructing Terrestrial Environmental Change. Annu. Rev. Earth Planet. Sci. 2022; 50:369–394. https://doi.org/10.1146/annurev-earth-032320- 095943.
19. Kantsler A J, Cook A C. Maturation patterns in the Perth Basin. Austr. Petrol. Explor. J. 1979;19, 94–107. https://doi.org/10.1071/AJ78011.
20. Kreuser T. Late Palaeozoic glacial sediments and transition to coal-bearing Lower Permian sediments in Tanzania. Facies 1987;17, 149–58.
21. Lewan MD. Factors controlling the proportionality of vanadium to nickel in crude oils. Geochim Cosmoch. Acta 1984; 48:2231–2238. https://doi.org/10.1016/0016-7037(84)90219-9.
22. Lineback JA, Keal J, Burroughs K. Source rock potential of East Africa progress report and preliminary geochemical data and interpretation for Mozambique and additional wells in Somalia, Ethiopia and Madagascar. Robertson Research. 1986;400.

23. Loegering MJ, Milkov AV. Geochemistry of Petroleum Gases and Liquids from the Inhassoro, Pande and Temane Fields Onshore Mozambique. Geosciences, 2007;7:33, doi.org/10.3390/geosciences7020033.
24. Mendonça Filho JG, Carvalho M, Menezes T. Palinofácies. in: Dutra, T.L. (Eds.), Técnicas e Procedimentos para o Trabalho com Fósseis e Formas Modernas Comparativas, Unisinos, São Leopoldo, 2002; 20–24.
25. Mendonça Filho JG, Gonçalves PA. Organic matter: concepts and definitions. In: Suárez-Ruiz, I., Mendonça Filho, J.G. (Eds.), Geology: Current and Future Developments. The Role of Organic Petrology in the Exploration of Conventional and Unconventional Hydrocarbon Systems, Bentham Science Publishers, United Arab Emirates, 2017;1–33
26. Moldowan, J.M., Sundararaman, P., Schoell, M., 1986. Sensitivity of biomarker properties to the depositional environment and/or source input in the Lower Toarcian of S. W. Germany. Org. Geochem. 10, 915–926.
27. Moldowan JM, Peters KE, Carlson RM, Schoell M, Abu-Ali MA. Diverse applications of petroleum biomarker maturity parameters. Arab. J. Sci. Eng. 1994; 19:273–98.
28. McCarthy K, Rojas K, Niemann M, Palmowski D, Peters K, Stankiewicz A. Basic petroleum geochemistry for source rock evaluation. Oilf. Rev. 2011; 23: 32–43.
29. McLoughlin S. The breakup history of Gondwana and its impact on pre-Cenozoic floristic provincialism. Austr. J. Bot. 2001; 49: 271–300.
30. Nesbitt HW, Young GM. Prediction of some weathering trends of plutonic and volcanic rocks based upon thermodynamic and kinetic consideration. Geochim. Cosmochim. Acta 1984; 48:1523–1534.
31. Nhamutole NE, Bamford MK, Araújo R. New species of *Protaxodioxylon* (conifer wood) from the middle Permian of the Metangula graben (Niassa province, Mozambique) and their implications. J. Afr. Earth Sci. 2021;183, 104323.
32. Nhamutole N, Bamford M, Souza P, Carmo D. Palynofacies analysis of the JOG16N-8 borehole, K5 formation from the Maniamba Basin (middle Permian), Mozambique: A contribution for hydrocarbon exploration. J. Afr. Earth Sci. 2023;205p. https://doi.org/10.1016/j.jafrearsci.2023.104997.
33. Nhamutole N, Bamford M, Souza P, Silva TF, Carmo D. Petroleum potential from Permian-Triassic strata of the Maniamba Basin, Mozambique: A preliminary characterization. S. Afr. J. Geol. 2024a; 127:117-130.

34. Nhamutole, N., Bamford, M., Souza, P., Félix, C.M., Carmo, D.A., Peu, J. Palynology of two drilling cores from the Maniamba Basin, Mozambique (central Gondwana): Insights on age and palaeoenvironments. Rev. Palaeob. Palynol. 2024b; 334:105271. https://doi.org/10.1016/j.revpalbo.2024.105271
35. Peters, KE, Walters CC, Moldovan JM. The Biomarker Guide. Biomarkers and Isotopes in the Environment and Human History. Cambridge University. 2005.
36. Roser BP, Korsch RJ. Determination of tectonic setting of sandstone-mudstone suites using SiO_2 content and K_2O/Na_2O ratio. J. Geo. 1986;91: 611-627.
37. Salman G, Abdula I. Development of the Mozambique and Ruvuma sedimentary basins, offshore Mozambique. Sediment. Geol. 1995; 96:7–41.
38. Seifert WK, Moldowan JM. Applications of steranes, terpenes, and monoaromatics to the maturation, migration, and source of crude oils. Geoch. Cosmoch. Acta 1978; 42: 77–95.
39. Seifert WK, Moldowan JM. The effect of thermal stress on source-rock quality as measured by hopane stereochemistry. Physic. Chem. Earth 1980; 12: 229–37.
40. Schwark L, Zink K, Lechtenbeck J. Reconstruction of postglacial to early Holocene vegetation history in terrestrial Central Europe via cuticular lipid biomarkers and pollen records from lake sediments. Geology 2002; 30:463–466.
41. Tissot BP, Welte DH. Petroleum formation and occurrence, 2nd ed. Berlin, Springer-Verlag, Berlin, 1984; 699.
42. Tyson RV. Palynofacies analysis. In: Jenkins, D.G. (Eds.), Applied Micropaleontology. Kluwer Academic Publication, Netherlands, 1993; 153–191.
43. Tyson RV. Sedimentary Organic Matter, Organic Facies, and Palynofacies. Chapman and Hall, London, 1995; 615.
44. Verniers J, Jourdan PP, Paulis RV, Frasca-Spada L, De Bock FR. The Karroo graben of Metangula northern Mozambique. J. Afr. Earth Sci. 1989; 9: 137–158. https://doi.org/10.1016/0899-5362(89)90016-X.
45. Whidden K, Sondergeld CH, Miller MA, Wood GD, Palmer-Koleman S, Larese DE, Cornick PA. Identification and prediction of source rock facies using integrated geoscience technologies: an example from the Kimmeridge Clay Formation, Fisher Bank Basin, North Sea, United Kingdom. Palynol. 1999; 24: 267-268.
46. Wood GD, Miller MA. Stratigraphic, paleoecologic, and petroleum-generating significance of Chlorophyta (Chlorococcalean algae) in the Cretaceous of Western Africa and South America. Afr. Geosci. Rev. 1999; 4:499-510.

Chapter Four

Palynology of two drilling cores from the Maniamba Basin, Mozambique (Central Gondwana): *Insights on age and palaeoenvironments*.

Adapted from Nhamutole, N, Bamford, M.K, Souza, P. A, Félix, C.M, Carmo, D.A, Peu, J.

Published by Review of Palaeobotany and Palynology

Review of Palaeobotany and Palynology 334 (2025) 105271

Contents lists available at ScienceDirect

Review of Palaeobotany and Palynology

journal homepage: www.elsevier.com/locate/revpalbo

Palynology of two drilling cores from the Maniamba Basin, Mozambique (Central Gondwana): Insights on age and palaeoenvironments

N. Nhamutole[a,b,*], M.K. Bamford[a], P.A. Souza[c], C.M. Félix[c], D.A. Carmo[d], J. Peu[e]

[a] Evolutionary Studies Institute and School of Geosciences, University of the Witwatersrand, P Bag 3, Wits, 2050 Johannesburg, South Africa
[b] Museu Nacional de Geologia, Av. 24 de Julho, 355, Maputo, Mozambique
[c] Laboratório de Palinologia Marleni Marques Toigo, Instituto de Geociências, UFRGS, Brazil
[d] Laboratório de Micropaleontologia da Universidade de Brasília, Brasília, DF, Brazil
[e] Eduardo Mondlane University, Departamento de Geologia, Av. Moçambique, Km 1.2, Maputo, Mozambique

Abstract

In the present work, dark siltstones, claystones, shales, coals and carbonaceous shale were critically investigated to identify palynofloral assemblages in Mozambique's overlooked Karoo-aged Maniamba Basin. The study was based on two borehole cores. It unveiled a rich and diversified microflora composed of four distinct palynoassemblages dominated by striate and non-striate bisaccate pollen grains that have prevailed under humid, warm and arid climate conditions in these Gondwana strata. The lower palynoassemblages 1 (P1) and 2 (P2) in both borehole cores are marked by the occurrence of common and abundant striate and non-striate bisaccate pollen, *Protohaploxypinus* spp., *P. limpidus*, *Striatopodocarpites cancellatus*, *Lueckisporites* spp., *Scheuringipollenites* spp. and colpate *Cycadopites cymbatus*. Late Permian key taxa such as *Marsupipollenites triradiatus*, *Plicatipollenites gondwanensis*, and *Guttulapollenites hannonicus* are found herein. The palynoassemblages 3 (P3) and 4 (P4), were assigned to the Early Triassic based on the FAD of key taxa, chiefly *Platysaccus papilonis*, *Lunatisporites* spp., *Lundbladispora* sp. and *Krauselisporites* sp. A younger age is assigned to the K5 Formation in the

Maniamba Basin correlating well-known Gondwana sequences from the Katberg and Balfour formations from the Main Karoo Basin (South Africa), the Moatize-Minjova Basin (Mozambique), Sakamena Group (Madagascar), Raniganj-Panchet formations (India), Mid-Zambezi valley (Zambia), and the Salt Range Basin (Pakistan). Fossil wood occurrences support the assigned ages. Although other proxies are needed to identify the Permo-Triassic transition, the obtained new palynological data could spark interest in exploring methane associated with coal beds.

1. Introduction

Among the four Karoo-aged basins in Mozambique, the Maniamba Basin is one of the most prominent sedimentary basins, extending over an area of 8000 km^2, along with the Zambezi River valley basins, Lugenda River Basin, and Mpotepote (Verniers et al., 1989). This basin displays a complete record of the Gondwana succession ranging from Permian to Upper Jurassic. Despite presenting a record of Gondwana events its stratigraphy based on palynology is still questionable. In Mozambique, palynological research has been comprehensively undertaken in the Moatize Minjova Basin (Lopes et al., 2014; Fernandes et al., 2015; Pereira et al., 2016; Gotz and Loyd, 2017; Fernandes et al., 2023), thus contributing to the enhancement of Gondwana correlations. Other palynological works have not been published because they were carried out by oil and gas companies. These surveys relate to ongoing oil and gas projects in the Mozambique and Rovuma basins. Here it should be noted that the Karoo sedimentary rocks do not outcrop in the coastal Rovuma Basin, except for small isolated patches that were mapped in the latest geological mapping undertaken by Norconsult (2007). The previous geological surveys carried out in the Rovuma and Mozambique basins did not reach the underlying Karoo sediments because the reservoir rocks of younger ages were the main target. Nevertheless, in order to understand the geology of the Karoo, rocks buried under the marine Jurassic in the Rovuma and the Mozambique basins, the study of similar formations in the Karoo basins on the continent, where these formations emerge based on drilling cores and geophysical profiles of boreholes in these basins, is needed. Above all, it has been hypothesised that the Karoo strata probably sourced the methane gas in the Mozambique and Rovuma basins since they two basins unconformably overlie the Karoo-aged strata. Furthermore, despite all the palynological work done in the

Mozambican basins, some remain overlooked such as the case of the Karoo-aged Maniamba Basin in the northern part of Mozambique. The latter palynological work undertaken in the Maniamba Basin dates to the 1980s (Verniers et al., 1989). In their study of these rocks, Verniers et al. (1989) identified three distinct assemblage zones and six subzones, thus correlating Ecca and Beaufort sections of the Maniamba Basin with surrounding areas include southwest Tanzania, Zambia, Zimbabwe, Madagascar and South Africa. The palynoassemblages identified by Verniers et al. (1989) were based on the variation of the bisaccate non-striate taxa such as *Protohaploxypinus* spp., *Vittatina africana*, and trilete spores of the genera *Acanthotriletes* and *Apiculatisporis*. However, no endemic Permian or Triassic taxa were reported. Moreover, several Gondwana studied sections have been well documented and correlated based on the distribution of organic-walled microfossils. A high-resolution Gondwana scheme is still debatable due to the lack of Permian marine microfossils, such as conodonts and benthic foraminifera, preventing a better correlation. Despite the aforementioned limitations, palynology remains are the most reliable tool for correlations of Gondwana terrestrially-derived sections as depicted by some authors (Jha et al., 2011; Pereira et al., 2016; Barbolini et al., 2018; Galasso et., 2019; Pereira et al., 2019; Agarwal et al., 2019; Fernandes et al., 2023). Therefore, the present work intends to draw up a concise palynological survey based on the existing knowledge, combined with newly obtained palynological data from two borehole cores JOG16N-6 and JOG16N-8 that could refine the biostratigraphy and palaeoenvironments of the late Permian from the Maniamba Basin. The results of this work will also aid future evaluation of unconventional hydrocarbon (coalbed methane). Additionally, since Mozambique was part of Gondwana during the Permian, this work, will provide important insights for an improved understanding of the Gondwana palynofloras during the Lopingian (Changhsingian).

2. Geology and Stratigraphy of the Maniamba Basin

Please see details regarding the geology of the Maniamba Basin in section 5.1

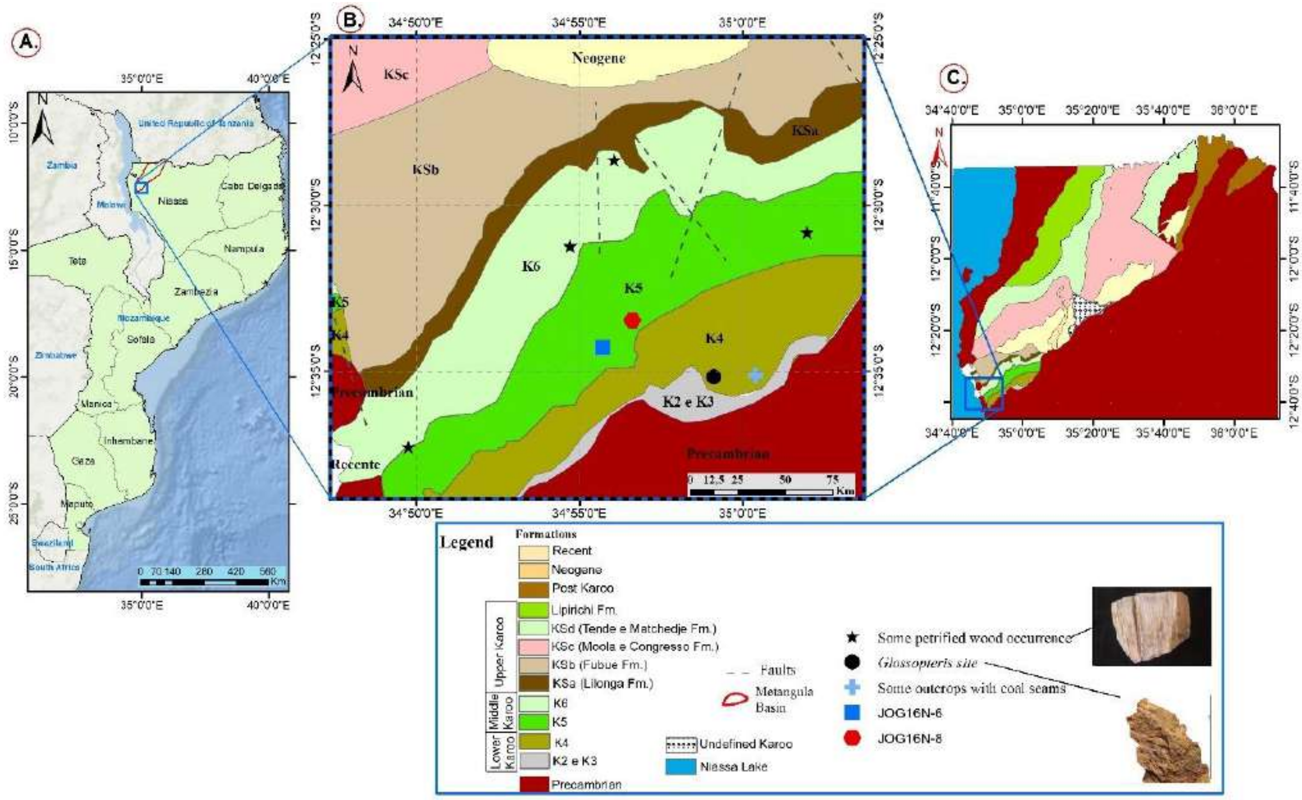

Fig. 1. Geological map of the Maniamba Basin (adapted from Verniers et al., 1989).

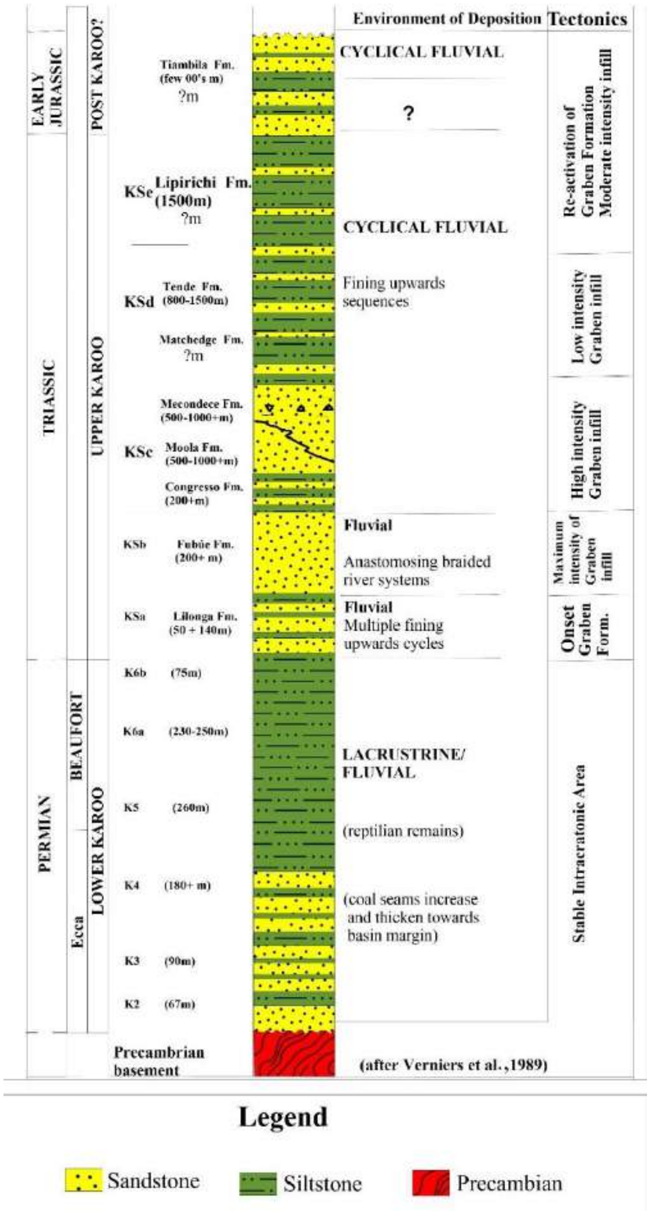

Fig. 2. The lithostratigraphic sequence of the Maniamba Basin emphasises the various depositional environments and tectonic events (after Verniers et al., 1989).

3. Methods and Materials

Thirty-nine (39) samples were taken from borehole JOG16N-6, but only nineteen (19) proved to be productive for palynomorphs. In borehole JOG16N-8, a total of nineteen (19) core samples were collected, out of which fourteen proved to be productive for palynomorphs (Fig. 3). The sampled lithologies consist of siltstones, carbonaceous shales, coal, fine-grained sandstones and dark-grey claystones. All samples from both cores were subjected to standard palynological preparation that includes acid preparation, oxidation and acetolysis (Moore et al., 1991; Traverse, 2007, Barbolini and Bamford 2014). The standard palynological procedures are described in section 6.2.

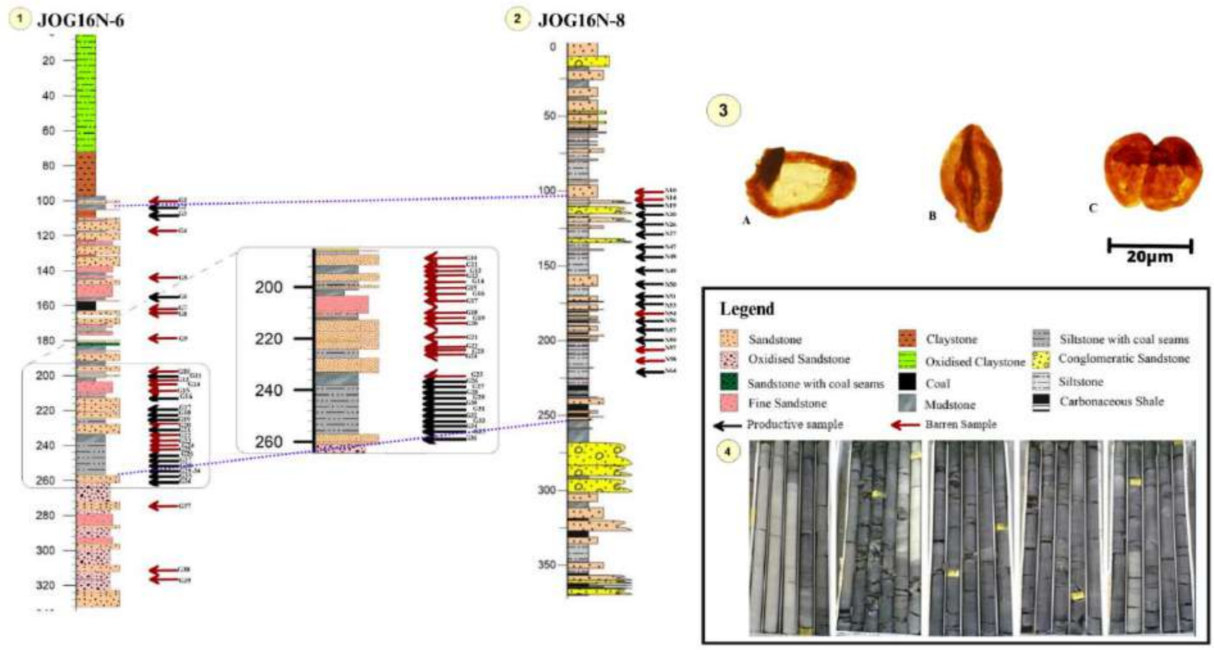

Fig. 3. A. Lithological log of JOG16N-6 core illustrating sampling points and correlatable sections with JOG16N-8, B. JOG16N-6 core illustrating sampling points and correlatable sections with JOG16N-8, C. Some palynotaxa found in the drilled cores in their taxonomical identification: A. represents *Caheniasaccites flavatus* Bose & Kar emend. Azcuy & Di Pasquo 2000, sample N53, JOG16N-8, B. *Gnetaceapollenites sinuosus* (Balme and Hennelly) Bharadwaj and Srivastava, 1969, sample G6, JOG16N-6, C. *Lueckisporites* spp., sample G20, JOG16N-6. Scale bar = 20 μ m.

4. Results

The studied borehole cores consist of sandstones, siltstones, mudstones, claystone, conglomerates, coal seams and carbonaceous shale (Fig. 3 A and B). The JOG16N-6 borehole is divided into three intervals based on lithological predominance. The deepest interval is sandstone dominated (350-260 m). The second interval (260-120 m) is dominated by siltstone-sandstone-coal and carbonaceous shales. One coal bed bearing carbonised leaves is identified within this interval with thickness >10 m (Fig. 3 A). Lastly, the upper unit ranges from 120 m to the top of the borehole and is dominated by coarse-grained to conglomeratic sandstone alternating with claystones. The

JOG16N-8 is characterised by the same lithologies observed in the JOG16N-6 borehole core (Fig. 3B). Here, three intervals were also identified. The deepest interval (370-275 m) is dominated by sandstones interbedded with conglomerates. The conglomerate's clasts are subrounded with no preferential orientation decreasing in size and quantity towards the top and displaying planar and abrupt contact at the base. Four coal beds with abrupt contact at the base are observed. The middle interval (270-100 m) is dominated by siltstone with coal seams and carbonaceous shale. Six coal seams were observed displaying a thickness of >5 m. The uppermost interval is found at the depth of 100m and extends to the top of the borehole core and is characterised by the dominance of sandstone alternating with siltstone (Fig 3B).

A well-preserved and diverse assemblage of pollen and spores, including trilete, monolete, monosaccate, bisaccate, and a few colpate palynotaxa, along with leaf cuticles and wood fragments was collected (Figs. 4-8). No marine palynoflora has been observed. The discrimination of the palynological assemblages as well as the related figures (Figs. 4-8) containing significant taxa are described in the following sections.

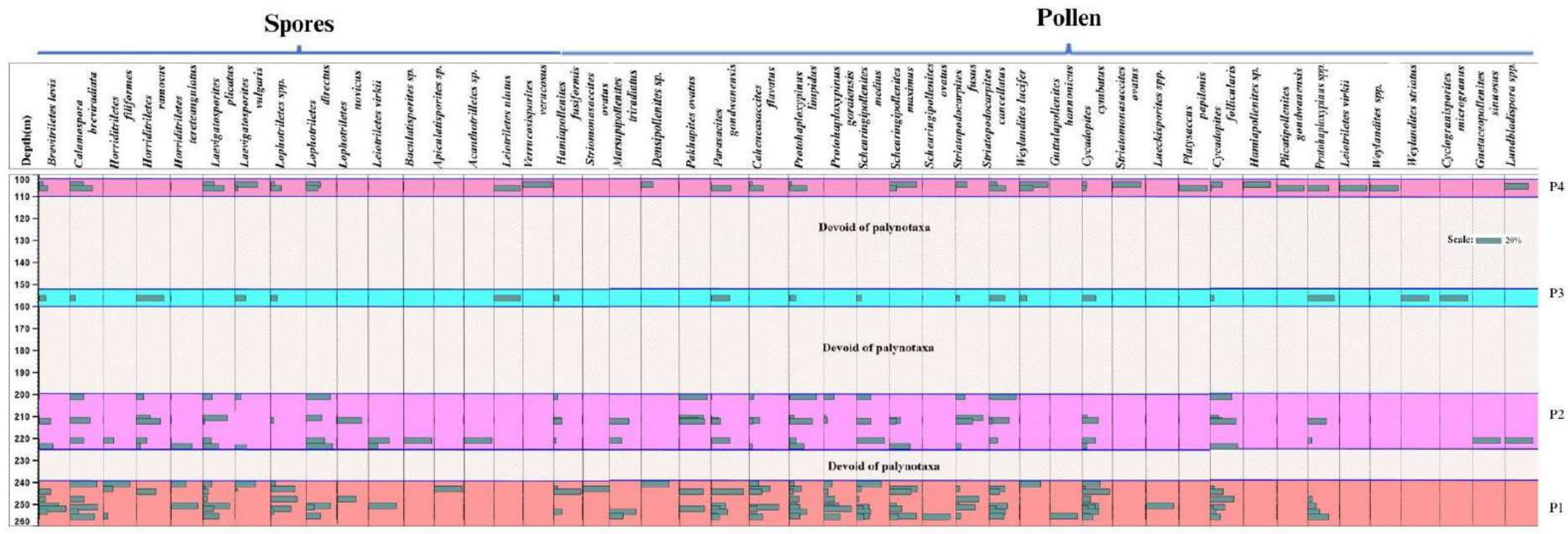

Fig. 4. Quantitative vertical distribution of the palynomorphs and the identified palynoassemblages from the JOG16N-6 borehole.

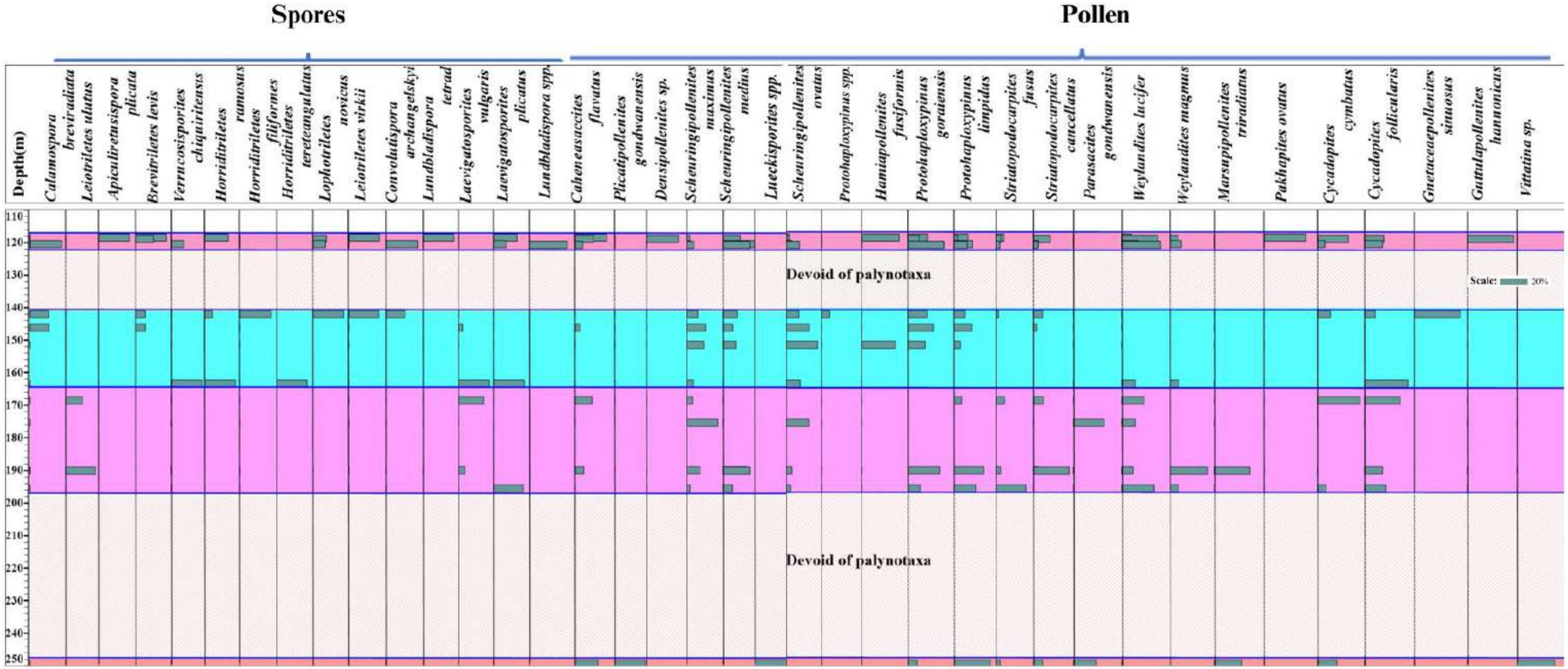

Fig. 5. Quantitative vertical distribution of the palynomorphs and the identified palynoassemblages from the JOG16N-8 borehole.

4.1 Palynology of the two borehole cores JOG16N-6 and JOG16N-8

4.1.1 Palynoassemblages from the JOG16N-6 Borehole

Palynoassemblage 1 (P1) (Fig. 4): This assemblage is characterised by the dominance of *Calamospora breviradiata, Cannanoropolis janakii, Cycadopites cymbatus, C. follicularis, Densipollenites* sp*., Hamiapollenites fusiformes, horriditrilletes tereteangulatus*. Rare and common occurrence includes *Laevigatosporites vulgaris, Leiotriletes* sp*., Lophotriletes directus*. In addition, for the occurrence of rare, common to abundant taxa species such as *Parasaccites gondwanensis*, *Protohaploxypinus limpidus*, *P. goraiensis*, *Scheuringipollenites medius*, *S. maximus*, *Striatopodocarpites cancellatus* and *S. fusus* is observed. On the other hand, the abundant palynotaxa include, *Lueckisporites* spp*., Portalites gondwanensis*, *Weylandites lucifer*, *Lophotriletes novicus*, *Guttulapollenites hannonicus, Densipollenites* sp., *Striomonosaccites ovatus*, and *Apiculatisporites* sp.

Palynoassemblage 2 (P2): The palynoassemblage 2 resembles the palynoassemblage 1, however, a clear increase of taxa such as *Protohaploxypinus limpidus*, *P. goraiensis*, *Cycadopites follicularis*, *Striatopodocarpites cancelatus* is identified. The first occurrence of taxa such as *Gnetaceaepollenites sinuous* combined with *Acanthotriletes* sp. and *Baculatisporites* sp. is observed.

Palynoassemblage 3 (P3): The palynoassemblage 3 is marked by the drop in the overall content of the palynomorphs. Most of the observed palynomorphs in palynoassemblage 2 disappear or have a lower abundance. However, the occurrence of stratigraphically important taxa such as *Platysaccus papilonis*, *Lunatisporites* spp*.,* and *Cyclogranisporites microgranus* is noted.

Palynoassemblage 4 (P4): The significant stratigraphic taxa observed in the palynoassemblage 3 increase their abundance in palynoassemblage 4. However, this palynoassemblage records the appearance of other key taxa such as *Verrucosisporites verucosus*, *Platysaccus papilonis, Lundbladispora* spp., and *Krauselisporites* sp. An increase in palynomorph content is observed, unlike the underlying palynoassemblage.

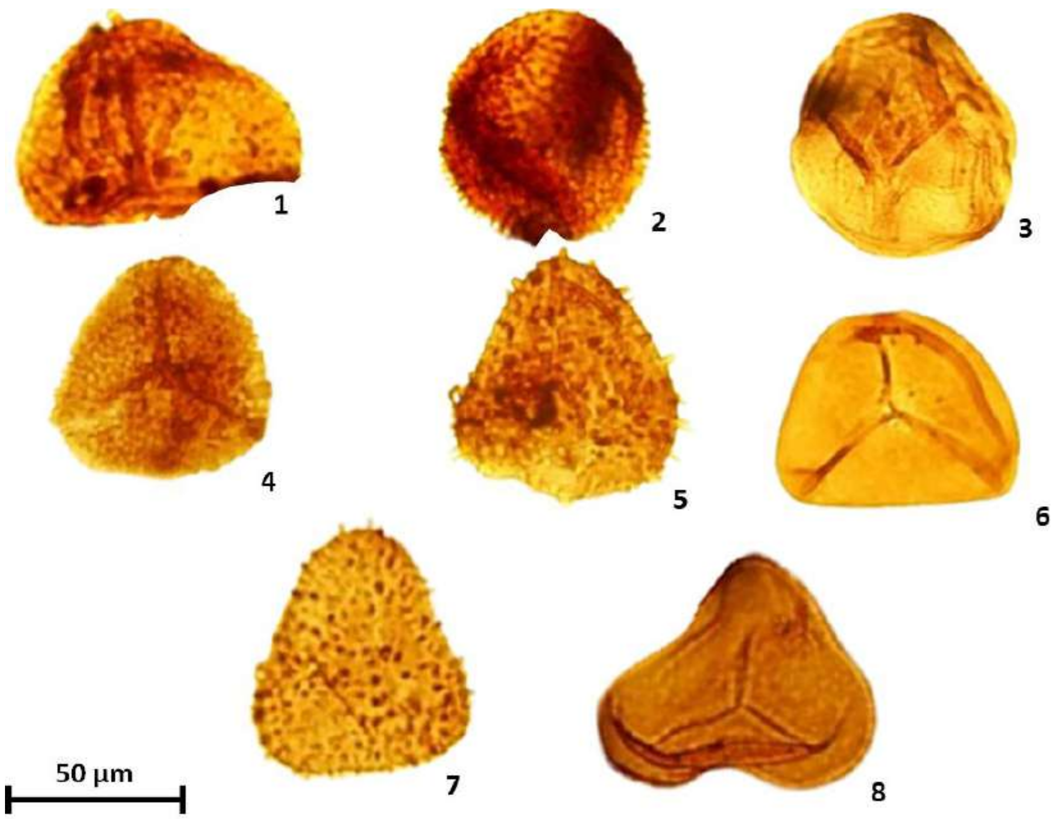

Fig. 6. Selected retrieved palynomorphs from the JOG16N-6 and JOG16N-8 borehole cores: 1. *Acanthotriletes* spp., sample G19, JOG16N-6, 2. *Baculatisporites* spp., sample G19, JOG16N-6, 3. *Cyclogranisporites parvigranulosus* (Leschik) Ybert 1975, sample G19, JOG16N-6, 4. *Lundbladispora* spp., sample G19, JOG16N-6, 5. *Horriditriletes tereteangulatus* (Balme and Hennelly) Backhouse, 1991, sample G19, JOG16N-6, 6. *Leiotriletes virkii* (Tiwari 1965), sample G19, JOG16N-6, 7. *Lophotriletes rectus* (Bharadwaj and Saluijha, 1964), sample G19, JOG16N-6, 8. *Lophotriletes* spp., sample G3, JOG16N-6. Scale bar = 50 μ m.

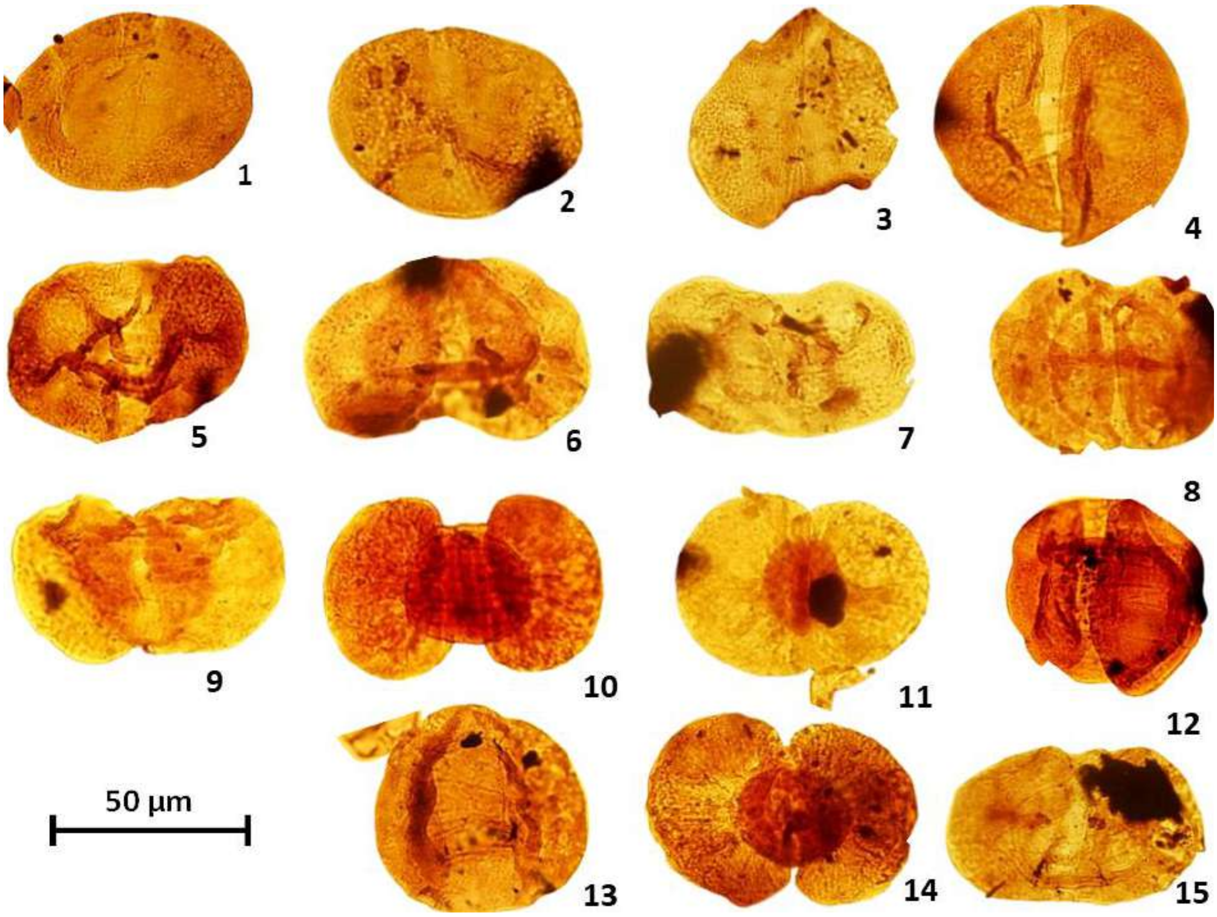

Fig. 7. Selected recovered palynomorphs from the JOG16N-6 and JOG16N-8 borehole cores: 1. *Striomonosaccites ovatus* (Bharadwaj 1962), sample G2, JOG16N-6, 2. *Scheuringipollenites maximus* (Hart) Tiwari (1973), sample G33, JOG16N-6, 3. *Scheuringipollenites medius* (Tiwari 1973), G33, JOG16N-6, 4. *Protohaploxypinus* spp., sample G19, JOG16N-6, 5. *Protohaploxypinus latissimus* (Luber in Luber and Waltz) Samoilovich 1953, sample G20, JOG16N-6, 6. *Protohaploxypinus* spp., sample N64, JOG16N-8, 7. *Protohaploxypinus goraiensis* (Potonié and Lele) Hart, 1964 sample N64, JOG16N-8, 8. *Protohaploxypinus limpidus* (Balme and Hennelly) Balme and Playford 1967, sample N64, JOG16N-8, 9. *Protohaploxypinus limpidus* (Balme and Hennelly) Balme and Playford 1967, sample N64, JOG16N-8, 10. *Striatopodocarpites cancellatus* (Balme and Hennelly) Hart 1963, sample N56, JOG16N-8, 11. *Striatopodocarpites fusus* (Balme and Hennelly) Potonie 1958, sample N64, JOG16-8, 12. *Lunatisporites* spp., sample G35, JOG16N-6. *Protohaploxypinus* spp., sample, N64, JOG16N-8, 14. *Platysaccus papilonis* (Naumova 1954), sample G28, JOG16N-6, 15. Unidentified bisaccate pollen grain, sample N6, JOG16N-8. Scale bar = 50 µm.

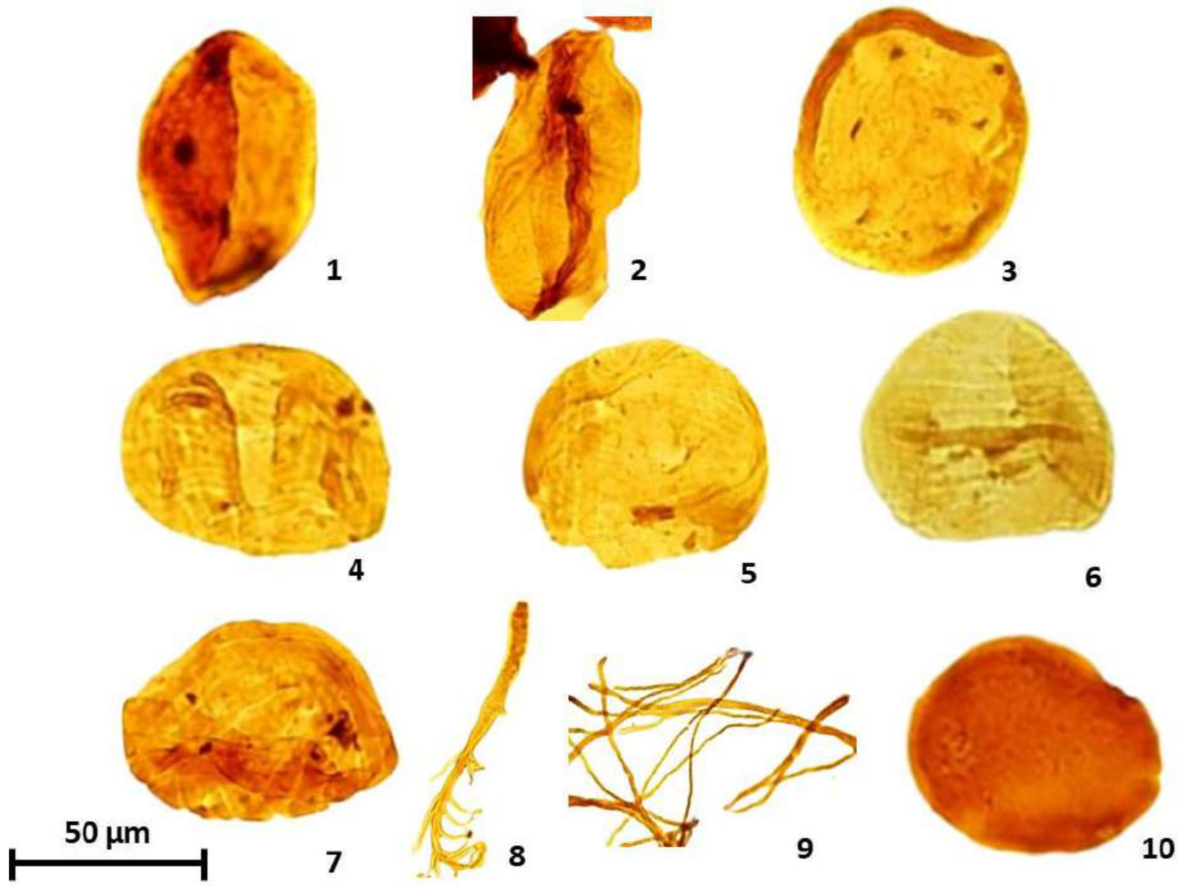

Fig. 8. Selected well-preserved sporomorphs from the JOG16N-6 and JOG16N-8 borehole cores:1. *Cycadopites cymbatus* (Balme and Hennelly) Segroves 1970, sample N64, JOG16N-8, 2. *Cycadopites folicularis* (Wilson and Webster 1946), sample N51, JOG16N-8, 3. *Marsupipollenites triradiatus* (Balme and Hennelly, 1956), sample N56, JOG16N-8, 4. *Weylandites lucifer* (Bharadwaj and Salujha) Foster 1975, sample N56, JOG16N-8, 5. *Weylandites lucifer* (Bharadwaj and Salujha) Foster 1975, sample N51, JOG16N-8, 6. *Vittatina* spp., sample N64, JOG16N-8, 7. *Weylandites* spp., sample G6, JOG16N-6, 8. Fungal hyphae, 9. Fungal hyphae, sample N47, JOG16N-8, 10. Unidentified fungal spore, sample N64, JOG16N-8. Scale bar = 50 µm.

4.1.2 Palynoassemblages from the JOG16N-8 borehole

Palynoassemblage 1 (P1) (Fig. 5): This assemblage contains abundant *Protohaploxypinus limpidus*, *Limitisporites rectus*, *Vittatina* sp., *Lueckisporites* spp., *Plicatipollenites gondwanensis* and *Caheniasaccites flavatus*. Here, we observed a rare occurrence of *P. goraiensis*, *Striatopodocarpites cancellatus* and the common occurrence of *Cycadopites cymbatus*.

Palynoassemblage 2 (P2): The assemblage contains moderate to abundant *Leiotriletes ulutus*, rare to common *Laevigatosporites vulgaris*, and abundant *L. plicatus*. Another notable occurrence includes *Parasaccites gondwanensis*, and rare to abundant occurrence of *S. maximus*, *S. ovatus* and *S. medius*. The latter taxa are also combined with rare and abundant occurrence of *Protohaploxypinus goraiensis*, *P. limpidus*, *Striatopodocarpites fusus*, *S. cancellatus*, *Weylandites lucifer*, *W. magmus*, *Cyacadopites cymbatus* and *C. follicularis*. *Marsupipollenites triradiatus* is also observed.

Palynoassemblage 3 (P3): This assemblage is marked by the presence of the selected and diagnostic species that also occur in the palynoassemblage 2, however a drop in the abundance of *Protohaploxypinus*, *Striatopodocarpites*, *Weylandites*, and *Cycadopites* is observed. The assemblage is characterised by the first occurrence of stratigraphically significant taxa such as *Calamospora breviradiata, Leiotriletes virkii* and species of the genera *Verrucosisporites*. Other taxa observed for the first time in the sequence include *Brevitriletes levis*, *Horriditriletes ramosus*, *H. filiformes*, *H. tereteangulatus*, *Lophotriletes novicus*, *Convulatispora archangelskii*, *Hamiapollenites fusiformes* and *Gnetaceaepollenites sinuosus.*

Palynoassemblage 4 (P4): This assemblage is marked by the same abundance of the palynomorphs observed in palynoassemblage 3. However, here was noted the appearance of significant biostratigraphic taxa such as *Lundbladispora sp.*, *Lundbladispora* tetrads, *Pakhapites ovatus*, *Krauselisporites* sp.

4.2 Age determination of the studied stratigraphical sequence based on palynotaxa

These borehole cores were drilled into the K5 Formation, and based on the vertical distribution and first appearance datum of stratigraphically significant taxa four palynoassemblages (P1, P2, P2, P4) for both borehole cores were identified. Aside from that, two intervals devoid of palynotaxa were observed for each of the borehole cores. The barren zones in these sections could be linked to poor preservation of the organic-walled microfossils. The palynological barren zones for the JOG16N are characteristic for the following depth intervals (160-200m), (110-152m), (225-240m). In its turn, for the JOG16N-8 core the barren sections are found in the range (198-249m) and (122-140m) respectively.

In summary, the P1 and P2 for borehole cores were mainly characterised by common occurrence of bisaccate striate pollen, non-striate, trilete spores and monocolpates as shown in Figures 4 and 5. Both lower palynoassemblages from both cores were assigned to the latest Permian. The Upper Permian strata for the JOG16N-6 are found in depths (240-260m) and (200-225m) whereas the depths (250-260m) and (165-198m) pertain to the JOG16N-8 core. In contrast, the palynoassemblages from the younger beds, in both boreholes are characterised by the initial appearance of Early Triassic taxa such as *Calamospora breviradiata, Verrucosisporites verucosus, Lundbladispora* sp.*, Hamiapollenites fusiforms* and *Krauselisporites* sp.

Our research corroborates the findings from Pereira et al. (2016) for the coeval Moatize-Minjova Basins in Mozambique as well as data from the southwest portion of the Maniamba Basin in Mozambique (Verniers et al., 1989). It should be noted that typical Triassic forms were not identified by Verniers et al. (1989). Here, we identify for the first time in the Maniamba Basin some important Early Triassic taxa that include *Lunatisporites* spp., *Platysaccus papilonis, Lundbladispora* spp., *Verrucosisporites verrucosus, Plicatipollenites gondwanensis, Cyclogranisporites microgranus* and *Krauselisporites* sp. In addition, several unidentified taxa, including some fungi and cuticles, appear at the top of the studied sequences (Fig. 6). The presence of unidentified taxa at the uppermost part of the sequence combined with the spike of fungal remains has been described as a marker for the Permian-Triassic transition in the southern part of the Main Karoo Basin (Steiner et al., 2003). However, the latter interpretations are still a matter of debate. The Permo-Triassic transition for the JOG16N-6 borehole is tentatively located at depths of 152-160m and 100-110m, while the JOG16N-8 borehole shows the transition at the depths of 140-165m and 117-122m. The minor difference is that Triassic forms are observed earlier in the latter borehole, even though both cores in those depths are characterised by lowering or absence of coal or carbonaceous samples and predominance of sandstones and claystones.

4.3 Age determination supported by fossil wood occurrences

According to Nhamutole et al. (2021) stratigraphically significant fossil wood taxa were collected from the K5 Formation, namely *A. africanum, Agathoxylon karooensis* and *Australoxylon teixeirae* (Figs. 9 and 10). *Agathoxylon africanum* is a widespread southern African species that ranges in age from late Permian (Lopingian) to Middle Triassic (Bamford and Phillipe, 2001). In its turn *A. karooensis* with triseriate araucarian tracheid pitting is endemic to Karoo rocks and has been recorded, so far, only in late Permian strata. Lastly, *A. teixeirae* is restricted to the Upper Permian and Lower Triassic formations such as Collingham, Middleton and Normandien (South Africa; Bamford, 1999; Bamford et al., 2020), Raniganj and Kamthi (India; Prasad, 1982), Teresina and Rio do Rasto (Brazil; Scheinedr et al., 1974). Shale Group in Malawi (Crisafulli, 2002), and in the Yaguary and Tacuary formations from Uruguay and Paraguay respectively (Crisafulli, 2002).

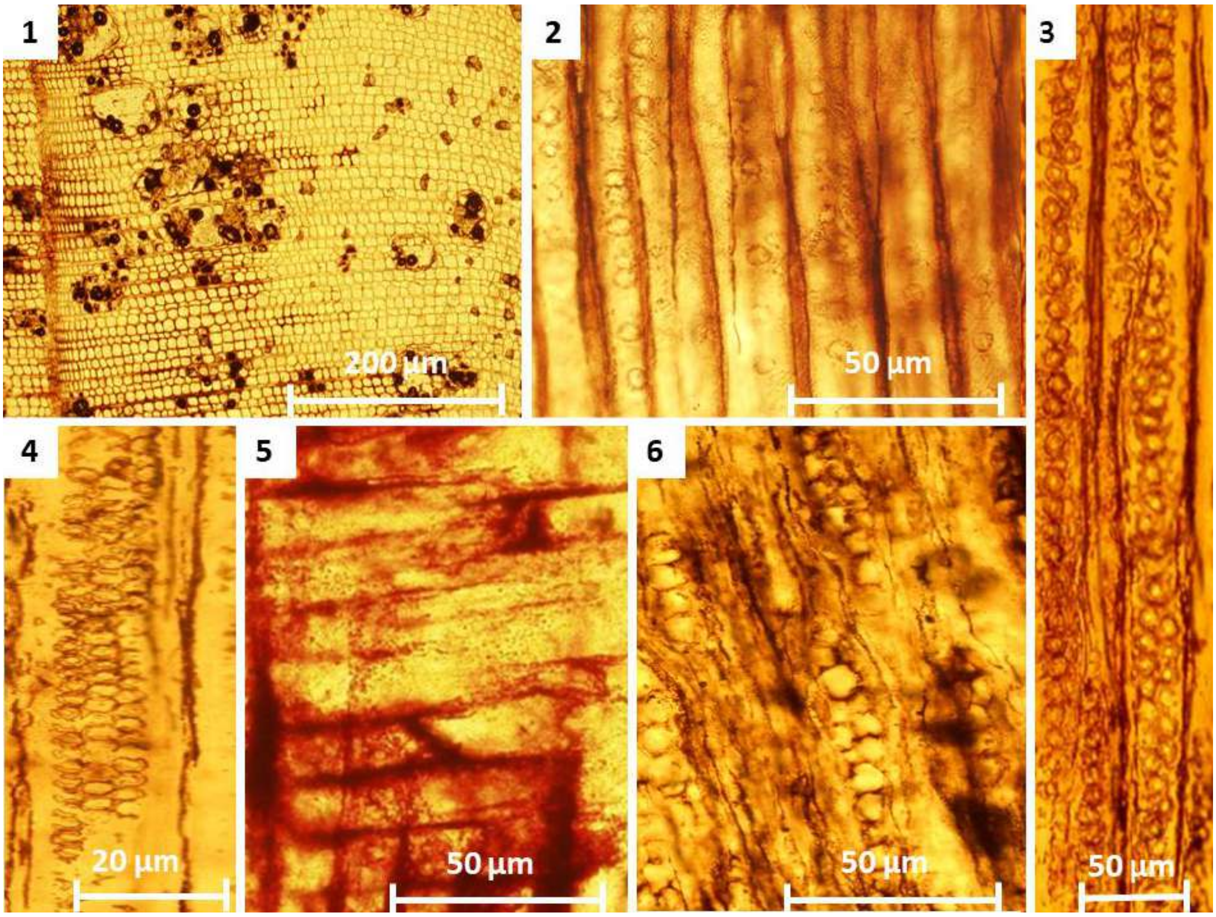

Fig. 9. Some characteristic fossil woods from the Karoo sequences: 1. Transverse section typical of late Permian wood displaying round to square tracheids, 2. Uniseriate bordered pits of the late Permian-Early Triassic *Agathoxylon africanum* wood in radial longitudinal section

(RLS), 3. Biseriate and alternate tracheid pits from Late-Permian-Early Triassic *A. africanum* fossil wood, 4. Endemic late Permian wood *A. karooensis* exhibiting triseriate bordered pits in RLS, 5. Uniseriate to biseriate rays typical of Permian wood from Karoo sequences in tangential longitudinal section (TLS).

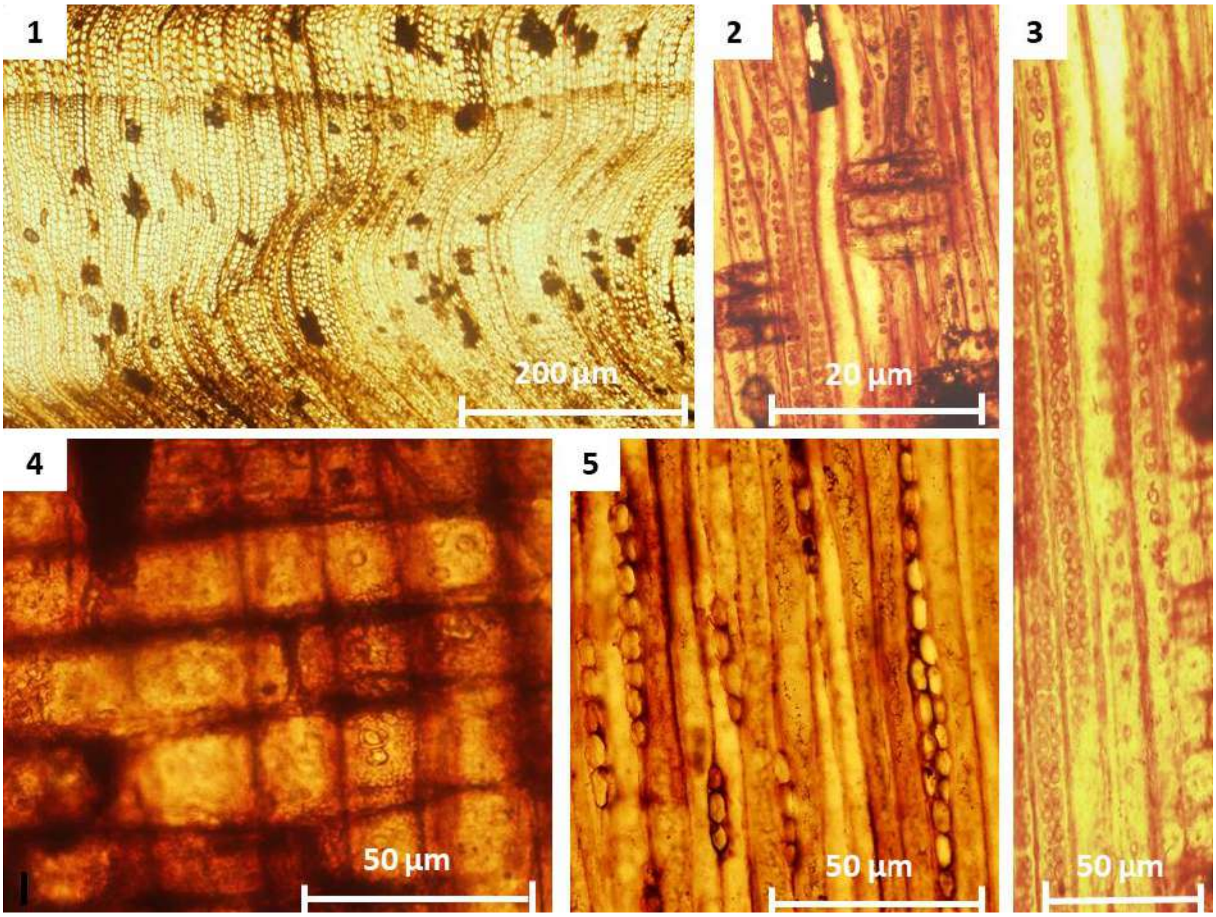

Fig. 10. 1. The transverse section shows slightly rounded to square and distorted pits (S-shaped), which is typical of Karoo woods, 2. Clusters of pits characteristics of *Australoxylon teixeirae*, 3. Alternate and opposite tracheids typical of *A. teixeirae* (Late Permian wood), 4. Radial longitudinal section (RLS) showing some pits in the cross-fields, 5. Well-preserved tangential section showing uniseriate to occasional biseriate rays pertaining to Late Permian *A. teixeirae*.

4.4 Correlations with Gondwana sections

Correlations with well-known biozones across Gondwana were done to establish the age of the Maniamba Basin cores (Table 1). Nevertheless, based on previous reports, intra- and inter-basinal correlations with closer affinity to the Maniamba Basin were selected. These include the Moatize-Minjova Basin, Mozambique (Pereira et al., 2016), Sakamena Group, Madagascar (Wright and Askin, 1987), Mid-Zambezi Valley, Zambia (Nyambe and Utting, 1997), Main Karoo Basin, South Africa (Steiner et al., 2003; Barbolini, 2014), Salt Range, Pakistan (Balme, 1970) and the Raniganj-Kamthi Formation (Godavari Basin), India (Jha et al., 2011; Jha and Aggarwal, 2012). Other stratigraphic sequences across Gondwana, that are diachronous with the Maniamba Basin, were not considered herein (South America and Australia). Therefore, the distribution of the key taxa from the target geological period is summarised below:

a) Moatize-Minjova Basin-Mozambique

Here, the Upper Permian strata are characterised by the common abundant occurrence of *Protohaploxypinus* spp., *Striatopodocarpites* spp., *Alisporites* spp., common *Guttulapollenites* and *Weylandites*, stratigraphical significant taxa include *Falcisporites*, *Krauselipollenites*, *Lueckisporites*, *Osmundacidites*, *Polipodiisporites*, etc. Early Triassic forms include *Lunatisporites pellucidus*, *Indospora clara*, *Lundbladispora sp*., *P. microcorpus*, *P. pantii* and *Guttulapollenites hannonicus*. The Karoo Moatize-Minjova Basin identified by Pereira et al. (2016), shows close affinity with the Karoo equivalent Maniamba Basin.

b) Mid Zambezi Valley-Zambia

According to Nyambe and Utting (1997), the Upper Permian marker taxa consist of *Protohaploxypinus limpidus*, *Protohaploxypinus goraiensis*, *Striatopodocarpites* spp., *Weylandites lucifer*, *Guttulapollenites hannonicus*, *Protohaploxypinus mutabilis*. In contrast, taxa such as *Platysaccus queenslandii*, *Verrucosisporites* sp., *Falcisporites stabilis*, *Alisporites* sp. and *Sulcatisporites* sp., characterize the Early Triassic. The Permian palynoassemblages studied by Nyambe and Utting (1997) in the Mid Zambezi Valley, Zambia including a few occurrences in the Lower Triassic resemble the flora described in this paper.

c) Katberg and Balfour Formations (Main Karoo Basin)-South Africa

In the Main Karoo Basin (MKB), several studies have been carried out aiming at refining the palynostratigraphy (Steiner et al., 2003; Gastaldo and Rolerson, 2008; Prevec et al., 2010; Barbolini, 2014). The Upper Permian strata are characterised by different species of *Protohaploxypinus* and *Falcisporites* combined with *Playfordiaspora crenulata* and *Triplexisporites playfordii*. In contrast, spores such as *Krauselisporites* spp., *Lundbladispora* spp., *Lunatisporites* spp., and *L. pellucidus* characterise the Early Triassic as suggested by Steiner et al. (2003). Prevec et al. (2010) described the late Permian palynoflora from the Southern Karoo Basin (Normandien Formation). The overlying Katberg Formation has been indicated as portraying the post-end Permian mass extinction (Smith and Botha, 2014; Botha et al., 2020; Gastaldo and Bamford, 2023), but with different interpretations. Nevertheless, the late Permian palynoflora from the Normandien Formation is characterised by abundant *Protohaploxypinus* and *Striatopodocarpites* combined with moderate *Lunatisporites* spp., *Falcisporites* and non-abundant spores. Further, another late Permian section from the Palingkloof Member of the Balfour Formation (uppermost Permian), yielded *Cycadopites cymbatus*, *Granulatisporites convexus*, *Marsupipollenites triradiatus*, *Plicatipollenites gondwanensis*, *Playfordiaspora crenulata*, *Protohaploxypinus limpidus* and *Vittatina fasciolata* (Barbolini et al., 2018). The Early Triassic taxa were retrieved from the overlying Katberg Formation include *Tripunatisporites maastrichtiensis* and *Aratrisporites tenuispinosus* (Barbolini et al., 2018). The Maniamba Basin resembles the late Permian-Early Triassic palynoassemblages described by Steiner et al. (2003) and Prevec et al. (2010). However, it differs from the Early Triassic palynoassemblages identified by Barbolini et al. (2018).

d) Sakamena Group-Madagascar

The well-established Permian palynoassemblages in Madagascar are known from the Lower and Mid Sakamena Group (Wright and Askin, 1987). The late Permian palynoassemblages are characterised by the abundant occurrence of *Weylandites* spp., *Guttulapollenites hannonicus*, *Protohaploxypinus* spp., *Striatopodocarpites* spp. and *Lueckisporites virkkiae*. Here, *P. microcorpus* occurs commonly. Another common occurrence includes *Falcisporites* spp., *Klausipollenites schaubergerii*, and *Platysaccus* spp. Here, the Early Triassic age is marked by common to abundant occurrence of relevant taxa that includes *Guttulapollenites hannonicus*, *Lundbladispora* spp., *Lunatisporites pellucidus*, *Protohaploxypinus microcorpus* and *Striatopodocarpites pantii*. These occurrences are combined with the first appearance datum of the Triassic marker, *Triplexisporites playfordii*. The Sakamena Group is characterised by non-striate and striate bisaccate pollen listed above that are also found in the Maniamba Basin.

e) Raniganj-Panchet Formations-India

According to Srivastava and Jha (1990) and Jha (2006) the late Permian palynoassemblages are characterised by an abundance of *Protohaploxypinus* spp., *Striatopodocarpites spp*., and *Faunipollenites spp*. Other common taxa include *Osmundacidites* sp., *Weylandites* spp., *Horriditriletes* spp., *Lophotriletes* spp., *Densipollenites magnicorpus*, *Playfordiapora crenulata*. Early Triassic abundant taxa include *Lunatisporites pellucidus*, *Densoisporites spp*., *Lundbladispora* spp., *Verrucosisporites* spp., *Alisporites* spp., *Klausipollenites schaubergerii*, and *T. playfordii* (Jha et al., 2011; Jha and Aggarwal, 2012). Typical Triassic taxa such as *Triplexisporites playfordii*, *Densoisporites spp*. and *K. schaubergeri* present in the Godavari basin in India, were not observed in the studied material from the Maniamba Basin, even though there are several other common occurrences between the two basins.

f) Salt Range Basin-Pakistan

The late Permian palynoassemblages for the Salt Range comprise the occurrence of dominant *Guttulapollenites hannonicus*, *Lueckisporites* spp., *Protohaploxypinus* spp., *Weylandites lucifer*, *Alisporites* spp., *Striatopodocarpites* spp., *Klausipollenites schaubergerii* and *Krauselisporites* spp. In contrast, the Early Triassic taxa include the abundance of *Lundbladispora obsoleta*, *Densoisporites playfordii*, and *L. brevicula*. Yet, *Guttulapollenites hannonicus* and *Lunatisporites* are commonly present. Aside from *Alisporites* spp., the dominance of striate bisaccates and similarities in the palynoassemblages in having many common palynotaxa depict a close similarity between Salt Range palynoassemblages with those from the Maniamba Basin.

Table 1 Permian–Triassic Gondwana sequences with closer affinity to the Maniamba Basin adapted from Pereira et al., 2016.

Period	Stage	**Madagascar** (Sakamena Group) (Wright and Askin, 1987)	**Pakistan (Salt Range)** (Balme, 1979; Hermann et al., 2012)	**Zambia** (Mid-Zambezi Valley) (Nyambe and Utting, 1997), Barbolini et al., 2016)	**India** (Raniganj and Panchet Fm.) (India) (Jha et al., 2011, Jha and Aggarwal, 2012)	**South Africa** (Katberg and Balfour Fm.) (Steiner, 2003, Prevec et al., 2010, Barbolini, 2018,)	**Mozambique** (Moatize Minjova Basin) (Pereira et al., 2016)	**Mozambique** (Maniamba Basin) (This study) JOG16N-6 and JOG16N 8 boreholes
Triassic	Olenekian Induan	Common Guttulapollenites. hannonicus, Lundbladispora spp., Lunatisporites pellucidus, Densoisporites playfordii, P. crenulate, T. playfordii.	Densoisporites playfordii, Lundbladispora brevicula, L. obsoleta, common,Uvaesporites spp., Lunatisporites pellucidus, L. noviaulensis and Guttulapollenites hannonicus	Falcisporites stabilis, Platysaccus queenslandii, L. pellucidus, Calamospora sp., Verurucosisporites sp., P. cancellata, Apiculatisporis sp.	Protohaploxypinus spp., Striatopodocarpites spp., Faunipollenites spp., common Osmundacidites sp., Weylandites spp., Hoditriletes spp., P. crenulata	Krauselisporites spp., Lundbladispora spp., Lunatisporites spp., Lunatisporites pellucidus, Tripunatisporites maastrichtiensis and Anatrisporites tenuispininosus	Lunatisporites pellucidus, Indospora clara, Lundbladispora spp., Triquitrites sp., P. microcorpus, P. pantii, Guttulapollenites hannonicus	Platysaccus papilonis, Lunatisporites spp., Verrucosisporites spp., Lundbladispora spp., Krauselisporites sp.
Permian	Changhsingian Wuchiapingian	Protohaploxypinus spp., Striadopodocarpites spp., Alisporites spp., P. microcorpus, G. hannonicus, Weylandites spp., L. virkkae, Falcisporites spp., Krauselisporites spp and rare L. pellucidus	Alisporites spp., G. hannonicus, Kraeuselisporites spp., K. wargalensis, Klausipollenites schaubergeri,Lueckisporites spp., Playfordiaspora sp., Protohaploxypinus spp.,Striatopodocarpites and Welandites lucifer	Protohaploxypinus limpidus, P. goraiensis, Striatopodocarpites spp., Guttulapollenites hannonicus, W. lucifer, Corisaccites alutas, Reticuloidosporites warchianus, Polypodiisporites mutabilis	Lunatisporites. pellucidus, Densoisporites spp., Lundbladispora spp., Verrucosisporites spp., Krausepollenites schaubergerii, Triplexisporites playfordii	Cycadopites cymbatus, Granulatisporites convexus, Marsupipollenites triradiatus, Plicatipollenites gondwanensis, Playfordiaspora crenulata, Protohaploxypinus limpidus and Vittatina fasciolata	Protohaploxypinus spp., Striatopodocarpites spp., Alisporites spp., common Guttulapollenites. hannonicus, Weylandites. Key taxa: Corisaccites, Falcisporites, Krauselisporites. Lueckisporites, Osmundacidites.	Protohaploxypinus spp., Striatopodocarpites spp., Guttulapollenites. hannonicus, Corisaccites alutas, Scheuringipollenites spp., Cycadopites cymbatus, Laevigatosporites spp, Plicatipollenites gondwanensis

5. Discussion

A detailed palynological combined with palaeobotany (fossil wood) work was undertaken in the present work. The occurrence of fossil wood taxa (Figs. 9 and 10), according to Bamford et al. (2020), suggests humid and warm periods in the Maniamba Basin during the Lopingian. Moreover, the predominance of rich and carbonaceous sediments in palynoassemblages 1 and 2 in fluvial-lacustrine environments indicates dense vegetation characterised by warm dry alternating with warm and humid periods, which were responsible for the deposition of vast coal beds during the Lopingian in an alluvial environment. Additionally, red-coloured sandstones are observed in the K5 Formation which can be linked to arid or semi-arid environments. These are also supported by the occurrence of concretions of calcilutite in the K5 Formation (Verniers et al., 1989). Based on the botanical affinity the high predominance of Glossopteridales with moderate contributions of Cordaitales, Coniferales and spores along the sequences represents a warm and humid climate characteristic of continental ecosystems across Gondwana (Guerra-Sommer et al., 1983; Lindström and McLoughlin, 2007; Aggarwal et al., 2019). Ongoing research based on the whole-rock geochemistry of major oxides SiO_2 versus Al_2O_3+K_2O+Na_2O pertaining to the samples from the top of the studied sequence suggests semi-arid climate conditions (Nhamutole et al., *in press*). The upper part of the sequence contains several taxa that have not been identified. If these unidentified taxa are combined with known Lower Triassic palynotaxa, the emergence of these new taxa could be interpreted as the phase of recovery for the flora following the end-Permian Mass Triassic Event (EPME). Nevertheless, the scarcity or existing barren zones in both borehole cores hinder recognising reliable floral trends that could provide us with more inputs regarding the EPME as reported in some coeval Gondwana sequences. Thus, this inference must be made with caution (Fig. 11).

Although a change in palynoflora is not recognised, the lithofacies along the studied sections indicate a shift from a complex dominated by sandstones and rich organic units at the bottom and the middle of the sequences to reddish claystone and sandstone units at the top of the sequence suggesting changes of the drainage system. Similar patterns regarding the changes in the drainage system are observed across the PT boundary in most Gondwana sequences. Additionally, from the studied material we observed a transgression of dominant striate and non-striate bisaccate forms from the bottom to the top of both studied sequences (Fig. 11). Similar patterns have already been observed in the earliest studies of the Permo-Triassic boundary between the Upper Raniganj and the overlying Panchet Formations in India as reported by Bharadwaj et al. (1979). Thus, only more comprehensive and wide-range sampling of the latest Permian floras in the Maniamba Basin, integrated with detailed taphonomic, molecular fossils (biomarkers), stable carbon isotopes curves, and lithostratigraphic data, can provide a more refined evaluation of the floral changes and more robust palaeoclimate inferences.

The palynofloral remains in the sediments from both borehole cores are reported to have been deposited in proximal settings under oxic, dysoxic and anoxic conditions based on the percentage of the bulk organic matter which includes dark woody material (opaque phytoclasts), brown woody material including cuticles and amorphous organic matter (Nhamutole et al., 2023). Recent palynofacies analysis undertaken in the Maniamba Basin has revealed the same paleoredox conditions, based on the ratios of the major elements, biomarkers including the isoprenoid Pristane and Phytane ratios, steranes, and terpanes.

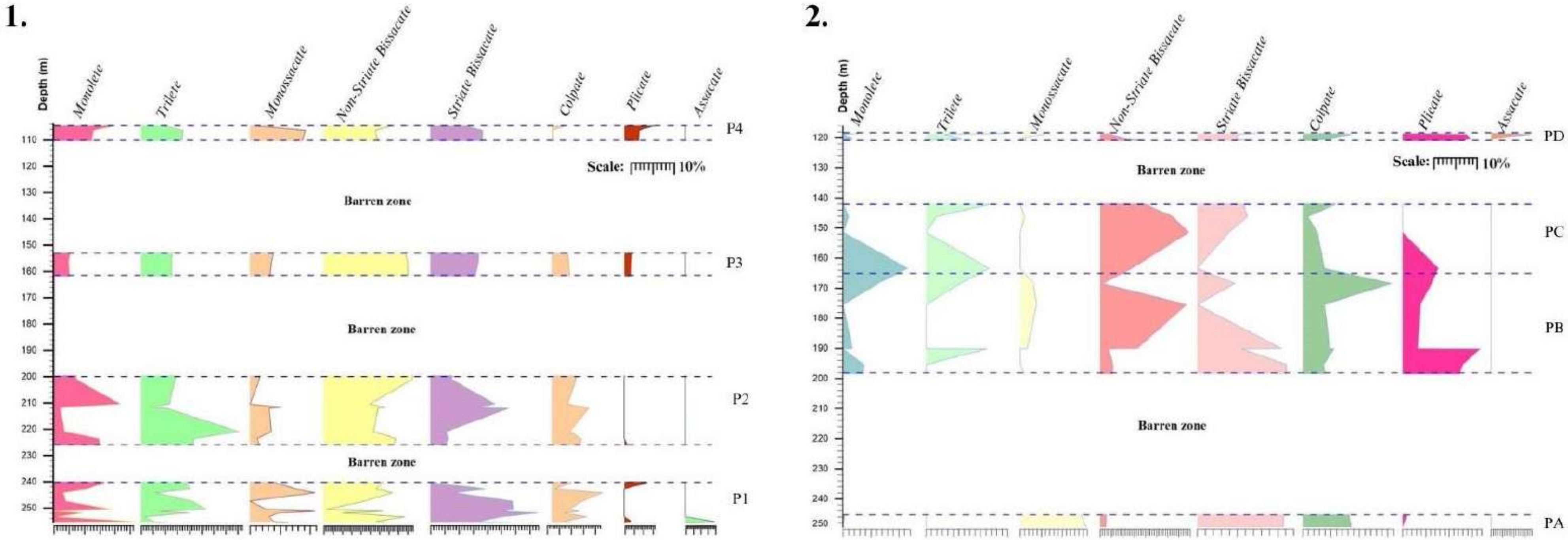

Fig. 11. Relative abundance of sporomorphs through the studied sequences. 1. JOG16N-6 borehole core 2. JOG16N-8 borehole core.

6. Conclusions

Drawing from the stratigraphic distribution of palynomorphs obtained from core samples taken from boreholes JOG16N-6 and JOG16N-8 in the Maniamba Basin, the following conclusions can be made regarding the K5 Formation:

1. The palynological study has revealed the presence of four distinct palynoassemblages for both borehole cores (palynoassemblages P1, P2, P3, and P4). The palynoassemblages yield abundant striate and non-striate bisaccate pollens coupled with ferns, sphenophytes and lycophytes, suggesting of thick arborescent palaeovegetation in the depositional settings. Warm and humid periods are inferred at the bottom of the sequence (P1 and P2 assemblages), with a shift to semi-arid and arid conditions inferred for the upper part of the studied sequence.
2. Palynoassemblages 1 and 2, are assigned to the latest Permian. In contrast, palynoassemblages 3 and 4 are attributed to the Early Triassic. This distinction arises from their closer connection to well-established Gondwana sequences due to the well-established correlation of these assemblages, to well-established Gondwana sequences, including the Moatize-Minjova Basin in Mozambique, Sakamena Group in Madagascar, the Raniganj-Kamthi Formation in India, Mid-Zambezi Valley in Zambia, the Salt Range in Pakistan, and the Balfour and Normandien Formations in South Africa. The other Gondwana sections depict dissimilarities due to the presence of endemic forms. It is important to stress that the presence of significant stratigraphical fossil wood species strongly corroborates the determined age.
3. The palynological age of the K5 presents a younger age than previously reported by Verniers et al. (1989). However, the studied flora is not typically Triassic since some Permian elements remain.
4. The Permian-Triassic boundary is cautiously interpreted in both borehole sections due to palynological barren zones, which complicate the tracking of vegetation changes. Therefore, alternative tools are necessary to gain a clear understanding.

References

Aggarwal, N., Agrawal, S., Thaku, B., 2019. Palynofloral, palynofacies and carbon isotope of Permian coal deposits from the Godavari Valley Coalfield, South India: Insights into the age, palaeovegetation and palaeoclimate. Inter. J. Coal Geol. https://doi.org/10.1016/j.coal.2019.103285.

Bamford, M., 1999. Permo-Triassic Fossil Woods from the South African Karoo Basin. Palaeont. afr. 35, 25-40.

Bamford, M.K., Philippe, M., 2001. Jurassic-Early Cretaceous Gondwanan homoxylous woods: a nomenclature revision of the genera with taxonomic notes. Rev. Palaeobot. Palynol. 113, 287-297.

Bamford, M.K., Cairncross, B., Lombard, H., 2020. Silicified fossil woods from the Late Permian Middleton Formation, Beaufort Group, Eastern Cape Province, South Africa and their paleoenvironmental significance. S. Afr. J. Geol. 123, 465-478.

Balme, B.E., 1970. Palynology of Permian and Triassic strata in the Salt Range and Surghar Range, West Pakistan. In: Kummel, B., Teichert, C. (Eds.), Stratigraphic Boundary Problems: Permian and Triassic of West Pakistan. The University Press of Kansas, Lawrence, KS, pp. 305–453.

Barbolini, N., 2014. Palynostratigraphy of the South African Karoo Supergroup and correlations with coeval Gondwanan successions. Unpublished PhD Thesis, University of the Witwatersrand (386 pp).

Barbolini, N., Bamford, M., 2014. Palynology of an Early Permian coal seam from the Karoo Supergroup of Botswana. J. Afr. Earth Sci. 100, 136-144.

Barbolini, N., Rubidge, B., Bamford, M.K., 2018. A new approach to biostratigraphy in the Karoo retroarc foreland system: Utilising restricted-range palynomorphs and their first appearance datums for correlation. J. Afr. Earth Sci. 140, 114–133

Botha, J., Huttenlocker, A.K., Smith, R.M.H., Prevec, R., Viglietti, P., Modesto, S.P.,2020. New geochemical and palaeontological data from the Permian-Triassic boundary in the South African Karoo Basin test the synchronicity of terrestrial and marine extinctions. Palaeogeogr. Palaeoclimatol. Palaeoecol. 540, 109467.

Bharadwaj, D., Tiwari, R., Prakash, A., 1979. Permo-Triassic Palynostratigraphy and lithological characteristics in Damodar Basin, India. Biological Memoir, 4,49-82.

Crisafulli, A., 2002. Contribución a la paleoxilología de la Formación Yaguarí, Pérmico Superior de Uruguay. Rev. Museo Argentino Ci. Nat. 4, 45-54.

Castanhinha, R., Araújo, R., Junior, L.C., Angielczyk, K.D., Martins, G.G., Martins, R.M. S., Chaouiya, C., Beckman, F., Wilde, F., 2013. Bringing Dicynodonts back to life: palaeobiology and anatomy of a new Emydopoid genus from the upper Permian of Mozambique. PLoS One 8 (12), e80974.

Falcon, R., 1975. Palyno-stratigraphy of the Lower Karroo sequence in the central Sebungwe District, Mid-Zambezi Basin, Rhodesia. Palaeontol. afr. 18, 1–29.

Fernandes, P., Hancox, P., Mendes, M., Pereira, Z., Lopes, G., Marques, J., Jorge, R., Albardeiro, L. 2023. The age and depositional environments of the lower Karoo Moatize Coalfield of Mozambique: insights into the postglacial history of central Gondwana. Palaeoworld, 33, 979–996.

Fernandes, P., Cogné, N., Chew, D., Rodrigues, B., Jorge, R.C.G.S., Marques, J., Jamal, D., Vasconcelos, L., 2015. The thermal history of the Karoo Moatize-Minjova Basin, Tete Province, Mozambique: An integrated vitrinite reflectance and apatite fission track thermochronology study. J.Afr. Earth Sci. 112, 55-72.

Galasso, F., Pereira, Z., Fernandes, P., Spina, A., Marques, J., 2019. First record of Permo-Triassic palynomorphs of the N'Condédzi sub-basin, Moatize-Minjova Coal Basin, Karoo Supergroup, Mozambique. Revue de Micropaléontologie. 64, 100357.

Gastaldo, R.A., Bamford, M.K., 2023. The influence of taphonomy and time on the paleobotanical record of the Permian–Triassic transition of the Karoo Basin (and elsewhere). Journal of African Earth Sciences 204, 1-24. JOAES-S-22-01322

Gastaldo, R.A., Rolerson, M.W., 2008. Katbergia *gen. nov*., a new trace fossil from the Late Permian and Early Triassic of the Karoo Basin: Implications for paleoenvironmental conditions at the P/Tr extinction event. Palaeont. 51, 215–229.

Gotz, A.E., Hancox, P.J., Lloyd, A., 2017. Permian climate change recorded in palynomorph assemblages of Mozambique (Moatize Basin, eastern Tete Province). Acta Palaeobotanica 57, 3–11.

Guerra-Sommer, M., Marques-Toigo, M., Paim, P.S.G., Henz, G.I., Skilveira, J.B.R. and Backeuser., Y. 1983. Estudomicoflorístico e petrológico dos carvões da Mina do Faxinal, Formação Rio Bonito (Permiano). Série Científica, 15, 73-83.

Jha, N., 2006. Permian Palynology from India and Africa: A phytogeographic paradigm. J. Palaeontol. Soc. India 51, 43–55.

Jha, N., Pauline, S.K., Mehrotra, N.C., 2011. Early Triassic palynomorphs from Manuguru area of Godavari Graben, Andhra Pradesh, India. J. Geol. Soc. India 78, 167–174.

Jha, N., Aggarwal, N., 2012. Permian–Triassic palynostratigraphy in Mailaram area, Godavari Graben, Andhra Pradesh, India. J. Earth Syst. Sci. 121, 1257–1285.

Lindstrom, ¨ S., McLoughlin, S., 2007. Synchronous palynofloristic extinction and recovery after the end-Permian event in the Prince Charles Mountains, Antarctica: implications for palynofloristic turnover across Gondwana. Rev. Palaeobot. Palynol. 145, 89–122.

Lopes, G., Pereira, Z., Fernandes, P., Marques, J., 2014. Datação Palinológica dos Sedimentos Glaciogénicos da Formação (Tilítica) de Vúzi, sondagem ETA 65, Bacia Carbonífera de Moatize–Minjova, Moçambique—Resultados Preliminares. Actas do IX Congresso Nacional de Geologia. 2º Congresso de Geologia dos Países de Língua Portuguesa, Porto, Portugal, p. 7.

Mahabeer, K.C., 2017. Palynology of the Permian Sanangoé-Mefidezi Coal Basin, Tete Province, Mozambique and correlations with Gondwanan microfloral assemblages. MSc thesis, University of Witwatersrand, Johannesburg, South Africa, 168 pp.

Moore, P.D., Webb, J.A., Collinson, M.E., 1991. Pollen Analysis. Blackwell Scientific Publications.

Nhamutole, N.E., Bamford, M.K., Araújo, R., 2021. New species of *Protaxodioxylon* (conifer wood) from the middle permian of the Metangula graben (Niassa province, Mozambique) and their implications. J. Afr. Earth Sci. 183, 104323.

Nhamutole N, Bamford M, Souza P, Do Carmo D (2023) Palynofacies analysis of the JOG16N-8 borehole, K5 formation from the Maniamba Basin (middle Permian), Mozambique: A contribution for hydrocarbon exploration. J. Afr. Earth Sci. 205(2):104997. https://doi.org/10.1016/j.jafrearsci.2023.104997.

Norconsult, C., 2007. Notícia explicativa das áreas de Niassa, Cabo Delgado e partes de Zambézia e Nampula. Maputo, Moçambique: Direcção Nacional de Geologia. Unpublished report.

Nyambe, I.A., Utting, J., 1997. Stratigraphy and palynostratigraphy, Karoo Supergroup (Permian and Triassic), mid-Zambesi Valley, southern Zambia. J. Afr. Earth Sci. 24, 563–583.

Pradhan, S., Goswami, S., Aggarwal, N., Mathews, R., Manoj, M., Suresh, S., Pillai, K., 2023. Integrative study of Permian coal-bearing horizons: biostratigraphy, palaeovegetation, and paleoclimate in the South Karanpura Basin. Environ. Geochem. Health. https://doi.org/10.1007/s10653-023-01701-w.

Pereira, Z., Fernandes, P., Lopes, G., Marques, J., Vasconcelos, L., 2016. The Permian– 685 Triassic transition in the Moatize–Minjova Basin, Karoo Supergroup, Mozambique: A 686 palynological perspective. Rev. Palaeob. and Palynol. 226, 1–19.

Pereira, Z., Fernandes, P., Lopes, G., Marques, J., Vaz, M., Costa, M., Correia, J., Castro, L., Galasso, F., 2019. Palynology of the Muara´dzi sub-basin, Moatize-Minjova Coal Basin, Karoo Supergroup, Mozambique. Rev. Palaeob. Palynol. 269, 78–93.

Prasad, M., 1982. An annotated synopsis of Indian Palaeozoic gymnospermous woods. Rev Palaeobot. Palynol. 38,119–156

Prevec, R., Gastaldo, R.A., Neveling, J., Reid, S.B., Looy, C.V., 2010. An autochthonous glossopterid flora with latest Permian palynomorphs and its depositional setting in the Dicynodon Assemblage Zone of the southern Karoo Basin, South Africa. Palaeogeogr. Palaeoclimatol. Palaeoecol. 292, 391–408.

Souza, P.A., 2003. New palynological data of the Itararé Subgroup from the Buri Coal (Late Carboniferous, Paraná Basin), São Paulo State, Brazil. Revista Brasileira de Paleontologia 5, 49–58.

Souza, P.A., Marques-Toigo, M., 2005. Progress on the palynostratigraphy of the Permian strata in Rio Grande do Sul State, Paraná Basin, Brazil. An. Acad. Bras. Ci. 77, 353–365.

Souza, P. A., Amaral, P. G.., Bernardes de Oliveira, M., 2006. A Late carboniferous palynoflora from the Itararé Subgroup (Paraná Basin) in Campinas, São Paulo State, Brazil. Rev. Micropaléont. 49, 105–115.

Smith, R.H.M., and Botha-Brink, J., 2014, Anatomy of a mass extinction: Sedimentological and taphonomic evidence for drought-induced die-offs at the Permo-Triassic boundary in the main Karoo Basin, South Africa.

Srivastava, S.C., Jha, N., 1990. Permian–Triassic palynofloral transition in Godavari Graben, Andra Pradesh. Palaeobotanist 38, 92–97.

Steiner, M.B., Eshet, Y., Rampino, M.R., Schwindt, D.M., 2003. Fungal abundance spike and the Permian–Triassic boundary in the Karoo Supergroup (South Africa). Palaeogeogr. Palaeoclimatol. Palaeoecol. 194, 405–414.

Stephenson, M.H., 2008. A review of the palynostratigraphy of Gondwanan Late 718 Carboniferous to Early Permian glacigene successions. Geol. Soc. Amer. 441, 317–330.

Traverse, A., 2007. Paleopalynology, Second Edition (Topics in Geobiology 28). Springer, Netherlands, Dordrecht.

Verniers, J., Jourdan, P.P., Paulis, R.V., Frasca-Spada, L., De Bock, F.R., 1989. The Karroo graben of Metangula northern Mozambique. J. Afr. Earth Sci. 9, 137–158.

Wright, R.P., Askin, R.A., 1987. The Permian–Triassic boundary in the southern Morondava basin of Madagascar as defined by plant microfossils. In: McKenzie, G.D. (Ed.), Gondwana Six: Stratigraphy, Sedimentology, and Paleontology. Geophysical Monograph Series, Washington, pp. 157–166.

New palynological data from Maniamba Basin, Mozambique (Karoo): correlations and implications for Lopingian floristic ecosystem reconstruction.

Adapted from Nhamutole, N, Bamford, M.K, Souza, P. A, Félix, C.M, Carmo, D.A, Aldevina, Z, Bande, P.

Published by Review of Palaeobotany and Palynology

Review of Palaeobotany and Palynology 336 (2025) 105310

Contents lists available at ScienceDirect

Review of Palaeobotany and Palynology

journal homepage: www.elsevier.com/locate/revpalbo

New palynological data from Maniamba Basin, Mozambique (Karoo): Correlations and implications for Lopingian floristic ecosystem reconstruction

Nhamutole Nelson [a,b,*], M. Bamford [a], P.A. Souza [c], C.M. Félix [c], D.A. Carmo [d], A. Zimba [e], P. Bande [a]

[a] Evolutionary Studies Institute and School of Geosciences, University of the Witwatersrand, P Bag 3, Wits, 2050 Johannesburg, South Africa
[b] Ministry of Mineral Resources and Energy, Av. 24 de Julho, 355, Maputo, Mozambique
[c] Palinology Laboratory Marleni Marques-Toigo, Geosciences Institute, UFRGS, Brazil
[d] Micropaleontology Laboratory, University of Brasília, Brasília, DF, Brazil
[e] Eduardo Mondlane University, Departamento de Geologia, Av. Moçambique, Km 1.2, Maputo, Mozambique

Abstract

Two borehole cores (JOG16N-5 and JOG16N-7) from the Maniamba Basin, northern Mozambique (central Gondwana) were studied for palynology. As a result, five palynoassemblages were identified from JOG16N-5 (T1, T2, T3, T4, T5) whereas only three were identified for the latter borehole (B1, B2 and B3). Palynoasssemblages T1, B1, B2, B3 were assigned to Wuchiapingian whereas the assemblages T2, T2, T3, T4 and T5 were are assigned to Changhsingian.

The age was assigned based on the common occurrence of Lopingian taxa (e.g., *Guttulapollenites*, *Alisporites*, *Weylandites*, *Cycadopites*, *Marsupipollenites, Scheuringipollenites, Protohaploxypinus,* and *Striatopodocarpites*) taxa together with abundant occurrence of stratigraphically important taxa, *Thymospora pseudothiessenii* as well as *Osmundacidites senectus.* Typical Gondwana vegetation is observed in both cores and is characterized by dominance of pollen grains assigned to the *Protohaploxypinus* and *Striatopodocarpites* whereas the monosaccate pollen indicators of upland vegetation are rare. Palynomorph indicators of a lowland setting

are common and include gingkoales, ferns (Filicopsida), sphenopsids, and lycopsids that can be interpreted as the existence of a vast lowland fluvial setting together with floodplains and wetlands in the Basin. Yet, variations in lithofacies indicate a change in the dynamic of the drainage system that prevailed during the Lopingian in the Maniamba Basin. Furthermore, similar palynoevents in Lopingian northern Karoo-aged basins of south-central Africa, and central Gondwana basins from Madagascar, India, and Antarctica are well correlated. However, in contrast, some distinct Lopingian palynoevents are observed with southern Karoo-aged basins which could suggest the existence of tectonic barriers that prevented floral exchange thus, confirming intra-Gondwanan floristic provincialism.

1. Introduction

The Mozambican Karoo basins contain some of the most exploited coal deposits in Gondwana, and are assumed to have been deposited during the Permian period [Cisuralian (298.9-273.1mya), Guadalupian (273.1-259.1mya), Lopingian (259.1-251.9mya)]. During this period there is strong evidence of a flourishing ecosystem comprising several plant groups viz., glossopterids, conifers, cycads, ginkgos and others. For instance, during the Lopingian ca. 60% of the worldwide flora consisted of seed plants (Gradstein and Kerp, 2012). Surprisingly, during the late Permian a mass extinction seems to have affected the fauna diversity more adversely than the plant groups as whole, except for some extinctions in the conifers that includes glossopterids and cordaites (Gradstein and Kerp, 2012). Most of the aforementioned conclusions were obtained through the use of palynology analysis with macroplant records playing a lesser role. Palynology can provide pivotal information regarding a chronological framework of continental stratigraphic sections, tectono-stratigraphy, and Basin evolution (Pereira et al., 2016; Barbolini et al., 2018; Gotz et al., 2018; Galasso et al., 2019; Lopes et al., 2021b; Fernandes et al., 2023), as well as the composition of ancient ecosystems, mainly regarding floristic biomes. In the present study, a palynological analysis in the Maniamba Basin is presented. This basin is located in northern Mozambique and is one of the Mozambican basins containing coal seams (Vasconcelos, 2009; Vasconcelos and Achimo, 2010). Here, the majority of studies have focused on the commercial evaluation of coal deposits (Vale Moçambique, 2014; JOGMEC, 2015). Few studies have focused in the stratigraphy of this Basin (Verniers et al., 1989; Norconsult, 2007). However, a recent palynological study helped to identify for the first time the Permian-Triassic transition in the Basin (Nhamutole et al., 2024a). Nevertheless, in the present work a palynological composition in two Permian successions drilled for coal exploration in the Maniamba Basin is analysed. The objective of this work is to identify palynostratigraphic succession with the help of retrieved sporomorphs and to place them into the existing Karoo sequences as well as into Gondwana paleogeographic provinces in order to supplement palaeoenvironment interpretations.

2. Geology and stratigraphy of the Maniamba Basin

Please see section 5.1 for details regarding the geology of the Maniamba Basin.

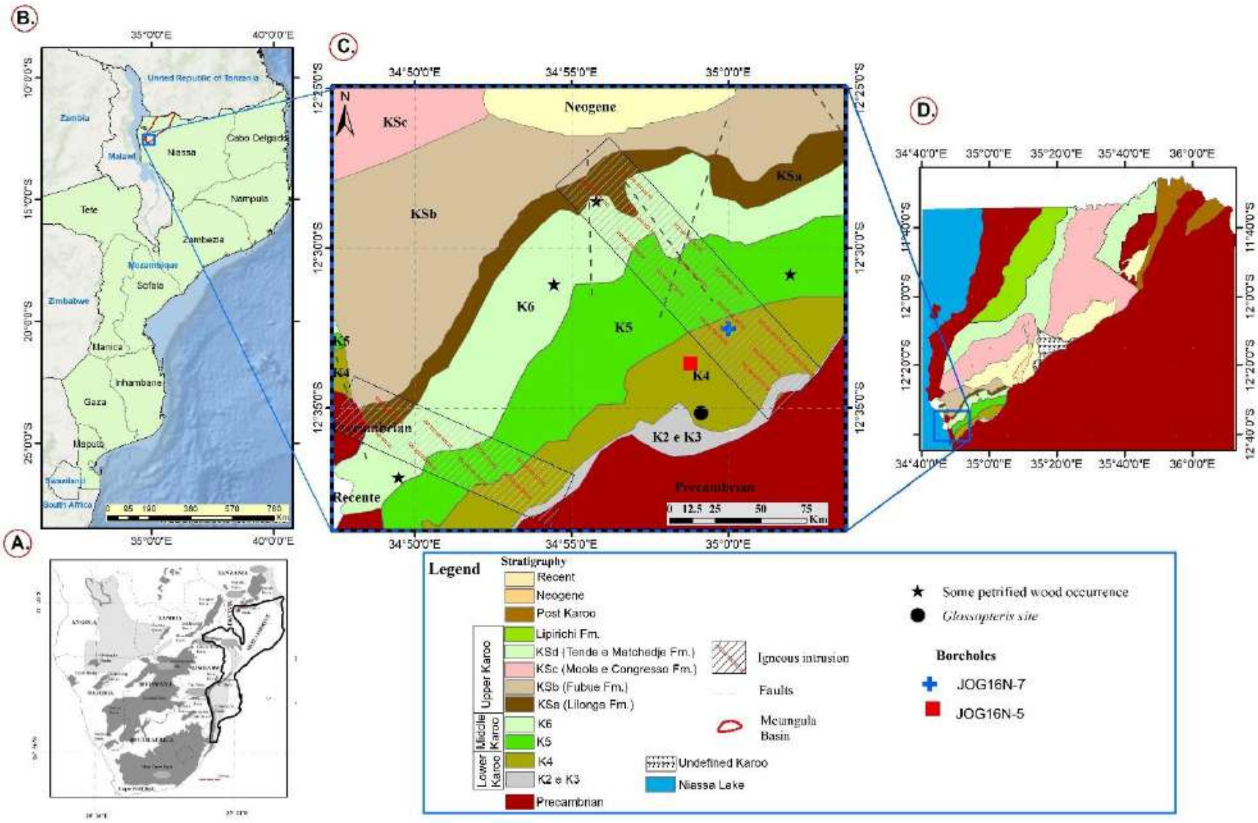

Fig. 1. A. Southern Africa map illustrating the location of Mozambique, B. Map of Mozambique showing the location of the Maniamba Basin (Niassa), C and D. Geology and stratigraphy of the Maniamba Basin (modified from Verniers et at., 1989).

3. Material and methods

Seventeen (17) samples were taken from borehole JOG16N-5 (*ca*. 220 m), but only fourteen (14) proved to be productive for palynomorphs (Fig. 2). Fifteen (15) samples were subsampled in the JOG16N-7 core (*ca*. 279 m) out of which nine (9) samples proved to be productive for palynological analysis. The collected samples in both cores were prepared using standard palynological extraction methods adapted from Phipps and Playford (1984) and Traverse (2007). The description of the standard palynological procedures is included in the section 6.2.

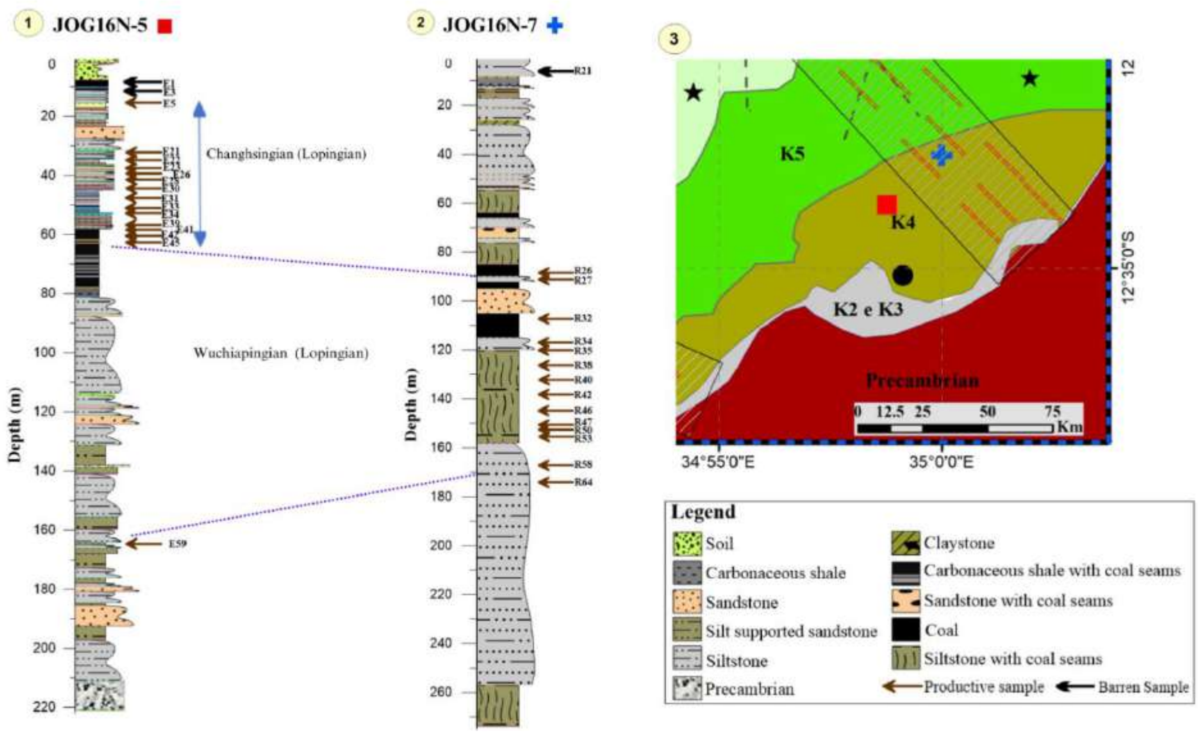

Fig. 2. 1 and 2. Lithological log of JOG16N-5 and JOG16N-7 cores showing sampling points (productive and barren) and correlatable sections based on palynoassemblages associations, 3. Detailed geologic section showing the two cores (modified from Verniers et al., 1989).

4. Results

4.1. Lithological description

4.1.1. Borehole JOG16N-5

The JOG16N-5 core depict has a total depth of *ca.* 220 m (Fig. 2). Its deepest section is made up of Precambrian basement that includes diolite rocks that are found from

203 m downwards. From 203 to 80 m the sequence is dominated by dark grey, reddish brown partly laminated siltstone. The siltstone section is intercalated by very fine-coarse sandstone, dark grey greenish grey, laminated with carbonaceous siltstone (190-160m). From 160 to 80 m the section is dominated by reddish brown, massive together with greenish grey sandstone. Lastly, four coal seams are observed from 80 m upwards. The first coal seam displays a thickness greater than 20 m. The coal seams are intercalated by dark grey, massive, siltstone with minor coal lenses. The uppermost unit consist of brownish grey, massive unit with medium and very coarse sandstones.

4.1.2. Borehole JOG16N-7

The JOG16N-7 core has a total depth of *ca.* 279 m and intercepts the Precambrian basement from 268-279 m (Fig. 2). An important section emerges with clear dominance of grey, reddish brown and massive siltstone (268-218 m). Along this siltstone dominated interval alternation with fine sandstone is observed. At a depth of 118 m is observed the first coal seam with > 30 m of thickness. The remaining three coal seams do not reach a thickness greater than 12 m. The coal seams sections end at depth 65 m, and are intercalated by grey, fine-coarse sandstones displaying some laminations. The Uppermost lithological unit, above 65 m is composed of dark grey, massive, laminated siltstone containing fine sandstones Palynological results

4.2. Palynological results

Different assemblages have been identified in the investigated two borehole cores (JOG16N-5 and JOG16N-7). The identification of the assemblages was based in the distribution of the palynomorphs along the sequences taking into consideration the relative abundance of prominent taxa as well as the first appearance datum (FAD) Here, five assemblages were observed for JOG16N-5 (T1-T5) and three for JOG16N-7 (B1-B3) (Tables 1 and 2). Taxa with stratigraphical importance and well preserved are illustrated in figures 3 to 8. Additionally, the stratigraphic sequence of the assemblages for each borehole core is as it follows.

4.2.1 Assemblages from JOG16N-5 borehole core

Assemblage T1: This palynofloral assemblage is recorded between the depth of 165-63.27 m. It is characterised by the dominance of spores, which are better preserved than the pollen grains. The more abundant spore taxa in this assemblage include *Laevigatosporites* spp., *Horriditriletes* spp., and *Converusisporites confluensis*. Also is observed the rare occurrence of taxa like *Thymospora* spp. The assemblage is complemented with rare occurrence of non-striate bisaccate pollen grains, such as *Scheuringipollentes maximus*, *Scheuringipollenites* spp., and *Protohaploxypinus limpidus*, *P. amplus*. Rare occurrences of colpate pollen grains, such as *Weylandites* spp, *Cycadopites cymbatus* are present. Stratigraphically important species *Thymospora pseudothiessenii,* and *Osmundacidities senectus* occur in the assemblage with the first one being abundant while the latter is rare.

Assemblage T2: This palynofloral assemblage is marked at a depth of 60.23–53.32 m. It is characterised by non-taeniate and taeniate bisaccate pollen grains. The main components of the assemblage include *Protohaploxypinus* spp. (e.g., *P.* sp., *P. limpidus*, *P. goraiensis* and *P. amplus*), *Striatopodocarpites* spp. (e.g., *S. cancelatus*, *S. fusus*, *S.* sp.), and *Alisporites* spp. Other recorded taxa include colpate pollen grains, such as *Weylandites lucifer*, *Weylandites* sp. (common occurrence), *W. striatus* (rare occurrence). *Lunatisporites* sp., *Corisaccites alutas*, *Florinites* sp., *Cycadopites* sp., were scarcely observed. In contrast, *Staurosaccites quadrifidus* occurs in greater abundance. Spores are rare in this assemblage and only three taxa were identified and includes *Cyclogranisporites* spp., and *Laevigatosporites* spp., and the key taxon *Osmundacidites senectus*.

Assemblage T3: This palynofloral assemblage (depth 50-58.37 m) is characterized by the dominance of striate bisaccate pollen grains over non-striate. Striate bisaccate pollen grains include common and abundant occurrence of *Striatopodocarpites fusus*, *Striatopodocarpites cancelatus*, and *S.* sp. The non-striate bisaccate taxa are observed rarely in this assemblage and include *Scheuringipollenites maximus*, *S. medius*, *S. ovatus,* and *Alisporites* spp. Other pollen taxa include *Striomonosaccites* spp., *Corisaccites* spp., *C. alutas* and colpate pollen grains, such as *Weylandites striatus* and *W.* spp. Spores complement the assemblage albeit in minor content. *Cyclogranisporites* marks its first appearance in this assemblage. Other spores include

Calamospora sp., and *Laevigatosprites* sp. *Osmundacidites senectus* is observed as common occurrence in the assemblage.

Assemblage T4: This palynofloral assemblage is marked at a depth of 45.2–39.9 m. It is characterised by the dominance of non-striate bisaccates and sub-dominance of striate bisaccates. Common palynotaxa include *Scheuringipollenites medius*, *S. ovatus*, *S. maximus*, *Protohaploxypinus limpidus*, *Protohaploxypinus goraiensis*, *P.* spp., and *Striatopodocarpites cancelatus*, *S. fusus*, and *Striatopodocarpites* spp. dominate the assemblage. Another abundant occurrence includes *Guttulapollenites hannonicus*, *Lunatisporites* spp., *Lueckisporites virkkiae* and *Weylandites lucifer*. Rare occurences of pollen comprise *Striomonosaccites incrassatus*, *Limitisporites* sp., *Staurosaccites quadrifidus*, *Corisaccites alutas*, *Vittatina costabilis*, *V.* sp., and *Cycadopites* sp. Spores are rarely observed herein, with *Calamospora* spp., *Cyclogranisporites* spp., and *Lophotriletes* spp., *Osmundacidites senectus,* and *Thymospora pseudothiessenii* being the only taxa (observed).

Assemblage T5: This palynofloral assemblage (depth 33.18-15.67 m) is characterized by a clear dominance of non-striate bisaccate pollen as observed in the previous assemblage (L4) however the content of striate bisaccate pollens is reduced herein. *Lunatisporites* spp., *Limitisporites amazonensis*, *Vittatina* spp., *Weylandites* spp, *Guttulapollenites hannonicus* and *Rhizomaspora* spp. are observed as rare occurrences. Spores such as *Osmundacidiies senectus* and *Laevigatosporites senectus* are observed in assemblage T5.

Table 1 Representation of palynoassemblages from borehole JOG16N-5 where A represent abundant (>50%), C=common (10-50%), R=rare (<10%), Al=algae.

Borehole	Samples number	Asssemblages	*Calamospora* spp.	*Cyclogranisporites* spp.	*Cyclogranisporites* spp.	*Laevigatosporites vulgaris*	*Laevigatosporites* spp.	*Horriditriletes* spp.	*Lophotriletes* spp.	*Osmundacidites senectus*	*Converrucosisporites confluens*	*Thymospora* spp.
			Spores									
Borehole JOG16N-5	E5	T5										
	E21									R		
	E22					R				R		
	E23	T4				R				R		
	E26		C						R	R		R
	E28									R		
	E30											
	E31	T3		C			R			R		
	E33		R		R		R			C		
	E34	T2								C		
	E39											
	E42				R		R					
	E45	T1				R	C	C		R	A	
	E59		R			R	C	R				A

Samples number	*Rhizomaspora* spp.	*Alisporites* spp.	*Scheuringipollenites maximus*	*Scheuringipollenites* spp.	*Protohaploxypinus limpidus*	*Protohaploxyoinus amplus*	*Protohaploxyoinus goraiensis*	*Protohaploxypinus hartii*	*Protohaploxypinus* spp.	*Striomonosaccites incrassatus*	*Striomonosaccites ovatus*	*Striomonosaccites* spp.	*Limitisporites amazonensis*	*Marsupipollenites tiradiatus*	*Limitisporites* spp.	*Lunatisporites* spp.	*Striatopodocarpites cancellatus*	*Striatopodocarpites fusus*	*Striatopodocarpites* spp.	*Guttulapollenites hannonicus*	*Lueckisporites virkkiae*	*Staurosaccites quadrifidus*	*Corisaccites alutas*	*Corisaccites* spp.	*Florinites* spp	*Vittatina costabilis*	*Vittatina* spp.	*Cycadopites* spp.	*Weylandites lucifer*	*Weylandites straitus*	*Weylandites magmus*	*Weylandites* spp.	Al
	Pollen																																
E5	R		C	C			C		C								R	R	R	R													
E21		R	C	C			R									R																R	R
E22		C		R	C	C	C			R			R			R				R							R						
E23	R		A		C	A	A	A	A							C	R			R	C						R						
E26		R	A		C	A	A	R	A	R					R		A	A	C	C	A	R	R					R	A				
E28			A		A	A	A		C										C	R			R			R	R		A				
E30			C	C	C	A	A																				R						
E31		C	R	R	R	R											C	C		R				R								R	
E33			R	R	R	R			A			R					C	C	A				A							R			R
E34		C	A	A			A		A																								
E39		R	R		C	A	A		A	R						R	C	C	C			A			R				C	R		C	
E42			A	C	A	C	C										C	C	C					R				R					R
E45			R	R	A	R																						C	R				
E59					R	R	R		R					R									R					R	R		R	R	

Marker for the assigned Wuchiapingian age (blue) — Marker for the assigned Changhsingian age (orange)

4.2.2. Assemblages from JOG16N-7 borehole core

Assemblage B1: This palynofloral assemblage is recorded at a depth of 272.84–144. 3 m. The assemblage is dominated by non-striate bisaccate pollen over striate pollen and comprises *Alisporites* spp., *Scheuringipollenites maximus*, *S.* spp., *Protohaploxypinus limpidus*, *P. goraiensis*, and *P.* spp. Rare occurrences of striate bisaccate pollen include *Striatopodocarpites fusus* and *Striatopodocarpites cancelatus*. Other pollen rare occurrences include *Caheniasaccites flavatus*, *Cannanoropolis mehtae*, *Lunatisporites variesectus*, *Lueckisporites virkkiae*, Potonie, *Potonieisporites lelei*, *Corisaccites* spp., *Pakhapites fusus*, *Weylandites* spp. Spores are rare and include *Laevigatosporites* spp., *Horriditrinletes* spp., *Converrucosisporites* spp*.,* and the stratigraphically important taxon *Thymospora pseudothiessenii* (rare to common occurrence).

Assemblage B2: This palynofloral assemblage is marked at a depth of 137.9–133.62 m. Here, striate and non-striate pollen decrease in abundance and occurs scarcely. Rare occurrence is also observed for *Weylandites* spp. Common occurrence of pollens includes Corisaccites spp., *Corisaccites alutas*, and *Alisporites* spp. Abundant occurrences of spores (Filicophyta) include *Converrucosisporites* spp., and *Granulatisporites austroamericanos*. However, rare occurrences were also observed and comprises *Verucosisporites* spp., *Leiotriletes* spp., *Laevigatosporites* spp., and *Horriditriletes* spp. Moreover, stratigraphical key species including *Thymospora pseudothiessenii*, *Indotriradites niger*, and *Osmundacidities senectus* are present.

Assemblage B3: This palynofloral assemblage (depth 116.93–88.38 m) has been identi fied by the dominance of non-striate bisaccates *Protohaploxypinus* spp., (*P. limpidus*, *P. goraiensis*, *P.* sp.), *Scheuringipollenites* spp., *S. maximus*, *S. ovatus*. Other common taxa include *Striomonosaccites incrassatus, Striatopodocarpites spp. Guttulapollenites hannonicus, Lueckisporites virkkiae, Corisaccites alutas, Illinites unicus, Vittatina* sp., *Weylandites lucifer* and *W.* sp., *Alisporites* sp., and *Meristocorpus explicatus* occur only rarely in the assemblage. All observed spore taxa are considered as occurring scarcely and include *Laevigatosporites* spp., *L. vulgaris*, *Lophotriletes* sp., *Thymospora pseudothiessenii* and *Osmundacidites senectus*. *Osmundacidites senectus* occurs as an isolated occurrence.

Additionally, several occurrences of algae (e.g., *Botrycoccus braunii*) have been observed along the studied palynoassemblages are good indicators of the presence of a fluvial-lacustrine depositional environment supported by the presence of phytoclasts (opaque and non-opaque), and cuticles representative of the palynoflora of the studied area. Lastly, it should be stressed that the borehole JOG16N-5 have samples relatively few spores, while borehole JOG16N-7 contains a greater abundance.

Table 2 Representation of palynoassemblages from borehole JOG16N-7 where A represent abundant, abundant (>50%), C=common (10-50%), R=rare (<10%), Al=algae.

Borehole	Samples number	Asssemblages	Spores: *Verrucosisporites* spp.	*Leiotriletes* spp.	*Lundbladispora brevicula*	*Laevigatosporites vulgaris*	*Laevigatosporites* spp.	*Horriditriletes* spp.	*Indotriradiates niger*	*Lophotriletes* spp.	*Thymospora pseudothiessenii*	*Converrucosisporites* spp.	*Granulatisporites austroamericanos*	*Meristocorpus explicatus*	*Alisporites* spp.	*Osmundacidities senectus*
Borehole JOG16N-7	R26				R	R	R	C			R			R		
	R27	B3			R						R				R	R
	E34						R	R		R	R				R	
	R40	B2	R				R	R			R				C	R
	R42			R					R		R	A	A		R	
	R46										R					
	R53	B1					R	R			R	R			C	
	R58										R	R				
	R64										C	R				

Borehole	Samples number	Asssemblages	Polen: *Scheuringipollenites maximus*	*Scheuringipollenites* spp.	*Protohaploxyoinus amplus*	*Protohaploxyoinus goraiensis*	*Protohaploxypinus limpidus*	*Protohaploxypinus* spp.	*Striomonosaccites incrassatus*	*Striomonosaccites ovatus*	*Caheniasaccites flavatus*	*Marsupipollenites triradiatus*	*Cannanoropolis mehtae.*	*Lunatisporites variesectus*	*Striatopodocarpites cancellatus*	*Striatopodocarpites fusus*	*Striatopodocarpites* spp.	*Guttulapollenites hannonicus*	*Lueckisporites virkkiae*	*Potonieisporites lelei*	*Corisaccites alutas*	*Corisaccites spp.*	*Illinites unicus*	*Vittatina costabilis*	*Vittatina spp.*	*Phakates fusus*	*Weylandites lucifer*	*Weylandites* spp.	Al
Borehole JOG16N-7	R26			C		C	C	C									R		C									R	
	R27	B3						C	C					R		R	C	R			R		R		R				
	E34		C	C																							R	R	
	R40	B2	C	R			R	R							R	R	R				C	C							R
	R42						R	R																				R	
	R46		C	R		C	C	A					R		R	R			R										
	R53	B1	C	C	R	A	A	C										R			R								R
	R58					A	A	A							R	R	R											R	
	R64		R	R		C	C	C			R	R								R						R			R

Marker for the assigned Wuchiapingian age

4.3. Palynostratigraphy

In the studied borehole cores distinct palynoassemblages were identified (Table 1 and, Figs. 3-7). For the borehole JOG16N-5 five palynoassemblages (T1-T5) whereas three palynoassemblages were identified for the borehole JOG16N-7 (B1-B3). The identification of the different biozones were mostly based in the relative abundance of the observed palynotaxa. Nevertheless, age assignment was based on correlation with local and regional schemes. The differences in the biozones are either abundance in bisaccate striate pollen or non-striate bisaccate pollen. Palynotaxa including *Protohaploxypinus*, *Striatopodocarpites*, and *Scheuringipollenites* are seen as dominant to sub-dominant throughout the entire section. Some sections unveil an abundance in spores if compared to others. Based on the occurrence of stratigraphically important taxa, Assemblage T1 from borehole core JOG16N-5 and assemblages B1, B2 and B3 from JOG16N-7 are correlated with Assemblage L2 proposed by Pereira et al. (2019) in her study in the Muarádzi sub-basin, Moatize-Minjova Coal Basin, Karoo supergroup from Mozambique. In its turn, the remaining assemblages from JOG16N-5 (T2, T3, T4, T5) are well correlated with the L3 assemblage proposed by Pereira et al. (2019). Based on the established correlation, the assemblages T1, B1, B2, and B3 (this work) are tentatively assigned to Middle to late Wuchiapingian whereas the assemblages T2, T3, T4, T5 depict a late Lopingian (Changhsingian) age.

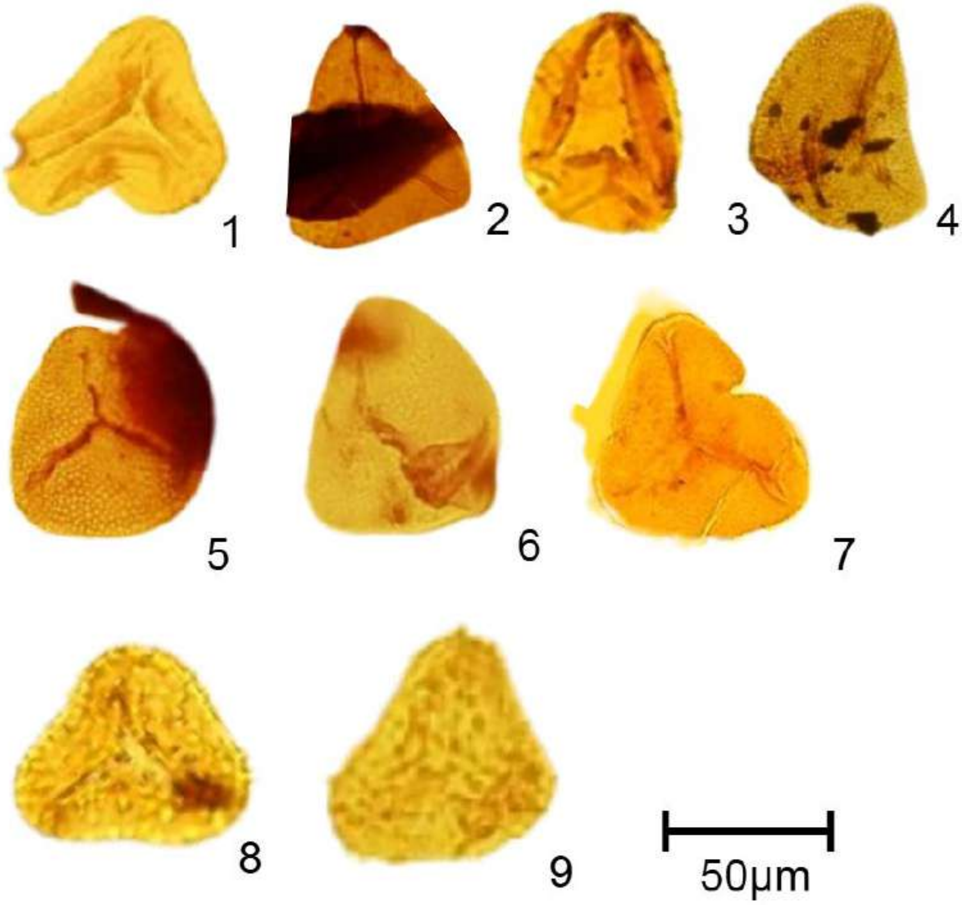

Fig. 3. Selected recovered palynomorphs from the JOG16N-5 and JOG16N-7 borehole cores: 1. *Lophotriles* spp., samples R34, JOG16N-7, 2. *Leiotriletes* spp., sample R42, JOG16N-7, 3. *Cyclogranisporites* spp., sample R42, 4. *Converrucosisporites confluensis* (Archangelsky and Gamero) Playford and Dino, 2002, sample R45, JOG16N-7, 5. *Converrucosisporites* spp., samples R42, JOG16N-7, 6. *Granulatisporites austroamericanus* (Archangelsky and Gamero, 1979), sample R42, JOG16N-7, 7. *Granulatisporites austroamericanus* (Archangelsky and Gamero, 1979), sample R42, JOG16N-7, *Horriditriletes* spp., sample R45, JOG16N-7, *Horriditriletes tereteangulatus* (Balme and Hennelly), Backhouse 1991, sample R40, JOG16N-7.

Fig. 4. Selected palynomorph specimens from the Maniamba Basin, Mozambique. 1. *Laevigatosporites* spp, sample E31, JOG16N-5, 2. *Laevigatosporites vulgaris*, sample E23, JOG16N-5, 3. *Osmundacidites senectus* (Balme, 1970), sample E26, JOG16N-5, 4. *Osmundacidites senectus* (Balme, 1970), sample E31, JOG16N-5, 5. *Osmundacidites senectus* (Balme, 1970), sample E33, JOG16N-5, 6. *Osmundacidites senectus*, 7. *Thymospora pseudothiessenii* (Kosanke) Wilson and Venkatachala 1963, sample R40, JOG16N-7, 8-*Thymospora pseudothiessenii* (Kosanke) Wilson and Venkatachala 1963, sample E59, JOG16N-7, 9. *Thymospora pseudothiessenii* (Kosanke) Wilson and Venkatachala 1963, sample R40, JOG16N-7, 10. *Thymospora pseudothiessenii* (Kosanke) Wilson and Venkatachala 1963, sample R64, JOG16N-7 11. *Thymospora pseudothiessenii* (Kosanke) Wilson and Venkatachala 1963, sample E59, JOG16N-5. Scale bar = 50 μ m.

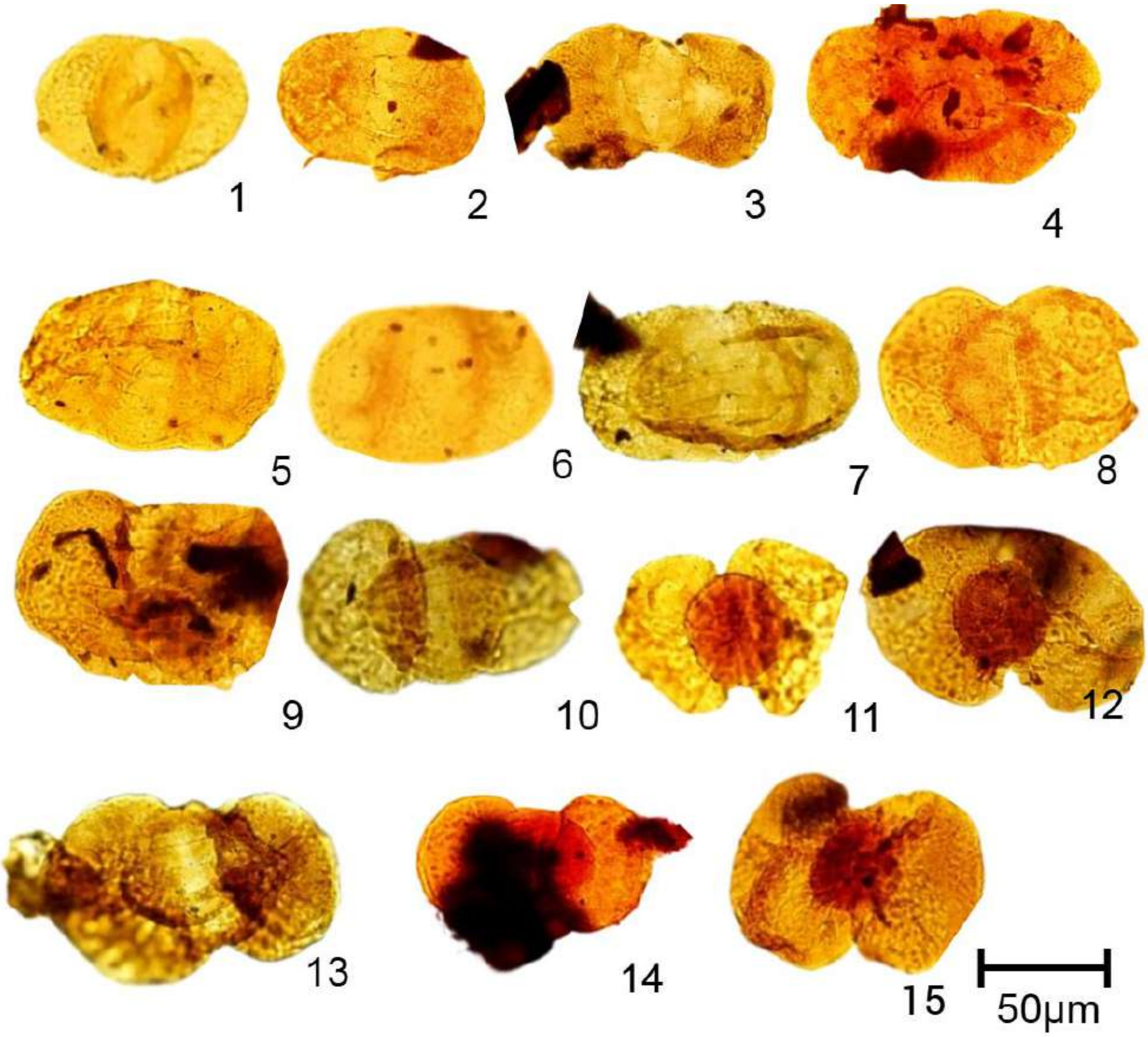

Fig. 5. Selected retrieved palynomoprhs from the Maniamba Basin, Mozambique. 1. *Alisporites* spp., sample E47, JOG16N-5, 2. *Ilinites unicus* Kosanke 1950 emend. Jansonius and Hills 1976, sample R27, JOG16N-7, 3. *Limitisporites amazonensis* Playford and Dino, 2000b, sample E22, JOG16N-5, 4. *Potonieisporites lelei* Maheshwari 1967 sample R64, JOG16N-7, 5. *Protohaploxypinus amplus* (Balme and Hennelly) Hart 1964, sample E22, JOG16N-5, 6. *Protohaploxypinus* spp., samples E22, JOG16N-5, 7. *Protohaploxypinus* spp., sample E28, JOG16N-5, 8. *Protohaploxypinus* spp., sample R27, JOG16N-7, 9. *Protohaploxypinus goraiensis* Potonié and Lele 1961, sample E42, JOG16N-5, 10. *Striatopodocarpites cancelatus* (Balme and Hennelly) Hart 1963, sample E39, JOG16N-5, 11. *Striatopodocarpites fusus* (Balme and Hennelly) Potonié 1956, sample E42, JOG16N-5, 12. *Striatopodocarpites fusus* (Balme and Hennelly) Potonié 1956, sample E42, JOG16N-5, sample E42, JOG16N-5, 13. *Striatopodocarpites* spp., sample E26, JOG16N-5, 14. *Striatopodocarpites* spp., sample R27, JOG16N-7, 15. *Rhizomaspora* spp., sample R27, JOG16N-7. Scale bar = 50 µ m.

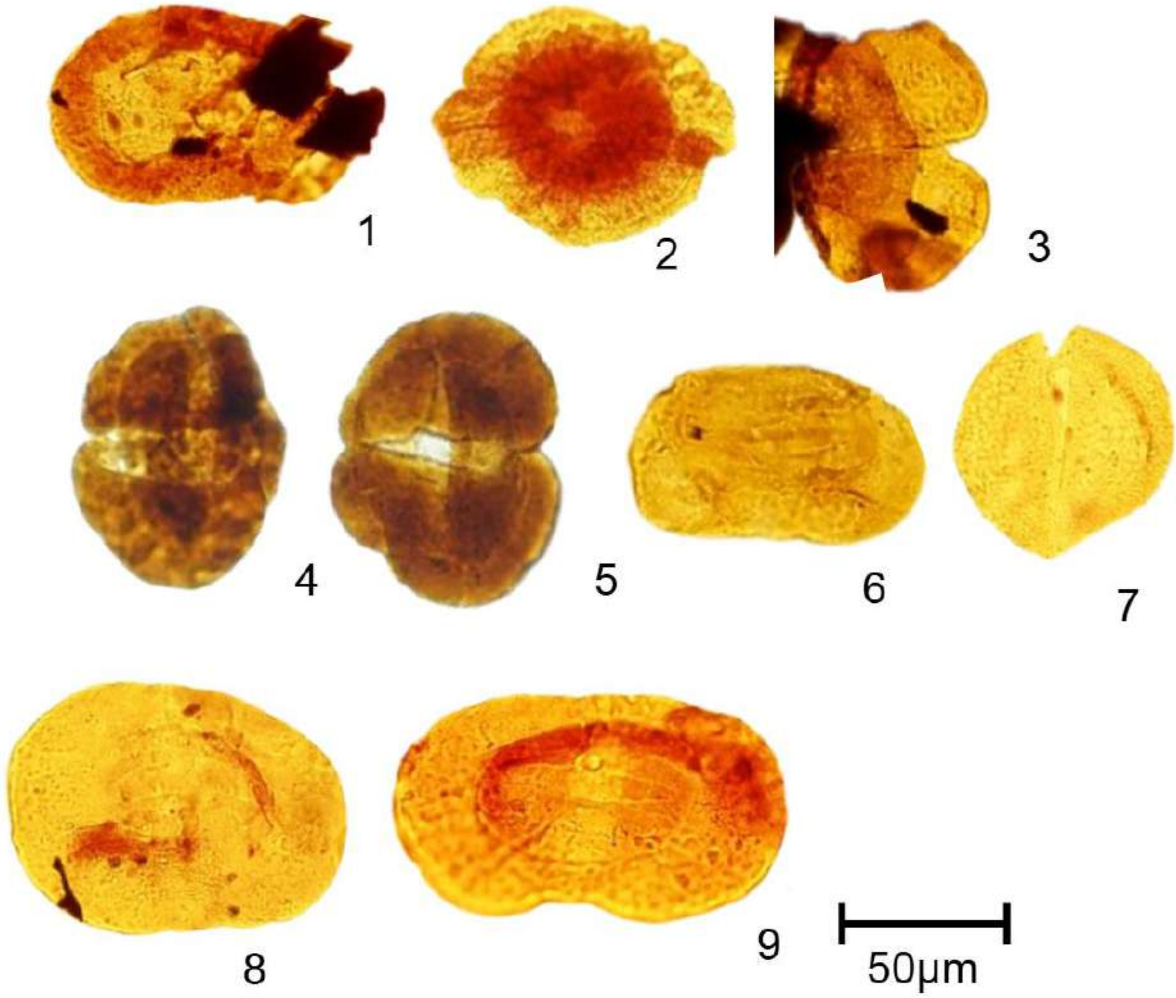

Fig. 6. Selected palynomorphs from the Maniamba Basin. 1. *Caheniasaccites flavatus*, Bose and Kar 1966, sample R64, JOG16N-7, 2. *Cannanoropolis mehtae* (Lele) Bose and Maheshwari 1968, sample R46, JOG16N-7. 3. *Corisaccites alutas* Venkatachala and Kar 1968, sample E33, JOG16N-5, 4. *Lueckisporites virkkiae* Potonié and Klaus 1954sample E26, JOG16N-5, 5. *Lueckisporites virkkiae* Potonié and Klaus 1954, sample E26, JOG16N-5, 6. *Lunatisporites* spp., sample E28, JOG16N-5, 7. *Scheuringipollenites maximus* (Hart) Tiwari (1973) sample R34, JOG16N-7, 8. *Striomonasaccites incrassatus* Playford and Dino, 2000, sample R27, JOG16N-7. 9. *Striomonosaccites incrassatus* Playford and Dino, 2000, sample R27, JOG16N-7. Scale bar = 50 µ m.

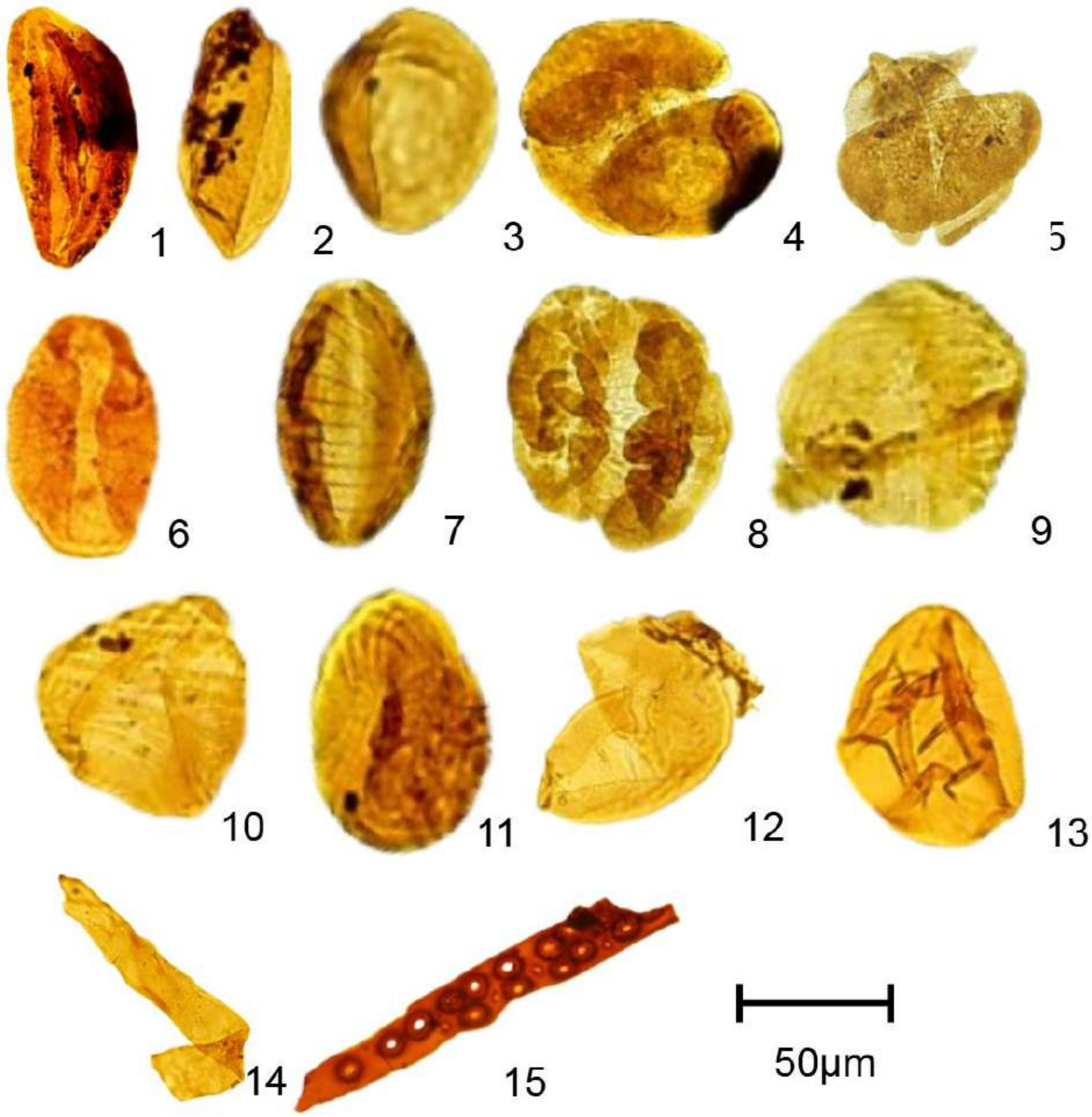

Fig. 7. Selected retrieved palynomoprhs from the Maniamba Basin, Mozambique. 1. *Gnetaceapollenites sinuosus* (Balme and Hennelly) Bharadwaj and Srivastava, 1969, sample E42, JOG16N-5, 2. *Cycadopites cymbatus* (Balme and Hennelly) Segroves 1970, sample E59, JOG16N-5, 3. *Marsupipollenites striatus* (Balme and Hennelly) Hart, 1965), sample E26, JOG16N-5, 4. *Guttulapollenites hannonicus*, Goubin 1965, sample E26, JOG16N-5, 5. *Guttulapollenites hannonicus*, Goubin 1965, sample E26, JOG16N-5, 6. *Phakites fusus* (Bose and Kar) Menéndez 1971, sample R64, JOG16N-7, 7. *Vittatina costabilis*, Wilson 1962, sample E28, JOG16N-5, 8. *Vittatina* spp., samples E26, JOG16N-5, 9. *Weylandites lucifer* (Bharadwaj and Salujha) Foster 1975, sample E39, 10. *Weylandites* spp., sample E21, JOG16N-5, 11. *Weylandites striatus* (Luber) Utting 1994, sample E39, JOG16N-5, 12. Unidentified algae, sample E33, JOG16N-5, 13. Unidentified algae, sample E33, JOG16N-5, 14. Fungal hyphae,

sample E21, JOG16N-5, 15. Translucent phytoclast with uni-bisseriate pitting, sample R64, JOG16N-7. Scale bar = 50 μ m.

4.4. Correlations

The establishment of a precise palynostratigraphy scheme across Gondwana sections is hindered due to the scarcity of marine faunas (Aggarwal et al., 2019) and others. However, in order to tentatively correlate the study section, a comparison was done with Karoo sections located in Mozambique and those paleogeographically closer sites as well with other Gondwana sequences (Table 3, and Fig. 8).

Table 3 Central Gondwana basins with similar palynoevents with the Maniamba Basin.

Chronostratigraphy			Zambia (Nyambe and Utting, 1997)	Madagascar, Sakamena Group (Wright and Askin, 1987)	India, Godavari Basin (Aggarwal and Jha, 2013, Tiwari and Tripathi, 1987)	Antarctica, Prince Charles Mountain (Lindström and McLoughlin, 2007)	Moatize-Minjova Basin (Mozambique) (Pereira et al., 2019)	Maniamba Basin, Mozambique (this study)
Permian	Lopingian	Changhsingian	**Madumabisa Fm.** ▪ P. *goraiensis*, P. *limpidus*, G. *hannonicus*, *Striatopodocarpites* spp., ***Thymospora pseudothiessenii***	▪ *Protohaploxypinus* spp., *Striatopodocarpites* spp., G. *hannonicus*, *Lueckisporites virkkiae*, ***Osmundacites senectus***	▪ *Striatopodocarpites* spp., G. *hannonicus*, ***Osmundacidites senectus***, *Weylandites* spp.	▪ *Protohaploxypinus* spp., *Striatopodocarpites* spp., *Osmundacidites* ***senectus***, *Horriditriletes* spp.	L3: ***Osmundacidites senectus***	T2, T3, T4, T5: ***Osmundacidites senectus***
		Wuchiapingian	**Upper Gwembe Fm.** ▪ **G. *hannonicus*, *Thymospora pseudothiessenii***				L2: ***Thymospora pseudothiessenii*** L1: *G. hannonicus*	T1, B1, B2, B3: ***Thymospora pseudothiessenii***

- The highlighted palynotaxa are regarded as stratigraphic markers.

4.4.1. Mozambique Karoo sub-basins

The palynological assemblages obtained through this study are well correlated with L2 and L3 assemblages proposed by Pereira et al. (2019), Lopes et al. (2021b), Galasso et al. (2019b) in the palynological work performed in the Muarádzi Basin and N'Condédzi sub-basin. This characteristic indicates that the palynostratigraphy of the sub-basins in Mozambican Karoo can easily be correlated (Table 3, and Fig. 8).

4.4.2. Northern and Southern Karoo schemes with similar Lopingian palynoevents

Northern Karoo schemes have proven to depict similar palynoevents as described in other studies (Pereira et al., 2016; Lopes et al., 2019, Nhamutole et al., 2024b). Here, northern Karoo Lopingian assemblages from Tanzania (Msaky and Srivastava, 1997), Zambia (Utting, 1979; Nyambe and Utting, 1997; Barbolini et al., 2016b) were compared (Table 3, Fig. 8).

The upper Madumabisa Formation in the mid-Zambezi valley (Zambia) is characterised by taxa including *Corisaccites alutas*, *Falcisporites australis*, *Guttulapollenites hannonicus*, *Klausipollenites schaubergerii*, *Polypodiisporites mutabilis*, *Protohaploxypinus goraiensis*, *Protohaploxypinus limpidus*, *Protohaploxypinus microcorpus*, *Striatopodocarpites spp*., *Thymospora pseudothiessenii*), *Vittatina* spp., and *Weylandites lucifer* assigned to Lopingian are well correlated with *Dulhuntyispora parvithola* Zone of Backhouse (1991) and the APP5 Zone of Price (1997), both dated as mid Wuchiapingian to late Changhsingian (Laurie et al., 2016) as well with the palynoflora of the Daptocephalus Assemblage Zone of the lower and middle Balfour Formation in the main Karoo Basin in South Africa (Barbolini et al., 2016a). Nevertheless, the presence of taxa listed above complemented with the occurrence of *Thymospora pseudothiessenii* is correlated with the assemblage T1 (Borehole JOG16-5) and assemblages B1, B2, B3 (Borehole JOG16N-7).

The upper part of the Gwembe Formation, in the lowermost unit of the Zambezi Basin is correlated with the *D. ericianus* Zone of Backhouse (1991), the *Guttulapollenites. hannonicus–P. rugatus* Zone (Zone VI) of Aitken (1998), Zone K8 (Barbolini et al., 2018), assemblage Zone III of the mid-Zambezi Basin, Zimbabwe. All these assemblages have a record of a common distinctive species as *Guttulapollenites* *hannonicus* and *Thymospora pseudothiessenii* which suggests a correlation with assemblages T1, B1, B2, B3 identified herein.

However, the southern Karoo basins (South Africa and Zimbabwe) depict different palynoevents compared with its northern counterpart probably due to the Cargonian Highlands that acted as a barrier for floral exchange between the southern and northern parts of the Karoo during the Permian as argued by Isbell et al. (2008). In addition, the Main Karoo Basin in South Africa displays a tectonic style related to the development of a foreland basin formed by the tectonic load of the Cape Fold Belt that differs from the tectonic control of the East Africa Rift basins. This different tectonic style could have influenced the existence of different sedimentary facies in the north and south. In addition, it may be argued that the plant colonization could have differed in these regions (Anderson, 1977; Barbolini, 2014). All the aforementioned aspects might have influenced the FAD (first appearance datum) of the key-taxa thus hindering the establishment of a precise correlation scheme across central Gondwana sequences (Catuneanu et al., 2005). Furthermore, it should be emphasized that different palynoevents within the Main Karoo Basin are not only restricted to the south and north part. For instance, the microflora encountered in the Prince Albert Formation located in the western region of the Basin display different restricted range taxa if compared to the microflora of the Prince Albert Formation located in the southern region (Barbolini, 2014). The existence of evident provincialism defined by endemic taxa has been a challenge for correlation of Gondwana microfloras (McLoughlin, 2001; Prevec et al., 2009). A classic example regarding provincialism across Gondwana that hampers correlation has to deal with the absence of stratigraphically useful Australian species in other parts of Gondwana (Truswell, 1981; Backhouse, 1991; Prevec et al., 2010).

4.4.3. Gondwana schemes with similar associations

Palynoassemblages T2, T3, T4, T5 from this study are correlated with assemblages from Morondova Basin, Madagascar (Lower Sakamena group) described by Wright and Askin, 1987) (Table 3, and Fig. 8). Key Lopingian taxa including *Protohaploxypinus* spp., *Striatopodocarpites* spp., *Guttulapollenites hannonicus*, *Lueckisporites virkkiae*, *Osmundacidites senectus* are observed in both sections. The aforementioned palynoassemblages are also well-correlated with Changhsingian palynoflora from Godavari Graben in India (Aggarwal and Jha, 2013; Tewari et al., 2015; Jha et al., 2018). Palynotaxa such as *Striatopodocarpites*, *Guttulapollenites*, *Lunatisporites*, *Corisaccites* together with some stratigraphically significant taxa such as *Alisporites* spp., *Osmundacidites* sp. and *Weylandites* spp., occur in these assemblages. Lastly, our palynoassemblages are tentatively correlated with Lopingian assemblages from Prince Charles Mountain, Antarctica (Lindström and McLoughlin, 2007). Species such as *Protohaploxypinus* spp., *Striatopodocarpites* spp., and spores assigned to the genera *Osmundacidites*, *Horriditriletes*, *Lophotriletes*, and *Laevigatosporites* depict similar palynoevents amongst the palynoassemblages from the Maniamba Basin with the ones observed from Prince Charles Mountain in Antarctica.

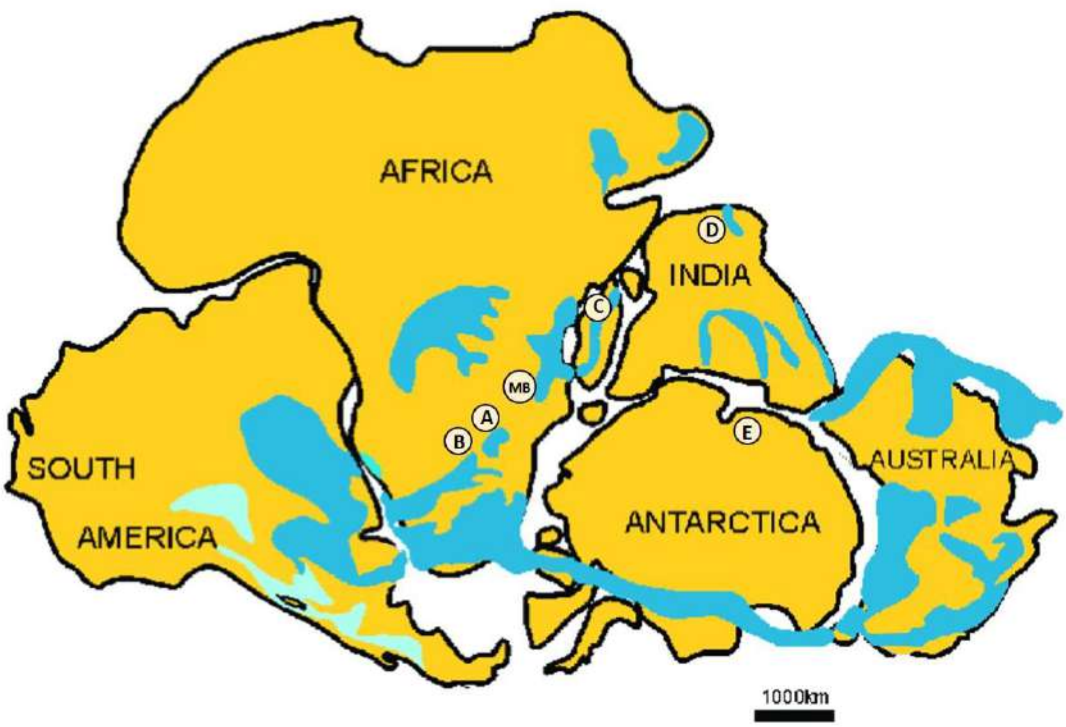

Fig. 8. Gondwana correlations during Lopingian (area with deep blue colour) depicting similar palynoevents modified from Pereira et al (2016). A. Moatize-Minjova Basin (Mozambique); B. Mid Zambezi valley Basin (Zambia); C. Sakamena group (Madagascar; D. Godovari Basin (India); E. Prince Charles Mountain (Antartica). MB=Maniamba Basin (Mozambique).

5. Discussion

Palynological analysis suggest a flora composed of luxuriant vegetation where the gymnosperm represented by *Striatopodocarpites*, *Protohaploxypinus*, and *Scheuringipollenites* completely dominate the assemblages, with non-glossopterids being sub-dominant throughout the entire section. Ferns, sphenopsids and lycopsids are common to abundant and are the typical vegetation of humid and warm lowland areas, with the rare influence of upland vegetation. The occurrence of silicified wood as reported by Nhamutole et al. (2021) support the fact that the plant growth in the area was climate and environment driven. Monosaccate pollen grains are scarce and the ones observed in the present study includes *Corisaccites alutas*, *Lueckisporites* sp., and *Marsupipollenites triradiatus*. The rare occurrence of monosaccate pollen indicates that drier areas existed but were probably located at greater distances from the floodplains. These were probably in upland regions of the river area as the gymnosperms that produced these palynomorphs (e.g., Cordaites) were unable to flourish in permanent wet soils and deeper swamps (Anderson and Anderson, 1985; Souza et al., 2015). Here, it should be stressed that only two Cordaitalean elements are known from the macrofloras of the Karoo Basin and include *Noeggerathiopsis hislopi* associated with coal macrofloras localities, being considered as hygrophilous and *Noeggerathiopsis spathulate*. The latter is rare in Upper Permian and is linked to flooding settings with absence of coal accumulation (Anderson and Anderson, 1985).

On the other hand, their low abundance indicates the influence of vast swamps and shallow lake environments existing during the deposition of the coal seam sequences observed in the Basin. Additionally, the high percentage of phytoclasts of different sizes, palynomorphs, and occurrence of algae (e.g., *Botrycoccus braunii*) described by previous studies corroborates with this palaeoenvironmental settings where water adapted higher seed ferns and gymnosperms thrived (e.g., Gotz et al., 2017; Wheeler and Gotz, 2017). These plants are responsible for the development of the thick coal beds in the Karoo basins, as shown by the occurrence of *Alisporites*, *Protohaploxipinus* and *Striatopodocarpites* in the palynomorph assemblages from both cores. Key palynotaxa *Thymospora* and *Osmundacidites* occur in the assemblages and they provide some critical paleonvironmental information as their occurrence is linked to humid and lowland environments. Spores related to lycophytes (e.g., *Indotriradites*), characteristic of very wet and humid environments are also present in low numbers in the palynomorph assemblages. However, an increase in abundance of spores along the sequences was not observed as expected for Lopingian sections suggesting that the Permian-Triassic boundary (PTB) was not reached. Similar results were also reported by Lopes et al. (2021) in the palynology work in the Muáradzi sub-Basin (Moatize-Minjova Basin). Palynofacies, Rock Eval, TOC (total organic carbon) and biomarker data from the studied borehole cores indicate deposition of sediments in a proximal-distal setting under oxic-dysoxic-anoxic conditions (Nhamutole et al., *in press*). The latter conditions are supported by the presence of pyrite, and high content of palynomorphs, moderate water level, low energy and depletetion in oxygen if compared to other organic matter components (Nhamutole et al., *in press*). Lastly, the observed changes in the lithofacies suggest a shift in the depositional environments. For instance, in both borehole cores is observed a clear shift from siltstone dominated environment to more coaly environment and then to siltstone-sandstone dominated environment. The observed sandstone could represent channel-fill successions, crevasse splay deposits linked to natural levees during the initial phases of flooding (Bicca et al., 2017). Carbonaceous shale horizons and coaly sections suggest overbank deposits with environmental conditions with the potential for coal formation and its accumulation. The intercalation of fine-siltstone and medium-to-fine grained sandstone units depict clastic deposition in the over banks during the flooding events. The sedimentation of silt and mud may have followed the peaks of the flooding events (Collinson, 1996; Bicca et al., 2017). The flooding intervals together with crevasse splay lenses suggest a meandering fluvial system characterised by high sinuosity that could have been triggered by tectonic activity during the Lopingian in the Maniamba Basin. The aforementioned variables were also responsible for sediment infilling in the Upper Karroo sequence from the Maniamba Basin.

6. Conclusions

Based on the stratigraphic distribution of palynomorphs recovered from two cores drilled in the Maniamba Basin, the following conclusions are derived:

- The palynological studies revealed the presence of five distinct palynoassemblages from JOG16N-5 core (T1: 165-63.27 m; T2: 60.23-53.32 m; T3: 50.0-48.37 m; T4: 45.2-36.9 m; T5: 33.18-15.67 m) and three palynoassemblages from JOG16N-7 core (B1: 272.84-144.3 m; B2: 137.9-133.62 m; B3: 116.93-88.38 m).

- The palynoassemblages T1 (JOG16N-5 core) and all the assemblages from JOG16N-7 (B1, B2, B3) were assigned to Middle-late Wuchiapingian whereas the assemblages T2, T2, T3, T4 and T5 from JOG16N-7 were are assigned to late Lopingian (Changhsingian).
- Palynoassemblages T1, B1, B2, B3 are characterized by the common occurrence of characteristic Lopingian taxa (*Guttulapollenites*, *Protohaploxypinus*, *Striatopodocarpites*, *Cannanoropolis*, *Cycadopites*, *Marsupipollenites*, *Striomonosaccites*, together with common occurrence of *Thymospora pseudothiessenii* whereas the palynoassemblages T2, T3, T4 and T5 were assigned based in occurrence of *Osmundacidites senectus* in all the sequences complemented with the occurrence of Lopingian taxa found in other palynoassemblages.
- In the studied boreholes, humid and warm climatic conditions are inferred based on the luxuriant vegetation as recorded by the dominance of pollen grains assigned to *Protohaploxypinus* and *Striatopodocarpites* whereas the presence of upland vegetation indicators such as monosaccate pollen grains is rare.
- The depositional environment was made up of several floodplains together with diversified wetlands characterised by forest swamps and lakes.
- Based on correlations the studied assemblages display similar palynoevents with northern Karoo-aged basins of south-central Africa and with Lopingian central Gondwana basins from Madagascar, India, and Antarctica. On the other hand, Southern Karoo-aged basins (e.g., South Africa and Zimbabwe) show distinct Lopingian palynoevents which suggest the existence of tectonic barriers that probably prevented floral exchange. Other variables that support provincialism across the Karoo include the existence of different sedimentary facies as well as different plant colonization
- Changes in lithofacies along the sections of both borehole cores indicate a change in the dynamics of the drainage system that prevailed during the Lopingian in the Maniamba Basin. In addition, channel-fill successions, crevasse splay deposits linked to natural levees, clastic deposition in the over banks are observed during the flooding events.

References

Aggarwal, N., Jha, N., 2013. Permian palynostratigraphy and palaeoclimate of Lingala Koyagudem Coalbelt, Godavari Graben, Andhra Pradesh, India. J. Asian Earth Sci. 64, 38–57.

Aitken, G., 1998. A Palynological and Palaeoenvironmental Analysis of Permian and Early Triassic Sediments of the Ecca and the Beaufort Groups, Northern Karoo Basin, South Africa. PhD Thesis. University of the Witwatersrand, Johannesburg, South Africa.

Anderson, J.M., 1977. The Biostratigraphy of the Permian and Triassic, Part 3. Memoirs of the Botanical Survey of South Africa No. 41.

Anderson, J.M., Anderson, H.M., 1985. Palaeoflora of southern Africa. Prodomus of South African megafloras, Devonian to Lower Cretaceous. Rotterdam, Balkema, 423 p.

Backhouse, J., 1991. Permian palynostratigraphy of the collie basin. W. Aust. Rev. Palaeobot. Palynol. 67, 237–314.

Barbolini., 2014. Palynostratigraphy of the south African supergroup and correlations with coeval Gondwanan successions. Unpublished PhD thesis. University of the Witwatersrand, South Africa.

Barbolini, N., Bamford, M.K., Rubidge, B., 2016~~c~~. Radiometric dating demonstrates that Permian spore-pollen zones of Australia and South Africa are diachronous. Gond wana Res. 37, 241–251.

Barbolini, N., Rubidge, B., Bamford, M.K., 2018. A new approach to biostratigraphy in the Karoo retroarc foreland system: utilising restricted-range palynomorphs and their f irst appearance datums for correlation. J. Afr. Earth Sci. 140, 114–133.

Bicca, M.M., Philipp, R.P., Jelinek, A.R., Ketzer, J.M.M., dos Santos Scherer, C.M., Jamal, D.L., Domingos dos Reis, A., 2017. Permian-Early triassic tectonics and stratigraphy of the Karoo Supergroup in northwestern Mozambique. J. Afr. Earth Sci. 130, 8–27.

Catuneanu, O., Wopfner, H., Eriksson, P.G., Cairncross, B., Rubidge, B.S., Smith, R.M.H., Hancox, P.J., 2005. The Karoo basins of south-central Africa. J. Afr. Earth Sci. 43, 211–253.

Collinson, J.D., 1996. Alluvial sediments. In: Reading, H.G. (Ed.), Sedimentary Environments: Processes, Facies and Stratigraphy. Blackwell Science, Oxford, pp. 37–82.

Fernandes, P., Hancox, P., Mendes, M., Pereira, Z., Lopes, G., Marques, J., Jorge, R., Albardeiro, L., 2023. The age and depositional environments of the lower Karoo Moatize Coalfield of Mozambique: insights into the postglacial history of central Gondwana. Palaeoworld 33, 979–996.

Galasso, F., Fernandes, P., Montesi, G., Pereira, Z., Spina, A., Marques, J., 2019a. Thermal history and basin evolution of the Moatize - minjova Coal Basin (N'Cond´ edzi Sub-basin, Mozambique) constrained by organic maturation levels. J. Afr. Earth Sci. 153, 219–238.

Gotz, A., Hancox, P.J., Lloyd, A., 2017. Permian climate change recorded in palynomorph assemblages of Mozambique (Moatize Basin, eastern Tete Province). Acta Paleobotanica 57 (1), 3–11.

Götz, A., Hancox, P.J., Lloyd, A., 2018. Southwestern Gondwana's Permian climate amelio ration recorded in coal-bearing deposits of the Moatize sub-basin (Mozambique). Paleoworld https://doi.org/10.1016/j.palwor.2018.08.004.

Gradstein, S.R., Kerp, H., 2012. A brief history of plants on Earth. In: Gradstein, F.M., Ogg, J.G., Schmitz, M., Ogg, G. (Eds.), The Geologic Time Scale. Elsevier, Amsterdam, pp. 233–237.

Isbell, J.L., Cole, D.I., Catuneanu, O., 2008. Carboniferous-Permian glaciation in the main Karoo Basin, South Africa: stratigraphy, depositional controls, and glacial dynamics. In: Fielding, C.R., Frank, T.D., Isbell, J.L. (Eds.), Resolving the Late Paleozoic Ice Age in Time and Space. Geological Society of America, Special Paper 441, pp. 71–82.

Jha, N., Aggarwal, N., Mishra, S., 2018. A review of the palynostratigraphy of Gondwana sediments from the Godavari Graben, India: global comparison and correlation of the Permian-Triassic palynoflora. J. Asian Earth Sci. 163, 1–21.

JOGMEC, 2015. The Results of Drilling Survey III in Mozambique. National Institute of Mines report, p. 40pp.

Laurie, J.R., Bodorkos, S., Nicoll, R.S., Crowley, J., Mantle, J.D., Mory, A.J., Wood, G.R., Backhouse, J., Holmes, E.K., Smith, T.E., Champion, D.C., 2016. Calibrating the middle and late Permian palynostratigraphy of Australia to the geologic timescale via U-Pb zircon CA-IDTIMS dating. Aust. J. Earth Sci. 63 (6), 701–730.

Lopes, G., Pereira, Z., Fernandes, P., Mendes, M., Marques, J., Jorge, R. 2021. Late Permian palaeoenvironmental evolution of the Matinde Formation in the Muará dzi Sub-basin, Moatize-Minjova Basin, Mozambique. J. afr. Earth sci. https://doi.org/10.1016/j.jafrearsci.2021.104138

Lindström, S., McLoughlin, S., 2007. Synchronous palynofloristic extinction and recovery after the end-Permian event in the Prince Charles Mountains, Antarctica: implications for palynofloristic turnover across Gondwana. Rev. Palaeobot. Palynol. 145, 89–122.

McLoughlin, S., 2001. The breakup history of Gondwana and its impact on pre-Cenozoic floristic provincialism. Australian Journal of Botany 49, 271-300.

Msaky, E., Srivastava, V., 1997. Lower Karoo (K5-K6) Palynological assemblage from Tanzania. Abstract 3rd Symposium of African Palynology. Johannesburg South Africa, p. 31.

Norconsult, C., 2007. Notícia explicativa das áreas de Niassa, Cabo Delgado e partes de Zamb´ ezia e Nampula. Direcção Nacional de Geologia, Maputo, Moçambique. Unpublished report.

Nhamutole, N., Araújo, R., Bamford, M. 2020. Fossil woods from the Permian and Triassic of Mozambique: taxonomy, palaeocology and geoconservation. Unpublisehd master dissertation. University of the Witwatersrand, South Africa.

Nhamutole, N., Bamford, M., Souza, P., Félix, C.M., Carmo, D.A., Peu, J., 2024b. Palynology of two drilling cores from the Maniamba Basin, Mozambique (central Gondwana): Insights on age and palaeoenvironments. Rev. Palaeob. Palynol. 334, 105271. https://doi.org/10.1016/j.revpalbo.2024.10527.

Nyambe, I.A., Utting, J., 1997. Stratigraphy and palynostratigraphy, Karoo Supergroup (Permian and Triassic), mid-Zambesi Valley, southern Zambia. J. Afr. Earth Sci. 24, 563–583.

Pereira, Z., Fernandes, P., Lopes, G., Marques, J., Vasconcelos, L., 2016. The Permian-Triassic transition in the Moatize-Minjova Basin, Karoo Supergroup, Mozambique: a palynological perspective. Rev. Palaeobot. Palynol. 226, 1–19.

Pereira, Z., Fernandes, P., Lopes, G., Marques, J., Vaz, M., Costa, M., Correia, J., Castro, L., Galasso, F., 2019. Palynology of the Muar´ adzi sub-Basin, moatize-minjova coal basin, Karoo Supergroup, Mozambique. Rev. Palaeobot. Palynol. 269, 78–93.

Phipps, D and Playford, G. 1984. Laboratory techniques for extraction of palynomorphs from sediment. University of Queensland, Australia. Papers, 33p.

Prevec, R., Labandeira, C.C., Neveling, J., Gastaldo, R.A., Bamford, M.K., Looy, C.V., 2009. Portrait of a Gondwanan Ecosystem: a new Late Permian locality from Kwazulu Natal, South Africa. Rev. Palaeobot. Palynol. 156, 454–493.

Prevec, R., Gastaldo, R.A., Neveling, J., Reid, S.B., Looy, C.V., 2010. An autochthonous glossopterid flora with latest Permian palynomorphs and its depositional setting in the Dicynodon Assemblage Zone of the southern Karoo Basin, South Africa. Palaeogeogr. Palaeoclimatol. Palaeoecol. 292, 391–408.

Souza, P.A., Perinotto, J.A.J., Félix, C.M., Araújo, B.C., 2015. Biostratigraphy and paleoecology of an unusual palynological record from the Aquidauana Formation, Late Pennsylvanian of Paraná Basin. An. Acad. Bras. Ciênc. 87, 611–622.

Tiwari, R.S., Vijaya, 1995. Differential morphographic identity of Gondwanic palynomorphs. Palaeobotanist 44, 62–115.

Traverse, A., 2007. Paleopalynology, Second Edition (Topics in Geobiology 28). Springer, Netherlands, Dordrecht.

Truswell, E. M., 1981. Pre-Cenozoic palynology and continental movements. Paleoreconstruction of the Continents. Geod. Series 2, 13-25.

Utting, J., 1979. Pollen and spore assemblages from the Upper Permian of the North Luangwa Valley, Zambia. IV International Palynological Conference, Lucknow (1976–77). vol. 2, pp. 165–174.

Vale Moçambique., 2014. Projecto, desenvolvimentos e avaliação da ocorrência de carvão existente na Bacia Carbonífera de Maniamba. Provincia de Niassa em Moçambique, p. 100 (in Portuguese).

Vasconcelos, L., 2009. Coal in Mozambique. 3° Simpósio de Carvões Gondwânicos. Brasilian Carbon Storage Research Center, Porto Alegre, Brasil, pp. 16–18.

Vasconcelos, L., Achimo, M., 2010. In: Cotelo Neiva, J.M., Ribeiro, A., Mendes Victor, L., Noronha, F., Ramalho, M.M. (Eds.), O carvão em Moçambique. Ciências Geológicas — Ensino e Investigação da sua História vol. 3. Geologia das Ex Colónias de África, Moçambique, Lisboa, pp. 191–206.

Verniers, J., Jourdan, P.P., Paulis, R.V., Frasca-Spada, L., De Bock, F.R., 1989. The Karroo graben of Metangula northern Mozambique. J. Afr. Earth Sci. 9, 137–158.

Wheeler, A., Gotz, A.E., 2017. Palynofacies as a tool for high-resolution palaeoenvironmental and palaeoclimatic reconstruction of Gondwanan post-glacial coal deposits: No.2 Coal Seam, Witbank Coalfield (South Africa). Palaeobiodivers. Palaeoenviron. 97 (2), 259–271.

Wright, R.P., Askin, R.A., 1987. The Permian–Triassic boundary in the southern Morondava basin of Madagascar as defined by plant microfossils. In: McKenzie, G.D. (Ed.), Gondwana Six: Stratigraphy, Sedimentology, and Paleontology. Geophysical Monograph Series, Washington, pp. 157–166

Part VI-General Conclusions

Conclusions

The present work was undertaken with the purpose of understanding the organic matter composition, thermal evolution, organic facies, mineral composition, age of the strata, paleoenvironments, provenance, potential for hydrocarbon in the boreholes and outcrop strata from the Maniamba Basin, Mozambique. The results obtained were divided based in the borehole cores and studied outcrops. Multiproxy analysis used yielded the following conclusions:

Borehole JOG16N-5

- Pyrolysis Rock Eval data and palynofacies indicates deposition under proximal-distal setting characterised by high energy conditions corroborates with high opaque phytoclast input that dilute other organic matter compounds.
- Thermal maturity variables (T_{max}, vitrinite reflectance, SCI) suggest immature to postmature levels of the organic matter (OM). The latter two parameters indicate the effect of kimberlite intrusions linked to rifting phases.
- The mineralogical composition consists of calcite, quartz, illite, kaolinite, smectite and trace of feldspars. The mineralogical composition determined the occurrence of Fe-shale and shale facies. The occurrence of illite is linked to diagenetic processes and igneous intrusions. The presence of Kaolinite is probably linked to the alteration of k-feldspar. Quartz, k-feldspar are associated to lithological variations observed along the studied sequence.
- Humid and warm paleoclimate linked to existing luxuriant glossopteris characterised by the dominance of *Protohaploxypinus* and *Striatopodocarpites* prevailed during the deposition and has influenced the paleoweathering. In its turn, there is a scarcity of upland covers indicators (monosaccate pollen).
- Most of samples were classified as good to excellent in regard to their potential to generate hydrocarbons (mostly gas).
- The palynotaxa events from JOG16N-5 borehole ressembles the northern Karoo aged basins as well as central Gondwana basins. On the other hand, the southern Karoo basins show distinct palynological events that could have been triggered by barriers of tectonic origin. These tectonic barriers could have hampered

palynoflora exchange. The aforementioned inferences are stressed by the existence of different sedimentary facies as well as different plant colonization.

- Five palynoassemblages were obtained in which the first is assigned to Middle-late Wuchiapingian whereas the last four are assigned to Changhsingian

Borehole JOG16N-6

- Non-marine influence for the organic matter is supported by four palynofacies associations, predominance of C_{27-31}, odd over even preference, abundant stigmastane under colestane, TAR>1 and high content of tryciclic terpanes.
- Thermal maturity parameters (SCI, vitrinite reflectance, CPI, OEP, ratios of 18α(H) trisneohopane (Ts) over 17α(H)-trisnorhopane (Tm), the C29 ααα S/(S+R) isomerization ratios in C29 steranes and C30 βα/(βα+αβ), C31 αβ S/(S+R) and C32αβ S/(S+R) suggest low thermal evolution.
- The mineral composition points to the dominance of quartz over other oxides, with the Al_2O_3/TiO_2) indicates intermediate rocks with minor contribution from felsic rocks that undergone incipient to strong paleoweathering.
- The organic matter is typical from proximal-distal environment which is influenced by variation in paleoredox conditions.
- Isoprenoids (Pr/C_{17} and Ph/C_{18} and palynofacies) points out to kerogen type III which indicates gas potential.
- Four palynoassemblages were obtained in which the first two are dated as latest Permian and the other two as Early Triassic. These assemblages are correlatable with well-established central Gondwana sections.
- Warm and humid paleoclimate were observed in the first two palynoassemblages whereas progressive aridification is observed for the remaining. These data agree with the lithofacies interpretation.

Borehole JOG16N-7

- Please see the conclusion in the JOG16N-6 section.
- Three palynoassemblages were obtained, and assigned to Middle-late Wuchiapingian.

- The common occurrence of characteristic Lopingian taxa (*Guttulapollenites*, *Protohaploxypinus*, *Striatopodocarpites*, *Cannanoropolis*, *Cycadopites*, *Marsupipollenites*, *Striomonosaccites*, together with common occurrence of *Thymospora pseudothiessenii* dominate the sequences.
- The depositional environment in the Maniamba was characterized by several floodplains together with diversified wetlands characterised by forest swamps and lakes.

Borehole JOG16N-8

- Please see the palynological dating information in the JOG16N-6 section.
- Phytoclasts dominates all the sequence with moderate contribution of sporomorphs and AOM.
- The deposition of the JOG16N-8 sediments occurred under typical lacustrine-fluvial environment favoured by oxidizing episodes that shifted with a seasonal shift to dysoxic.
- SCI indicates a low thermal evolution for the OM.
- The abundant type III and IV kerogens suggest potential source rocks for gas.

Outcrops (Luiga, Michunwa, Nhamago, Luchai)

- Palynofacies and biomarker data indicates terrestrially and bacterial derived organic matter with no marine influence
- Thermal maturity variables (Ts/Tm ratio, methlyphenantrane, 2-methlylantracene) suggest immature to overmature with some strata being influenced by kimberlite emplacement which are associated with the first or second graben faulting stages).
- Environmental settings changed from oxic-suboxic-anoxic conditions.
- In general, all units, are characterised by two categories of pollen that includes bisaccate striate and non-striate.
- Hypautocthonous sedimentation is inferred based on the co-existence of lycopsids, filicopsids and sphenopsids vegetation.

- Luchai and Nhamago were dated to Late Permian-Early Triassic whereas Luchai and Nhamago pertain to Guadalupian.
- Mineral composition, the range of organic richness (good to excellent) suggest the existence of potential source rocks for gas.

From the paleoenvironmental point of view the Maniamba Basin is quite complex, however it should be highlighted that during Middle-late Permian to possibly Early Triassic this Basin was made up of fluvio-lacustrine settings together with coal seams which comprise floodplain, crevasse splay and typical associations of lithofacies derived from fluvial channels. This depicts a typical fluvial/lacustrine environment where the co-existence of sub environments comprising very high and low energy was possible.

Contribution to the existing Knowledge

The highlights of this research project are as follows:

- The Permian sequences of the Maniamba Basin are rich in regard to OM and their maturation place them into gas and oil windows. However, the strata are more gas prone than oil.
- Iintegrative approaches of palynology, palynofacies, Rock Eval pyrolysis, vitrinite reflectance together with biomarkers have demonstrated a great potential to complement existing studies (e., sedimentological, lithostratigraphic) in the Maniamba Basin as well as in other contemporaneous basins. The vitrinite reflectance were always correlatable with SCI, T_{max}, and at some extent with biomarkers.
- The present study also highlights the record of Permo-Triassic transition in the Maniamba Basin reinforcing Gondwana correlations in Central Gondwana as well as corroborating previously proposed vertebrate extinction events in the Karoo Basin.
- The possible existence of intra Gondwanan provincialism that often hampers Gondwana correlation is also identified in the present research project in which northern Karoo palynoevents show dissimilarities with its southern Karoo counterpart.

- Through this research, it can be precisely stated that the petroleum fluids from the Rovuma Basin are not sourced from the deeper Permian Karoo rocks in the Maniamba Basin differing from previous assumptions.
- Stratigraphically a Wuchiapingian age was suggested for the K4, whereas a Changhsingian-Induan age is inferred for the K5 formations in the Maniamba Basin contradicting previous thoughts. This work represents the first comprehensive palynological biozonation scheme for the Maniamba Basin.
- This work emphasizes the importance of the use of biomarkers (oil fingerprint) to assess hydrocarbon pathway and migration (source-oil correlation).
- The occurrence of considerably thicker coals in the Basin opens perspective for future exploration of coal bed methane (CBM) in the Basin regarded as clean energy in the context of energy transition.

In overall, these findings are highly encouraging follow up studies aiming at delineating the possible presence of other key elements essential for hydrocarbon research.

Future research

Main possibilities for future research may include:

- Use 2D model for a better interpretation of the thermal history of the buried formations from the Maniamba Basin.
- Sampling of outcrop strata in a smaller distance closer to kimberlite intrusions are needed for further understanding of the effect of the OM preservation and as well as maturity since volcanic thermal alteration significantly matures source rocks, often leading to high-to-overmature level.
- The Permian-Triassic boundary identification was hindered due to the lack of palynotaxa changes across the boundary as well as the existing barren zones, hence the identification of molecular fossils and biogeochemical anomalies which are contemporaneous with the Permian-Triassic Event are required.
- Evaluation of the paleoredox conditions changes across the Permian-Triassic boundary since they are considered the triggers of the extinction.
- Undertake isotopes analysis in order to interpret the changes on carbon incursion through the sequence that depict the Permian-Triassic transition.

- In order to further our understanding regarding the stratigraphy of the Maniamba Basin all formations must be palynologically investigated (e.g., K2, K3, K6, KSb, KSc, KSd, and others).
- Due to the excellent floral and faunal fossil record of the Maniamba Basin, future studies integrating different elements of the ecosystem (e.g., fauna, macroplants, microfloras) together with radiometric dating can possibly make Maniamba Basin the standard type section to which other Gondwana successions could be compared.

In summary, it is crucial therefore that integrated methods are considered in future works in order to deepen our understanding regarding the geodynamics of the Maniamba Basin.

Part VII-Appendix

Reconstructing the Late Permian-Early Triassic environment of a coal-bearing succession in the Maniamba Basin, Mozambique (Central Gondwana): A multiproxy palynological and geochemical approach.

Supplementary Materials

Figure S1: Cuticule observed under transmitted white light.

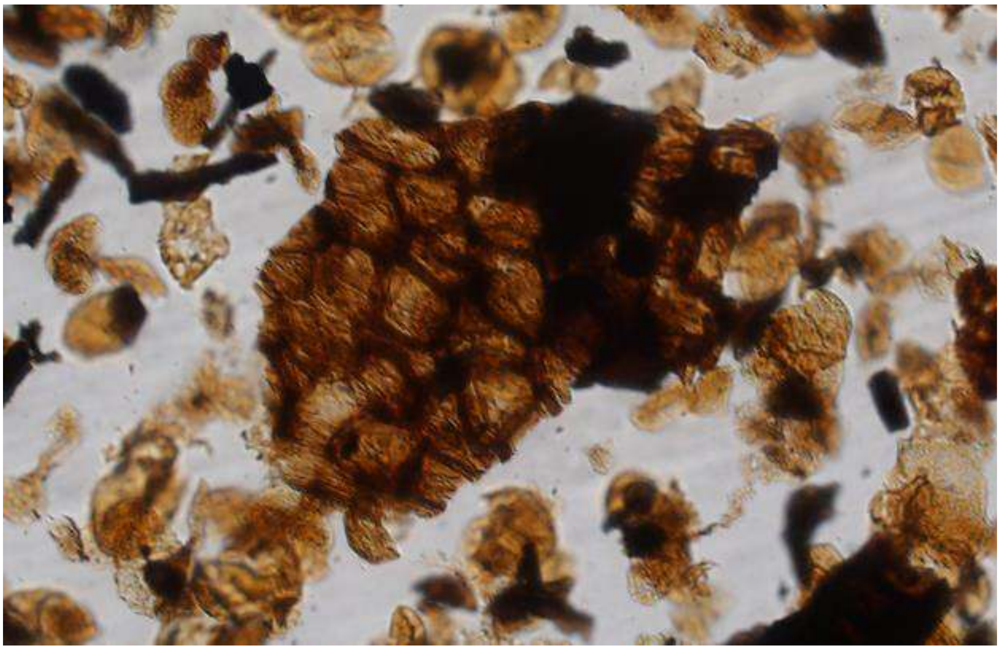

Figure S2: Cuticle from S1 image observed under blue light and exhibiting dark or no fluorescence.

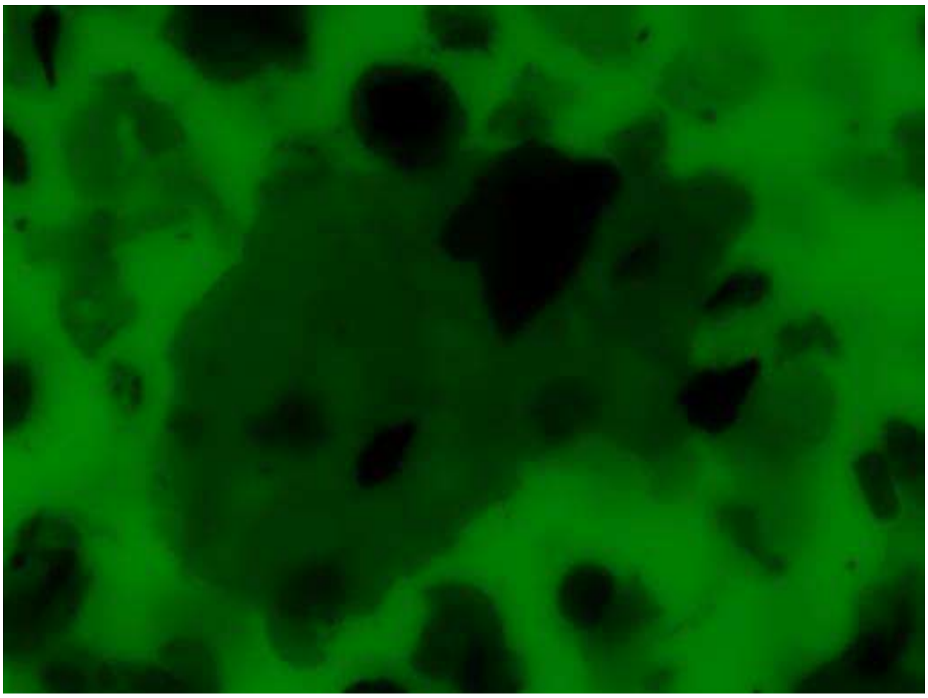

Figure S3: Amorphous organic matter in transmitted white light.

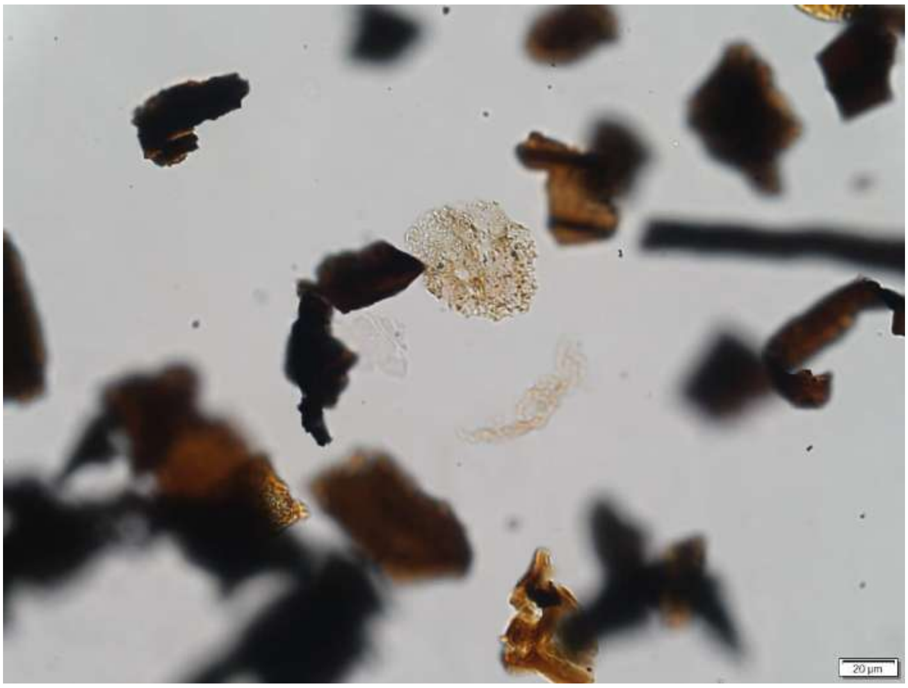

Figure S4: Amorphous organic from figure S3 in fluorescence mode.

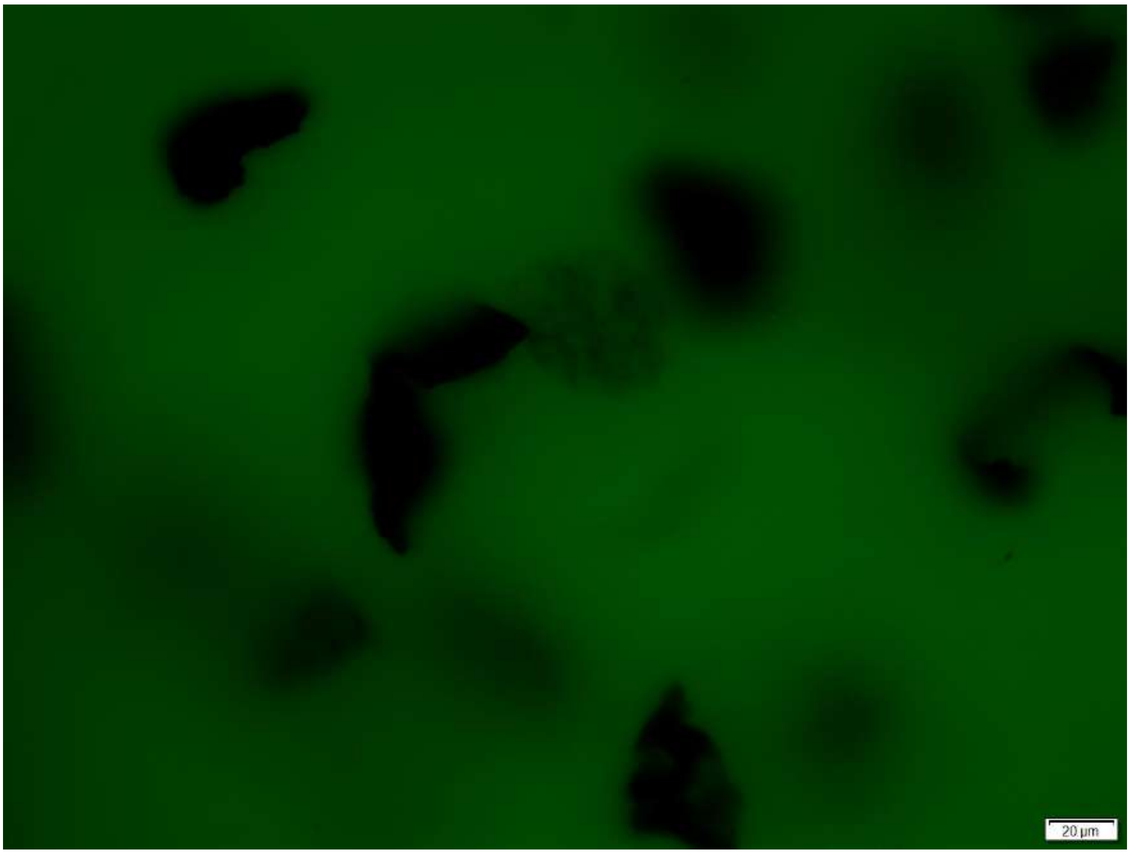

Table S1 Palynofacies data of the outcrop strata. The Spore Coloration Index (SCI) interpretation was obtained from Makled and Tahoun (2015) and references therein.

Outcrops (samples)	Opaque (%)			Non-Opaque (%)					Palynomorphs (%)		AOM (%)		Thermal maturity	
	Equid.	Elongated	Corroded	Biostructured	Non-Biostructured	Cuticles	Membranes	Fungal hyphae	Pollen	Spores	AOM	Resin	SCI	Maturity
1NN (3)	0	4.0	50.3	1.0	0	0	0	0.7	40.0	2.6	0.3	0.7	Light yellow	Immature
1NN (2)	2.1	4.7	50.0	1.3	0.5	0.3	0	0.5	39.7	0.6	0.3	0.0	Dark yellow	Early mature
1NN (1)	0.7	1.6	42.7	5.0	1.3	1.3	0	0	30.0	7.4	10.0	0.0	Light yellow	Immature
23NN (4)	0.0	6.3	7.6	5.7	1.2	0.0	0.0	0.0	48.2	10.0	18.0	3.0	Light yellow	Immature
23NN (2)	0.0	1.0	70.3	1.7	0.0	0.0	1.0	0.0	10.3	5.0	10.0	0.7	Dark yellow	Early mature
31NN (4)	0.3	6.0	6.9	3.0	3.0	0.5	0.7	0.3	50.0	12.0	15	2.3	Black	Overmature
31NN (3)	0.0	15.7	63.3	5.7	0.0	1.3	0.0	0.3	9.7	0.0	4.0	0.0	Yellow brown	Mature
31NN (1)	0.0	8.3	46.0	10.0	0.3	1.0	0.0	0.2	24.5	5.5	3.2	0.7	Brown	Late mature
40NN (1)	0.4	4.7	61.3	3.0	0.6	0.6	0.5	0.3	18.3	1.7	8.5	0.1	Light yellow	Immature
40NN (2)	0.0	2.2	4.7	4.0	8.0	0.0	0.0	0.0	50.0	10.4	18	2.5	Dark yellow	Early mature
40NN (4)	0.0	10.7	66.0	2.3	1.3	0.0	0.0	0.0	8.3	1.4	10.0	0.0	Dark	Overmature

*AOM=Amorphous organic matter; SCI=Spore coloration index.